SELECTION AND CHARACTERIZATION OF DNA APTAMERS FOR ESTRADIOL AND ETHYNYLESTRADIOL FOR APTASENSOR DEVELOPMENT

BY

SPURTI UMESH AKKI

DISSERTATION

Submitted in partial fulfillment of the requirements
for the degree of Doctor of Philosophy in Environmental Engineering in Civil Engineering
in the Graduate College of the
University of Illinois at Urbana-Champaign, 2018

Urbana, Illinois

Doctoral Committee:

Assistant Professor Jeremy S. Guest, Chair
Professor Charles J. Werth, Director of Research
Professor Scott K. Silverman
Assistant Professor Roland Cusick

ABSTRACT

Small organic contaminants have been widely detected in the surface and ground waters of this nation. A sub-class of these contaminants called endocrine disrupting compounds (EDCs) are known to have adverse effects on aquatic and human health. Among the EDCs, natural hormone 17β-estradiol (E2) and synthetic hormone 17α-ethynylestradiol (EE) possess high estrogenic potency and hence are contaminants of interest. Conventional methods to detect these compounds are expensive, time consuming and need implementation by an expert. By contrast, antibody-based assays are relatively inexpensive and commercially available but suffer from poor selectivity. A promising alternative makes use of DNA aptamers as molecular recognition elements. In order to evaluate the potential of DNA aptamers and aptasensors to detect small organics in natural waters, the following objectives were pursued: (1) critically review DNA aptamers and aptasensors developed for small organic molecules and assess their use for monitoring environmentally relevant organics, (2) select and characterize DNA aptamers that bind to E2 and EE and, (3) study the effect of immobilization on the binding affinity of the selected E2 and EE aptamers.

A review of ~80 aptamers and ~200 aptasensors for small organics was conducted to identify factors that affect binding affinity of the aptamer and limits of detection (LODs) of the aptasensor. Based on regression analyses, aptamer binding affinities are found to have a weak relationship with hydrophobicity of the target and length of the aptamer (p-values<0.05). Independent t-tests comparing aptasensor LODs suggest that the electrochemical platform is significantly more sensitive than colorimetric and fluorescence-based platforms. The inherent binding affinity of the aptamer was found to have a significant effect on the LOD of the aptasensor. While some fabricated aptasensors are sufficiently sensitive to detect contaminants at

environmentally relevant concentrations, they are often associated with complex fabrication steps, and/or interference from structurally similar analogs. As a result, aptasensor commercialization faces many challenges including reusability, reproducibility and robustness.

In vitro selections were conducted with different selection pressures to isolate sensitive and selective DNA aptamers for E2 and EE. An equilibrium-filtration assay was used to determine dissociation constants (K_d) of the aptamer towards its parent target and its analogues. The E2 aptamers, E2Apt1 and E2Apt2 were found to have K_d values of 0.6 μM. They bound to analogue estrone (E1) with a similar affinity but were at least 74-fold more selective over EE. The EE aptamers K_d values are 0.5-1 μM. While one EE aptamer (EEApt1) was 53-fold more selective for EE over E2 and E1, the second EE aptamer (EEApt2) bound to all three EDCs (E1, E2 and EE) with similar affinities. The aptamers maintained their binding affinities in natural waters samples (tap water and lake water). DMS probing of the structure of the DNA aptamer revealed that the binding regions were mostly located in the single-stranded loop regions of the aptamer.

Aptasensors typically employ immobilized aptamers though the aptamers are selected and characterized while free or unattached in solution. The K_d values of immobilized selective aptamers were evaluated using magnetic microbeads surface for attachment. E2Apt1 immobilized at either end (5′ or 3′) and E2Apt2 immobilized at the 3′ end retain their binding affinity. The binding affinity is inversely correlated to the average linear distance of the binding pocket from the immobilized end. This result suggests that unwanted interactions between the aptamer and other moieties are more likely when the binding pocket is further away from the surface. Binding curve of E2Apt2 immobilized at the 5′ end indicates potential dimerization at high loadings of aptamer on the beads due to increased proximity between aptamer strands.

EEApt1 loses its binding affinity upon immobilization potentially due to disruption in its tertiary structure upon attachment to the surface. Despite no loss in binding affinity upon immobilization, E2Apt1 (5′) shows no significant change in electrochemical current on binding to E2 when incorporated into an electrochemical sensor. This result implies an insufficient conformational change of the aptamer on binding to the target.

Overall, this work identifies the first aptamers for EE and selective aptamers for E2, while also highlighting the issues with development of aptamers and their eventual incorporation into aptasensors to detect small organics. Two major concerns are (1) immobilizing aptamers in sensor platforms while selections of aptamers are conducted with free/unattached aptamers, resulting in loss of binding affinity and (2) insufficient conformational change of the aptamer on binding to small molecule targets, resulting in a lack of change in the sensor signal. The findings from this dissertation support additional research directions regarding employing free aptamers in sensors and/or conducting new selections for aptamers using a DNA pool that is attached to a surface.

To Mummy and Appa

For being wonderful parents and my pillars of strength

ACKNOWLEDGEMENTS

I would like to thank my advisor, Prof. Charles Werth, for his tremendous patience, support & guidance through all these years of my research. I would also like to express my gratitude towards Prof. Scott Silverman for co-advising me, helping with aptamer development & characterization during the first phase of my PhD & serving on my doctoral committee. I extend my thanks to Prof. Jeremy Guest & Prof. Roland Cusick for serving on my doctoral committee & providing me with valuable feedback on my research. Special thanks to Prof. Richard Crooks & Dr. Josephine Hofstetter at the University of Texas at Austin for all the help with the electrochemical techniques.

I could not have done this without the love & unwavering support from my parents – thank you for believing in me. My thoughtful husband, Raylan, has been by my side through thick & thin. Ajja has been a constant inspiration through all these years. Both Ajjis always wished me the best & prayed for me. My brother, Shreyu, has been a silent yet integral presence & I am proud that he has done well for himself. Special thanks to Chikka Aunty for talking me through some tough times. Thank you Mumma & Dada for keeping me in your prayers.

I would like to thank the Werth Group, particularly Allison for being a supportive friend & a sounding board. I really appreciate the Silverman Group for teaching me the ways of the lab & including me in all their activities right from research talks to coffee break conversations. I extend my thanks to the Crooks Group for helping me figure out electrochemistry. I appreciate help from Dr. Shaoying Qi for maintaining lab equipment & applying for permits. Melissa Pollard has been integral in helping with timely purchasing. Champaign & Austin became home to me because of my dearest friends Nisha, Maria, Neetika, Amrita & Shivani – thank you for tolerating my worst & bringing out my best.

TABLE OF CONTENTS

CHAPTER 1
INTRODUCTION

1.1 Motivation

Anthropogenic small organics which include solvents, pesticides, and pharmaceuticals have been detected in surface and ground waters of this nation[1-2]. These compounds originate from industrial effluent, agricultural run-off and/or landfill leachate subsequently seeping into water resources. An emerging sub-class of such small organic contaminants called endocrine disrupting compounds (EDCs) are found to have a negative impact on aquatic and human health[3-5]. Among the EDCs, natural hormone 17β-estradiol (E2) and synthetic hormone 17α-ethynylestradiol (EE) possess high estrogenic potency[6-7] and have been detected in surface waters[1]. Therefore, E2 and EE were required to be monitored in water resources from 2013 through 2015 in accordance with the EPA's Unregulated Contaminant Monitoring Rule 3 (UCMR3).

Conventional methods to detect these compounds include chromatographic-spectrometric techniques (e.g., LC-MS, GC-MS) which are sensitive[8-9] but time-consuming, expensive, and require instrumentation which needs to be operated by an expert. Alternatively, Enzyme Linked Immunosorbent Assays (ELISAs) employ antibodies as recognition elements to detect E2/EE. ELISAs are sensitive, cost-effective, easy-to-use and are commercially available which makes them a good alternative. However, they suffer from false positives due to interference of natural matrix components and/or analogues[10-12] because of the poor selectivity of the antibodies used in the assays. Therefore, there is a need to develop sensitive and selective sensors to detect these compounds.

1.2 Background

Aptamers are single stranded oligonucleotides (DNA or RNA) that are selected to bind to a target of interest with desired sensitivity and selectivity[13-15]. Aptamers are identified through a process called Systematic Evolution of Ligands by EXponential enrichment (SELEX). The relative ease of selection and synthesis, and tolerance to a broader range of physiological conditions makes DNA aptamers favorable molecular recognition elements. DNA aptamers have been identified for a variety of targets ranging from proteins (e.g., thrombin[16], abrin[17]) to cations (K^{+}[18], As^{5+}[19]), including small organics (e.g., cocaine[20], ATP[21]). The binding affinity of aptamers for their targets are characterized by a dissociation constant (K_d) – lower the value of K_d, higher the affinity of the aptamer and vice versa.

DNA aptamers can be functionalized and have been coupled to a range of sensor platforms (e.g., electrochemical[22], fluorescence-based[23], colorimetric[24], surface enhanced Raman spectroscopy[25], surface plasmon resonance[26]) to create aptamer-based sensors or aptasensors. They have been reported for a variety of organic compounds, some of which are environmentally relevant. A few studies on aptasensors for small organics have reported limits of detection (LODs) in the attomolar range[26-27]. Aptasensors have also been successfully tested in a multitude of matrices including tap water[28], wastewater[29], blood[30], serum[31], and urine[32]. In one case, a thrombin aptasensor was developed using materials such as wax-printed chromatographic paper and carbon electrodes which reduced the cost to \$0.33/sensor[33]. Yet, there are no commercially available aptasensors for organic contaminants.

Specifically, E2 aptamers have been reported in multiple studies[34-36], and some[34, 36] have been successfully converted to aptasensors. Kim et al. identified the first E2 aptamer (K_d = 0.13μM)[34] which has been widely incorporated into sensors with LODs as low as 1fM[37-38].

However, the selectivity of this aptamer is limited, in some cases with only a 5-fold difference in signal change between the parent target and its analogue[29]. Vanschoenbeek et al. identified an E2 aptamer with lower binding affinity (K_d = 0.9μM)[35] and poorer selectivity[39] than the E2 aptamer from Kim et al. In a 2014 study, Alsager et al. identified a high binding affinity aptamer (K_d = 0.05μM)[36] with ~100-fold selectivity towards E2 compared to its analogues[39]. However, EE aptamers had not been reported in the literature.

In order to develop aptasensors, aptamers are typically immobilized on a sensor platform[40-42]. Upon binding to the target, the aptamer undergoes a conformational change which is transduced into a signal change by the platform. This signal change is quantified and correlated to the concentration of the target. For instance, aptamers are immobilized on electrodes[41-42] (gold or carbon) in electrochemical sensors. The change in conformation of the aptamer alters the resistance at the electrode resulting in a change in the current due to the redox species in solution or attached to the aptamer (Figure 1.1). However, aptamers are identified and characterized for their binding affinity typically in the free or unattached state. Also, conformational change of the aptamer upon target binding is not selected for during the conventional aptamer selection process. These factors could potentially lead to issues during aptasensor development.

1.3 Research Objectives

The overall goal of my research was to select, characterize and evaluate DNA aptamers as potential candidates to develop alternative sensors for small organics. The model small organic contaminants used are E2 and EE. The primary objectives of my work were as follows:

Objective 1: To critically review DNA aptamers and aptasensors developed for small organic molecules and assess their use for monitoring environmentally relevant organics.

Multiple linear regression analyses were conducted between logK_d and a suite of aptamer and target properties to gain insight into causes for improved binding affinity. Alternative sensing platforms were compared to determine their strengths and weaknesses. Aptasensor LODs were compared to environmentally relevant concentrations of small organics to assess their utility as environmental sensors.

Objective 2: To select and characterize DNA aptamers that bind to E2 and EE. Conventional SELEX was employed to select aptamers for E2 and EE. Additional selection pressures were applied during this process to isolate sensitive binders. The aptamers' dissociation constants for the parent target as well as its analogues were evaluated in buffered nanopore water and buffered environmental water samples. Chemical probing methods were used to identify the binding regions on the aptamers.

Objective 3: To study the effect of immobilization on the binding affinity of the selected E2 and EE aptamers. The biotin-labeled aptamers were immobilized on streptavidin-coated magnetic beads and their binding affinity was assessed. One E2 aptamer was immobilized on gold nanoparticles to investigate if different surfaces affect the binding affinity. This aptamer was also immobilized on a gold electrode to test for electrochemical signal change upon binding to the target.

1.4 Dissertation Outline

- Chapter 2 contains a manuscript submitted to *Environmental Science and Technology* titled "Critical Review: DNA aptasensors, Are they ready for monitoring organic pollutants in natural and treated water sources?" with co-author C.J. Werth. This work addresses objective 1.

- Chapter 3 contains a manuscript published in *Environmental Science and Technology* titled "Selective Aptamers for Detection of Estradiol and Ethynylestradiol in Natural Waters" with co-authors C.J. Werth and S.K. Silverman. This work addresses objective 2.
- Chapter 4 contains a manuscript in preparation for submission to *ACS Sensors* titled "Effects of Immobilizing DNA Aptamers on Binding to Estradiol and Ethynylestradiol" with co-author C.J. Werth. This work addresses objective 3.
- Chapter 5 contains major conclusions based on this work and future research directions.
- Appendix A contains supplementary information for Chapter 2.
- Appendix B contains supplementary information for Chapter 3.
- Appendix C contains supplementary information for Chapter 4.

1.5 Figure

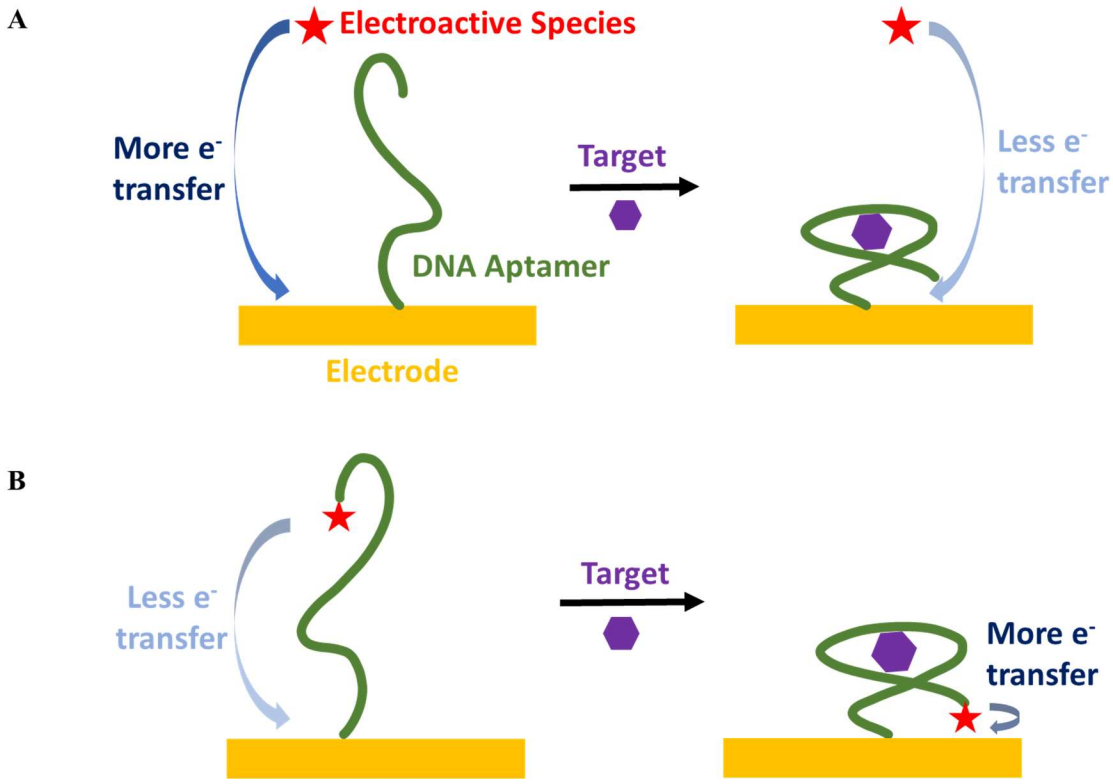

Figure 1.1. Conceptual model of an electrochemical aptasensor with (A) exogenous electroactive or redox species or (B) endogenous (attached to the DNA aptamer) redox species.

1.6 REFERENCES

1. Kolpin, D. W.; Furlong, E. T.; Meyer, M. T.; Thurman, E. M.; Zaugg, S. D.; Barber, L. B.; Buxton, H. T., Pharmaceuticals, Hormones, and Other Organic Wastewater Contaminants in U.S. Streams, 1999−2000: A National Reconnaissance. *Environmental Science & Technology* **2002,** *36* (6), 1202-1211.
2. Barnes, K. K.; Kolpin, D. W.; Furlong, E. T.; Zaugg, S. D.; Meyer, M. T.; Barber, L. B., A national reconnaissance of pharmaceuticals and other organic wastewater contaminants in the United States — I) Groundwater. *Science of The Total Environment* **2008,** *402* (2), 192-200.
3. Sharpe, R. M.; Skakkebaek, N. E., Are oestrogens involved in falling sperm counts and disorders of the male reproductive tract? *The Lancet* **1993,** *341* (8857), 1392-1396.
4. Jobling, S.; Williams, R.; Johnson, A.; Taylor, A.; Gross-Sorokin, M.; Nolan, M.; Tyler, C. R.; van Aerle, R.; Santos, E.; Brighty, G., Predicted Exposures to Steroid Estrogens in U.K. Rivers Correlate with Widespread Sexual Disruption in Wild Fish Populations. *Environmental Health Perspectives* **2006,** *114* (Suppl 1), 32-39.
5. Kidd, K. A.; Blanchfield, P. J.; Mills, K. H.; Palace, V. P.; Evans, R. E.; Lazorchak, J. M.; Flick, R. W., Collapse of a fish population after exposure to a synthetic estrogen. *Proceedings of the National Academy of Sciences* **2007,** *104* (21), 8897.
6. Van den Belt, K.; Berckmans, P.; Vangenechten, C.; Verheyen, R.; Witters, H., Comparative study on the in vitro/in vivo estrogenic potencies of 17β-estradiol, estrone, 17α-ethynylestradiol and nonylphenol. *Aquatic Toxicology* **2004,** *66* (2), 183-195.
7. Pillon, A.; Boussioux, A.-M.; Escande, A.; Aït-Aïssa, S.; Gomez, E.; Fenet, H.; Ruff, M.; Moras, D.; Vignon, F.; Duchesne, M.-J.; Casellas, C.; Nicolas, J.-C.; Balaguer, P., Binding of Estrogenic Compounds to Recombinant Estrogen Receptor-α: Application to Environmental Analysis. *Environmental Health Perspectives* **2005,** *113* (3), 278-284.
8. Hutchins, S. R.; White, M. V.; Hudson, F. M.; Fine, D. D., Analysis of Lagoon Samples from Different Concentrated Animal Feeding Operations for Estrogens and Estrogen Conjugates. *Environmental Science & Technology* **2007,** *41* (3), 738-744.
9. Grover, D. P.; Zhang, Z. L.; Readman, J. W.; Zhou, J. L., A comparison of three analytical techniques for the measurement of steroidal estrogens in environmental water samples. *Talanta* **2009,** *78* (3), 1204-1210.
10. Sawaya, W. N.; Lone, K. P.; Husain, A.; Dashti, B.; Al-Zenki, S., Screening for estrogenic steroids in sheep and chicken by the application of enzyme-linked immunosorbent assay and a comparison with analysis by gas chromatography–mass spectrometry. *Food Chemistry* **1998,** *63* (4), 563-569.
11. Farré, M.; Brix, R.; Kuster, M.; Rubio, F.; Goda, Y.; López de Alda, M. J.; Barceló, D., Evaluation of commercial immunoassays for the detection of estrogens in water by comparison with high-performance liquid chromatography tandem mass spectrometry HPLC–MS/MS (QqQ). *Analytical and Bioanalytical Chemistry* **2006,** *385* (6), 1001-1011.
12. Viganò, L.; Benfenati, E.; Cauwenberge, A. v.; Eidem, J. K.; Erratico, C.; Goksøyr, A.; Kloas, W.; Maggioni, S.; Mandich, A.; Urbatzka, R., Estrogenicity profile and estrogenic compounds determined in river sediments by chemical analysis, ELISA and yeast assays. *Chemosphere* **2008,** *73* (7), 1078-1089.
13. Tuerk, C.; Gold, L., Systematic evolution of ligands by exponential enrichment: RNA ligands to bacteriophage T4 DNA polymerase. *Science* **1990,** *249* (4968), 505.
14. Ellington, A. D.; Szostak, J. W., In vitro selection of RNA molecules that bind specific ligands. *Nature* **1990,** *346* (6287), 818-822.
15. Ellington, A. D.; Szostak, J. W., Selection in vitro of single-stranded DNA molecules that fold into specific ligand-binding structures. *Nature* **1992,** *355* (6363), 850-852.

16. Bock, L. C.; Griffin, L. C.; Latham, J. A.; Vermaas, E. H.; Toole, J. J., Selection of single-stranded DNA molecules that bind and inhibit human thrombin. *Nature* **1992,** *355* (6360), 564-566.
17. Tang, J.; Yu, T.; Guo, L.; Xie, J.; Shao, N.; He, Z., In vitro selection of DNA aptamer against abrin toxin and aptamer-based abrin direct detection. *Biosensors and Bioelectronics* **2007,** *22* (11), 2456-2463.
18. Wang, L.; Liu, X.; Hu, X.; Song, S.; Fan, C., Unmodified gold nanoparticles as a colorimetric probe for potassium DNA aptamers. *Chemical Communications* **2006,** (36), 3780-3782.
19. Kim, M.; Um, H.-J.; Bang, S.; Lee, S.-H.; Oh, S.-J.; Han, J.-H.; Kim, K.-W.; Min, J.; Kim, Y.-H., Arsenic Removal from Vietnamese Groundwater Using the Arsenic-Binding DNA Aptamer. *Environmental Science & Technology* **2009,** *43* (24), 9335-9340.
20. Stojanovic, M. N.; de Prada, P.; Landry, D. W., Aptamer-Based Folding Fluorescent Sensor for Cocaine. *Journal of the American Chemical Society* **2001,** *123* (21), 4928-4931.
21. Huizenga, D. E.; Szostak, J. W., A DNA Aptamer That Binds Adenosine and ATP. *Biochemistry* **1995,** *34* (2), 656-665.
22. Hayat, A.; Marty, J. L., Aptamer based electrochemical sensors for emerging environmental pollutants. *Frontiers in Chemistry* **2014,** *2*, 41.
23. Emrani, A. S.; Danesh, N. M.; Lavaee, P.; Ramezani, M.; Abnous, K.; Taghdisi, S. M., Colorimetric and fluorescence quenching aptasensors for detection of streptomycin in blood serum and milk based on double-stranded DNA and gold nanoparticles. *Food Chemistry* **2016,** *190*, 115-121.
24. Yang, C.; Wang, Y.; Marty, J.-L.; Yang, X., Aptamer-based colorimetric biosensing of Ochratoxin A using unmodified gold nanoparticles indicator. *Biosensors and Bioelectronics* **2011,** *26* (5), 2724-2727.
25. Pang, S.; Labuza, T. P.; He, L., Development of a single aptamer-based surface enhanced Raman scattering method for rapid detection of multiple pesticides. *Analyst* **2014,** *139* (8), 1895-1901.
26. Kim, S.; Lee, H. J., Gold Nanostar Enhanced Surface Plasmon Resonance Detection of an Antibiotic at Attomolar Concentrations via an Aptamer-Antibody Sandwich Assay. *Analytical Chemistry* **2017,** *89* (12), 6624-6630.
27. Meng, F.; Ma, X.; Duan, N.; Wu, S.; Xia, Y.; Wang, Z.; Xu, B., Ultrasensitive SERS aptasensor for the detection of oxytetracycline based on a gold-enhanced nano-assembly. *Talanta* **2017,** *165*, 412-418.
28. Wu, L.; Qi, P.; Fu, X.; Liu, H.; Li, J.; Wang, Q.; Fan, H., A novel electrochemical PCB77-binding DNA aptamer biosensor for selective detection of PCB77. *Journal of Electroanalytical Chemistry* **2016,** *771*, 45-49.
29. Yildirim, N.; Long, F.; Gao, C.; He, M.; Shi, H.-C.; Gu, A. Z., Aptamer-Based Optical Biosensor For Rapid and Sensitive Detection of 17β-Estradiol In Water Samples. *Environmental Science & Technology* **2012,** *46* (6), 3288-3294.
30. Ferguson, B. S.; Hoggarth, D. A.; Maliniak, D.; Ploense, K.; White, R. J.; Woodward, N.; Hsieh, K.; Bonham, A. J.; Eisenstein, M.; Kippin, T. E.; Plaxco, K. W.; Soh, H. T., Real-Time, Aptamer-Based Tracking of Circulating Therapeutic Agents in Living Animals. *Science Translational Medicine* **2013,** *5* (213), 213ra165.
31. Lavaee, P.; Danesh, N. M.; Ramezani, M.; Abnous, K.; Taghdisi, S. M., Colorimetric aptamer based assay for the determination of fluoroquinolones by triggering the reduction-catalyzing activity of gold nanoparticles. *Microchimica Acta* **2017,** *184* (7), 2039-2045.
32. Ragavan, K. V.; Selvakumar, L. S.; Thakur, M. S., Functionalized aptamers as nano-bioprobes for ultrasensitive detection of bisphenol-A. *Chemical Communications* **2013,** *49* (53), 5960-5962.
33. Cunningham, J. C.; Brenes, N. J.; Crooks, R. M., Paper Electrochemical Device for Detection of DNA and Thrombin by Target-Induced Conformational Switching. *Analytical Chemistry* **2014,** *86* (12), 6166-6170.

34. Kim, Y. S.; Jung, H. S.; Matsuura, T.; Lee, H. Y.; Kawai, T.; Gu, M. B., Electrochemical detection of 17β-estradiol using DNA aptamer immobilized gold electrode chip. *Biosensors and Bioelectronics* **2007,** *22* (11), 2525-2531.
35. Vanschoenbeek, K.; Vanbrabant, J.; Hosseinkhani, B.; Vermeeren, V.; Michiels, L., Aptamers targeting different functional groups of 17β-estradiol. *The Journal of Steroid Biochemistry and Molecular Biology* **2015,** *147*, 10-16.
36. Alsager, O. A.; Kumar, S.; Willmott, G. R.; McNatty, K. P.; Hodgkiss, J. M., Small molecule detection in solution via the size contraction response of aptamer functionalized nanoparticles. *Biosensors and Bioelectronics* **2014,** *57*, 262-268.
37. Chen, J.; Wen, J.; Yang, G.; Zhou, S., A target-induced three-way G-quadruplex junction for 17β-estradiol monitoring with a naked-eye readout. *Chemical Communications* **2015,** *51* (62), 12373-12376.
38. Na, W.; Park, J. W.; An, J. H.; Jang, J., Size-controllable ultrathin carboxylated polypyrrole nanotube transducer for extremely sensitive 17β-estradiol FET-type biosensors. *Journal of Materials Chemistry B* **2016,** *4* (29), 5025-5034.
39. Svobodova, M.; Skouridou, V.; Botero, M. L.; Jauset-Rubio, M.; Schubert, T.; Bashammakh, A. S.; El-Shahawi, M. S.; Alyoubi, A. O.; O'Sullivan, C. K., The characterization and validation of 17β-estradiol binding aptamers. *Journal of Steroid Biochemistry and Molecular Biology* **2017,** *167*, 14-22.
40. Liu, J.; Lu, Y., Fast Colorimetric Sensing of Adenosine and Cocaine Based on a General Sensor Design Involving Aptamers and Nanoparticles. *Angewandte Chemie International Edition* **2006,** *45* (1), 90-94.
41. Baker, B. R.; Lai, R. Y.; Wood, M. S.; Doctor, E. H.; Heeger, A. J.; Plaxco, K. W., An Electronic, Aptamer-Based Small-Molecule Sensor for the Rapid, Label-Free Detection of Cocaine in Adulterated Samples and Biological Fluids. *Journal of the American Chemical Society* **2006,** *128* (10), 3138-3139.
42. Zhu, Y.; Zhou, C.; Yan, X.; Yan, Y.; Wang, Q., Aptamer-functionalized nanoporous gold film for high-performance direct electrochemical detection of bisphenol A in human serum. *Analytica Chimica Acta* **2015,** *883*, 81-89.

CHAPTER 2
CRITICAL REVIEW: DNA APTASENSORS, ARE THEY READY FOR MONITORING ORGANIC POLLUTANTS IN NATURAL AND TREATED WATER SOURCES?

Submitted to *Environmental Science & Technology*

2.1 Abstract

There is a growing need to monitor anthropogenic organic contaminants detected in water sources. DNA aptamers are synthetic single-stranded oligonucleotides, selected to bind to target contaminants with favorable selectivity and sensitivity. These aptamers can be functionalized and are used with a variety of sensing platforms to develop sensors, or aptasensors. In this critical review, we: 1) identify the state-of-the-art in DNA aptamer selection, 2) evaluate target and aptamer properties that make for sensitive and selective binding and sensing, 3) determine strengths and weaknesses of alternative sensing platforms, and 4) assess the potential for aptasensors to quantify the concentrations of environmentally relevant organic contaminants in water. Among a suite of target and aptamer properties, binding affinity is either directly (e.g., organic carbon partition coefficient) or inversely (e.g., polar surface area) correlated to properties that indicate greater target hydrophobicity results in the strongest binding aptamers, and binding affinity is correlated to aptasensor limits of detection. Electrochemical-based aptasensors show the greatest sensitivity, which is similar to that of ELISA-based methods. Only a handful of aptasensors can detect organic pollutants at environmentally relevant concentrations, and interference from structurally similar analogs commonly present in natural waters is a yet-to-be overcome challenge. These findings lead to recommendations to improve aptasensor performance.

2.2 Introduction

A wide variety of organic pollutants are found in natural and treated water sources, including solvents, fuels, pesticides, pharmaceuticals, and personal care products[1-2]. These pollutants originate primarily from anthropogenic sources such as urban and agricultural runoff, municipal and industrial wastewater effluent, landfill leachate, railroad tank car accidents, leaking underground storage tanks, and livestock waste lagoons. Traditional methods to detect and quantify these pollutants involve mass spectrometry, often in combination with gas or liquid chromatography (i.e., GC-MS, LC-MS); they are expensive, time consuming, and require analyses at a central facility by an expert. To overcome these limitations, many researchers have been trying to develop low cost, easy, point of use sensors for pollutants in water using highly specific chemical binding agents coupled to colorimetric, fluorescence, or electrochemical sensing.

Inexpensive, easy, point of use commercial sensors for organic compounds are common in personal healthcare; a prime example is the pregnancy test kit. It involves the detection of a pregnancy hormone (hCG) using two sets of antibodies that bind to the hormone. The first set of antibodies is functionalized with a dye while the second set with an enzyme; in the presence of hCG, an antibody1-hCG-antibody2 sandwich is formed,[3] which causes the enzyme to react with the dye yielding a visible color change on the test strip. Analogous sensors for organic pollutant detection in natural waters are much more limited, and are restricted to a few antibody-based assays for pesticides. Referred to as Enzyme Linked ImmunoSorbent Assays (ELISAs), these sensors are inexpensive and easy to use, but suffer from false positives and/or overestimation due to interference from analogues and/or sample matrices[4-9]. For instance, one study screened for estrogenic steroids in sheep urine and chicken muscles, and found that the ELISAs showed false

positives in 18.5% of urine samples and 12.6% of muscle samples, while GC-MS indicated no estrogens were present in those samples[4]. In another study[5], an ELISA test kit overestimated the concentration of herbicide atrazine by 49% in finished water samples, potentially due to the presence of oxidants. In a different study[6], an ELISA overestimated the concentration of pharmaceutical carbamazepine by up to 29% in wastewater samples, potentially due to matrix effects and/or analogues. The antibody used in the ELISA was found to have significant cross reactivity with the analogue epoxycarbamazepine (83%). Similarly, an ELISA for the insecticide diazinon was found to have 29% cross reactivity with the analogue diazoxon, and also showed false positives in storm runoff samples due to potential matrix effects[7]. In another case[9], the antibody used in an ELISA for veterinary antibiotic tylosin A had significant cross-reactivity (26-121%) with its analogues, making it unfit to quantify the target contaminant. Also, antibodies must be harvested from animals, so widespread use might result in objections from animal rights groups.

Two emerging methods involve using either RNA or DNA aptamers for pollutant binding. Aptamers are single strands of RNA or DNA that can be selected to bind to a target molecule with high sensitivity and selectivity. They can fold into tertiary structures to form binding pockets for their target (Figure 2.1), and bind to the target through hydrogen bond, electrostatic and hydrophobic interactions[10]. RNA aptamers were identified first, resulting in a wide range of RNA aptamer targets including small organic molecules (e.g., flavin mononucleotide[11], theophylline[12]), proteins (e.g., HIV-1 reverse transcriptase[13], bacteriophage R17 coat protein[14]) and pathogens (e.g., *E. coli*[15], *Salmonella*[16]). DNA aptamers have also been developed for many targets including small organic molecules (e.g., estradiol[17], kanamycin[18], microcystin[19]), proteins (e.g., ricin[20], abrin[21]), pathogens (e.g., *Salmonella*[22], Norovirus[23]) and

even metal ions (e.g., K^{+}[24], As^{5+}[25]). Although RNA aptamers are relatively larger in number, DNA aptamers have advantages given their stability under a wide range of buffer conditions, resistance to base-catalyzed hydrolysis, and ease of selection; therefore, they are the focus of this critical review.

DNA aptamers have been integrated into a number of sensing platforms, e.g., primarily ones that rely on fluorescent or colorimetric signaling molecules, or electrochemical signaling via suppression or enhancement of electron transfer to an electrode surface. These DNA-based sensors are referred to as aptasensors. They have been used to detect organics in tap water[26], lake water[27], wastewater[28-29], synthetic saliva[30], plasma[31], serum[32-33], urine[34] and even whole blood[35], in many cases without sample pre-processing. In some cases[27, 36-40], detection limits as low as 1 fM have been obtained. Aptamer regeneration is possible[28, 41], which allows multiple uses, and aptasensors have been integrated into paper and wax-based[42] microfluidic devices at very low costs ($0.30/sensor)[43].

Companies that commercially develop aptamers (e.g., Aptagen, LLC; BasePair Biotechnologies, Inc.; AptaMatrix, Inc.) provide services that include tuning the sensitivity and structure-switching ability of aptamers. However, there are no commercially available aptasensors for sensing environmentally relevant organic pollutants, including the 53 organic chemicals regulated by the safe drinking water act (SDWA), and the 75 unregulated organic wastewater pollutants detected in 2002 by Kolpin et al in a nationwide survey of contamination in 139 stream locations[1]. Significant concerns over their widespread distribution and persistence remain, due to their potentially negative environmental effects, and possible unknown synergistic modes of action. Therefore, there is a need for low-cost point of use environmental sensors. Aptasensors appear to be a promising option but there are concerns regarding their

implementation, including identifying aptamers that strongly and selectively bind to pollutants of interest, retain their binding properties when integrated into a sensor platform, undergo sufficient conformational change upon binding to activate a sensing mechanism, and are stable over long term storage.

The objectives of this critical review are to 1) identify the state-of-the-art in the field of DNA aptamer selections, 2) evaluate the properties of targets and aptamers that make for sensitive and selective binding and sensing based on 81 aptamers identified in literature 3) determine the primary strengths and weaknesses of alternative sensing platforms in aptasensors for organic pollutant detection from ~200 aptasensors developed, 4) assess the potential for aptasensors to quantify the concentrations of environmentally relevant organic contaminants in natural and treated waters, and 5) provide recommendations for aptasensor development to improve their potential for commercialization. While previous reviews [44-47] provided important insights, they primarily focused on summarizing the state-of-art in aptamer selection and sensor development, and did not quantitatively evaluate and compare the target and aptamer properties that affect binding and sensing, the limits of detection for alternative sensing platforms, and the ability of existing aptasensors to detect environmentally relevant concentrations of target pollutants in the presence of structurally similar analogs that can compete for binding in natural waters. Our approach allows us to critically evaluate the feasibility of aptasensors to serve as a reliable sensing platform for small organic pollutants in natural and treated waters, and to provide recommendations for moving aptasensor development forward to commercialization.

2.3 Selection of DNA Aptamers

Aptamers are single stranded oligonucleotides that have been selected to bind to a target with high sensitivity, and either high selectivity or general selectivity for a class of compounds.

DNA aptamers are typically identified by a process called Systematic Evolution of Ligands by EXponential enrichment (SELEX)[48-49]. Traditionally, a radiolabeled pool of single-stranded DNA (~10^{12}-10^{14} unique sequences), containing a random region of fixed length (typically 20- to 60-mer) flanked by primer binding regions on either side, is used for selections. Selections occur in columns or vials containing a support matrix with or without bound target(s). Typical support matrices are agarose and nitrocellulose, and selections are done in a binding buffer, typically containing monovalent (Na^+, K^+) and divalent (Mg^{2+}, Ca^{2+}) ions for screening the negatively charged phosphate backbone of the DNA and favor folding to enable binding to the target. The random DNA pool in binding buffer is first incubated with only the support matrix to eliminate any non-specific binding sequences. The eluent from this pre-selection step is then exposed to support that has the desired target immobilized on it. Sequences that bind to the target remain on the support, which are then eluted with either a denaturing buffer[23] or with free target in buffer solution[17]. The DNA sequences in the eluent are amplified using PCR. This enriched pool is put through the same cycle until 30-50% of the pool exhibits binding activity to the target (usually after 8-15 rounds)[50]. Binding activity can be monitored by tracking the radiolabeled DNA that is put through the selection cycle.

Additional selection pressures can be applied in later rounds to enhance selectivity. For example, counter-selections can be done by eluting the column with analogues of the target prior to eluting with the desired target to eliminate any sequences that are not selective[51-52]. Alternatively, detection can be broadened; DNA sequences that bind to a class of compounds can be selected by either eluting the support column with a cocktail of compounds or by eluting the column with a different analogue during each successive selection round[53]. Eventually, the pool

is cloned and sequenced, and individual sequences are characterized for their sensitivity and selectivity. An illustrative figure of the selection process is in Appendix A (Figure A.1).

The dissociation constant (K_d) is typically used to quantify the sensitivity of aptamer binding. It is the equilibrium constant of an aptamer as defined by equation 2.1.

$$K_d = \frac{[free\ aptamer][free\ target]}{[aptamer{-}tar \quad complex]} \tag{2.1}$$

A larger value of K_d is associated with weaker binding affinity and inversely a lower value of K_d is associated with better binding affinity. Dissociation constants are typically determined by a method called equilibrium filtration[12], where varying concentrations of aptamer are incubated in binding buffer with a constant concentration of target, which is usually radiolabeled. Upon equilibration, ~50% of the solution is passed through a molecular weight cut-off filter which allows separation of the free target and aptamer-bound target. Upon quantifying and plotting the amount of bound target against the DNA concentration, a curve can be fit through the data to determine the K_d of an aptamer to its target.

The aptamer's binding domain can sometimes be identified by truncation[54-57], mutation[58] and chemical probing methods[17]. Most cases of successful truncation of the aptamer lead to shorter sequences that have the same binding affinity as the parent aptamer[57]. In some cases, mutations and/or truncations can lead to enhanced binding affinity[55, 59] or improved affinity and selectivity[54, 56] (i.e., ratio of aptamer K_d values for target and analogue) since the unwanted nucleotides are eliminated from interacting with the target. Truncation of aptamers reduces synthesis costs and enables easier incorporation of the aptamers into various sensor platforms. Chemical probe compounds include dimethyl sulfate (DMS) and diethyl pyrocarbonate (DEPC)[17, 60-61]. DMS probing involves the methylation of the N7 position of the guanine residues on the DNA. The guanines interacting with the target are not (or less) available for methylation.

On subsequent base-catalyzed cleavage, the guanines interacting with the target are identified by gel electrophoresis and imaging. DEPC works in a similar manner by carbethoxylating the N7 position of adenines, if available, making them sensitive to base-catalyzed cleavage which can be imaged on gels. Some studies report that the concentration and species[51] of divalent ions used in the binding buffer impact the dissociation constant of the aptamer. Hence, these buffer conditions are optimized for subsequent detection purposes where the samples are diluted with optimized buffer.

The SELEX process has been modified in multiple ways either to reduce the number of selection cycles or to improve the efficiency and ease of selections. FluMag SELEX[62] involves the use of fluorescent tagged DNA sequences to monitor binding activity through the rounds of selections instead of conventional radiolabeled sequences. Additionally, magnetic microbeads are used as the support on which the target is immobilized, as these enable easy separation of the bound sequences from the unbound sequences. Capillary Electrophoresis-SELEX (CE-SELEX)[63-64] is another modification where selections are conducted in free solution by employing CE in the separation step. This step helps distinguish the bound sequences from the unbound sequences based on their different migration times; i.e., the size and charge of the aptamer-target complex is different than unbound sequences. Due to the stringency of separation, CE-SELEX requires fewer rounds (2-4 rounds) in order to identify aptamers. However, CE-SELEX is mostly used to isolate aptamers for large targets like proteins[63-64] and in some limited cases for small molecules[65]. Not all small molecules can be easily immobilized on a support. As a result of this, capture-SELEX[66] was developed, where the DNA pool is hybridized onto a support containing complementary DNA sequences. The sequences that bind to the free target in solution are eluted off the support, amplified, and then put through additional cycles until the

desired binding activity is attained. Graphene Oxide SELEX (GO-SELEX)[67-72] is another way to overcome the necessity of immobilizing small molecules on a surface. In this method, the DNA pool is incubated with the target in solution followed by exposure to GO sheets. DNA that is not involved in binding with the target is adsorbed onto GO through π-π stacking. Bound sequences are separated from the GO-bound DNA by centrifugation, amplified and then put through additional rounds.

In general, the aptamer selection process is time-consuming, but it can be tailored to incorporate desirable characteristics such as selectivity and structure-switching upon binding. However, there are no definitive methods to improve sensitivity of an aptamer towards its target, and there is always randomness, which affects the number of cycles to obtain strongly binding aptamers and the final sensitivity and selectivity of the selected aptamer. A trait of selected aptamers is that they usually only maintain their binding affinity in buffer that matches or is close to that used for selection, so samples must be diluted in buffer for detection in natural matrices. This is because the buffer contains cations, which aid in folding of the negatively charged DNA aptamer in order to adopt a favorable conformation while binding to the target. Also, DNA aptamers are typically selected independent of their incorporation into sensing platforms, so selected aptamer characteristics may not be ideal for optimal aptasensor performance.

2.4 Targets for DNA Aptamers

A complete list of the 81 DNA aptamers for small organics considered in this chapter is listed in Table A.1 (Appendix A). The first DNA aptamer was identified in 1992 for an azo dye (reactive green 19, MW 1419Da), and the dissociation constant (K_d) is 33 μM[73]. The smallest molecule for which a DNA aptamer has been identified is ethanolamine (MW 61Da), with a K_d

of 6 nM[74]. However, most of the small-molecule aptamers have larger dissociation constants, ranging from high nanomolar to low micromolar range. For some targets, like L-arginine and L-argininamide, the K_d values lie in the millimolar range (K_d arginine = 2.5 mM, K_d argininamide = 0.25 mM[75]). This could potentially be because these aptamers were among the first to be identified when selection of aptamers by SELEX was not optimized. This is supported by the plot of dissociation constants for small molecules versus the year of publication in Figure A.2, indicating that "poor binders" were primarily identified before 2005, and after this the K_ds are significantly improved. One likely reason for this trend is that >60% of the studies through 2005 do not incorporate negative/counter selections, while over 90% of those after 2005 do.

Aptamers for small molecules in different molecular weight (MW) categories were grouped and their K_d values are plotted versus molecular weight in Figure 2.2. Independent-sample t-tests were conducted on the logK_d values for different MW groups and a p-value <0.05 (alpha value) was used to identify a statistical difference between any two groups[76]. In addition to statistical significance, Cohen's d values were used to compare the effect size between different MW groups. A d-value $\geq$ 0.8 is considered a visibly large effect, while a value less than this and $\geq$0.5 is considered a medium effect[77]. From Figure 2.2, logK_d values are statistically smaller (p-values <0.05) for the largest targets, i.e., proteins, relative to those for small (<200Da) organic molecules, all medium (200-1700Da) organic molecules combined, as well as all small and medium organic molecules combined (<1700Da), and the differences are considered large (d-values >0.8, data not shown). The logK_d values for the proteins are also statistically smaller than those for each of the small and medium organic MW groups (p-value < 0.05) and the effect size is large (d value >0.8), except the 400-500Da MW group (p value > 0.05, d value < 0.8).

None of the logK_d values for individual small or medium MW groups are statistically different from each other (p-value >0.05, data not shown).

Smaller organic molecules typically have a lower number of unique functional groups for the aptamer to recognize and bind to, potentially resulting in lower binding affinity. Unique binding groups promote specific hydrogen bonding, electrostatic, Van der Waals, and/or entropic interactions[10, 78]; the lack of these binding groups might explain the weaker affinity for small and medium molecules <1700Da, and the higher affinity for proteins. The greater the number of unique interactions between an aptamer and its target also likely contributes to improved selectivity of the aptamer. For example, the aptamer for human immunoglobulin E (IgE)[79] is at least 1000 times more selective towards its target when compared to mouse and rat IgE, and at least 2000 times more selective over human IgG. In contrast, small molecule aptamers identified in two studies[17, 80] for estradiol show relatively poor selectivity (~2-100 times) compared to those for the analogues testosterone and progesterone[81].

Apart from MW, thirteen additional target properties, i.e., polarizability, molar volume, log of Henry's constant ($logK_H$), polar surface area (PSA), lipophilicity/hydrophilicity (based on four partition coefficients), enthalpy of vaporization, entropy of vaporization, number of freely rotating bonds, number of hydrogen bond acceptors, and number of hydrogen bond donors were individually compared to logK_d values. Lipophilicity/hydrophilicity was based on the octanol-water partition coefficient ($logK_{ow}$ from EPI Suite or logP from ACD labs), a pH-dependent octanol-water distribution coefficient (logD at pH 7.4) and an organic carbon-water partition coefficient ($logK_{oc}$). Weakly negative linear proportionality constants, associated with p-values <0.05, were identified between logK_d and either $logK_{oc}$ or logD, and $logK_{oc}$ and logD are correlated to each other (correlation coefficient=0.85); both one-variable regression models

indicate a more lipophilic/hydrophobic target molecule would have a lower K_d value. The aptamer properties of length and free energy of folding were also individually compared to logK_d values. A weakly negative linear proportionality constant was identified between logK_d and length of aptamer, suggesting that longer aptamers can form more specific binding pockets for the target.

Multivariable linear regressions were also conducted using logK_d as the dependent variable and combinations of the independent target and aptamer properties noted above. Variables whose correlation coefficients were $\geq$ 0.7 were considered mutually correlated and mutually correlated variables were not used simultaneously in the same regression model. This resulted in ~1200 models tested, varying from two to seven independent variables. Among these models, only six two-variable models showed a relationship (p-values <0.05) to logK_d. Four two-variable models that incorporate molecular weight (MW) and either number of hydrogen bond donors, PSA, logK_H or logD were found to have a significant (p-value<0.05) but weak relationship to log K_d, and all four of these parameters (i.e., number of hydrogen bond donors, PSA, logK_H and logD) are mutually correlated (correlation coefficients >0.7). A negative proportionality constant for MW in all of these models was found. The regression models show low, positive proportionality constants for PSA and number of hydrogen bond donors, suggesting that more hydrophobic targets, with lower number of hydrogen bond donors or less polar surface area, yield better binding aptamers. They also show low, negative proportionality constants for logK_H and logD, suggesting that more lipophilic/hydrophobic targets yield better binding aptamers. Tabulated p-values and proportionality constants for all models (Table A.3) as well as plots of logK_d versus MW and either number of hydrogen bond donors or PSA are in Figure A.3 in Appendix A. The fifth and sixth two-variable models showed a relationship (p-value < 0.05)

of log K_d to logD and either enthalpy or entropy of vaporization. The logD proportionality constant is weakly negative in both of these models, and the enthalpy and entropy of vaporization proportionality constants are weakly to moderately negative, respectively. These results are consistent with hydrophobic targets binding more strongly to DNA aptamers. None of the other tested models (varying from two to seven independent variables) showed a correlation with logK_d. Based on the single and two-variable regression models, the hydrophobicity/lipophilicity of organic molecules is the dominant characteristic that affects binding of organic molecules to DNA aptamers.

2.5 Sensing Platforms for Aptasensors

A wide range of sensing platforms has been used to make aptasensors. The only commercially available ones are for heavy metal ions (e.g., lead, mercury, cadmium) in water, and are manufactured by a company named ANDalyze. They employ catalytic DNA coupled with a fluorescence-based platform ($8/test), and can be operated using a hand-held fluorimeter. In the literature, colorimetric, fluorescence, and electrochemical platforms are most commonly used in conjunction with aptamers to make aptasensors. Other platforms include Surface-Enhanced Raman Spectroscopy (SERS), quartz crystal microbalance, cantilever and luminescence based platforms[82]. In this section, the three most common platforms, i.e., colorimetric, fluorescence, and electrochemical are discussed.

Colorimetric Aptasensors

Colorimetric aptasensors are visual in nature and typically involve the use of gold nanoparticles (AuNPs)[83-87], which are red in color when dispersed in solution. In most sensors[86-87], the electropositive amino groups of the bases on the DNA aptamer non-covalently bind to the negatively charged AuNPs, which stabilize the AuNPs in the presence of high salt concentrations

(see Figure 2.3A). Upon introduction of the target, the DNA aptamer preferentially binds to the target, leaving the AuNPs bare and susceptible to aggregation, which causes a blue shift. The extent of the blue shift, quantified by a ratio of absorbance at ~620 nm to ~520 nm ($\sim A_{620}/A_{520}$)[88-90], is correlated to the concentration of the target. In a few cases[83-84], a reactive chromogenic agent like tetramethylbenzidine (TMB) is used in conjunction with H_2O_2. This chemical reacts on the surface of AuNPs, and serves as a catalyst to promote peroxidase-like activity. Upon binding of the DNA to the target, the surface of the AuNPs is made available to catalyze the oxidation of colorless TMB to form TMB diimine, which is blue in color. Therefore, the color of the solution changes from red (dispersed AuNPs) to purplish-blue, which is then correlated to the target concentration. In other cases[85], a thiolated aptamer is covalently bound to AuNPs. A secondary sequence complementary to two different segments of the aptamer holds the aptamer-bound AuNPs together, making the solution blue in color. Upon introducing the target to this construct, the aptamers preferentially bind to the target, dispersing the AuNPs in solution, and leading to a red shift.

Several AuNP-based aptasensors have been successfully tested in matrices different from binding buffers (~67% of those listed in Table A.4), including synthetic saliva, serum, tap water, lake water, wastewater, milk and soil samples. However, AuNP-based sensors are dependent on salt-induced aggregation, which seems to make them more susceptible to interference by environmental matrices. Natural matrices are typically diluted in buffer prior to sensing, so only matrices with high salt concentrations, particularly divalent ions, pose a problem.

Fluorescence-based Sensors

Fluorescence-based aptasensors require a fluorophore and quencher; the former is typically attached to one terminus of the aptamer, and a quencher to the other[34]. Alternatively, a

surface (on which the fluorophore-labeled aptamer can be adsorbed when in an unbound state such as a graphene oxide sheet) behaves as a quencher[91]. In some other cases[92], the quencher is attached to a complementary DNA sequence (cDNA) which gets unbound from the aptamer upon target binding. When the fluorophore and quencher are spatially apart, the fluorescence signal is high. Upon binding of the aptamer to the target, the change in conformation of the aptamer causes the fluorophore and quencher to approach each other, resulting in a loss of fluorescence (Figure 2.3B) – these are signal-off sensors; this loss of fluorescence signal can be correlated to the concentration of the target. Alternatively, the initial conformation of the aptamer could have the fluorophore and quencher close to each other resulting in low fluorescence. Upon binding to the target, the aptamer's change in conformation could separate the fluorophore and quencher resulting in a higher fluorescence signal (signal-on sensors). The latter approach is typical of sensors that use cDNA sequences that carry the quencher.

Like colorimetric-based aptasensors, fluorescence-based aptasensors (~90% of those listed in Table A.4) have been successfully tested in a wide variety of matrices including tap water, lake water, river water, wastewater, maize sample extracts, soil sample extracts and human serum. Challenges include identifying the right length and position of the cDNA, or the exact location of the fluorophore and quencher on the aptamer, in order to gain maximum signal change upon binding. This could be particularly tedious for long aptamers without prior knowledge of secondary and/or tertiary structures. Moreover, labeling aptamers with fluorophores and/or quenchers increases the cost of synthesis.

Electrochemical Sensors

Electrochemical sensors typically require immobilization of the aptamer on an electrode with either an exogenous[93-94] or endogenous[95] redox reporter. The binding of the aptamer to the

target causes a change in conformation of the aptamer on the electrode surface, resulting in a change in the surface resistance and current at a fixed potential (Figure 2.3C). This change in current can be correlated to the concentration of the target. In some cases, the surface of the electrode is modified with nanosheets and/or nanoparticles, which adds complexity to synthesis but aids lowering limits of detections (LODs). Electrochemical sensors could be signal-on or signal-off, depending on the conformation change and the type of reporter used. Most electrochemical sensors are signal-off sensors, since the aptamer adopts a more compact conformation upon binding to the target, making the electrode less accessible to exogenous reporters. For example, the thrombin binding aptamer folds into a more compact conformation, which involves the formation of a G-quartet upon binding to thrombin[96]. This makes approach of an exogenous redox reporter like ferrocyanide/ferricyanide to an electrode surface more difficult, and reduces the extent of oxidation/reduction at a given potential.

Electrochemical sensors (~80% of those electrochemical sensors listed in Table A.4) have also been successfully tested in a wide range of matrices – water samples, milk, maize extracts, wine, human serum and blood. However, inadequate conformational change of such sensors upon binding can lead to poor sensitivity, as in the case of an immunoglobulin E aptasensor[97].

Comparison of Sensor Platforms

Limits of detection for aptasensors for all targets (see Table A.4) for colorimetric, fluorescent, and electrochemical detectors are shown in Figure 2.4. In general, colorimetric and fluorescent sensors have poorer limits of detection compared to electrochemical sensors (p-value $<<0.05$, d-value >0.8). In experiments performed by the authors, extensive (40-98%) non-specific adsorption of two small organics (i.e., estradiol and ethynylestradiol) to the surface of

citrate-capped AuNPs was observed (Figure A.4). Colorimetric sensors use AuNPs, and nonspecific binding to Au may interfere with their sensitivity. Colorimetric and fluorescent aptasensors are both based on optical detection, and are prone to interference from colored or turbid samples. Additionally, fluorescent sensor aptamers need to be labeled, which increases their complexity and cost.

Electrochemical aptasensors fare best amongst the three platforms (t-test p-values $<<0.05$ and d-values > 0.8). This trend generally holds even when compared across three different molecular weight categories (Figure A.5). They have the lowest limits of detection and can be reused in some cases upon regenerating the electrode surface[58, 98]. However, they require instrumentation for their functioning (eg. potentiostats, power source). Electrochemical detection often involves the immobilization of aptamers onto electrodes, which can cause reduction or complete loss in the binding affinity of the aptamer, rendering the sensor ineffective. Nonspecific adsorption of target analytes to gold electrodes can also reduce sensitivity. Electrochemical sensors with the lowest LODs mostly involve complex fabrication steps that include more expensive components like nanoparticles and polymer films. Additionally, some reports indicate that exogenous electroactive reporters like ferri/ferrocyanide can lead to severe alteration of the electrode due to polymerization and subsequent corrosion of electrodes[99].

An aptasensor's LOD is impacted by the inherent affinity of the aptamer to the target as well as the sensitivity of the sensor platform employed. The relationship between K_ds and LODs was evaluated (Figure 2.5), and it was found that a lower K_d (higher binding affinity) yields lower LODs (more sensitive sensors). A linear regression analysis between the logarithms of K_d and LOD yielded a positive value for the slope (+1.01) with a p-value $<10^{-9}$ for the slope indicating >99.99% confidence in the correlation.

2.6 Aptasensors for Detecting Environmentally Relevant Contaminants

The EPA mandates the regulation of certain organic chemicals in drinking water. Of the 53 organic chemicals in the national primary drinking water regulations, aptamers have been developed in research studies for 6 compounds, namely carbofuran[100], diethylhexyl phthalate (DEHP)[101], polychlorinated biphenyls (PCBs)[102], chlorpyrifos[103], atrazine[104] and pentachlorophenol[105]. Aptasensors have been successfully identified for 3 of the 6 compounds – one each for carbofuran[100] and DEHP[101], and 7 sensors for two congeners of PCBs (i.e. PCB77 and PCB72)[26, 102, 106-110]. The limit of quantification (LOQ) of the sensors for carbofuran and DEHP are below the compounds' maximum contaminant limits (MCL), making these sensors potentially viable options for environmental detection. However, the DEHP aptamer was identified by conducting selections using dibutyl phthalate (DBP) and therefore has poor selectivity. The DEHP aptamer binds to other phthalic acid esters such as DBP and butyl benzyl phthalate (BBP) with similar affinity (i.e. <1.5-fold selectivity). Additionally, the DEHP sensor has not been tested in natural matrices.

In contrast, the carbofuran sensor[100] exhibits good selectivity (ratio of signal change for target to that of analogue) against many small organics, and was tested in fruit and vegetable samples. The sensor readings were reproducible and stable over a period of 10 days. However, construction of the sensor involves AuNP-modified electrodes with carbon-dot modified thiolated DNA aptamers, and electrochemiluminescence. The latter is an instrument-heavy technique, making it unfavorable for use in the field. Lastly, 2 of the 5 PCB77 sensors could be used to detect this organic chemical at or below the MCL. However, there are 209 PCB congeners, and these aptasensors[26, 102] are shown to have partial affinity (30-50% sensor signal change compared to parent target) for 4 of the 9 congeners tested, indicating poor selectivity.

More useful for environmental detection would be a general use PCB aptamer that can detect total PCB concentrations, or a larger subset of PCBs.

Among other organics detected in the nation's surface waters by Kolpin et al[1], aptasensors have been developed in research studies for lincomycin, oxytetracycline (OTC), sulfadimethoxine (SDM), tetracycline (TET), codeine, bisphenol A (BPA), estradiol (E2) and progesterone. LOQs for OTC, SDM and progesterone sensors are above environmentally relevant concentrations (Figure 2.6), making them less useful in natural waters. LOQ for some E2, TET and BPA sensors, and the lincomycin sensor, are below environmentally relevant concentrations. However, the construction of these sensors with favorable LOQs usually involves nanomaterials and other instrumentation-heavy components. Most such sensors have not been tested for robustness, reproducibility and stability.

Selectivity of aptasensors is another key parameter that requires further consideration. Ciprofloxacin and tetracycline aptamers used in the sensors reported in Table A.4 were selected for a group of antibiotics, quinolones and tetracyclines, respectively. Hence, these sensors are not very selective against analogues. For instance, the ciprofloxacin sensor[111] bound with similar affinity (~80% signal change) to equivalent concentrations of ofloxacin and levofloxacin. The tetracycline aptamer bound to an equivalent concentration of doxycycline with 40% signal change in one sensor[112], while another sensor showed 20% signal change with OTC[113]. This is concerning because the median environmental concentration of OTC is ~3 times that of tetracycline[1]. Similarly, an E2 sensor[28] showed 20% signal change in the presence of an equivalent concentration of carbaryl, 4-n-nonylphenol or estriol. Although one can only speculate the synergistic effects of these analogues on the selectivity of an aptasensor, the median environmental concentrations of the aforementioned analogues are altogether ~100 times

the median concentration of E2. Moreover, other closely related analogues such as estrone, ethynylestradiol, BPA and progesterone all together are ~40 times the concentration of E2[1]. These factors will likely result in false positives or elevated signal changes[114], falsely indicating higher concentrations reported by the sensor. Additionally, because of non-specific interactions through matrix interference, the LODs of sensors are higher in natural matrices compared to that in buffered pure water. With a ciprofloxacin sensor[32], the LOD increased from 1.2 nM in buffered water to 2.6 nM in serum samples and 3.2 nM in milk samples. In the case of a BPA sensor[34], the LOD increased from 0.01 pg/mL in water to 0.1 pg/mL in urine.

2.7 Perspectives and Future Development

Literature studies on aptamers and aptasensors thus far show promise regarding their ability to sense targets in a wide range of matrices with minimal sample pretreatment. However, the number of environmentally relevant targets for developed aptasensors is a small fraction of the many contaminants present in natural waters. In many cases, the aptasensor is not sensitive enough to detect contaminants at concentrations present in natural waters, and in other cases the construction of the sensor involves complex fabrication steps. Moreover, the selectivity of the sensors in natural matrices at environmentally relevant concentrations has not been widely evaluated, but is often relatively poor given the concentrations of analogues in natural waters. Aptasensors for small organics that appear to have sufficient sensitivity and selectivity still have to go through commercialization challenges, which include portability, ease-of-use, stability, robustness, reproducibility and most importantly, cost of production.

Aptamers broke into the therapeutics market in 2004 with pegaptanib (brand name Macugen), which is a drug containing a modified RNA aptamer that is used to treat neo-vascular age-related macular degeneration. Upon binding of the aptamer to a key protein [vascular

endothelial growth factor (VEGF)] in the disease-causing pathway, VEGF is rendered inactive. However, this drug was soon replaced by an antibody (i.e., protein)-based drug, likely due to the difference in cost ($800/dose vs $50/dose). Besides cost, another concern is that aptamers may not be as sensitive or selective as proteins. The lowest LODs of lab-based aptasensors, commercially available ELISAs, laboratory-based (i.e., not commercial) ELISAs, and immunosensors (i.e., proteins coupled with sensing platforms) for 11 small organic pollutants are plotted in Figure 2.7. Aptasensors appear to have an edge in terms of sensitivity for 6 of the 11 target pollutants, and can detect median environmental concentrations of 8 of the 11 compounds. Their sensitivity ranges from ~50 to 2300-fold greater for four targets, and 10^7-fold greater for two targets (i.e., TET and OTC). Both TET and OTC sensors[115-116] that showed attomolar sensitivity (LOD ~10^{-18} M) employ methods like surface plasmon resonance and Raman spectroscopy, which require expensive instrumentation. The commercially available ELISAs have LODs that enable detection of median environmental concentrations of 7 of the 11 compounds. Immunosensors possess LODs that enable detection of 10 compounds. The results suggest that neither aptamers nor protein-based sensors hold a definitive edge in terms of sensitivity. Also, cross reactivity with analogue compounds, potential matrix effects, and false positives for both approaches suggest that neither holds a definitive edge in terms of selectivity.

Commercially available aptasensors for environmentally relevant organic pollutants are yet to be realized. New approaches and/or efforts are needed to meet the grand challenge of developing aptamers for such targets that are highly sensitive and selective in both the free and surface bound states, and that undergo sufficient conformation change upon target binding either to alter agglomeration of AuNPs, or to unbind from a complementary DNA strand, or to increase resistance at an electrode surface. The current selection approach typically makes use of free

(i.e., unbound) aptamers. I recommend performing selection of aptamers in a state that reflects their use in the desired aptasensor platform. For example, aptamers can be selected when bound to surfaces or hybridized to cDNA, as in the case for capture-SELEX or GO-SELEX, respectively. These approaches also increase the likelihood of selecting aptamers with larger conformational change upon binding. I also recommend applying more stringent selection pressures, such as lowering concentrations of the target during elution, in order to enhance the binding affinity of aptamers. I further recommend incorporating counter-selections against close analogues of the target in order to improve aptasensor selectivity. Additional challenges for aptasensors are improving robustness, stability, reusability and/or reproducibility. While these have been addressed for a handful of metal sensing aptasensors, they will need to be addressed anew for any commercially viable aptasensors that emerge for environmental organic pollutants. Hence, aptasensors for environmental organic pollutants require additional innovation and investment before commercialization is realized.

2.8 Figures

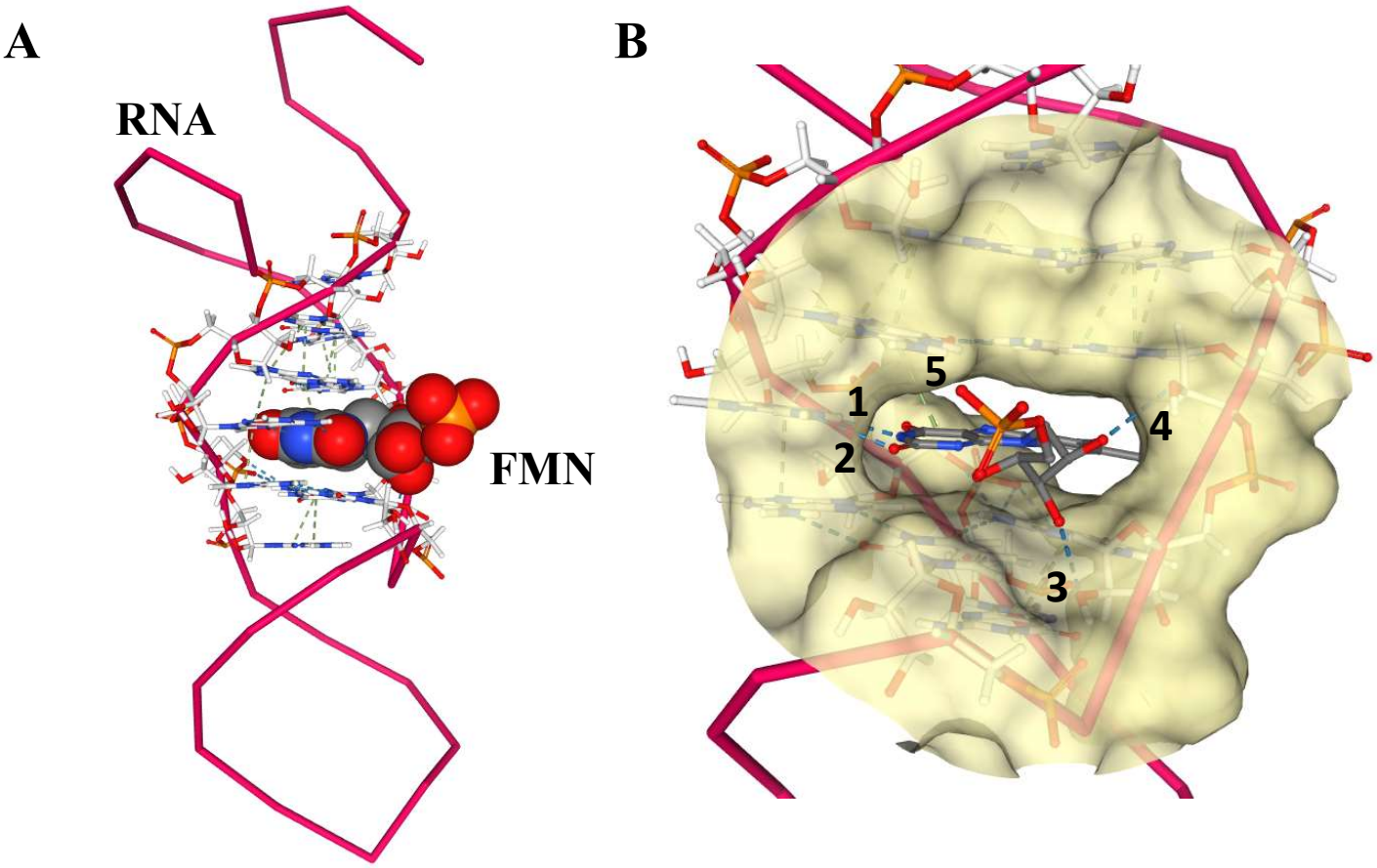

Figure 2.1. NMR structure of an RNA aptamer that binds to Flavin Mononucleotide (FMN)[117]. (A) Full NMR structure of aptamer-ligand complex. RNA backbone is depicted as a pink line with the binding pocket-bases shown in ball-and-stick format. The target (FMN) is shown in space-fill format and fits into the binding pocket. (B) Magnified image of the binding pocket of the aptamer from a different angle. FMN is depicted in the ball-and-stick format while part of the RNA's binding pocket is depicted as a surface. Four hydrogen bonds (labels 1-4) between the FMN and RNA are shown as blue bonds, while the one π-π hydrophobic stacking (label 5) is depicted as a green bond. The images were created from the protein data bank (filename: FMN1) using the NGL Viewer[118-119].

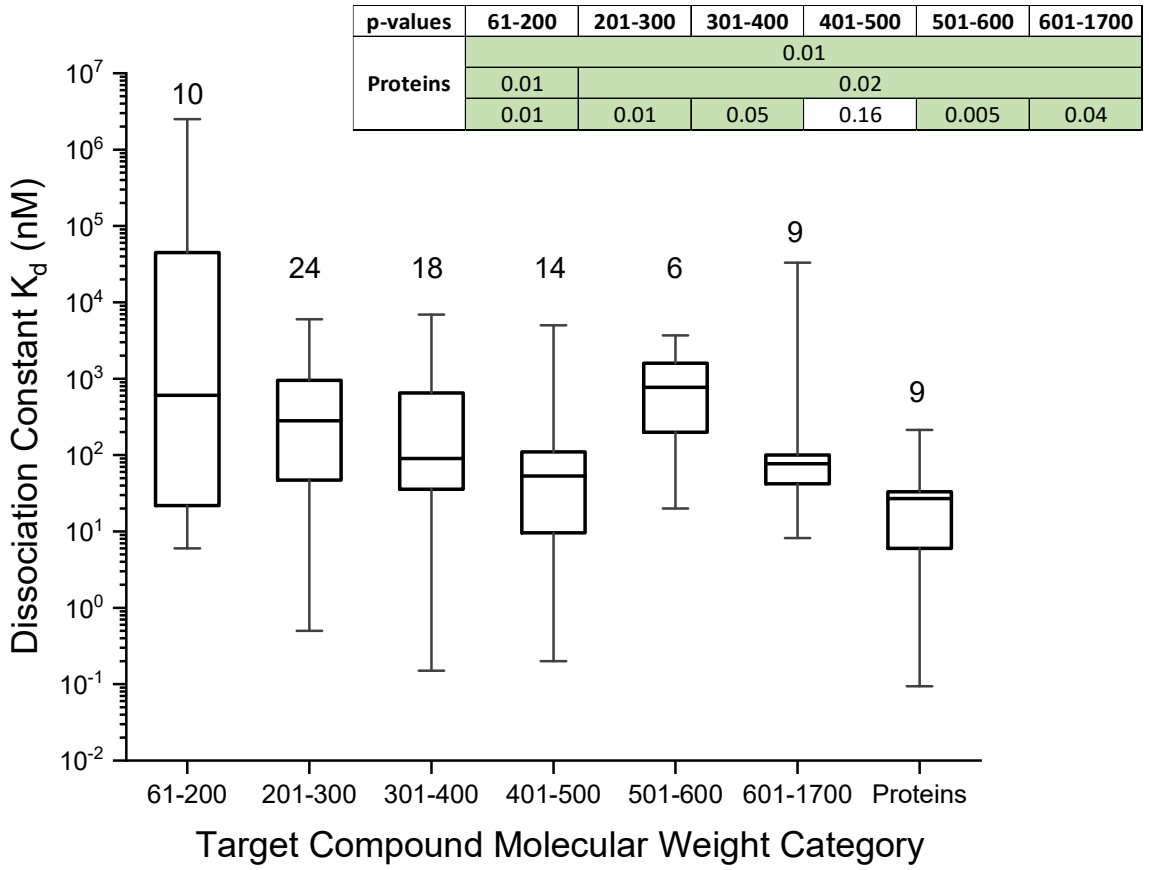

Figure 2.2. Box plot of the lowest dissociation constants for different molecular weight categories. The number against each box indicates the number of samples used to create each box. Independent samples t-tests were conducted between small molecules (<1700Da), and large molecules (proteins). The data for this plot is listed in Tables A1 and A2 in Appendix A derived from references [17-18, 20-21, 51-52, 57-58, 64-66, 68-75, 79, 101-102, 104, 120-182].

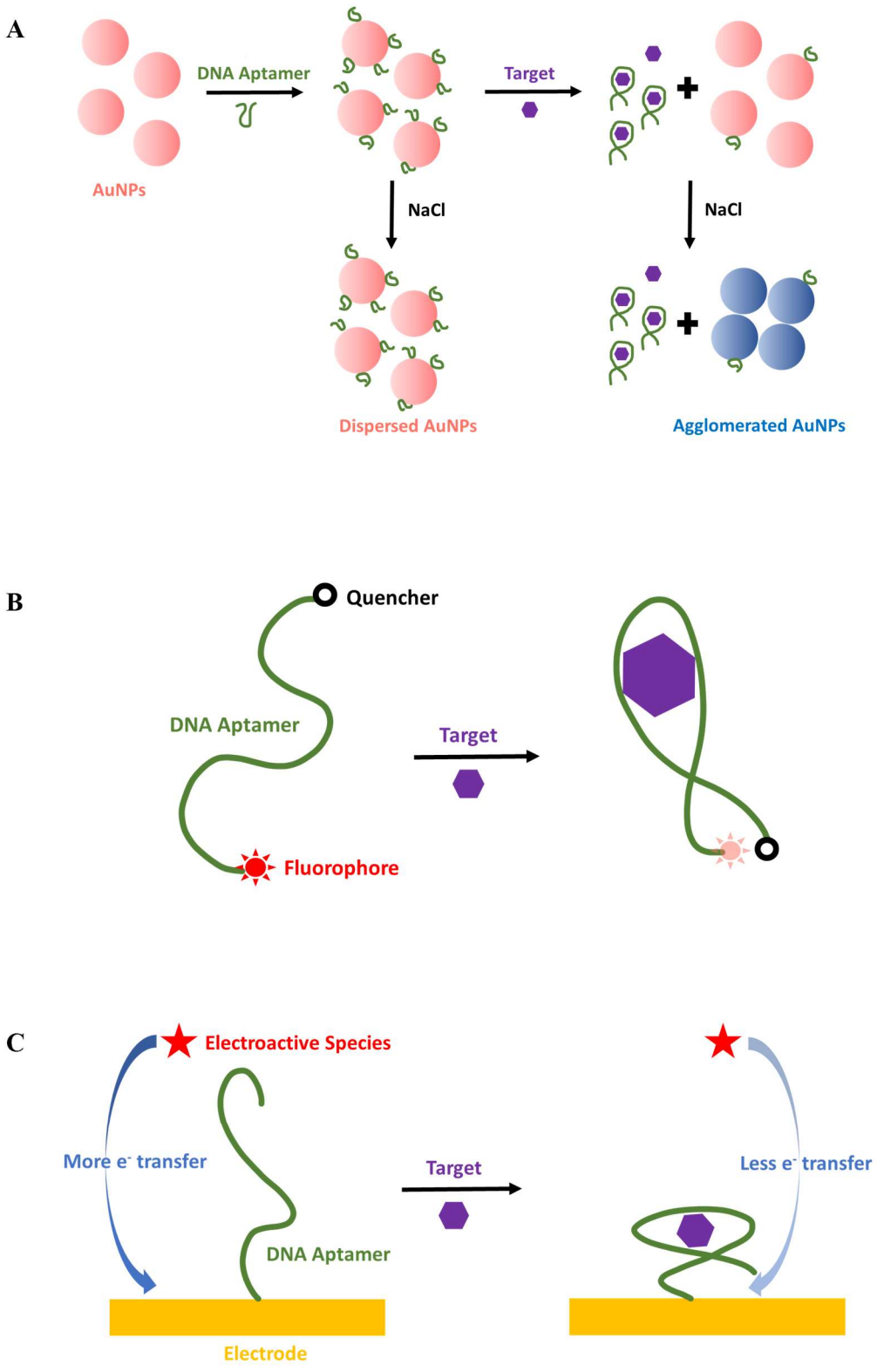

Figure 2.3. Conceptual models of a (A) colorimetric sensor (B) fluorescence-based sensor and (C) electrochemical sensor

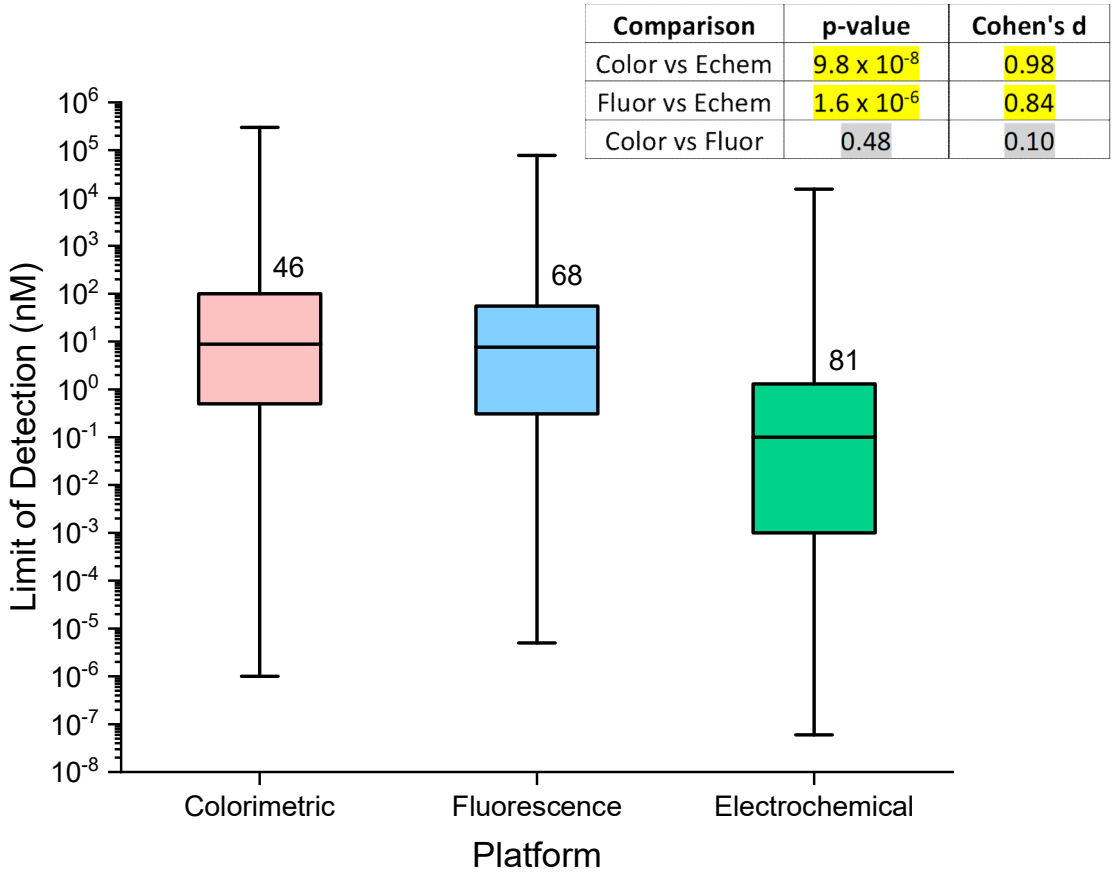

Figure 2.4. Box plot of limits of detection of aptasensors employing colorimetric, fluorescence or electrochemical platforms. The p-value is obtained by comparing any two platforms using an independent samples t-test while the effect size is computed using the Cohen's d-value. The number against each box indicates the number of samples used to create each box. The data used for this plot is listed in Table A.4 and derived from references [18, 26-27, 29-34, 36-40, 54, 83-87, 90-91, 93-95, 98, 100-103, 109-110, 112-114, 128, 150, 177, 183-314]

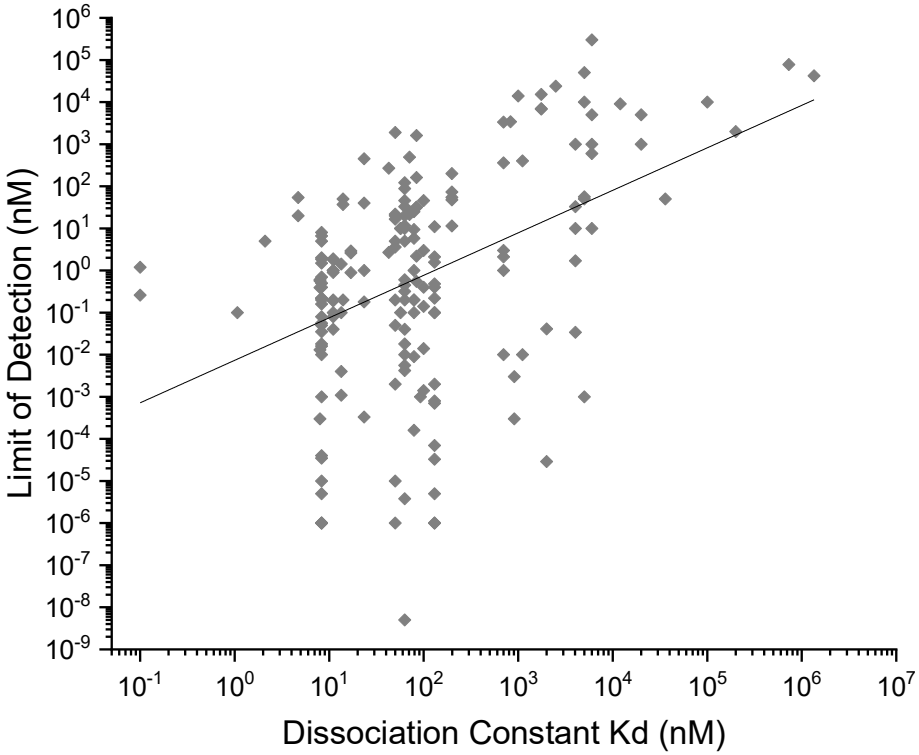

Figure 2.5. DNA aptasensor limit of detection (in nM) versus DNA aptamer dissociation constant K_d (in nM) for small organic molecules. A linear regression on the log values of LOD and K_d yielded the following parameters: $R^2 = 0.19$ and slope = 1.01 ($p < 10^{-9}$).The data for this plot was derived from the following references [18, 26-34, 36-40, 58, 83-87, 90-91, 93-95, 98, 102, 106-108, 112-114, 116, 128, 141, 145, 150, 154, 163-164, 177-178, 183-189, 194-195, 197-200, 204-212, 214-225, 227-260, 262-264, 266-276, 278-290, 292-293, 296, 298-327]

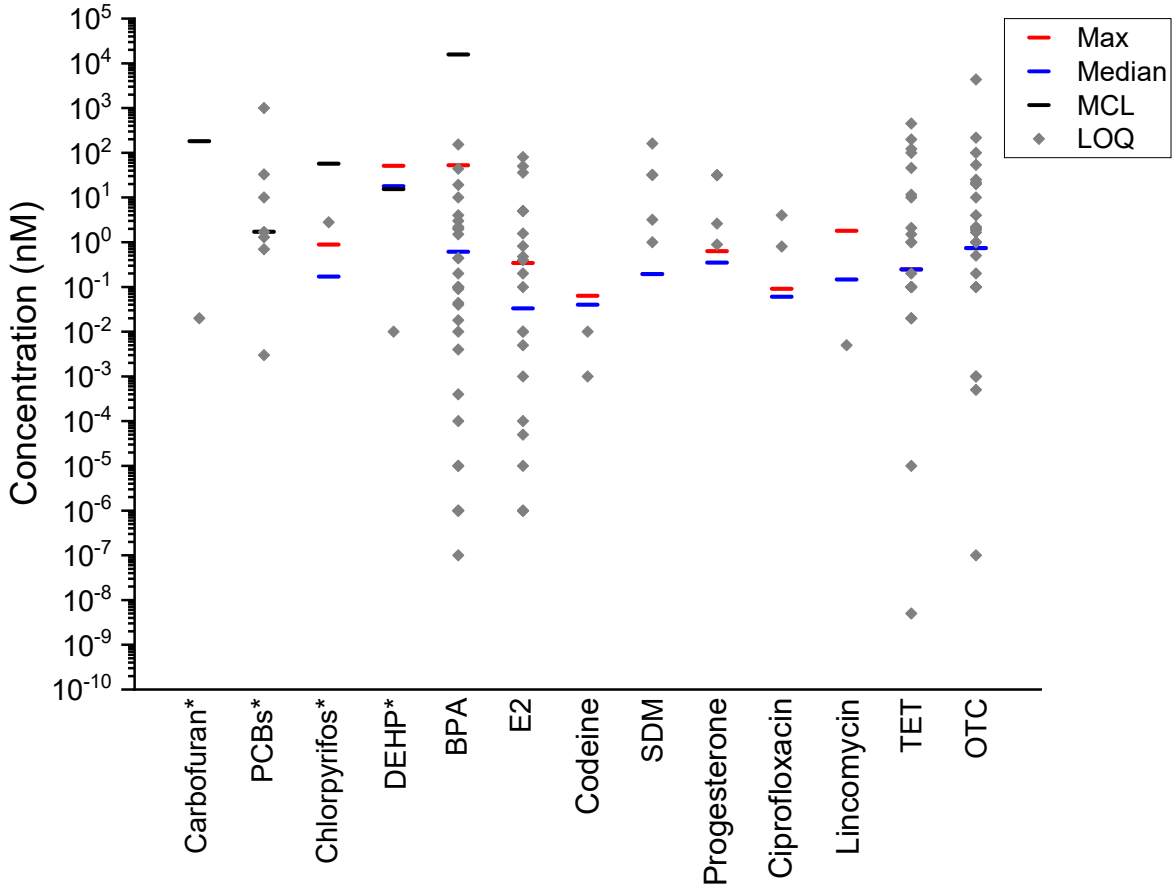

Figure 2.6. Median and maximum concentrations of compounds detected in surface waters of the US[1] plotted alongside the lower limit of the linear range (or limit of quantification) of various aptasensors developed for these compounds. Compounds with the * sign are regulated per the Safe Drinking Water Act. The data for this plot was derived from the following references [26-30, 32-34, 36-40, 54, 58, 83-84, 90-91, 93-94, 98, 100-103, 106-110, 112-116, 128, 145, 154, 163-164, 178, 204-222, 228-238, 241, 250-254, 265-297, 315-319, 322-324, 328]

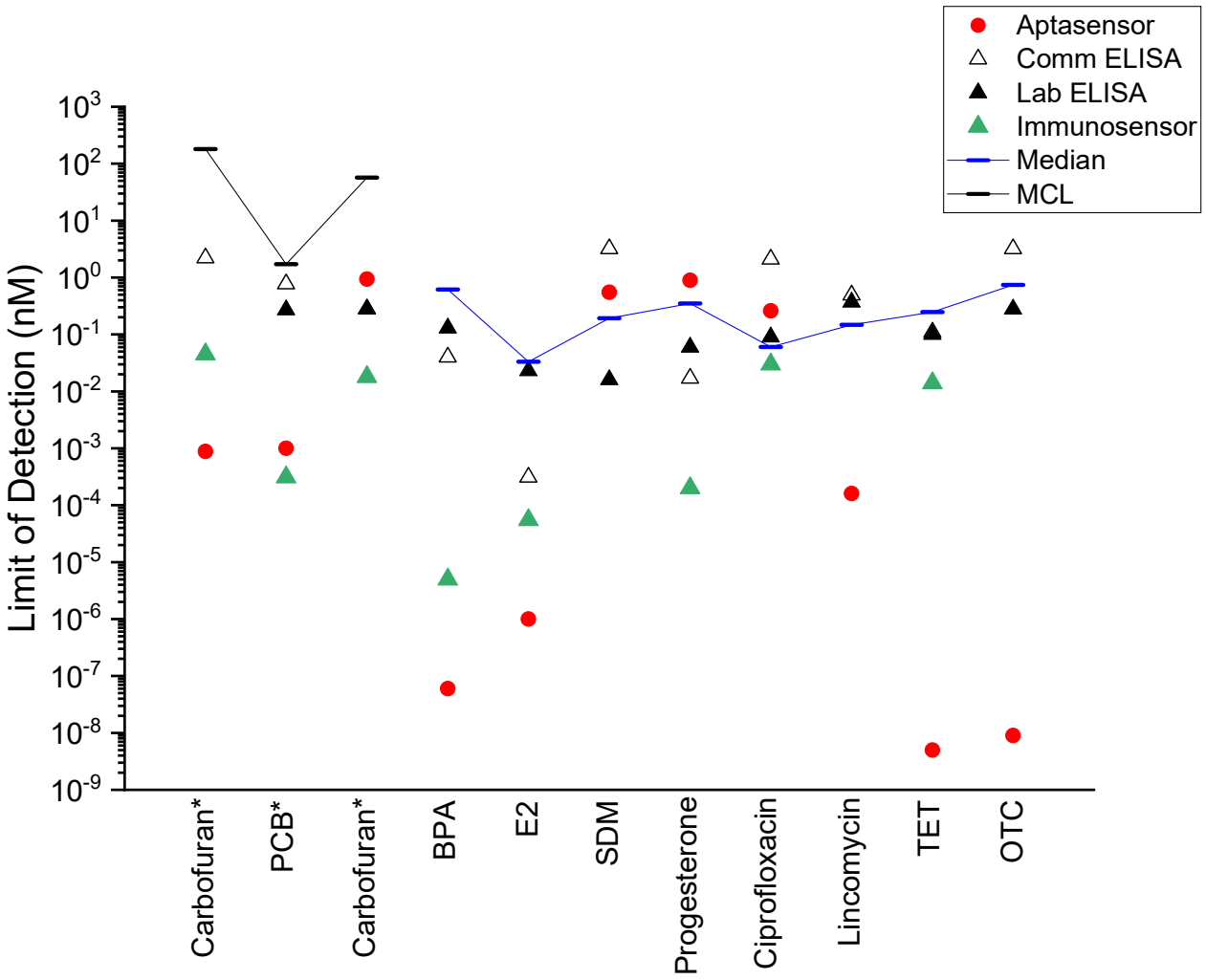

Figure 2.7. Lowest LODs of commercial ELISAs, lab based ELISAs, immunosensors and aptasensors for environmentally relevant contaminants. Compounds with the * sign are regulated in accordance with the Safe Drinking Water Act for which MCL values are considered instead of median environmental concentrations. The MCL and median environmental concentrations [1] are connected with a line to help identify sensors that can be used for environmental sensing. The LODs for sensors are derived from the following references[27, 33, 39-40, 100, 103, 110, 115-116, 213, 252, 254, 265, 329-358]

2.9 REFERENCES

1. Kolpin, D. W.; Furlong, E. T.; Meyer, M. T.; Thurman, E. M.; Zaugg, S. D.; Barber, L. B.; Buxton, H. T., Pharmaceuticals, Hormones, and Other Organic Wastewater Contaminants in U.S. Streams, 1999−2000: A National Reconnaissance. *Environmental Science & Technology* **2002,** *36* (6), 1202-1211.
2. Bradley, P. M.; Journey, C. A.; Romanok, K. M.; Barber, L. B.; Buxton, H. T.; Foreman, W. T.; Furlong, E. T.; Glassmeyer, S. T.; Hladik, M. L.; Iwanowicz, L. R.; Jones, D. K.; Kolpin, D. W.; Kuivila, K. M.; Loftin, K. A.; Mills, M. A.; Meyer, M. T.; Orlando, J. L.; Reilly, T. J.; Smalling, K. L.; Villeneuve, D. L., Expanded Target-Chemical Analysis Reveals Extensive Mixed-Organic-Contaminant Exposure in U.S. Streams. *Environmental Science & Technology* **2017,** *51* (9), 4792-4802.
3. Wada, H. G.; Danisch, R. J.; Baxter, S. R.; Federici, M. M.; Fraser, R. C.; Brownmiller, L. J.; Lankford, J. C., Enzyme immunoassay of the glycoprotein tropic hormones--choriogonadotropin, lutropin, thyrotropin--with solid-phase monoclonal antibody for the alpha-subunit and enzyme-coupled monoclonal antibody specific for the beta-subunit. *Clinical Chemistry* **1982,** *28* (9), 1862.
4. Sawaya, W. N.; Lone, K. P.; Husain, A.; Dashti, B.; Al-Zenki, S., Screening for estrogenic steroids in sheep and chicken by the application of enzyme-linked immunosorbent assay and a comparison with analysis by gas chromatography–mass spectrometry. *Food Chemistry* **1998,** *63* (4), 563-569.
5. Graziano, N.; McGuire, M. J.; Roberson, A.; Adams, C.; Jiang, H.; Blute, N., 2004 National Atrazine Occurrence Monitoring Program Using the Abraxis ELISA Method. *Environmental Science & Technology* **2006,** *40* (4), 1163-1171.
6. Calisto, V.; Bahlmann, A.; Schneider, R. J.; Esteves, V. I., Application of an ELISA to the quantification of carbamazepine in ground, surface and wastewaters and validation with LC–MS/MS. *Chemosphere* **2011,** *84* (11), 1708-1715.
7. Sullivan, J. J.; Goh, K. S., Evaluation and Validation of a Commercial ELISA for Diazinon in Surface Waters. *Journal of Agricultural and Food Chemistry* **2000,** *48* (9), 4071-4078.
8. Byer, J. D.; Struger, J.; Klawunn, P.; Todd, A.; Sverko, E., Low Cost Monitoring of Glyphosate in Surface Waters Using the ELISA Method: An Evaluation. *Environmental Science & Technology* **2008,** *42* (16), 6052-6057.
9. Hu, D.; Fulton, B.; Henderson, K.; Coats, J., Identification of Tylosin Photoreaction Products and Comparison of ELISA and HPLC Methods for Their Detection in Water. *Environmental Science & Technology* **2008,** *42* (8), 2982-2987.
10. Feigon, J.; Dieckmann, T.; Smith, F. W., Aptamer structures from A to ζ. *Chemistry & Biology* **1996,** *3* (8), 611-617.
11. Burgstaller, P.; Famulok, M., Isolation of RNA Aptamers for Biological Cofactors by In Vitro Selection. *Angewandte Chemie International Edition in English* **1994,** *33*, 1084-1087.
12. Jenison, R. D.; Gill Sc Fau - Pardi, A.; Pardi A Fau - Polisky, B.; Polisky, B., High-resolution molecular discrimination by RNA. (0036-8075 (Print)).
13. Tuerk, C.; MacDougal, S.; Gold, L., RNA Pseudoknots that Inhibit Human Immunodeficiency Virus Type 1 Reverse Transcriptase. *Proceedings of the National Academy of Sciences of the United States of America* **1992,** *89* (15), 6988-6992.
14. Schneider, D.; Tuerk, C.; Gold, L., Selection of high affinity RNA ligands to the bacteriophage R17 coat protein. *Journal of Molecular Biology* **1992,** *228* (3), 862-869.
15. Dua, P.; Ren, S.; Lee, S. W.; Kim, J.-K.; Shin, H.-s.; Jeong, O. K. C.; Kim, S.; Lee, D.-K., Cell-SELEX Based Identification of an RNA Aptamer for Escherichia coli and Its Use in Various Detection Formats. *Molecules and Cells* **2016,** *39* (11), 807-813.

16. Hyeon, J.-Y.; Chon, J.-W.; Choi, I.-S.; Park, C.; Kim, D.-E.; Seo, K.-H., Development of RNA aptamers for detection of Salmonella Enteritidis. *Journal of Microbiological Methods* **2012,** *89* (1), 79-82.
17. Akki, S. U.; Werth, C. J.; Silverman, S. K., Selective Aptamers for Detection of Estradiol and Ethynylestradiol in Natural Waters. *Environmental Science & Technology* **2015,** *49* (16), 9905-9913.
18. Song, K.-M.; Cho, M.; Jo, H.; Min, K.; Jeon, S. H.; Kim, T.; Han, M. S.; Ku, J. K.; Ban, C., Gold nanoparticle-based colorimetric detection of kanamycin using a DNA aptamer. *Analytical Biochemistry* **2011,** *415* (2), 175-181.
19. Ng, A.; Chinnappan, R.; Eissa, S.; Liu, H.; Tlili, C.; Zourob, M., Selection, Characterization, and Biosensing Application of High Affinity Congener-Specific Microcystin-Targeting Aptamers. *Environmental Science & Technology* **2012,** *46* (19), 10697-10703.
20. Tang, J.; Xie, J.; Shao, N.; Yan, Y., The DNA aptamers that specifically recognize ricin toxin are selected by two in vitro selection methods. *Electrophoresis* **2006,** *27* (7), 1303-1311.
21. Tang, J.; Yu, T.; Guo, L.; Xie, J.; Shao, N.; He, Z., In vitro selection of DNA aptamer against abrin toxin and aptamer-based abrin direct detection. *Biosensors and Bioelectronics* **2007,** *22* (11), 2456-2463.
22. Dwivedi, H. P.; Smiley, R. D.; Jaykus, L.-A., Selection of DNA aptamers for capture and detection of Salmonella Typhimurium using a whole-cell SELEX approach in conjunction with cell sorting. *Applied Microbiology and Biotechnology* **2013,** *97* (8), 3677-3686.
23. Giamberardino, A.; Labib, M.; Hassan, E. M.; Tetro, J. A.; Springthorpe, S.; Sattar, S. A.; Berezovski, M. V.; DeRosa, M. C., Ultrasensitive Norovirus Detection Using DNA Aptasensor Technology. *PLOS ONE* **2013,** *8* (11), e79087.
24. Wang, L.; Liu, X.; Hu, X.; Song, S.; Fan, C., Unmodified gold nanoparticles as a colorimetric probe for potassium DNA aptamers. *Chemical Communications* **2006,** (36), 3780-3782.
25. Kim, M.; Um, H.-J.; Bang, S.; Lee, S.-H.; Oh, S.-J.; Han, J.-H.; Kim, K.-W.; Min, J.; Kim, Y.-H., Arsenic Removal from Vietnamese Groundwater Using the Arsenic-Binding DNA Aptamer. *Environmental Science & Technology* **2009,** *43* (24), 9335-9340.
26. Wu, L.; Qi, P.; Fu, X.; Liu, H.; Li, J.; Wang, Q.; Fan, H., A novel electrochemical PCB77-binding DNA aptamer biosensor for selective detection of PCB77. *Journal of Electroanalytical Chemistry* **2016,** *771*, 45-49.
27. Chen, J.; Wen, J.; Yang, G.; Zhou, S., A target-induced three-way G-quadruplex junction for 17[small beta]-estradiol monitoring with a naked-eye readout. *Chemical Communications* **2015,** *51* (62), 12373-12376.
28. Yildirim, N.; Long, F.; Gao, C.; He, M.; Shi, H.-C.; Gu, A. Z., Aptamer-Based Optical Biosensor For Rapid and Sensitive Detection of 17β-Estradiol In Water Samples. *Environmental Science & Technology* **2012,** *46* (6), 3288-3294.
29. Fan, L.; Zhao, G.; Shi, H.; Liu, M.; Wang, Y.; Ke, H., A Femtomolar Level and Highly Selective 17β-estradiol Photoelectrochemical Aptasensor Applied in Environmental Water Samples Analysis. *Environmental Science & Technology* **2014,** *48* (10), 5754-5761.
30. Soh, J. H.; Lin, Y.; Rana, S.; Ying, J. Y.; Stevens, M. M., Colorimetric Detection of Small Molecules in Complex Matrixes via Target-Mediated Growth of Aptamer-Functionalized Gold Nanoparticles. *Analytical Chemistry* **2015,** *87* (15), 7644-7652.
31. Bagheri, H.; Talemi, R. P.; Afkhami, A., Gold nanoparticles deposited on fluorine-doped tin oxide surface as an effective platform for fabricating a highly sensitive and specific digoxin aptasensor. *RSC Advances* **2015,** *5* (72), 58491-58498.
32. Lavaee, P.; Danesh, N. M.; Ramezani, M.; Abnous, K.; Taghdisi, S. M., Colorimetric aptamer based assay for the determination of fluoroquinolones by triggering the reduction-catalyzing activity of gold nanoparticles. *Microchimica Acta* **2017,** *184* (7), 2039-2045.

33. Abnous, K.; Danesh, N. M.; Alibolandi, M.; Ramezani, M.; Taghdisi, S. M.; Emrani, A. S., A novel electrochemical aptasensor for ultrasensitive detection of fluoroquinolones based on single-stranded DNA-binding protein. *Sensors and Actuators B: Chemical* **2017,** *240*, 100-106.
34. Ragavan, K. V.; Selvakumar, L. S.; Thakur, M. S., Functionalized aptamers as nano-bioprobes for ultrasensitive detection of bisphenol-A. *Chemical Communications* **2013,** *49* (53), 5960-5962.
35. Ferguson, B. S.; Hoggarth, D. A.; Maliniak, D.; Ploense, K.; White, R. J.; Woodward, N.; Hsieh, K.; Bonham, A. J.; Eisenstein, M.; Kippin, T. E.; Plaxco, K. W.; Soh, H. T., Real-Time, Aptamer-Based Tracking of Circulating Therapeutic Agents in Living Animals. *Science Translational Medicine* **2013,** *5* (213), 213ra165.
36. Lee, J. S.; Kim, S. G.; Jun, J.; Shin, D. H.; Jang, J., Aptamer-Functionalized Multidimensional Conducting-Polymer Nanoparticles for an Ultrasensitive and Selective Field-Effect-Transistor Endocrine-Disruptor Sensors. *Advanced Functional Materials* **2014,** *24* (39), 6145-6153.
37. Kim, S. G.; Lee, J. S.; Jun, J.; Shin, D. H.; Jang, J., Ultrasensitive Bisphenol A Field-Effect Transistor Sensor Using an Aptamer-Modified Multichannel Carbon Nanofiber Transducer. *ACS Applied Materials & Interfaces* **2016,** *8* (10), 6602-6610.
38. Lin, X.; Cheng, C.; Terry, P.; Chen, J.; Cui, H.; Wu, J., Rapid and sensitive detection of bisphenol a from serum matrix. *Biosensors and Bioelectronics* **2017,** *91*, 104-109.
39. Na, W.; Park, J. W.; An, J. H.; Jang, J., Size-controllable ultrathin carboxylated polypyrrole nanotube transducer for extremely sensitive 17[small beta]-estradiol FET-type biosensors. *Journal of Materials Chemistry B* **2016,** *4* (29), 5025-5034.
40. Zhu, B.; Alsager, O. A.; Kumar, S.; Hodgkiss, J. M.; Travas-Sejdic, J., Label-free electrochemical aptasensor for femtomolar detection of 17β-estradiol. *Biosensors and Bioelectronics* **2015,** *70*, 398-403.
41. Hu, X.; Mu, L.; Zhou, Q.; Wen, J.; Pawliszyn, J., ssDNA Aptamer-Based Column for Simultaneous Removal of Nanogram Per Liter Level of Illicit and Analgesic Pharmaceuticals in Drinking Water. *Environmental Science & Technology* **2011,** *45* (11), 4890-4895.
42. Cunningham, J. C.; Brenes, N. J.; Crooks, R. M., Paper Electrochemical Device for Detection of DNA and Thrombin by Target-Induced Conformational Switching. *Analytical Chemistry* **2014,** *86* (12), 6166-6170.
43. Cunningham, J. C.; Scida, K.; Kogan, M. R.; Wang, B.; Ellington, A. D.; Crooks, R. M., Paper diagnostic device for quantitative electrochemical detection of ricin at picomolar levels. *Lab on a Chip* **2015,** *15* (18), 3707-3715.
44. McKeague, M.; DeRosa, M. C., Challenges and Opportunities for Small Molecule Aptamer Development. *Journal of Nucleic Acids* **2012,** *2012*, 748913.
45. Pfeiffer, F.; Mayer, G., Selection and Biosensor Application of Aptamers for Small Molecules. *Frontiers in Chemistry* **2016,** *4*, 25.
46. Hayat, A.; Marty, J. L., Aptamer based electrochemical sensors for emerging environmental pollutants. *Frontiers in Chemistry* **2014,** *2*, 41.
47. Nguyen, V.-T.; Kwon, Y. S.; Gu, M. B., Aptamer-based environmental biosensors for small molecule contaminants. *Current Opinion in Biotechnology* **2017,** *45*, 15-23.
48. Tuerk, C.; Gold, L., Systematic evolution of ligands by exponential enrichment: RNA ligands to bacteriophage T4 DNA polymerase. *Science* **1990,** *249* (4968), 505.
49. Ellington, A. D.; Szostak, J. W., In vitro selection of RNA molecules that bind specific ligands. *Nature* **1990,** *346* (6287), 818-822.
50. Jayasena, S. D., Aptamers: An Emerging Class of Molecules That Rival Antibodies in Diagnostics. *Clinical Chemistry* **1999,** *45* (9), 1628.
51. Cruz-Aguado, J. A.; Penner, G., Determination of Ochratoxin A with a DNA Aptamer. *Journal of Agricultural and Food Chemistry* **2008,** *56* (22), 10456-10461.
52. McKeague, M.; Bradley, C. R.; De Girolamo, A.; Visconti, A.; Miller, J. D.; DeRosa, M. C., Screening and Initial Binding Assessment of Fumonisin B(1) Aptamers. *International Journal of Molecular Sciences* **2010,** *11* (12), 4864-4881.

53. Niazi, J. H.; Lee, S. J.; Gu, M. B., Single-stranded DNA aptamers specific for antibiotics tetracyclines. *Bioorganic & Medicinal Chemistry* **2008,** *16* (15), 7245-7253.
54. Lee, E.-H.; Lim, H. J.; Lee, S.-D.; Son, A., Highly Sensitive Detection of Bisphenol A by NanoAptamer Assay with Truncated Aptamer. *ACS Applied Materials & Interfaces* **2017,** *9* (17), 14889-14898.
55. Macdonald, J.; Houghton, P.; Xiang, D.; Duan, W.; Shigdar, S., Truncation and Mutation of a Transferrin Receptor Aptamer Enhances Binding Affinity. *Nucleic Acid Therapeutics* **2016,** *26* (6), 348-354.
56. Ha, N.-R.; Jung, I.-P.; La, I.-J.; Jung, H.-S.; Yoon, M.-Y., Ultra-sensitive detection of kanamycin for food safety using a reduced graphene oxide-based fluorescent aptasensor. **2017,** *7*, 40305.
57. Gu, H.; Duan, N.; Wu, S.; Hao, L.; Xia, Y.; Ma, X.; Wang, Z., Graphene oxide-assisted non-immobilized SELEX of okdaic acid aptamer and the analytical application of aptasensor. **2016,** *6*, 21665.
58. Huang, L.; Yang, X.; Qi, C.; Niu, X.; Zhao, C.; Zhao, X.; Shangguan, D.; Yang, Y., A label-free electrochemical biosensor based on a DNA aptamer against codeine. *Analytica Chimica Acta* **2013,** *787*, 203-210.
59. Mei, H.; Bing, T.; Yang, X.; Qi, C.; Chang, T.; Liu, X.; Cao, Z.; Shangguan, D., Functional-Group Specific Aptamers Indirectly Recognizing Compounds with Alkyl Amino Group. *Analytical Chemistry* **2012,** *84* (17), 7323-7329.
60. Beylot, B.; Spassky, A., Chemical Probing Shows That the Intron-encoded Endonuclease I-SceI Distorts DNA through Binding in Monomeric Form to Its Homing Site. *Journal of Biological Chemistry* **2001,** *276* (27), 25243-25253.
61. Chinnapen, D. J. F.; Sen, D., Hemin-Stimulated Docking of Cytochrome c to a Hemin−DNA Aptamer Complex. *Biochemistry* **2002,** *41* (16), 5202-5212.
62. Stoltenburg, R.; Reinemann C Fau - Strehlitz, B.; Strehlitz, B., FluMag-SELEX as an advantageous method for DNA aptamer selection. *Analytical & Bioanalytical Chemistry* **2005,** *383* (1), 83-91.
63. Mosing, R. K.; Bowser, M. T., Isolating Aptamers Using Capillary Electrophoresis–SELEX (CE–SELEX). In *Nucleic Acid and Peptide Aptamers: Methods and Protocols*, Mayer, G., Ed. Humana Press: Totowa, NJ, 2009; pp 33-43.
64. Mendonsa, S. D.; Bowser, M. T., In Vitro Evolution of Functional DNA Using Capillary Electrophoresis. *Journal of the American Chemical Society* **2004,** *126* (1), 20-21.
65. Yang, J.; Bowser, M. T., Capillary Electrophoresis–SELEX Selection of Catalytic DNA Aptamers for a Small-Molecule Porphyrin Target. *Analytical Chemistry* **2013,** *85* (3), 1525-1530.
66. Stoltenburg, R.; Nikolaus, N.; Strehlitz, B., Capture-SELEX: Selection of DNA Aptamers for Aminoglycoside Antibiotics. *Journal of Analytical Methods in Chemistry* **2012,** *2012*, 14.
67. Park, J.-W.; Tatavarty, R.; Kim, D. W.; Jung, H.-T.; Gu, M. B., Immobilization-free screening of aptamers assisted by graphene oxide. *Chemical Communications* **2012,** *48* (15), 2071-2073.
68. Wu, S.; Duan, N.; Zhang, W.; Zhao, S.; Wang, Z., Screening and development of DNA aptamers as capture probes for colorimetric detection of patulin. *Analytical Biochemistry* **2016,** *508*, 58-64.
69. Gao, S.; Hu, B.; Zheng, X.; Cao, Y.; Liu, D.; Sun, M.; Jiao, B.; Wang, L., Gonyautoxin 1/4 aptamers with high-affinity and high-specificity: From efficient selection to aptasensor application. *Biosensors and Bioelectronics* **2016,** *79*, 938-944.
70. Lee, A. Y.; Ha, N.-R.; Jung, I.-P.; Kim, S.-H.; Kim, A. R.; Yoon, M.-Y., Development of a ssDNA aptamer for detection of residual benzylpenicillin. *Analytical Biochemistry* **2017,** *531*, 1-7.
71. Zhang, Y.; You, Y.; Xia, Z.; Han, X.; Tian, Y.; Zhou, N., Graphene oxide-based selection and identification of ofloxacin-specific single-stranded DNA aptamers. *RSC Advances* **2016,** *6* (101), 99540-99545.
72. Kwon, Y. S.; Nguyen, V.-T.; Park, J. G.; Gu, M. B., Detection of Iprobenfos and Edifenphos using a new Multi-aptasensor. *Analytica Chimica Acta* **2015,** *868*, 60-66.

73. Ellington, A. D.; Szostak, J. W., Selection in vitro of single-stranded DNA molecules that fold into specific ligand-binding structures. *Nature* **1992,** *355* (6363), 850-852.
74. Mann, D.; Reinemann, C.; Stoltenburg, R.; Strehlitz, B., In vitro selection of DNA aptamers binding ethanolamine. *Biochemical and Biophysical Research Communications* **2005,** *338* (4), 1928-1934.
75. Harada, K.; Frankel, A. D., Identification of two novel arginine binding DNAs. *The EMBO Journal* **1995,** *14* (23), 5798-5811.
76. Fisher, R. A., The Arrangement of Field Experiments. In *Breakthroughs in Statistics: Methodology and Distribution*, Kotz, S.; Johnson, N. L., Eds. Springer New York: New York, NY, 1992; pp 82-91.
77. Cohen, J., CHAPTER 2 - The t Test for Means. In *Statistical Power Analysis for the Behavioral Sciences (Revised Edition)*, Academic Press: 1977; pp 19-74.
78. Robertson, S. A.; Harada, K.; Frankel, A. D.; Wemmer, D. E., Structure Determination and Binding Kinetics of a DNA Aptamer−Argininamide Complex. *Biochemistry* **2000,** *39* (5), 946-954.
79. Wiegand, T. W.; Williams, P. B.; Dreskin, S. C.; Jouvin, M. H.; Kinet, J. P.; Tasset, D., High-affinity oligonucleotide ligands to human IgE inhibit binding to Fc epsilon receptor I. *The Journal of Immunology* **1996,** *157* (1), 221.
80. Kim, Y. S.; Jung Hs Fau - Matsuura, T.; Matsuura T Fau - Lee, H. Y.; Lee Hy Fau - Kawai, T.; Kawai T Fau - Gu, M. B.; Gu, M. B., Electrochemical detection of 17beta-estradiol using DNA aptamer immobilized gold electrode chip. (0956-5663 (Print)).
81. Svobodova, M.; Skouridou, V.; Botero, M. L.; Jauset-Rubio, M.; Schubert, T.; Bashammakh, A. S.; El-Shahawi, M. S.; Alyoubi, A. O.; O'Sullivan, C. K., The characterization and validation of 17beta-estradiol binding aptamers. (1879-1220 (Electronic)).
82. Sassolas, A.; Blum, L. J.; Leca-Bouvier, B. D., Optical detection systems using immobilized aptamers. *Biosensors and Bioelectronics* **2011,** *26* (9), 3725-3736.
83. Yan, J.; Huang, Y.; Zhang, C.; Fang, Z.; Bai, W.; Yan, M.; Zhu, C.; Chen, A., Aptamer based photometric assay for the antibiotic sulfadimethoxine based on the inhibition and reactivation of the peroxidase-like activity of gold nanoparticles. *Microchimica Acta* **2017,** *184* (1), 59-63.
84. Wang, A.; Zhao, H.; Chen, X.; Tan, B.; Zhang, Y.; Quan, X., A colorimetric aptasensor for sulfadimethoxine detection based on peroxidase-like activity of graphene/nickel@palladium hybrids. *Analytical Biochemistry* **2017,** *525*, 92-99.
85. Liu, J.; Lu, Y., Fast Colorimetric Sensing of Adenosine and Cocaine Based on a General Sensor Design Involving Aptamers and Nanoparticles. *Angewandte Chemie International Edition* **2006,** *45* (1), 90-94.
86. Yang, C.; Wang, Y.; Marty, J.-L.; Yang, X., Aptamer-based colorimetric biosensing of Ochratoxin A using unmodified gold nanoparticles indicator. *Biosensors and Bioelectronics* **2011,** *26* (5), 2724-2727.
87. Sarreshtehdar Emrani, A.; Danesh, N. M.; Lavaee, P.; Jalalian, S. H.; Ramezani, M.; Abnous, K.; Taghdisi, S. M., Sensitive and selective detection of digoxin based on fluorescence quenching and colorimetric aptasensors. *Analytical Methods* **2015,** *7* (8), 3419-3424.
88. Alsager Oa Fau - Kumar, S.; Kumar, S.; Zhu, B.; Travas-Sejdic, J.; McNatty, K. P.; Hodgkiss, J. M., Ultrasensitive colorimetric detection of 17beta-estradiol: the effect of shortening DNA aptamer sequences. (1520-6882 (Electronic)).
89. Wei, H.; Li, B.; Li, J.; Wang, E.; Dong, S., Simple and sensitive aptamer-based colorimetric sensing of protein using unmodified gold nanoparticle probes. *Chemical Communications* **2007,** (36), 3735-3737.
90. Liu, J.; Bai, W.; Niu, S.; Zhu, C.; Yang, S.; Chen, A., Highly sensitive colorimetric detection of 17β-estradiol using split DNA aptamers immobilized on unmodified gold nanoparticles. *Scientific Reports* **2014,** *4*, 7571.

91. Zhao, H.; Gao, S.; Liu, M.; Chang, Y.; Fan, X.; Quan, X., Fluorescent assay for oxytetracycline based on a long-chain aptamer assembled onto reduced graphene oxide. *Microchimica Acta* **2013,** *180* (9), 829-835.
92. Nutiu, R.; Li, Y., Structure-Switching Signaling Aptamers. *Journal of the American Chemical Society* **2003,** *125* (16), 4771-4778.
93. Zhu, Y.; Zhou, C.; Yan, X.; Yan, Y.; Wang, Q., Aptamer-functionalized nanoporous gold film for high-performance direct electrochemical detection of bisphenol A in human serum. *Analytica Chimica Acta* **2015,** *883*, 81-89.
94. Zhou, L.; Li, D.-J.; Gai, L.; Wang, J.-P.; Li, Y.-B., Electrochemical aptasensor for the detection of tetracycline with multi-walled carbon nanotubes amplification. *Sensors and Actuators B: Chemical* **2012,** *162* (1), 201-208.
95. Baker, B. R.; Lai, R. Y.; Wood, M. S.; Doctor, E. H.; Heeger, A. J.; Plaxco, K. W., An Electronic, Aptamer-Based Small-Molecule Sensor for the Rapid, Label-Free Detection of Cocaine in Adulterated Samples and Biological Fluids. *Journal of the American Chemical Society* **2006,** *128* (10), 3138-3139.
96. Macaya, R. F.; Schultze, P.; Smith, F. W.; Roe, J. A.; Feigon, J., Thrombin-Binding DNA Aptamer Forms a Unimolecular Quadruplex Structure in Solution. *Proceedings of the National Academy of Sciences of the United States of America* **1993,** *90* (8), 3745-3749.
97. Xiao, Y.; Uzawa, T.; White, R. J.; DeMartini, D.; Plaxco, K. W., On the Signaling of Electrochemical Aptamer-Based Sensors: Collision- and Folding-Based Mechanisms. *Electroanalysis* **2009,** *21* (11), 1267-1271.
98. Chen, L.; Zeng, X.; Ferhan, A. R.; Chi, Y.; Kim, D.-H.; Chen, G., Signal-on electrochemiluminescent aptasensors based on target controlled permeable films. *Chemical Communications* **2015,** *51* (6), 1035-1038.
99. Lazar, J.; Schnelting, C.; Slavcheva, E.; Schnakenberg, U., Hampering of the Stability of Gold Electrodes by Ferri-/Ferrocyanide Redox Couple Electrolytes during Electrochemical Impedance Spectroscopy. *Analytical Chemistry* **2016,** *88* (1), 682-687.
100. Li, S.; Wu, X.; Liu, C.; Yin, G.; Luo, J.; Xu, Z., Application of DNA aptamers as sensing layers for detection of carbofuran by electrogenerated chemiluminescence energy transfer. *Analytica Chimica Acta* **2016,** *941*, 94-100.
101. Han, Y.; Diao, D.; Lu, Z.; Li, X.; Guo, Q.; Huo, Y.; Xu, Q.; Li, Y.; Cao, S.; Wang, J.; Wang, Y.; Zhao, J.; Li, Z.; He, M.; Luo, Z.; Lou, X., Selection of Group-Specific Phthalic Acid Esters Binding DNA Aptamers via Rationally Designed Target Immobilization and Applications for Ultrasensitive and Highly Selective Detection of Phthalic Acid Esters. *Analytical Chemistry* **2017,** *89* (10), 5270-5277.
102. Xu, S.; Yuan, H.; Chen, S.; Xu, A.; Wang, J.; Wu, L., Selection of DNA aptamers against polychlorinated biphenyls as potential biorecognition elements for environmental analysis. *Analytical Biochemistry* **2012,** *423* (2), 195-201.
103. Jiao, Y.; Jia, H.; Guo, Y.; Zhang, H.; Wang, Z.; Sun, X.; Zhao, J., An ultrasensitive aptasensor for chlorpyrifos based on ordered mesoporous carbon/ferrocene hybrid multiwalled carbon nanotubes. *RSC Advances* **2016,** *6* (63), 58541-58548.
104. Williams, R. M.; Crihfield, C. L.; Gattu, S.; Holland, L. A.; Sooter, L. J., In Vitro Selection of a Single-Stranded DNA Molecular Recognition Element against Atrazine. *International Journal of Molecular Sciences* **2014,** *15* (8), 14332-14347.
105. Bruno, J. G., In VitroSelection of DNA to Chloroaromatics Using Magnetic Microbead-Based Affinity Separation and Fluorescence Detection. *Biochemical and Biophysical Research Communications* **1997,** *234* (1), 117-120.
106. Lu, Y.; Huang, Q.; Meng, G.; Wu, L.; Jingjing, Z., Label-free selective SERS detection of PCB-77 based on DNA aptamer modified SiO2@Au core/shell nanoparticles. *Analyst* **2014,** *139* (12), 3083-3087.

107. Fu, C.; Wang, Y.; Chen, G.; Yang, L.; Xu, S.; Xu, W., Aptamer-Based Surface-Enhanced Raman Scattering-Microfluidic Sensor for Sensitive and Selective Polychlorinated Biphenyls Detection. *Analytical Chemistry* **2015,** *87* (19), 9555-9558.
108. Sun, K.; Huang, Q.; Meng, G.; Lu, Y., Highly Sensitive and Selective Surface-Enhanced Raman Spectroscopy Label-free Detection of 3,3′,4,4′-Tetrachlorobiphenyl Using DNA Aptamer-Modified Ag-Nanorod Arrays. *ACS Applied Materials & Interfaces* **2016,** *8* (8), 5723-5728.
109. Chen, M.; Gan, N.; Zhang, H.; Yan, Z.; Li, T.; Chen, Y.; Xu, Q.; Jiang, Q., Electrochemical simultaneous assay of chloramphenicol and PCB72 using magnetic and aptamer-modified quantum dot-encoded dendritic nanotracers for signal amplification. *Microchimica Acta* **2016,** *183* (3), 1099-1106.
110. Yan, Z.; Gan, N.; Wang, D.; Cao, Y.; Chen, M.; Li, T.; Chen, Y., A "signal-on'' aptasensor for simultaneous detection of chloramphenicol and polychlorinated biphenyls using multi-metal ions encoded nanospherical brushes as tracers. *Biosensors and Bioelectronics* **2015,** *74*, 718-724.
111. Reinemann, C.; Freiin von Fritsch, U.; Rudolph, S.; Strehlitz, B., Generation and characterization of quinolone-specific DNA aptamers suitable for water monitoring. *Biosensors and Bioelectronics* **2016,** *77*, 1039-1047.
112. Jahanbani, S.; Benvidi, A., Comparison of two fabricated aptasensors based on modified carbon paste/oleic acid and magnetic bar carbon paste/Fe3O4@oleic acid nanoparticle electrodes for tetracycline detection. *Biosensors and Bioelectronics* **2016,** *85*, 553-562.
113. Luo, Y.; Xu, J.; Li, Y.; Gao, H.; Guo, J.; Shen, F.; Sun, C., A novel colorimetric aptasensor using cysteamine-stabilized gold nanoparticles as probe for rapid and specific detection of tetracycline in raw milk. *Food Control* **2015,** *54*, 7-15.
114. Zhang, D.; Zhang, W.; Ye, J.; Zhan, S.; Xia, B.; Lv, J.; Xu, H.; Du, G.; Wang, L., A Label-Free Colorimetric Biosensor for 17β-Estradiol Detection Using Nanoparticles Assembled by Aptamer and Cationic Polymer. *Australian Journal of Chemistry* **2016,** *69* (1), 12-19.
115. Meng, F.; Ma, X.; Duan, N.; Wu, S.; Xia, Y.; Wang, Z.; Xu, B., Ultrasensitive SERS aptasensor for the detection of oxytetracycline based on a gold-enhanced nano-assembly. *Talanta* **2017,** *165*, 412-418.
116. Kim, S.; Lee, H. J., Gold Nanostar Enhanced Surface Plasmon Resonance Detection of an Antibiotic at Attomolar Concentrations via an Aptamer-Antibody Sandwich Assay. *Analytical Chemistry* **2017,** *89* (12), 6624-6630.
117. Fan, P.; Suri, A. K.; Fiala, R.; Live, D.; Patel, D. J., Molecular Recognition in the FMN – RNA Aptamer Complex. *Journal of Molecular Biology* **1996,** *258* (3), 480-500.
118. Rose, A. S.; Hildebrand, P. W., NGL Viewer: a web application for molecular visualization. *Nucleic Acids Research* **2015,** *43* (W1), W576-W579.
119. Rose, A. S.; Bradley, A. R.; Valasatava, Y.; Duarte, J. M.; Prlic, A.; Rose, P. W., Web-based molecular graphics for large complexes. In *Proceedings of the 21st International Conference on Web3D Technology*, ACM: Anaheim, California, 2016; pp 185-186.
120. Huizenga, D. E.; Szostak, J. W., A DNA Aptamer That Binds Adenosine and ATP. *Biochemistry* **1995,** *34* (2), 656-665.
121. Yang, Q.; Goldstein, I. J.; Mei, H.-Y.; Engelke, D. R., DNA ligands that bind tightly and selectively to cellobiose. *Proceedings of the National Academy of Sciences* **1998,** *95* (10), 5462-5467.
122. Wilson, C.; Szostak, J. W., Isolation of a fluorophore-specific DNA aptamer with weak redox activity. *Chemistry & Biology* **1998,** *5* (11), 609-617.
123. Kato, T.; Takemura, T.; Yano, K.; Ikebukuro, K.; Karube, I., In vitro selection of DNA aptamers which bind to cholic acid. *Biochimica et Biophysica Acta (BBA) - Gene Structure and Expression* **2000,** *1493* (1), 12-18.
124. Okazawa, A.; Maeda, H.; Fukusaki, E.; Katakura, Y.; Kobayashi, A., In vitro selection of hematoporphyrin binding DNA aptamers. *Bioorganic & Medicinal Chemistry Letters* **2000,** *10* (23), 2653-2656.

125. Vianini, E.; Palumbo, M.; Gatto, B., In vitro selection of DNA aptamers that bind l-tyrosinamide. *Bioorganic & Medicinal Chemistry* **2001,** *9* (10), 2543-2548.
126. Mehedi Masud, M.; Kuwahara, M.; Ozaki, H.; Sawai, H., Sialyllactose-binding modified DNA aptamer bearing additional functionality by SELEX. *Bioorganic & Medicinal Chemistry* **2004,** *12* (5), 1111-1120.
127. Shoji, A.; Kuwahara, M.; Ozaki, H.; Sawai, H., Modified DNA Aptamer That Binds the (R)-Isomer of a Thalidomide Derivative with High Enantioselectivity. *Journal of the American Chemical Society* **2007,** *129* (5), 1456-1464.
128. Kim, Y. S.; Jung, H. S.; Matsuura, T.; Lee, H. Y.; Kawai, T.; Gu, M. B., Electrochemical detection of 17β-estradiol using DNA aptamer immobilized gold electrode chip. *Biosensors and Bioelectronics* **2007,** *22* (11), 2525-2531.
129. Wochner, A.; Menger, M.; Orgel, D.; Cech, B.; Rimmele, M.; Erdmann, V. A.; Glökler, J., A DNA aptamer with high affinity and specificity for therapeutic anthracyclines. *Analytical Biochemistry* **2008,** *373* (1), 34-42.
130. Niazi, J. H.; Lee, S. J.; Kim, Y. S.; Gu, M. B., ssDNA aptamers that selectively bind oxytetracycline. *Bioorganic & Medicinal Chemistry* **2008,** *16* (3), 1254-1261.
131. Miyachi, Y.; Shimizu, N.; Ogino, C.; Fukuda, H.; Kondo, A., Selection of a DNA aptamer that binds 8-OHdG using GMP-agarose. *Bioorganic & Medicinal Chemistry Letters* **2009,** *19* (13), 3619-3622.
132. Joeng, C. B.; Niazi, J. H.; Lee, S. J.; Gu, M. B., ssDNA aptamers that recognize diclofenac and 2-anilinophenylacetic acid. *Bioorganic & Medicinal Chemistry* **2009,** *17* (15), 5380-5387.
133. Walsh, R.; DeRosa, M. C., Retention of function in the DNA homolog of the RNA dopamine aptamer. *Biochemical and Biophysical Research Communications* **2009,** *388* (4), 732-735.
134. Kim, Y. S.; Hyun, C. J.; Kim, I. A.; Gu, M. B., Isolation and characterization of enantioselective DNA aptamers for ibuprofen. *Bioorganic & Medicinal Chemistry* **2010,** *18* (10), 3467-3473.
135. Luo, X.; McKeague, M.; Pitre, S.; Dumontier, M.; Green, J.; Golshani, A.; Derosa, M. C.; Dehne, F., Computational approaches toward the design of pools for the in vitro selection of complex aptamers. *RNA* **2010,** *16* (11), 2252-2262.
136. He, J.; Liu, Y.; Fan, M.; Liu, X., Isolation and Identification of the DNA Aptamer Target to Acetamiprid. *Journal of Agricultural and Food Chemistry* **2011,** *59* (5), 1582-1586.
137. Jo, M.; Ahn, J.-Y.; Lee, J.; Lee, S.; Hong, S. W.; Yoo, J.-W.; Kang, J.; Dua, P.; Lee, D.-k.; Hong, S.; Kim, S., Development of Single-Stranded DNA Aptamers for Specific Bisphenol A Detection. *Oligonucleotides* **2011,** *21* (2), 85-91.
138. Mehta, J.; Van Dorst, B.; Rouah-Martin, E.; Herrebout, W.; Scippo, M.-L.; Blust, R.; Robbens, J., In vitro selection and characterization of DNA aptamers recognizing chloramphenicol. *Journal of Biotechnology* **2011,** *155* (4), 361-369.
139. Yang, X.; Bing, T.; Mei, H.; Fang, C.; Cao, Z.; Shangguan, D., Characterization and application of a DNA aptamer binding to l-tryptophan. *Analyst* **2011,** *136* (3), 577-585.
140. Barthelmebs, L.; Jonca, J.; Hayat, A.; Prieto-Simon, B.; Marty, J.-L., Enzyme-Linked Aptamer Assays (ELAAs), based on a competition format for a rapid and sensitive detection of Ochratoxin A in wine. *Food Control* **2011,** *22* (5), 737-743.
141. Song, K.-M.; Jeong, E.; Jeon, W.; Cho, M.; Ban, C., Aptasensor for ampicillin using gold nanoparticle based dual fluorescence–colorimetric methods. *Analytical and Bioanalytical Chemistry* **2012,** *402* (6), 2153-2161.
142. Kiani, Z.; Shafiei, M.; Rahimi-Moghaddam, P.; Karkhane, A. A.; Ebrahimi, S. A., In vitro selection and characterization of deoxyribonucleic acid aptamers for digoxin. *Analytica Chimica Acta* **2012,** *748*, 67-72.
143. Rouah-Martin, E.; Mehta, J.; van Dorst, B.; de Saeger, S.; Dubruel, P.; Maes, B. U. W.; Lemiere, F.; Goormaghtigh, E.; Daems, D.; Herrebout, W.; van Hove, F.; Blust, R.; Robbens, J., Aptamer-Based Molecular Recognition of Lysergamine, Metergoline and Small Ergot Alkaloids. *International Journal of Molecular Sciences* **2012,** *13* (12), 17138-17159.

144. Mehta, J.; Rouah-Martin, E.; Van Dorst, B.; Maes, B.; Herrebout, W.; Scippo, M.-L.; Dardenne, F.; Blust, R.; Robbens, J., Selection and Characterization of PCB-Binding DNA Aptamers. *Analytical Chemistry* **2012,** *84* (3), 1669-1676.
145. Song, K.-M.; Jeong, E.; Jeon, W.; Jo, H.; Ban, C., A coordination polymer nanobelt (CPNB)-based aptasensor for sulfadimethoxine. *Biosensors and Bioelectronics* **2012,** *33* (1), 113-119.
146. Grozio, A.; Gonzalez, V. M.; Millo, E.; Sturla, L.; Vigliarolo, T.; Bagnasco, L.; Guida, L.; D'Arrigo, C.; De Flora, A.; Salis, A.; Martin, E. M.; Bellotti, M.; Zocchi, E., Selection and Characterization of Single Stranded DNA Aptamers for the Hormone Abscisic Acid. *Nucleic Acid Therapeutics* **2013,** *23* (5), 322-331.
147. Gong, S.; Ren, H.-L.; Tian, R.-Y.; Lin, C.; Hu, P.; Li, Y.-S.; Liu, Z.-S.; Song, J.; Tang, F.; Zhou, Y.; Li, Z.-H.; Zhang, Y.-Y.; Lu, S.-Y., A novel analytical probe binding to a potential carcinogenic factor of N-glycolylneuraminic acid by SELEX. *Biosensors and Bioelectronics* **2013,** *49*, 547-554.
148. Eissa, S.; Ng, A.; Siaj, M.; Tavares, A. C.; Zourob, M., Selection and Identification of DNA Aptamers against Okadaic Acid for Biosensing Application. *Analytical Chemistry* **2013,** *85* (24), 11794-11801.
149. Zheng, X.; Hu, B.; Gao, S. X.; Liu, D. J.; Sun, M. J.; Jiao, B. H.; Wang, L. H., A saxitoxin-binding aptamer with higher affinity and inhibitory activity optimized by rational site-directed mutagenesis and truncation. *Toxicon* **2015,** *101*, 41-47.
150. Zhou, N.; Wang, J.; Zhang, J.; Li, C.; Tian, Y.; Wang, J., Selection and identification of streptomycin-specific single-stranded DNA aptamers and the application in the detection of streptomycin in honey. *Talanta* **2013,** *108*, 109-116.
151. Bae, H.; Ren, S.; Kang, J.; Kim, M.; Jiang, Y.; Jin, M. M.; Min, I. M.; Kim, S., Sol-Gel SELEX Circumventing Chemical Conjugation of Low Molecular Weight Metabolites Discovers Aptamers Selective to Xanthine. *Nucleic Acid Therapeutics* **2013,** *23* (6), 443-449.
152. Chen, X.; Huang, Y.; Duan, N.; Wu, S.; Ma, X.; Xia, Y.; Zhu, C.; Jiang, Y.; Wang, Z., Selection and identification of ssDNA aptamers recognizing zearalenone. *Analytical and Bioanalytical Chemistry* **2013,** *405* (20), 6573-6581.
153. Vanschoenbeek, K.; Vanbrabant, J.; Hosseinkhani, B.; Vermeeren, V.; Michiels, L., Aptamers targeting different functional groups of 17β-estradiol. *The Journal of Steroid Biochemistry and Molecular Biology* **2015,** *147*, 10-16.
154. Alsager, O. A.; Kumar, S.; Willmott, G. R.; McNatty, K. P.; Hodgkiss, J. M., Small molecule detection in solution via the size contraction response of aptamer functionalized nanoparticles. *Biosensors and Bioelectronics* **2014,** *57*, 262-268.
155. Malhotra, S.; Pandey, A. K.; Rajput, Y. S.; Sharma, R., Selection of aptamers for aflatoxin M1 and their characterization. *Journal of Molecular Recognition* **2014,** *27* (8), 493-500.
156. Zhu, Z.; Song, Y.; Li, C.; Zou, Y.; Zhu, L.; An, Y.; Yang, C. J., Monoclonal Surface Display SELEX for Simple, Rapid, Efficient, and Cost-Effective Aptamer Enrichment and Identification. *Analytical Chemistry* **2014,** *86* (12), 5881-5888.
157. Williams, R. M.; Kulick, A. R.; Yedlapalli, S.; Battistella, L.; Hajiran, C. J.; Sooter, L. J., In Vitro Selection of a Single-Stranded DNA Molecular Recognition Element Specific for Bromacil. *Journal of Nucleic Acids* **2014,** *2014*, 102968.
158. Martin, J. A.; Chávez, J. L.; Chushak, Y.; Chapleau, R. R.; Hagen, J.; Kelley-Loughnane, N., Tunable stringency aptamer selection and gold nanoparticle assay for detection of cortisol. *Analytical and Bioanalytical Chemistry* **2014,** *406* (19), 4637-4647.
159. Elshafey, R.; Siaj, M.; Zourob, M., In Vitro Selection, Characterization, and Biosensing Application of High-Affinity Cylindrospermopsin-Targeting Aptamers. *Analytical Chemistry* **2014,** *86* (18), 9196-9203.
160. Chen, X.; Huang, Y.; Duan, N.; Wu, S.; Xia, Y.; Ma, X.; Zhu, C.; Jiang, Y.; Ding, Z.; Wang, Z., Selection and characterization of single stranded DNA aptamers recognizing fumonisin B1. *Microchimica Acta* **2014,** *181* (11), 1317-1324.

161. Nikolaus, N.; Strehlitz, B., DNA-Aptamers Binding Aminoglycoside Antibiotics. *Sensors (Basel, Switzerland)* **2014,** *14* (2), 3737-3755.
162. McKeague, M.; Velu, R.; Hill, K.; Bardóczy, V.; Mészáros, T.; DeRosa, M. C., Selection and Characterization of a Novel DNA Aptamer for Label-Free Fluorescence Biosensing of Ochratoxin A. *Toxins* **2014,** *6* (8), 2435-2452.
163. Kim, C.-H.; Lee, L.-P.; Min, J.-R.; Lim, M.-W.; Jeong, S.-H., An indirect competitive assay-based aptasensor for detection of oxytetracycline in milk. *Biosensors and Bioelectronics* **2014,** *51*, 426-430.
164. Contreras Jiménez, G.; Eissa, S.; Ng, A.; Alhadrami, H.; Zourob, M.; Siaj, M., Aptamer-Based Label-Free Impedimetric Biosensor for Detection of Progesterone. *Analytical Chemistry* **2015,** *87* (2), 1075-1082.
165. Chen, X.; Huang, Y.; Duan, N.; Wu, S.; Xia, Y.; Ma, X.; Zhu, C.; Jiang, Y.; Wang, Z., Screening and Identification of DNA Aptamers against T-2 Toxin Assisted by Graphene Oxide. *Journal of Agricultural and Food Chemistry* **2014,** *62* (42), 10368-10374.
166. Priyanka; Shorie, M.; Bhalla, V.; Pathania, P.; Suri, C. R., Nanobioprobe mediated DNA aptamers for explosive detection. *Chemical Communications* **2014,** *50* (9), 1080-1082.
167. Elshafey, R.; Siaj, M.; Zourob, M., DNA aptamers selection and characterization for development of label-free impedimetric aptasensor for neurotoxin anatoxin-a. *Biosensors and Bioelectronics* **2015,** *68*, 295-302.
168. Eissa, S.; Siaj, M.; Zourob, M., Aptamer-based competitive electrochemical biosensor for brevetoxin-2. *Biosensors and Bioelectronics* **2015,** *69*, 148-154.
169. Gu, C.; Lan, T.; Shi, H.; Lu, Y., Portable Detection of Melamine in Milk Using a Personal Glucose Meter Based on an in Vitro Selected Structure-Switching Aptamer. *Analytical Chemistry* **2015,** *87* (15), 7676-7682.
170. Tang, X. L.; Hua, Y.; Guan, Q.; Yuan, C. H., Improved detection of deeply invasive candidiasis with DNA aptamers specific binding to (1→3)-β-D-glucans from Candida albicans. *European Journal of Clinical Microbiology & Infectious Diseases* **2016,** *35* (4), 587-595.
171. Setlem, K.; Mondal, B.; Ramlal, S.; Kingston, J., Immuno Affinity SELEX for Simple, Rapid, and Cost-Effective Aptamer Enrichment and Identification against Aflatoxin B1. *Frontiers in Microbiology* **2016,** *7*, 1909.
172. Kim, U.-J.; Kim, B. C., DNA aptamers for selective identification and separation of flame retardant chemicals. *Analytica Chimica Acta* **2016,** *936*, 208-215.
173. Wang , H.; Wang, J.; Sun, N.; Cheng , H.; Chen, H.; Pei, R., Selection and Characterization of Malachite Green Aptamers for the Development of Light–up Probes. *ChemistrySelect* **2016,** *1* (8), 1571-1574.
174. Wang, H.; Wang, J.; Xu, L.; Zhang, Y.; Chen, Y.; Chen, H.; Pei, R., Selection and characterization of thioflavin T aptamers for the development of light-up probes. *Analytical Methods* **2016,** *8* (48), 8461-8465.
175. Valenzano, S.; De Girolamo, A.; DeRosa, M. C.; McKeague, M.; Schena, R.; Catucci, L.; Pascale, M., Screening and Identification of DNA Aptamers to Tyramine Using in Vitro Selection and High-Throughput Sequencing. *ACS Combinatorial Science* **2016,** *18* (6), 302-313.
176. Skouridou, V.; Jauset-Rubio, M.; Ballester, P.; Bashammakh, A. S.; El-Shahawi, M. S.; Alyoubi, A. O.; O'Sullivan, C. K., Selection and characterization of DNA aptamers against the steroid testosterone. *Microchimica Acta* **2017,** *184* (6), 1631-1639.
177. Ha, N.-R.; Jung, I.-P.; La, I.-J.; Jung, H.-S.; Yoon, M.-Y., Ultra-sensitive detection of kanamycin for food safety using a reduced graphene oxide-based fluorescent aptasensor. *Scientific Reports* **2017,** *7*, 40305.
178. Alhadrami, H. A.; Chinnappan, R.; Eissa, S.; Rahamn, A. A.; Zourob, M., High affinity truncated DNA aptamers for the development of fluorescence based progesterone biosensors. *Analytical Biochemistry* **2017,** *525*, 78-84.

179. Bock, L. C.; Griffin, L. C.; Latham, J. A.; Vermaas, E. H.; Toole, J. J., Selection of single-stranded DNA molecules that bind and inhibit human thrombin. *Nature* **1992,** *355* (6360), 564-566.
180. Green, L. S.; Jellinek, D.; Jenison, R.; Östman, A.; Heldin, C.-H.; Janjic, N., Inhibitory DNA Ligands to Platelet-Derived Growth Factor B-Chain. *Biochemistry* **1996,** *35* (45), 14413-14424.
181. Rotherham, L. S.; Maserumule, C.; Dheda, K.; Theron, J.; Khati, M., Selection and Application of ssDNA Aptamers to Detect Active TB from Sputum Samples. *PLOS ONE* **2012,** *7* (10), e46862.
182. Stoltenburg, R.; Schubert, T.; Strehlitz, B., In vitro Selection and Interaction Studies of a DNA Aptamer Targeting Protein A. *PLoS ONE* **2015,** *10* (7), e0134403.
183. Zheng, Y.; Wang, Y.; Yang, X., Aptamer-based colorimetric biosensing of dopamine using unmodified gold nanoparticles. *Sensors and Actuators B: Chemical* **2011,** *156* (1), 95-99.
184. Li, B.-R.; Hsieh, Y.-J.; Chen, Y.-X.; Chung, Y.-T.; Pan, C.-Y.; Chen, Y.-T., An Ultrasensitive Nanowire-Transistor Biosensor for Detecting Dopamine Release from Living PC12 Cells under Hypoxic Stimulation. *Journal of the American Chemical Society* **2013,** *135* (43), 16034-16037.
185. Zhou, J.; Wang, W.; Yu, P.; Xiong, E.; Zhang, X.; Chen, J., A simple label-free electrochemical aptasensor for dopamine detection. *RSC Advances* **2014,** *4* (94), 52250-52255.
186. Jarczewska, M.; Sheelam, S. R.; Ziółkowski, R.; Górski, Ł., A Label-Free Electrochemical DNA Aptasensor for the Detection of Dopamine. *Journal of The Electrochemical Society* **2016,** *163* (3), B26-B31.
187. Azadbakht, A.; Roushani, M.; Abbasi, A. R.; Menati, S.; Derikvand, Z., A label-free aptasensor based on polyethyleneimine wrapped carbon nanotubes in situ formed gold nanoparticles as signal probe for highly sensitive detection of dopamine. *Materials Science and Engineering: C* **2016,** *68*, 585-593.
188. Huang, R.; Xiong, W.; Wang, D.; Guo, L.; Lin, Z.; Yu, L.; Chu, K.; Qiu, B.; Chen, G., Label-free aptamer-based partial filling technique for enantioseparation and determination of dl-tryptophan with micellar electrokinetic chromatography. *ELECTROPHORESIS* **2013,** *34* (2), 254-259.
189. Yang, X.; Han, Q.; Zhang, Y.; Wu, J.; Tang, X.; Dong, C.; Liu, W., Determination of free tryptophan in serum with aptamer—Comparison of two aptasensors. *Talanta* **2015,** *131*, 672-677.
190. Zhang, C.; Wang, L.; Tu, Z.; Sun, X.; He, Q.; Lei, Z.; Xu, C.; Liu, Y.; Zhang, X.; Yang, J.; Liu, X.; Xu, Y., Organophosphorus pesticides detection using broad-specific single-stranded DNA based fluorescence polarization aptamer assay. *Biosensors and Bioelectronics* **2014,** *55*, 216-219.
191. Dou, X.; Chu, X.; Kong, W.; Luo, J.; Yang, M., A gold-based nanobeacon probe for fluorescence sensing of organophosphorus pesticides. *Analytica Chimica Acta* **2015,** *891*, 291-297.
192. Tang, T.; Deng, J.; Zhang, M.; Shi, G.; Zhou, T., Quantum dot-DNA aptamer conjugates coupled with capillary electrophoresis: A universal strategy for ratiometric detection of organophosphorus pesticides. *Talanta* **2016,** *146*, 55-61.
193. Wang, P.; Wan, Y.; Ali, A.; Deng, S.; Su, Y.; Fan, C.; Yang, S., Aptamer-wrapped gold nanoparticles for the colorimetric detection of omethoate. *Science China Chemistry* **2016,** *59* (2), 237-242.
194. Zhang, C.; Lin, B.; Cao, Y.; Guo, M.; Yu, Y., Fluorescence Determination of Omethoate Based on a Dual Strategy for Improving Sensitivity. *Journal of Agricultural and Food Chemistry* **2017,** *65* (14), 3065-3073.
195. Fan, L.; Zhao, G.; Shi, H.; Liu, M.; Li, Z., A highly selective electrochemical impedance spectroscopy-based aptasensor for sensitive detection of acetamiprid. *Biosensors and Bioelectronics* **2013,** *43*, 12-18.
196. Shi, H.; Zhao, G.; Liu, M.; Fan, L.; Cao, T., Aptamer-based colorimetric sensing of acetamiprid in soil samples: Sensitivity, selectivity and mechanism. *Journal of Hazardous Materials* **2013,** *260*, 754-761.

197. Weerathunge, P.; Ramanathan, R.; Shukla, R.; Sharma, T. K.; Bansal, V., Aptamer-Controlled Reversible Inhibition of Gold Nanozyme Activity for Pesticide Sensing. *Analytical Chemistry* **2014,** *86* (24), 11937-11941.
198. Yang, Z.; Qian, J.; Yang, X.; Jiang, D.; Du, X.; Wang, K.; Mao, H.; Wang, K., A facile label-free colorimetric aptasensor for acetamiprid based on the peroxidase-like activity of hemin-functionalized reduced graphene oxide. *Biosensors and Bioelectronics* **2015,** *65*, 39-46.
199. Jiang, D.; Du, X.; Liu, Q.; Zhou, L.; Dai, L.; Qian, J.; Wang, K., Silver nanoparticles anchored on nitrogen-doped graphene as a novel electrochemical biosensing platform with enhanced sensitivity for aptamer-based pesticide assay. *Analyst* **2015,** *140* (18), 6404-6411.
200. Li, H.; Qiao, Y.; Li, J.; Fang, H.; Fan, D.; Wang, W., A sensitive and label-free photoelectrochemical aptasensor using Co-doped ZnO diluted magnetic semiconductor nanoparticles. *Biosensors and Bioelectronics* **2016,** *77*, 378-384.
201. Guo, J.; Li, Y.; Wang, L.; Xu, J.; Huang, Y.; Luo, Y.; Shen, F.; Sun, C.; Meng, R., Aptamer-based fluorescent screening assay for acetamiprid via inner filter effect of gold nanoparticles on the fluorescence of CdTe quantum dots. *Analytical & Bioanalytical Chemistry* **2016,** *408* (2), 557-566.
202. Lin, B.; Yu, Y.; Li, R.; Cao, Y.; Guo, M., Turn-on sensor for quantification and imaging of acetamiprid residues based on quantum dots functionalized with aptamer. *Sensors and Actuators B: Chemical* **2016,** *229*, 100-109.
203. Hu, W.; Chen, Q.; Li, H.; Ouyang, Q.; Zhao, J., Fabricating a novel label-free aptasensor for acetamiprid by fluorescence resonance energy transfer between NH2-NaYF4: Yb, Ho@SiO2 and Au nanoparticles. *Biosensors and Bioelectronics* **2016,** *80*, 398-404.
204. Mei, Z.; Chu, H.; Chen, W.; Xue, F.; Liu, J.; Xu, H.; Zhang, R.; Zheng, L., Ultrasensitive one-step rapid visual detection of bisphenol A in water samples by label-free aptasensor. *Biosensors and Bioelectronics* **2013,** *39* (1), 26-30.
205. Xue, F.; Wu, J.; Chu, H.; Mei, Z.; Ye, Y.; Liu, J.; Zhang, R.; Peng, C.; Zheng, L.; Chen, W., Electrochemical aptasensor for the determination of bisphenol A in drinking water. *Microchimica Acta* **2013,** *180* (1), 109-115.
206. Zhang, Y.; Cao, T.; Huang, X.; Liu, M.; Shi, H.; Zhao, G., A Visible-Light Driven Photoelectrochemical Aptasensor for Endocrine Disrupting Chemicals Bisphenol A with High Sensitivity and Specificity. *Electroanalysis* **2013,** *25* (7), 1787-1795.
207. Zhou, L.; Wang, J.; Li, D.; Li, Y., An electrochemical aptasensor based on gold nanoparticles dotted graphene modified glassy carbon electrode for label-free detection of bisphenol A in milk samples. *Food Chemistry* **2014,** *162*, 34-40.
208. Yildirim, N.; Long, F.; He, M.; Shi, H.-C.; Gu, A. Z., A portable optic fiber aptasensor for sensitive, specific and rapid detection of bisphenol-A in water samples. *Environmental Science: Processes & Impacts* **2014,** *16* (6), 1379-1386.
209. Zhu, Y.; Cai, Y.; Xu, L.; Zheng, L.; Wang, L.; Qi, B.; Xu, C., Building An Aptamer/Graphene Oxide FRET Biosensor for One-Step Detection of Bisphenol A. *ACS Applied Materials & Interfaces* **2015,** *7* (14), 7492-7496.
210. Xu, J.; Li, Y.; Bie, J.; Jiang, W.; Guo, J.; Luo, Y.; Shen, F.; Sun, C., Colorimetric method for determination of bisphenol A based on aptamer-mediated aggregation of positively charged gold nanoparticles. *Microchimica Acta* **2015,** *182* (13), 2131-2138.
211. Ding, J.; Gu, Y.; Li, F.; Zhang, H.; Qin, W., DNA Nanostructure-Based Magnetic Beads for Potentiometric Aptasensing. *Analytical Chemistry* **2015,** *87* (13), 6465-6469.
212. Duan, N.; Zhang, H.; Nie, Y.; Wu, S.; Miao, T.; Chen, J.; Wang, Z., Fluorescence resonance energy transfer-based aptamer biosensors for bisphenol A using lanthanide-doped KGdF4 nanoparticles. *Analytical Methods* **2015,** *7* (12), 5186-5192.
213. Cheng, C.; Wang, S.; Wu, J.; Yu, Y.; Li, R.; Eda, S.; Chen, J.; Feng, G.; Lawrie, B.; Hu, A., Bisphenol A Sensors on Polyimide Fabricated by Laser Direct Writing for Onsite River Water

Monitoring at Attomolar Concentration. *ACS Applied Materials & Interfaces* **2016,** *8* (28), 17784-17792.
214. Zhang, D.; Yang, J.; Ye, J.; Xu, L.; Xu, H.; Zhan, S.; Xia, B.; Wang, L., Colorimetric detection of bisphenol A based on unmodified aptamer and cationic polymer aggregated gold nanoparticles. *Analytical Biochemistry* **2016,** *499*, 51-56.
215. Li, Y.; Xu, J.; Wang, L.; Huang, Y.; Guo, J.; Cao, X.; Shen, F.; Luo, Y.; Sun, C., Aptamer-based fluorescent detection of bisphenol A using nonconjugated gold nanoparticles and CdTe quantum dots. *Sensors and Actuators B: Chemical* **2016,** *222*, 815-822.
216. Chen, J.; Zhou, S., Label-free DNA Y junction for bisphenol A monitoring using exonuclease III-based signal protection strategy. *Biosensors and Bioelectronics* **2016,** *77*, 277-283.
217. Guo, X.; Wu, S.; Duan, N.; Wang, Z., Mn2+-doped NaYF4:Yb/Er upconversion nanoparticle-based electrochemiluminescent aptasensor for bisphenol A. *Analytical and Bioanalytical Chemistry* **2016,** *408* (14), 3823-3831.
218. Kazane, I.; Gorgy, K.; Gondran, C.; Spinelli, N.; Zazoua, A.; Defrancq, E.; Cosnier, S., Highly Sensitive Bisphenol-A Electrochemical Aptasensor Based on Poly(Pyrrole-Nitrilotriacetic Acid)-Aptamer Film. *Analytical Chemistry* **2016,** *88* (14), 7268-7273.
219. Deiminiat, B.; Rounaghi, G. H.; Arbab-Zavar, M. H.; Razavipanah, I., A novel electrochemical aptasensor based on f-MWCNTs/AuNPs nanocomposite for label-free detection of bisphenol A. *Sensors and Actuators B: Chemical* **2017,** *242*, 158-166.
220. He, M.-Q.; Wang, K.; Wang, J.; Yu, Y.-L.; He, R.-H., A sensitive aptasensor based on molybdenum carbide nanotubes and label-free aptamer for detection of bisphenol A. *Analytical and Bioanalytical Chemistry* **2017,** *409* (7), 1797-1803.
221. Zhang, Y.; Wang, Y.; Zhu, W.; Wang, J.; Yue, X.; Liu, W.; Zhang, D.; Wang, J., Simultaneous colorimetric determination of bisphenol A and bisphenol S via a multi-level DNA circuit mediated by aptamers and gold nanoparticles. *Microchimica Acta* **2017,** *184* (3), 951-959.
222. Beiranvand, Z. S.; Abbasi, A. R.; Dehdashtian, S.; Karimi, Z.; Azadbakht, A., Aptamer-based electrochemical biosensor by using Au-Pt nanoparticles, carbon nanotubes and acriflavine platform. *Analytical Biochemistry* **2017,** *518*, 35-45.
223. Bala, R.; Sharma, R. K.; Wangoo, N., Development of gold nanoparticles-based aptasensor for the colorimetric detection of organophosphorus pesticide phorate. *Analytical and Bioanalytical Chemistry* **2016,** *408* (1), 333-338.
224. Zhu, C.; Zeng, Z.; Li, H.; Li, F.; Fan, C.; Zhang, H., Single-Layer MoS2-Based Nanoprobes for Homogeneous Detection of Biomolecules. *Journal of the American Chemical Society* **2013,** *135* (16), 5998-6001.
225. Zhang, Z.; Oni, O.; Liu, J., New insights into a classic aptamer: binding sites, cooperativity and more sensitive adenosine detection. *Nucleic Acids Research* **2017,** *45* (13), 7593-7601.
226. Song, Y.; Tang, T.; Wang, X.; Xu, G.; Wei, F.; Wu, Y.; Song, Q.; Ma, Y.; Ma, Y.; Cen, Y.; Hu, Q., Highly selective and sensitive detection of adenosine utilizing signal amplification based on silver ions-assisted cation exchange reaction with CdTe quantum dots. *Sensors and Actuators B: Chemical* **2017,** *247*, 305-311.
227. Sergelen, K.; Liedberg, B.; Knoll, W.; Dostalek, J., A surface plasmon field-enhanced fluorescence reversible split aptamer biosensor. *Analyst* **2017,** *142* (16), 2995-3001.
228. Lin, Z.; Chen, L.; Zhang, G.; Liu, Q.; Qiu, B.; Cai, Z.; Chen, G., Label-free aptamer-based electrochemical impedance biosensor for 17[small beta]-estradiol. *Analyst* **2012,** *137* (4), 819-822.
229. Long, F.; Shi, H.; Wang, H., Fluorescence resonance energy transfer based aptasensor for the sensitive and selective detection of 17[small beta]-estradiol using a quantum dot-bioconjugate as a nano-bioprobe. *RSC Advances* **2014,** *4* (6), 2935-2941.
230. Ke, H.; Liu, M.; Zhuang, L.; Li, Z.; Fan, L.; Zhao, G., A Fetomolar Level 17β-estradiol Electrochemical Aptasensor Constructed On Hierachical Dendritic Gold Modified Boron-Doped Diamond Electrode. *Electrochimica Acta* **2014,** *137*, 146-153.

231. Huang, K.-J.; Liu, Y.-J.; Zhang, J.-Z.; Cao, J.-T.; Liu, Y.-M., Aptamer/Au nanoparticles/cobalt sulfide nanosheets biosensor for 17β-estradiol detection using a guanine-rich complementary DNA sequence for signal amplification. *Biosensors and Bioelectronics* **2015,** *67*, 184-191.
232. Fan, L.; Zhao, G.; Shi, H.; Liu, M., A simple and label-free aptasensor based on nickel hexacyanoferrate nanoparticles as signal probe for highly sensitive detection of 17β-estradiol. *Biosensors and Bioelectronics* **2015,** *68*, 303-309.
233. Li, Y.; Xu, J.; Jia, M.; Yang, Z.; Liang, Z.; Guo, J.; Luo, Y.; Shen, F.; Sun, C., Colorimetric determination of 17β-estradiol based on the specific recognition of aptamer and the salt-induced aggregation of gold nanoparticles. *Materials Letters* **2015,** *159*, 221-224.
234. Alsager, O. A.; Kumar, S.; Zhu, B.; Travas-Sejdic, J.; McNatty, K. P.; Hodgkiss, J. M., Ultrasensitive Colorimetric Detection of 17β-Estradiol: The Effect of Shortening DNA Aptamer Sequences. *Analytical Chemistry* **2015,** *87* (8), 4201-4209.
235. Zheng, H. Y.; Alsager, O. A.; Wood, C. S.; Hodgkiss, J. M.; Plank, N. O. V., Carbon nanotube field effect transistor aptasensors for estrogen detection in liquids. *Journal of Vacuum Science & Technology B, Nanotechnology and Microelectronics: Materials, Processing, Measurement, and Phenomena* **2015,** *33* (6), 06F904.
236. Dou, M.; Garcia, J. M.; Zhan, S.; Li, X., Interfacial nano-biosensing in microfluidic droplets for high-sensitivity detection of low-solubility molecules. *Chemical Communications* **2016,** *52* (17), 3470-3473.
237. Huang, H.; Shi, S.; Gao, X.; Gao, R.; Zhu, Y.; Wu, X.; Zang, R.; Yao, T., A universal label-free fluorescent aptasensor based on Ru complex and quantum dots for adenosine, dopamine and 17β-estradiol detection. *Biosensors and Bioelectronics* **2016,** *79*, 198-204.
238. Ni, X.; Xia, B.; Wang, L.; Ye, J.; Du, G.; Feng, H.; Zhou, X.; Zhang, T.; Wang, W., Fluorescent aptasensor for 17β-estradiol determination based on gold nanoparticles quenching the fluorescence of Rhodamine B. *Analytical Biochemistry* **2017,** *523*, 17-23.
239. Kashefi-Kheyrabadi, L.; Mehrgardi, M. A., Design and construction of a label free aptasensor for electrochemical detection of sodium diclofenac. *Biosensors and Bioelectronics* **2012,** *33* (1), 184-189.
240. Derikvand, H.; Roushani, M.; Abbasi, A. R.; Derikvand, Z.; Azadbakht, A., Design of folding-based impedimetric aptasensor for determination of the nonsteroidal anti-inflammatory drug. *Analytical Biochemistry* **2016,** *513*, 77-86.
241. Niu, X.; Huang, L.; Zhao, J.; Yin, M.; Luo, D.; Yang, Y., An ultrasensitive aptamer biosensor for the detection of codeine based on a Au nanoparticle/polyamidoamine dendrimer-modified screen-printed carbon electrode. *Analytical Methods* **2016,** *8* (5), 1091-1095.
242. Stojanovic, M. N.; de Prada, P.; Landry, D. W., Aptamer-Based Folding Fluorescent Sensor for Cocaine. *Journal of the American Chemical Society* **2001,** *123* (21), 4928-4931.
243. Zhang, J.; Wang, L.; Pan, D.; Song, S.; Boey, F. Y. C.; Zhang, H.; Fan, C., Visual Cocaine Detection with Gold Nanoparticles and Rationally Engineered Aptamer Structures. *Small* **2008,** *4* (8), 1196-1200.
244. Zuo, X.; Xiao, Y.; Plaxco, K. W., High Specificity, Electrochemical Sandwich Assays Based on Single Aptamer Sequences and Suitable for the Direct Detection of Small-Molecule Targets in Blood and Other Complex Matrices. *Journal of the American Chemical Society* **2009,** *131* (20), 6944-6945.
245. Wang, J.; Song, J.; Wang, X.; Wu, S.; Zhao, Y.; Luo, P.; Meng, C., An ATMND/SGI based label-free and fluorescence ratiometric aptasensor for rapid and highly sensitive detection of cocaine in biofluids. *Talanta* **2016,** *161*, 437-442.
246. Yu, H.; Canoura, J.; Guntupalli, B.; Lou, X.; Xiao, Y., A cooperative-binding split aptamer assay for rapid, specific and ultra-sensitive fluorescence detection of cocaine in saliva. *Chemical Science* **2017,** *8* (1), 131-141.
247. Rauf, S.; Zhang, L.; Ali, A.; Liu, Y.; Li, J., Label-Free Nanopore Biosensor for Rapid and Highly Sensitive Cocaine Detection in Complex Biological Fluids. *ACS Sensors* **2017,** *2* (2), 227-234.

248. Liu, Y.; Zhao, Q., Direct fluorescence anisotropy assay for cocaine using tetramethylrhodamine-labeled aptamer. *Analytical and Bioanalytical Chemistry* **2017,** *409* (16), 3993-4000.
249. Su, F.; Zhang, S.; Ji, H.; Zhao, H.; Tian, J.-Y.; Liu, C.-S.; Zhang, Z.; Fang, S.; Zhu, X.; Du, M., Two-Dimensional Zirconium-Based Metal–Organic Framework Nanosheet Composites Embedded with Au Nanoclusters: A Highly Sensitive Electrochemical Aptasensor toward Detecting Cocaine. *ACS Sensors* **2017,** *2* (7), 998-1005.
250. Chen, A.; Jiang, X.; Zhang, W.; Chen, G.; Zhao, Y.; Tunio, T. M.; Liu, J.; Lv, Z.; Li, C.; Yang, S., High sensitive rapid visual detection of sulfadimethoxine by label-freeaptasensor. *Biosensors and Bioelectronics* **2013,** *42*, 419-425.
251. Niu, S.; Lv, Z.; Liu, J.; Bai, W.; Yang, S.; Chen, A., Colorimetric Aptasensor Using Unmodified Gold Nanoparticles for Homogeneous Multiplex Detection. *PLOS ONE* **2014,** *9* (10), e109263.
252. Okoth, O. K.; Yan, K.; Liu, Y.; Zhang, J., Graphene-doped Bi2S3 nanorods as visible-light photoelectrochemical aptasensing platform for sulfadimethoxine detection. *Biosensors and Bioelectronics* **2016,** *86*, 636-642.
253. Du, G.; Zhang, D.; Xia, B.; Xu, L.; Wu, S.; Zhan, S.; Ni, X.; Zhou, X.; Wang, L., A label-free colorimetric progesterone aptasensor based on the aggregation of gold nanoparticles. *Microchimica Acta* **2016,** *183* (7), 2251-2258.
254. Du, G.; Wang, L.; Zhang, D.; Ni, X.; Zhou, X.; Xu, H.; Xu, L.; Wu, S.; Zhang, T.; Wang, W., Colorimetric aptasensor for progesterone detection based on surfactant-induced aggregation of gold nanoparticles. *Analytical Biochemistry* **2016,** *514*, 2-7.
255. Daprà, J.; Lauridsen, L. H.; Nielsen, A. T.; Rozlosnik, N., Comparative study on aptamers as recognition elements for antibiotics in a label-free all-polymer biosensor. *Biosensors and Bioelectronics* **2013,** *43*, 315-320.
256. Wang, H.; Wang, Y.; Liu, S.; Yu, J.; Xu, W.; Guo, Y.; Huang, J., Target-aptamer binding triggered quadratic recycling amplification for highly specific and ultrasensitive detection of antibiotics at the attomole level. *Chemical Communications* **2015,** *51* (39), 8377-8380.
257. Wang, X.; Dong, S.; Gai, P.; Duan, R.; Li, F., Highly sensitive homogeneous electrochemical aptasensor for antibiotic residues detection based on dual recycling amplification strategy. *Biosensors and Bioelectronics* **2016,** *82*, 49-54.
258. Sheng, L.; Ren, J.; Miao, Y.; Wang, J.; Wang, E., PVP-coated graphene oxide for selective determination of ochratoxin A via quenching fluorescence of free aptamer. *Biosensors and Bioelectronics* **2011,** *26* (8), 3494-3499.
259. Bonel, L.; Vidal, J. C.; Duato, P.; Castillo, J. R., An electrochemical competitive biosensor for ochratoxin A based on a DNA biotinylated aptamer. *Biosensors and Bioelectronics* **2011,** *26* (7), 3254-3259.
260. Wu, S.; Duan, N.; Ma, X.; Xia, Y.; Wang, H.; Wang, Z.; Zhang, Q., Multiplexed Fluorescence Resonance Energy Transfer Aptasensor between Upconversion Nanoparticles and Graphene Oxide for the Simultaneous Determination of Mycotoxins. *Analytical Chemistry* **2012,** *84* (14), 6263-6270.
261. Lu, Z.; Chen, X.; Hu, W., A fluorescence aptasensor based on semiconductor quantum dots and MoS2 nanosheets for ochratoxin A detection. *Sensors and Actuators B: Chemical* **2017,** *246*, 61-67.
262. Lv, L.; Li, D.; Liu, R.; Cui, C.; Guo, Z., Label-free aptasensor for ochratoxin A detection using SYBR Gold as a probe. *Sensors and Actuators B: Chemical* **2017,** *246*, 647-652.
263. Samokhvalov, A. V.; Safenkova, I. V.; Eremin, S. A.; Zherdev, A. V.; Dzantiev, B. B., Use of anchor protein modules in fluorescence polarisation aptamer assay for ochratoxin A determination. *Analytica Chimica Acta* **2017,** *962*, 80-87.
264. Yang, Y.; Li, W.; Shen, P.; Liu, R.; Li, Y.; Xu, J.; Zheng, Q.; Zhang, Y.; Li, J.; Zheng, T., Aptamer fluorescence signal recovery screening for multiplex mycotoxins in cereal samples based on photonic crystal microsphere suspension array. *Sensors and Actuators B: Chemical* **2017,** *248*, 351-358.

265. Li, S.; Liu, C.; Yin, G.; Zhang, Q.; Luo, J.; Wu, N., Aptamer-molecularly imprinted sensor base on electrogenerated chemiluminescence energy transfer for detection of lincomycin. *Biosensors and Bioelectronics* **2017,** *91*, 687-691.
266. Kim, Y.-J.; Kim, Y. S.; Niazi, J. H.; Gu, M. B., Electrochemical aptasensor for tetracycline detection. *Bioprocess and Biosystems Engineering* **2009,** *33* (1), 31.
267. Jeong, S.; Rhee Paeng, I., Sensitivity and Selectivity on Aptamer-Based Assay: The Determination of Tetracycline Residue in Bovine Milk. *The Scientific World Journal* **2012,** *2012*, 10.
268. He, L.; Luo, Y.; Zhi, W.; Wu, Y.; Zhou, P., A Colorimetric Aptamer Biosensor Based on Gold Nanoparticles for the Ultrasensitive and Specific Detection of Tetracycline in Milk. *Australian Journal of Chemistry* **2013,** *66* (4), 485-490.
269. He, L.; Luo, Y.; Zhi, W.; Zhou, P., Colorimetric Sensing of Tetracyclines in Milk Based on the Assembly of Cationic Conjugated Polymer-Aggregated Gold Nanoparticles. *Food Analytical Methods* **2013,** *6* (6), 1704-1711.
270. Wang, S.; Yong, W.; Liu, J.; Zhang, L.; Chen, Q.; Dong, Y., Development of an indirect competitive assay-based aptasensor for highly sensitive detection of tetracycline residue in honey. *Biosensors and Bioelectronics* **2014,** *57*, 192-198.
271. Kwon, Y. S.; Ahmad Raston, N. H.; Gu, M. B., An ultra-sensitive colorimetric detection of tetracyclines using the shortest aptamer with highly enhanced affinity. *Chemical Communications* **2014,** *50* (1), 40-42.
272. Luo, Y.; He, L.; Zhan, S.; Wu, Y.; Liu, L.; Zhi, W.; Zhou, P., Ultrasensitive Resonance Scattering (RS) Spectral Detection for Trace Tetracycline in Milk Using Aptamer-Coated Nanogold (ACNG) as a Catalyst. *Journal of Agricultural and Food Chemistry* **2014,** *62* (5), 1032-1037.
273. Shen, G.; Guo, Y.; Sun, X.; Wang, X., Electrochemical Aptasensor Based on Prussian Blue-Chitosan-Glutaraldehyde for the Sensitive Determination of Tetracycline. *Nano-Micro Letters* **2014,** *6* (2), 143-152.
274. Guo, Y.; Shen, G.; Sun, X.; Wang, X., Electrochemical Aptasensor Based on Multiwalled Carbon Nanotubes and Graphene for Tetracycline Detection. *IEEE Sensors Journal* **2015,** *15* (3), 1951-1958.
275. Wang, S.; Liu, J.; Yong, W.; Chen, Q.; Zhang, L.; Dong, Y.; Su, H.; Tan, T., A direct competitive assay-based aptasensor for sensitive determination of tetracycline residue in Honey. *Talanta* **2015,** *131*, 562-569.
276. Guo, Y.; Wang, X.; Sun, X., *A label-free electrochemical aptasensor based on electrodeposited gold nanoparticles and methylene blue for tetracycline detection*. 2015; Vol. 10, p 3668-3679.
277. Jalalian, S. H.; Taghdisi, S. M.; Danesh, N. M.; Bakhtiari, H.; Lavaee, P.; Ramezani, M.; Abnous, K., Sensitive and fast detection of tetracycline using an aptasensor. *Analytical Methods* **2015,** *7* (6), 2523-2528.
278. Taghdisi, S. M.; Danesh, N. M.; Ramezani, M.; Abnous, K., A novel M-shape electrochemical aptasensor for ultrasensitive detection of tetracyclines. *Biosensors and Bioelectronics* **2016,** *85*, 509-514.
279. Zhan, X.; Hu, G.; Wagberg, T.; Zhan, S.; Xu, H.; Zhou, P., Electrochemical aptasensor for tetracycline using a screen-printed carbon electrode modified with an alginate film containing reduced graphene oxide and magnetite (Fe3O4) nanoparticles. *Microchimica Acta* **2016,** *183* (2), 723-729.
280. Xue, J.; Liu, J.; Wang, C.; Tian, Y.; Zhou, N., Simultaneous electrochemical detection of multiple antibiotic residues in milk based on aptamers and quantum dots. *Analytical Methods* **2016,** *8* (9), 1981-1988.
281. Ouyang, Q.; Liu, Y.; Chen, Q.; Guo, Z.; Zhao, J.; Li, H.; Hu, W., Rapid and specific sensing of tetracycline in food using a novel upconversion aptasensor. *Food Control* **2017,** *81*, 156-163.
282. Kim, Y. S.; Niazi, J. H.; Gu, M. B., Specific detection of oxytetracycline using DNA aptamer-immobilized interdigitated array electrode chip. *Analytica Chimica Acta* **2009,** *634* (2), 250-254.

283. Kim, Y. S.; Kim, J. H.; Kim, I. A.; Lee, S. J.; Jurng, J.; Gu, M. B., A novel colorimetric aptasensor using gold nanoparticle for a highly sensitive and specific detection of oxytetracycline. *Biosensors and Bioelectronics* **2010,** *26* (4), 1644-1649.
284. Zheng, D.; Zhu, X.; Zhu, X.; Bo, B.; Yin, Y.; Li, G., An electrochemical biosensor for the direct detection of oxytetracycline in mouse blood serum and urine. *Analyst* **2013,** *138* (6), 1886-1890.
285. Yan, K.; Liu, Y.; Yang, Y.; Zhang, J., A Cathodic "Signal-off" Photoelectrochemical Aptasensor for Ultrasensitive and Selective Detection of Oxytetracycline. *Analytical Chemistry* **2015,** *87* (24), 12215-12220.
286. Liu, C.; Lu, C.; Tang, Z.; Chen, X.; Wang, G.; Sun, F., Aptamer-functionalized magnetic nanoparticles for simultaneous fluorometric determination of oxytetracycline and kanamycin. *Microchimica Acta* **2015,** *182* (15), 2567-2575.
287. Yuan, F.; Zhao, H.; Zhang, Z.; Gao, L.; Xu, J.; Quan, X., Fluorescent biosensor for sensitive analysis of oxytetracycline based on an indirectly labelled long-chain aptamer. *RSC Advances* **2015,** *5* (72), 58895-58901.
288. Lu, C.; Tang, Z.; Liu, C.; Kang, L.; Sun, F., Magnetic-nanobead-based competitive enzyme-linked aptamer assay for the analysis of oxytetracycline in food. *Analytical and Bioanalytical Chemistry* **2015,** *407* (14), 4155-4163.
289. Seo, H. B.; Kwon, Y. S.; Lee, J.-e.; Cullen, D.; Noh, H.; Gu, M. B., A novel reflectance-based aptasensor using gold nanoparticles for the detection of oxytetracycline. *Analyst* **2015,** *140* (19), 6671-6675.
290. Tan, B.; Zhao, H.; Du, L.; Gan, X.; Quan, X., A versatile fluorescent biosensor based on target-responsive graphene oxide hydrogel for antibiotic detection. *Biosensors and Bioelectronics* **2016,** *83*, 267-273.
291. Chen, M.; Gan, N.; Zhou, Y.; Li, T.; Xu, Q.; Cao, Y.; Chen, Y., An electrochemical aptasensor for multiplex antibiotics detection based on metal ions doped nanoscale MOFs as signal tracers and RecJf exonuclease-assisted targets recycling amplification. *Talanta* **2016,** *161*, 867-874.
292. Hosseini, M.; Mehrabi, F.; Ganjali, M. R.; Norouzi, P., A fluorescent aptasensor for sensitive analysis oxytetracycline based on silver nanoclusters. *Luminescence* **2016,** *31* (7), 1339-1343.
293. Su, R.; Xu, J.; Luo, Y.; Li, Y.; Liu, X.; Bie, J.; Sun, C., Highly selective and sensitive visual detection of oxytetracycline based on aptamer binding-mediated the anti-aggregation of positively charged gold nanoparticles. *Materials Letters* **2016,** *180*, 31-34.
294. Yan, Z.; Gan, N.; Li, T.; Cao, Y.; Chen, Y., A sensitive electrochemical aptasensor for multiplex antibiotics detection based on high-capacity magnetic hollow porous nanotracers coupling exonuclease-assisted cascade target recycling. *Biosensors and Bioelectronics* **2016,** *78*, 51-57.
295. Liu, S.; Wang, Y.; Xu, W.; Leng, X.; Wang, H.; Guo, Y.; Huang, J., A novel sandwich-type electrochemical aptasensor based on GR-3D Au and aptamer-AuNPs-HRP for sensitive detection of oxytetracycline. *Biosensors and Bioelectronics* **2017,** *88*, 181-187.
296. Li, Y.; Tian, J.; Yuan, T.; Wang, P.; Lu, J., A sensitive photoelectrochemical aptasensor for oxytetracycline based on a signal "switch off-on" strategy. *Sensors and Actuators B: Chemical* **2017,** *240*, 785-792.
297. Babaei, M.; Jalalian, S. H.; Bakhtiari, H.; Ramezani, M.; Abnous, K.; Taghdisi, S. M., Aptamer-Based Fluorescent Switch for Sensitive Detection of Oxytetracycline. *Australian Journal of Chemistry* **2017,** *70* (6), 718-723.
298. Zhu, Y.; Chandra, P.; Song, K.-M.; Ban, C.; Shim, Y.-B., Label-free detection of kanamycin based on the aptamer-functionalized conducting polymer/gold nanocomposite. *Biosensors and Bioelectronics* **2012,** *36* (1), 29-34.
299. Li, R.; Liu, Y.; Cheng, L.; Yang, C.; Zhang, J., Photoelectrochemical Aptasensing of Kanamycin Using Visible Light-Activated Carbon Nitride and Graphene Oxide Nanocomposites. *Analytical Chemistry* **2014,** *86* (19), 9372-9375.

300. Li, H.; Sun, D.-e.; Liu, Y.; Liu, Z., An ultrasensitive homogeneous aptasensor for kanamycin based on upconversion fluorescence resonance energy transfer. *Biosensors and Bioelectronics* **2014,** *55*, 149-156.
301. Sun, X.; Li, F.; Shen, G.; Huang, J.; Wang, X., Aptasensor based on the synergistic contributions of chitosan-gold nanoparticles, graphene-gold nanoparticles and multi-walled carbon nanotubes-cobalt phthalocyanine nanocomposites for kanamycin detection. *Analyst* **2014,** *139* (1), 299-308.
302. Wang, C.; Chen, D.; Wang, Q.; Tan, R., Kanamycin detection based on the catalytic ability enhancement of gold nanoparticles. *Biosensors and Bioelectronics* **2017,** *91*, 262-267.
303. Sharma, A.; Istamboulie, G.; Hayat, A.; Catanante, G.; Bhand, S.; Marty, J. L., Disposable and portable aptamer functionalized impedimetric sensor for detection of kanamycin residue in milk sample. *Sensors and Actuators B: Chemical* **2017,** *245*, 507-515.
304. Chen, M.; Gan, N.; Zhou, Y.; Li, T.; Xu, Q.; Cao, Y.; Chen, Y., A novel aptamer- metal ions-nanoscale MOF based electrochemical biocodes for multiple antibiotics detection and signal amplification. *Sensors and Actuators B: Chemical* **2017,** *242*, 1201-1209.
305. Zuo, X.; Song, S.; Zhang, J.; Pan, D.; Wang, L.; Fan, C., A Target-Responsive Electrochemical Aptamer Switch (TREAS) for Reagentless Detection of Nanomolar ATP. *Journal of the American Chemical Society* **2007,** *129* (5), 1042-1043.
306. Wang, J.; Wang, L.; Liu, X.; Liang, Z.; Song, S.; Li, W.; Li, G.; Fan, C., A Gold Nanoparticle-Based Aptamer Target Binding Readout for ATP Assay. *Advanced Materials* **2007,** *19* (22), 3943-3946.
307. Mohammad Danesh, N.; Ramezani, M.; Sarreshtehdar Emrani, A.; Abnous, K.; Taghdisi, S. M., A novel electrochemical aptasensor based on arch-shape structure of aptamer-complimentary strand conjugate and exonuclease I for sensitive detection of streptomycin. *Biosensors and Bioelectronics* **2016,** *75*, 123-128.
308. Emrani, A. S.; Danesh, N. M.; Lavaee, P.; Ramezani, M.; Abnous, K.; Taghdisi, S. M., Colorimetric and fluorescence quenching aptasensors for detection of streptomycin in blood serum and milk based on double-stranded DNA and gold nanoparticles. *Food Chemistry* **2016,** *190*, 115-121.
309. Taghdisi, S. M.; Danesh, N. M.; Nameghi, M. A.; Ramezani, M.; Abnous, K., A label-free fluorescent aptasensor for selective and sensitive detection of streptomycin in milk and blood serum. *Food Chemistry* **2016,** *203*, 145-149.
310. Wu, S.; Duan, N.; Li, X.; Tan, G.; Ma, X.; Xia, Y.; Wang, Z.; Wang, H., Homogenous detection of fumonisin B1 with a molecular beacon based on fluorescence resonance energy transfer between NaYF4: Yb, Ho upconversion nanoparticles and gold nanoparticles. *Talanta* **2013,** *116*, 611-618.
311. Zhao, Y.; Luo, Y.; Li, T.; Song, Q., Au NPs driven electrochemiluminescence aptasensors for sensitive detection of fumonisin B1. *RSC Advances* **2014,** *4* (101), 57709-57714.
312. Shi, Z.-Y.; Zheng, Y.-T.; Zhang, H.-B.; He, C.-H.; Wu, W.-D.; Zhang, H.-B., DNA Electrochemical Aptasensor for Detecting Fumonisins B1 Based on Graphene and Thionine Nanocomposite. *Electroanalysis* **2015,** *27* (5), 1097-1103.
313. Emrani, A. S.; Taghdisi, S. M.; Danesh, N. M.; Jalalian, S. H.; Ramezani, M.; Abnous, K., A novel fluorescent aptasensor for selective and sensitive detection of digoxin based on silica nanoparticles. *Analytical Methods* **2015,** *7* (9), 3814-3818.
314. Mashhadizadeh, M. H.; Naseri, N.; Mehrgardi, M. A., A digoxin electrochemical aptasensor using Ag nanoparticle decorated graphene oxide. *Analytical Methods* **2016,** *8* (39), 7247-7253.
315. Chung, E.; Jeon, J.; Yu, J.; Lee, C.; Choo, J., Surface-enhanced Raman scattering aptasensor for ultrasensitive trace analysis of bisphenol A. *Biosensors and Bioelectronics* **2015,** *64*, 560-565.
316. Marks, H. L.; Pishko, M. V.; Jackson, G. W.; Coté, G. L., Rational Design of a Bisphenol A Aptamer Selective Surface-Enhanced Raman Scattering Nanoprobe. *Analytical Chemistry* **2014,** *86* (23), 11614-11619.

317. Kuang, H.; Yin, H.; Liu, L.; Xu, L.; Ma, W.; Xu, C., Asymmetric Plasmonic Aptasensor for Sensitive Detection of Bisphenol A. *ACS Applied Materials & Interfaces* **2014,** *6* (1), 364-369.
318. Luo, Z.; Zhang, J.; Wang, Y.; Chen, J.; Li, Y.; Duan, Y., An aptamer based method for small molecules detection through monitoring salt-induced AuNPs aggregation and surface plasmon resonance (SPR) detection. *Sensors and Actuators B: Chemical* **2016,** *236*, 474-479.
319. Hao, L.; Gu, H.; Duan, N.; Wu, S.; Wang, Z., A chemiluminescent aptasensor for simultaneous detection of three antibiotics in milk. *Analytical Methods* **2016,** *8* (44), 7929-7936.
320. Dai, S.; Wu, S.; Duan, N.; Chen, J.; Zheng, Z.; Wang, Z., An ultrasensitive aptasensor for Ochratoxin A using hexagonal core/shell upconversion nanoparticles as luminophores. *Biosensors and Bioelectronics* **2017,** *91*, 538-544.
321. Wang, C.; Wang, C.; Wang, Q.; Chen, D., Resonance light scattering method for detecting kanamycin in milk with enhanced sensitivity. *Analytical and Bioanalytical Chemistry* **2017,** *409* (11), 2839-2846.
322. Hou, H.; Bai, X.; Xing, C.; Gu, N.; Zhang, B.; Tang, J., Aptamer-Based Cantilever Array Sensors for Oxytetracycline Detection. *Analytical Chemistry* **2013,** *85* (4), 2010-2014.
323. Fang, C.; Wu, S.; Duan, N.; Dai, S.; Wang, Z., Highly sensitive aptasensor for oxytetracycline based on upconversion and magnetic nanoparticles. *Analytical Methods* **2015,** *7* (6), 2585-2593.
324. Zhang, H.; Fang, C.; Wu, S.; Duan, N.; Wang, Z., Upconversion luminescence resonance energy transfer-based aptasensor for the sensitive detection of oxytetracycline. *Analytical Biochemistry* **2015,** *489*, 44-49.
325. Hun, X.; Xu, Y.; Xie, G.; Luo, X., Aptamer biosensor for highly sensitive and selective detection of dopamine using ubiquitous personal glucose meters. *Sensors and Actuators B: Chemical* **2015,** *209*, 596-601.
326. Chen, X.; Bai, X.; Li, H.; Zhang, B., Aptamer-based microcantilever array biosensor for detection of fumonisin B-1. *RSC Advances* **2015,** *5* (45), 35448-35452.
327. Pang, S.; Labuza, T. P.; He, L., Development of a single aptamer-based surface enhanced Raman scattering method for rapid detection of multiple pesticides. *Analyst* **2014,** *139* (8), 1895-1901.
328. Kim, K.; Gu, M.-B.; Kang, D.-H.; Park, J.-W.; Song, I.-H.; Jung, H.-S.; Suh, K.-Y., High-sensitivity detection of oxytetracycline using light scattering agglutination assay with aptasensor. *ELECTROPHORESIS* **2010,** *31* (18), 3115-3120.
329. Creative Diagnostics Bisphenol A ELISA kit. http://www.creative-diagnostics.com/Bisphenol-A-EIA-Kit-3972-464.htm.
330. Creative Diagnostics Carbofuran ELISA kit. http://www.creative-diagnostics.com/Carbofuran-EIA-Kit-244088-471.htm.
331. Creative Diagnostics Lincomycin EIA kit. http://www.creative-diagnostics.com/Lincomycin-EIA-Kit-244064-471.htm.
332. Creative Diagnostics Sulfadimethoxine ELISA kit. http://www.creative-diagnostics.com/Sulfadimethoxine-ELISA-Kit-3575-464.htm.
333. Modernwater Monitoring Rapid Assay for PCBs. http://www.modernwater-monitoring.com/pdf/MW_Factsheet_Rapid-Assay_PCB.pdf.
334. Strategic Diagnostics Inc Chlorpyrifos RaPID assay https://www.nemi.gov/methods/method_pdf/7261/.
335. DRG International Salivary Estradiol ELISA https://store.drg-international.com/shop/salivary-estradiol-elisa.asp.
336. DRG International Salivary Progesterone ELISA. https://store.drg-international.com/shop/salivary-progesterone-elisa.asp.
337. BiooScientific MaxSignal Ciprofloxacin ELISA kit. http://www.biooscientific.com/Antibiotic-Residue-Test-Kits/MaxSignal-Ciprofloxacin-ELISA-Test-Kit.
338. BiooScientific MaxSignal Oxytetracycline ELISA kit. http://www.biooscientific.com/Antibiotic-Residue-Test-Kits/MaxSignal-Oxytetracycline-ELISA-Kit.

339. MyBioSource Tetracyclines ELISA kit. https://www.mybiosource.com/prods/ELISA-Kit/Tetracyclines/TET/datasheet.php?products_id=280466.
340. Razak, C. N. A.; Salam, F.; Ampon, K.; Basri, M.; Salleh, A. B., Development of an ELISA for Detection of Parathion, Carbofuran, and 2,4-Dichlorophenoxyacetic Acid in Water, Soil, Vegetables, and Fruits. *Annals of the New York Academy of Sciences* **1998,** *864* (1), 479-484.
341. Sun, X.; Du, S.; Wang, X., Amperometric immunosensor for carbofuran detection based on gold nanoparticles and PB-MWCNTs-CTS composite film. *European Food Research and Technology* **2012,** *235* (3), 469-477.
342. Inui, H.; Takeuchi, T.; Uesugi, A.; Doi, F.; Takai, M.; Nishi, K.; Miyake, S.; Ohkawa, H., Enzyme-Linked Immunosorbent Assay with Monoclonal and Single-Chain Variable Fragment Antibodies Selective to Coplanar Polychlorinated Biphenyls. *Journal of Agricultural and Food Chemistry* **2012,** *60* (7), 1605-1612.
343. Endo, T.; Okuyama, A.; Matsubara, Y.; Nishi, K.; Kobayashi, M.; Yamamura, S.; Morita, Y.; Takamura, Y.; Mizukami, H.; Tamiya, E., Fluorescence-based assay with enzyme amplification on a micro-flow immunosensor chip for monitoring coplanar polychlorinated biphenyls. *Analytica Chimica Acta* **2005,** *531* (1), 7-13.
344. Liu, Y. H.; Chen, J.; Guo, Y. R.; Wang, C. M.; Liang, X.; Zhu, G. N., A sensitive monoclonal antibody-based enzyme-linked immunosorbent assay for chlorpyrifos residue determination in Chinese agricultural samples. *Journal of Environmental Science and Health, Part B* **2011,** *46* (4), 313-320.
345. Sun, Z.; Wang, W.; Wen, H.; Gan, C.; Lei, H.; Liu, Y., Sensitive electrochemical immunoassay for chlorpyrifos by using flake-like Fe3O4 modified carbon nanotubes as the enhanced multienzyme label. *Analytica Chimica Acta* **2015,** *899* (Supplement C), 91-99.
346. Lei, Y.; Fang, L.; Hamid Akash, M. S.; Liu, Z.; Shi, W.; Chen, S., Development and comparison of two competitive ELISAs for the detection of bisphenol A in human urine. *Analytical Methods* **2013,** *5* (21), 6106-6113.
347. Kim, K. S.; Jang, J.-r.; Choe, W.-S.; Yoo, P. J., Electrochemical detection of Bisphenol A with high sensitivity and selectivity using recombinant protein-immobilized graphene electrodes. *Biosensors and Bioelectronics* **2015,** *71* (Supplement C), 214-221.
348. Lacorn, M.; Fleischer, K.; Willig, S.; Gremmel, S.; Steinhart, H.; Claus, R., Use of biotinylated 17β-estradiol in enzyme-immunoassay development: Spacer length and chemical structure of the bridge are the main determinants in simultaneous streptavidin–antibody binding. *Journal of Immunological Methods* **2005,** *297* (1), 225-236.
349. Zhang, S.; Du, B.; Li, H.; Xin, X.; Ma, H.; Wu, D.; Yan, L.; Wei, Q., Metal ions-based immunosensor for simultaneous determination of estradiol and diethylstilbestrol. *Biosensors and Bioelectronics* **2014,** *52* (Supplement C), 225-231.
350. Peng, C.-F.; Duan, X.-H.; Pan, Q.-L.; Liu, L.-Q.; Xue, F., Ultrasensitive Nano-ELISA for Detecting Sulfadimethoxine in Chicken Tissue. *Journal of Chemistry* **2013,** *2013*, 5.
351. Saha, B.; Das, C., Development of a Highly Sensitive Enzyme Linked Immunosorbent Assay for Human Serum Progesterone using Penicillinase. *Journal of Immunoassay* **1991,** *12* (3), 391-412.
352. Dong, X.-X.; Yuan, L.-P.; Liu, Y.-X.; Wu, M.-F.; Liu, B.; Sun, Y.-M.; Shen, Y.-D.; Xu, Z.-L., Development of a progesterone immunosensor based on thionine-graphene oxide composites platforms: Improvement by biotin-streptavidin-amplified system. *Talanta* **2017,** *170* (Supplement C), 502-508.
353. Chen, J.-J.; Jiang, J.-Q., Monoclonal antibody-based solvent tolerable indirect competitive ELISA for monitoring ciprofloxacin residue in poultry samples. *Food and Agricultural Immunology* **2013,** *24* (3), 331-344.
354. Ionescu, R. E.; Jaffrezic-Renault, N.; Bouffier, L.; Gondran, C.; Cosnier, S.; Pinacho, D. G.; Marco, M. P.; Sánchez-Baeza, F. J.; Healy, T.; Martelet, C., Impedimetric immunosensor for the specific label free detection of ciprofloxacin antibiotic. *Biosensors and Bioelectronics* **2007,** *23* (4), 549-555.

355. Wang, Y.; Wang, R.; Wang, J.; Yang, H.; Song, J.; Wang, Y.; Deng, A., A sensitive and specific enzyme-linked immunosorbent assay for the detection of lincomycin in food samples. *Journal of the Science of Food and Agriculture* **2010,** *90* (12), 2083-2089.
356. Jeon, M.; Kim, J.; Paeng, K.-J.; Park, S.-W.; Paeng, I. R., Biotin–avidin mediated competitive enzyme-linked immunosorbent assay to detect residues of tetracyclines in milk. *Microchemical Journal* **2008,** *88* (1), 26-31.
357. Que, X.; Chen, X.; Fu, L.; Lai, W.; Zhuang, J.; Chen, G.; Tang, D., Platinum-catalyzed hydrogen evolution reaction for sensitive electrochemical immunoassay of tetracycline residues. *Journal of Electroanalytical Chemistry* **2013,** *704* (Supplement C), 111-117.
358. Le, T.; Yu, H.; Zhao, Z.; Wei, W., Development of a Monoclonal Antibody-Based ELISA for the Detection of Oxytetracycline and 4-Epi-Oxytetracycline Residues in Chicken Tissues. *Analytical Letters* **2012,** *45* (4), 386-394.

CHAPTER 3
SELECTIVE APTAMERS FOR DETECTION OF ESTRADIOL AND ETHYNYLESTRADIOL IN NATURAL WATERS

Published in *Environmental Science & Technology*, 2015

Akki, S. U.; Werth, C. J.; Silverman, S. K., Selective Aptamers for Detection of Estradiol and Ethynylestradiol in Natural Waters. *Environmental Science & Technology* **2015,** *49* (16), 9905-9913

3.1 Abstract

In vitro selections were used to identify new DNA aptamers for two endocrine disrupting compounds often found in treated and natural waters, 17β-estradiol (E2) and 17α-ethynylestradiol (EE). Equilibrium filtration was used to determine aptamer sensitivity/selectivity and dimethyl sulfate (DMS) probing to explore aptamer binding sites. The new E2 aptamers are at least 74-fold more sensitive for E2 than is a previously reported DNA aptamer, with dissociation constants (K_d values) of 0.6 μM. Similarly, the EE aptamers are highly sensitive for EE, with K_d of 0.5−1.0 μM. Selectivity values indicate that the E2 aptamers bind E2 and a structural analogue, estrone (E1), equally well and are at least 74-fold selective over EE. One EE aptamer is at least 53-fold more selective for EE over E2 or E1, but the other binds EE, E2, and E1 with similar affinity. The new aptamers do not lose sensitivity or selectivity in natural water from a local lake, despite the presence of natural organic matter (∼4 mg/L TOC). DMS probing suggests that E2 binding occurs in relatively flexible single-stranded DNA regions, an important finding for rational redesign of aptamers and their incorporation into sensing platforms. This is the first report of aptamers with strong selectivity for E2 and E1 over EE, or with strong selectivity for EE over E2 and E1. Such selectivity is important for achieving

the goal of creating practically useful DNA-based sensors that can distinguish structurally similar estrogenic compounds in natural waters.

3.2 Introduction

Endocrine-disrupting compounds (EDCs) compose a class of emerging contaminants that are a growing concern due to their negative impacts on human and aquatic life[1-6]. They originate from various municipal, industrial, and institutional sources including wastewater effluent and solid waste, as well as from feedlot runoff containing animal waste. Among the EDCs, 17β-estradiol (E2), 17α-ethynylestradiol (EE), and estrone (E1) (Figure 3.1A) have been widely detected in groundwater and surface water samples (~nM)[7]. The EPA included these three compounds in the list of contaminants that require monitoring in public water samples from 2013 to 2015 in accordance with the Unregulated Contaminant Monitoring Rule 3 (UCMR3). Of these contaminants, E2 and EE have the highest estrogenic potencies[8-9]. Therefore, sensitive, selective, rapid, and inexpensive methods for detection of E2 and EE in natural water samples are needed.

The current state-of-the-art for EDC detection includes chromatographic−spectroscopic methods (e.g., LC-MS, GCMS) and antibody-based molecular recognition assays such as ELISAs (enzyme-linked immunosorbent assays). The former techniques are associated with high sensitivity (~pM)[10-11] but are expensive, sometimes require extensive sample pretreatment (e.g., sample derivatization), are instrumentation- and time-intensive, and cannot be practically used for real-time analysis. The antibody-based molecular recognition assays are sensitive enough for natural samples (~nM to pM)[12-13] and are relatively inexpensive, but they can suffer from poor selectivity due to interference by analogues and matrix components[14-16]. Additionally, antibodies used in ELISAs need to be harvested from animals, which makes the process time-consuming[17] and a social concern[18].

An emerging field in sensor studies is based on molecular recognition by single-stranded DNA or RNA oligonucleotides called aptamers. Especially for DNA, the low-cost synthesis of an aptamer, coupled with its tolerance to a wide range of physiological conditions compared to antibodies, suggests that aptamers can be used in complex environmental matrixes. Moreover, aptamers can be readily functionalized to facilitate their integration into a variety of sensor platforms. Aptamer-based sensors[19-28], also referred to as aptasensors, can have high sensitivity (as low as fM)[29-31] and can be employed for real-time detection of contaminants and other compounds[32-34].

To date, only a single aptamer for E2 or its analogues has been reported. It does not discriminate strongly among E2, E1, and EE, and a binding constant as low as 0.13 μM was reported by Kim et al[35]. This published aptamer (no particular designation was used in ref 35) has been integrated into a number of sensing platforms, with detection based on fluorescence[36], a color change[37], or an electrochemical signal[35, 38]. Sensors developed using this aptamer had detection limits for E2 as low as 33 fM[30] and good binding affinity in natural waters[27, 30]. These reports highlight the improved detection limits of aptamer-based sensors relative to the binding affinities of the aptamers themselves. While these reports represent a major step forward in real-time monitoring of E2 in natural waters, greater selectivity for E2 over its analogues is needed to create sensors for selective monitoring of the many different estrogenic compounds of varying concentrations in natural waters.

The objectives of this study are to use in vitro selection to identify a new suite of DNA aptamers that bind with high sensitivity and selectively to E2 or EE; to determine if binding affinities change in natural waters that contain nontarget constituents (e.g., natural organic matter); and to explore the binding regions of the selected aptamers. In vitro selection was used,

often called SELEX (Systematic Evolution of Ligands by EXponential enrichment)[39-40], to identify DNA aptamers for E2 and EE (Figure 3.1B). Selection pressures were applied by increasing elution times to elute stronger binding aptamers (which have lower off-rates) or by decreasing eluent concentrations to identify aptamers that are sensitive to lower concentrations of the target. The equilibrium filtration assay was used to determine DNA binding affinities to E2, E1, and EE in clean selection buffer as well as in both tap water and natural water from a small urban lake, each amended with selection buffer after a one-step filtration. Binding affinities were used to determine sensitivities of the DNA aptamers, while the ratio of sensitivities for one EDC to another was used to calculate selectivities of the aptamers. Dimethyl sulfate (DMS) probing was used to methylate guanosine nucleotides of aptamers in the presence of the target compound (E2 or EE), with the expectation that only guanosine nucleotides not involved in the binding interaction with the target compound are accessible for methylation. Insights from these results suggest potential approaches for rational improvement of DNA aptamers.

3.3 Materials and Methods

Materials

The EDCs E2 (>98%), E1 (>99%), and EE (>98%) were obtained from Sigma-Aldrich. Tritiated EDCs 2,4,6,7-^{3}H-E2 (81 Ci/mmol) and 2,4,6,7-3H-E1 (94 Ci/mmol) were purchased from PerkinElmer, and 6,7-3H-EE (60 Ci/mmol) was obtained from American Radiolabeled Chemicals. DMS (dimethyl sulfate, >99%) was obtained from Acros. DNA oligonucleotides were prepared by solid-phase synthesis on an ABI 394 instrument using reagents from Glen Research or purchased from Integrated DNA Technologies (IDT). The oligonucleotides were purified either by PAGE (polyacrylamide gel electrophoresis) or phenol/chloroform extraction, followed by ethanol precipitation. For PAGE purification, 7 M urea denaturing PAGE was used

with running buffer TBE (89 mM each Tris and boric acid, 2 mM EDTA, pH 8.3), and oligonucleotides were extracted from the polyacrylamide with TEN buffer (10 mM Tris, pH 8.0, 1 mM EDTA, 300 mM NaCl). DNA oligonucleotides used in selections contained 40 consecutive random nucleotides (N_{40}) with known primer-binding regions on both ends (see Appendix B for details).

Immobilization of E2 and EE on Agarose Support

E2 and EE were immobilized on epoxy-activated agarose support (Sepharose 6B, GE Healthcare, catalog number 17-0480-01) by reaction of the phenolic hydroxy group of E2/EE with the epoxy group. The extent of derivatization was quantified by UV−visible spectroscopy (see Appendix B for details).

In Vitro Selection Procedure

In vitro selection was performed, seeking E2-selective and EE-selective aptamers. The selection strategy (Figure 3.1B) involved an initially random N_{40} pool of DNA sequences, of which 0.1% was 5′-^{32}P radiolabeled, in binding buffer (50 mM Tris, pH 7.5, 5 mM $MgCl_2$, and 300 mM NaCl). A 40-nucleotide random region was chosen as a trade-off between the ease of incorporating shorter aptamers into sensors and improved sensitivity and selectivity of long aptamers due to more complex folding. This DNA pool was exposed to agarose support contained in a preselection column to eliminate sequences that bind to the support at room temperature (23 °C). The flow-through from the preselection column was exposed to immobilized (agarose support-bound) E2/EE contained in a selection column. The selection column was washed with binding buffer containing 20% ethanol to remove any nonspecifically bound sequences. The E2/EE-bound sequences were eluted for a total of 1 h from the selection column with binding buffer containing 200 μM E2 or binding buffer containing 20 μM EE.

Eluted sequences were PCR-amplified and taken into the next selection round (the desired, forward single strand was separable because the reverse strand was initiated with a primer that includes a nonamplifiable spacer). After each round, the binding activity of the pool was quantified according to the fraction of sequences that eluted specifically with E2/EE. For rounds 9+ of the E2 selection, a longer elution time pressure was applied (6 h total elution time) to promote elution of tighter-binding sequences, which have slower off-rates. In the EE selection, a lower eluent concentration of EE was used as a concentration pressure from the beginning of the selection to identify aptamers that were sensitive to lower concentrations of EE. After 10 rounds of both selections, cloning and sequencing of the pools were performed. The clones were screened using a preliminary binding assay with immobilized E2/EE (see Appendix B for details).

Determining Aptamer Dissociation Constants (K_d Values) for E2 and Analogues by Equilibrium Filtration Assay

In the equilibrium filtration assay, a known DNA aptamer concentration was incubated in a 1.7 mL tube with 0.5 μM of EDC (including ~5 nM ^{3}H-EDC) in 200 μL of binding buffer with 2% (v/v) ethanol for 1 h at 23 °C. (For assays of the published aptamer from ref 35, their reported buffer was used instead: 100 mM Tris, pH 8.0, 10 mM $MgCl_2$, 200 mM NaCl, 25 mM KCl, and 5% ethanol.) The solution was transferred to a 10000 MW cutoff filter (Microcon YM-10, Millipore) and centrifuged at 5000g for 10 min. The volume of filtrate, ν_F, was measured (±2 μL) by pipet; a typical value was 90−95 μL. The filtrate was transferred to a 7 mL HDPE scintillation vial containing 5 mL of scintillation fluid (EcoScint O, National Diagnostics). The inner column of the cutoff filter was inverted and centrifuged at 1000g for 3 min to collect the retentate, for which the volume, ν_R, was typically 85−90 μL. The retentate was similarly

transferred to a scintillation vial. The inner column was washed with 2 × 300 µL of selection buffer (5 min incubation in inner tube, inversion, and centrifugation). Finally, the inner tube was flushed with 2 × 300 µL of ethanol by centrifugation at 17200g for 15 min. A scintillation counter (Beckman Coulter LS 6500) was used to quantify amounts of ^{3}H. For the retentate, the counts, C_R, were taken as the sum of the counts in the retentate and the two washes. For the filtrate, the counts, C_F, were taken as the sum of the counts in the filtrate and the two flushes.

The chemical binding equilibrium between an aptamer and its ligand is governed by equation 3.1, where A is the DNA aptamer and L is the ligand (here E2, EE, or E1). The equilibrium constant for this reaction, which is the dissociation constant K_d, is representative of the binding affinity of the aptamer to the ligand. Lower values of K_d indicate better binding affinities of the aptamer with the ligand. The total concentration c of L was fixed at 0.5 µM, although in several cases other values of c (e.g., 10 µM) were evaluated experimentally, with quantitatively similar outcomes (data not shown). The total DNA aptamer concentration, a, was varied from 0.01 to 50 µM. The concentration in a particular sample of the aptamer-ligand (A·L) complex, y, is related to c and a by equation 3.2. Solving for y leads to equation 3.3.

$$A \bullet L \leftrightarrow A + L \tag{3.1}$$

$$K_d = \frac{(a-y)(c-y)}{y} \tag{3.2}$$

$$y = \frac{(c+a+K_d)-\sqrt{(c+a+K_d)^2-4ca}}{2} \tag{3.3}$$

Equation 3.3 is used to determine K_d, where y is derived from the experimental data using equation 3.4. The midpoint of the plot of y versus a (as in Figure 3.2A) is derived from equation 3.3 by taking $y = c/2$, which results in equation 3.5. This allows correlation of the visually apparent midpoint with the actual K_d value; there is an offset of $c/2$.

$$y = \left(\frac{C_R - C_F \times \frac{\nu_R}{\nu_F}}{C_R + C_F}\right) \times c \tag{3.4}$$

$$a_{1/2} = K_d + \frac{c}{2} \tag{3.5}$$

In some cases, the data did not fit the model represented by a simple bimolecular interaction given by equation 3.1. Similar cases showing more complex DNA aptamer binding have been reported[31, 41], and equation 3.6 was applied, which incorporates a Hill coefficient, *n*, in order to accommodate the degree of cooperativity in binding. The equilibrium constant K_d for equation 3.6 is described by equation 3.7.

$$\mathrm{A} \bullet \mathrm{L}_n \leftrightarrow \mathrm{A} + n\mathrm{L} \tag{3.6}$$

$$K_d = \frac{(a-y)(c-ny)^n}{y} \tag{3.7}$$

As seen from equation 3.7, the concentration of the complex $\mathrm{A{\cdot}L_n}$, *y*, cannot be easily separated from the independent variable (*a*) and fit variables (K_d, *n*). Therefore, MATLAB was used to cover a landscape of K_d and *n* values and computed *y* for a given range of values of *a*. The best-fit values of K_d and *n* were found by minimizing the root-mean-square error between the computed and experimentally derived values of *y*. The plots with the Hill coefficient model fits are in Appendix B (Figure B.4), with errors of the fit values computed as described in Appendix B. For certain combinations of aptamer and ligand with weak binding, precise K_d values could not be determined because a limiting concentration of the aptamer−ligand complex could not be reached. In such cases, the lower limit of K_d was estimated as the maximum DNA concentration at which the data was obtained, i.e., $K_d \geq 50$ μM. For ease of comparison of different aptamers, a half-saturation constant $K_{1/2} = K_d^{1/n}$ was calculated, where $K_{1/2}$ represents the concentration of the ligand at which half the aptamer sites are occupied. When an aptamer−ligand interaction was modeled well by equation 3.1, $n = 1$ and $K_{1/2} = K_d$. Selectivity of each aptamer for the parent

ligand (E2 or EE) over its analogues was evaluated by taking the ratio of the half-saturation constants, i.e., $K_{1/2,\text{ analogue}} / K_{1/2,\text{ parent}}$.

DMS Probing

Probing by dimethyl sulfate (DMS) was used to interrogate the folded structures of nucleic acids. Each 5′-^{32}P-radiolabeled aptamer was incubated with a series of concentrations of E2 or EE, followed by treatment with DMS, which methylates the physically accessible N7 nitrogen atoms of guanosine nucleotides (see Appendix B for full procedures)[42]. Such methylation blocks the enzymatic activity of DNA polymerase, which therefore allows readout of the methylation sites. The DMS accessibilities of individual nucleotides change as the aptamer folds, typically by decreasing because the initially accessible N7 atoms become buried within the folded structure. The samples were treated with piperidine followed by PAGE. The methylated guanine nucleobases are good leaving groups, such that treatment with base (10% piperidine) leads to depurination followed by base-promoted strand scission (Figure 3.4A). Each PAGE band corresponds to a unique and assignable guanosine nucleotide of the aptamer. Band intensities for guanosine nucleotides that changed with E2/EE concentration were quantified and normalized.

Band intensities for individual guanosine nucleotides were first normalized within each lane to a particular guanosine nucleotide whose intensity did not appear to depend upon E2/EE concentration (G45 for E2Apt1, G56 for E2Apt2, G57 for EEApt1, and G38 for EEApt2). For each nucleotide, the resulting band intensities were renormalized to a value of 1 for the band intensity at the lowest nonzero E2/EE concentration of 1 nM. The final normalized band intensity was plotted against the concentration of E2/EE (c) according to equation 3.8, leading to a K_d value as determined from the data for that nucleotide. Fitted parameters I_{low} and I_{high} are the

limiting band intensities at low and high concentrations of EE/EE. All fitted values of I_{low} were 1.00 ± 0.03. The DMS probing data were modeled well by the equilibrium of equation 3.1, and therefore the more complicated fitting process associated with the equilibrium of equation 3.6 was unnecessary.

$$I_{obs} = \left(\frac{I_{low} + I_{high} \times \frac{c}{K_d}}{1 + \frac{c}{K_d}} \right) \tag{3.8}$$

3.4 Results

Identification of E2-Selective Aptamers

In vitro selection was performed to identify E2-selective aptamers (Figure 3.1B). The E2-binding activity was undetectable above background (~3%) until rounds 7 and 8, where 29% and 24% of the pool were bound to the immobilized E2 and then specifically eluted by free E2 with a 1 h elution step (Figure B.1 in Appendix B). Selection pressure for tighter binding (i.e., lower value of the dissociation constant, K_d) was imposed by increasing the elution time to 6 h, which enables elution of aptamers with slower off-rate and therefore tighter binding. In rounds 9 and 10 with the longer elution time, 23% and 35% binding were observed. Individual E2 aptamers were cloned from round 10 and screened according to their ability to bind to immobilized E2. On this basis, 16 unique E2-binding sequences were identified; these sequences did not segregate into any specific families (not shown). Preliminary experiments were performed, involving both (1) immobilized E2-binding assays analogous to the binding step used during selection itself and (2) dimethyl sulfate (DMS) probing experiments as described below. On the basis of these preliminary data, two aptamers designated as E2Apt1 and E2Apt2 (Figure B.2) were studied in greater detail because of their high binding affinities.

Characterization of E2-Selective Aptamers by Equilibrium Filtration Assay

The equilibrium filtration assay was used to quantify binding constants for E2Apt1 and E2Apt2, as well as the E2 aptamer reported by Kim et al[35]. The assays for the published aptamer were performed in the binding buffer reported in ref 35. The equilibrium distribution profile for E2Apt1 is shown in Figure 3.2A (same for E2Apt2 as shown in Figure B.3); the E2 data is not fit well at high E2 concentration by the curve corresponding to equation 3.3. Therefore, the Hill coefficient model of equations 3.6 and 3.7 were used, which allowed a better fit to the entire data set (Figure B.4). E2Apt1 and E2Apt2 were found to have K_d values for E2 of 0.60 and 0.56 μM, respectively, with Hill n values for E2 of 1.3 and 1.5, respectively (see Table 3.1 for tabulation of all K_d and n values in this report). In parallel, a reproducible and unexpectedly high K_d value ≥50 μM (with Hill n = 1) was determined for the E2 aptamer reported by Kim et al[35]. (Figure B.3), although its K_d was reported by those authors as 0.13 μM. This discrepancy in K_d for the E2 aptamer from ref 35 cannot be explained, but there is confidence in the reproducibility of measurements, which were made with each aptamer not immobilized in any way.

The equilibrium filtration assay was also used to assess K_d of E2Apt1 and E2Apt2 for binding to the E2 analogues E1 and EE. The Hill n values for the analogues were 1, as the data fit well to equation 3.3. To facilitate comparisons of aptamer sensitivity, in Figure 3.2B inverse K_d values of E2Apt1 and E2Apt2 was plotted for each of E2, E1, and EE binding, where higher values correspond to better sensitivity. It was observed that E2Apt1 and E2Apt2 bind with greatest affinity to E2 followed by E1 and last EE. For each E2 analogue, the aptamer selectivity was quantified as $K_{1/2,\text{analogue}} / K_{1/2,E2}$, where $K_{1/2} = K_d^{1/n}$ represents the EDC concentration at which the aptamer is half-saturated. Both aptamers gave similar results for their selectivity (Figure 3.3). Each aptamer bound to E1 nearly as well as E2, with only 4−7-fold selectivity for

E2. In contrast, each aptamer bound much less well to EE than to E2, with ≥74-fold selectivity for E2.

Characterization of E2-Selective Aptamers by Dimethyl Sulfate (DMS) Probing

DMS probing was used to identify guanosine N7 atoms (Figure 3.4A) in E2Apt1 and E2Apt2 whose accessibilities decrease with increasing E2/EE concentration. These locations are indicated in the representative PAGE images in Figure 3.4B with decreasing band intensities, which are quantified and plotted in Figure 3.4C. For both E2Apt1 and E2Apt2, numerous guanosines showed E2-dependent changes in guanosine methylation (7 guanosines for E2Apt1; 10 for E2Apt2). E2 induced changes in nucleobase accessibilities at a much lower concentration than did EE for these E2 aptamers, in accord with the equilibrium filtration assay data. The quantitative K_d values for E2 as determined by DMS probing are in the same range as the K_d values as determined by equilibrium filtration, using the Hill coefficient model. K_d values for all nucleotide positions as determined by DMS probing are collected in Table B.1.

The nucleotide sites of DMS methylation were mapped consistently to aptamer sequence components that are predicted by the mfold secondary structure prediction algorithm[43]. These sites are located within single-stranded regions rather than double-stranded regions, as illustrated in Figure 3.4D for E2Apt1 (see Figure B.6 for analogous data for the other three aptamers). The N7 atoms of guanosine nucleotides in these relatively flexible single-stranded regions are more likely to become buried upon aptamer folding and ligand binding. Single-stranded regions can adopt more complex binding sites with greater potential for molecular recognition.

Identification of EE-Selective Aptamers

Via the same selection approach, EE-selective aptamers were sought. Because the E2 selections gave aptamers with K_d values ≤1 μM, 20 μM rather than 200 μM EE in the elution step

was used, with the intention of fostering tighter EE binding. Using a constant 1 h elution time, binding was first observed as 10% at round 6, reaching 30% at round 10 (Figure B.1). Individual EE aptamers were cloned, and three unique clones that did not share any common binding motifs were identified. Two unique aptamers, EEApt1 and EEApt2 (Figure B.2), were studied further based on their high affinities.

Characterization of EE-Selective Aptamers by Equilibrium Filtration and DMS Probing

The same equilibrium filtration assay was used to characterize binding of EEApt1 and EEApt2 to each of EE, E2, and E1. EEApt1 and EEApt2 were found to have K_d values for EE of 0.95 and 0.46 μM, respectively (Table 3.1). Aptamer sensitivities of the EE aptamers are compared in Figure 3.2B, obtained by plotting inverse K_d values of EEApt1 and EEApt2 for each of E2, E1, and EE. EEApt1 shows the greatest affinity toward EE and significantly lower affinity toward E1 and E2. Conversely, EEApt2 binds with similar affinity to E2, EE, and E1.

Selectivity of the EE aptamers against E2 and E1 is compared in Figure 3.3. EEApt1 was the more selective of the two aptamers, with ≥53-fold selectivity for EE over both E1 and E2. Thus, EEApt1 had selectivity for its EE target that is comparable in magnitude to the E2 (versus EE) selectivity of both E2Apt1 and E2Apt2. In contrast, EEApt2 was only 3-fold selective for EE over E1 and essentially unselective between EE and E2. Given the relatively strong binding (low K_d value) of EEApt2, it can reasonably be considered as a general E2/EE/E1-binding aptamer (binding to EDCs other than these three was not evaluated).

DMS probing of EEApt1 revealed four guanosine sites where methylation depended upon the EE concentration, and these sites mapped onto the more flexible loop regions in the mfold-predicted secondary structure (Figure B.6). This is similar to the mapping of binding-affected guanosine sites in E2Apt1 and E2Apt2. However, analogous probing experiments with

EEApt2 revealed no guanosines whose accessibilities changed substantially with EE concentration. Although the underlying reason is unclear, it is interesting that only the more general aptamer (i.e., the one with little selectivity for one EDC over another) showed no change in guanosine methylation with ligand concentration.

Sensitivity and Selectivity of the New Aptamers in Natural Water Samples

Practical applications of aptamer-based sensors require that they function well under realistic conditions[44]. All four new aptamers (E2Apt1, E2Apt2, EEApt1, and EEApt2) were evaluated for their performance in a natural water sample collected from the small urban lake in Crystal Lake Park, Urbana, IL. The lake water was filtered through a 0.22 μm filter and stored at 4 °C. The lake water was characterized for anions, cations, and organics (see Table B.2 for water characterization). The TOC (~NVOC) of the lake sample, which could potentially interfere with the aptamer performance, was 4.43 mg/L. This is much greater than the amount of E2/EE/E1 used in the assays (~0.14 mg/L). The natural water was mixed with binding buffer (2:1) and spiked with 0.5 μM of one of E2, EE, or E1, and equilibrium filtration assays were performed. Neither K_d values (Table 3.1) nor aptamer selectivities (Figure 3.3) were significantly altered by the presence of the natural water, relative to K_d values and selectivities in binding buffer alone, which indicates that aptamer binding is specific to EDCs rather than general for a range of organic compounds. This finding suggests that the aptamer-based sensors should be able to detect contaminants in natural water without compromising detection limits due to interference from the environmental matrix. The aptamers were also tested in tap water from Urbana, IL (Table B.2), and the sensitivities and selectivities of the aptamers were conserved.

3.5 Discussion

In this study, four new DNA aptamers that have submicromolar dissociation constants (K_d values) for the EDCs 17β-estradiol (E2) and its artificial derivative 17α-ethynylestradiol (EE) were identified. Although Kim et al.[35] reported an E2 aptamer with K_d of 0.13 μM, in my hands and in accord with some[45-46] but not all other reports[31], I was unable to obtain this low K_d value, instead reproducibly finding $K_d \geq 50$ μM for their published aptamer. Because the original authors did not describe their selection procedure and provided no experimental data regarding their K_d value[35], this discrepancy cannot be explained.

Our new aptamers have one of two behaviors with regard to ligand selectivity. Those aptamers identified by in vitro selection for binding to E2 (E2Apt1 and E2Apt2) bind strongly to both E2 and estrone (E1) but not EE. In contrast, one of the aptamers identified for binding to EE (EEApt1) binds to EE and with at least 53-fold selectivity over E2 or E1. This outcome suggests that EEApt1 discriminates between E2/ E1 and EE via interactions that specifically involve the ethynyl functional group of EE, whereas selectivity between E2 and E1 would require a more subtle type of interaction. The data require that the ethynyl group either interferes with aptamer binding (for the E2-selective aptamers) or is part of a required binding interaction (for the EE-selective aptamers). Finally, EEApt2 does not discriminate among E2, E1, and EE. This result means that EEApt2 must interact only with functional groups common to all three compounds but not the ethynyl group.

Aptamers are known to be specific to their targets when identified by appropriate selection methods. For instance, the theophylline RNA aptamer binds to its target 10,000 times better than to caffeine, which differs from theophylline by a methyl group[47]. However, not all aptamers have such high selectivites. A study that identified DNA aptamers for PCBs found that

the aptamers display little selectivity toward specific congeners[48]. In natural waters, EDCs are detected at varying levels that span orders of magnitude. For example, in one study the maximum EE concentration in sewage treatment plant effluent was 3.7 pM (1.1 ng/L), while the maximum E1 concentration was 300 pM (82 ng/L)[49]. This 81-fold difference in concentration would require an EE aptamer with an even greater difference in selectivity to enable quantification.

In most cases, the DMS probing data suggest that specific guanosine nucleotides are involved in key aspects of ligand binding. From DMS probing of E2Apt1, E2Apt2, and EEApt1, these guanosine nucleotides lie either in the interior loops or at the base of stems of the lowest-energy configuration of the aptamer predicted by mfold. This is similar to another study in which an essential binding motif (which contains four guanosines) was located in the loop regions of multiple thyroxine aptamers[50]. Additionally, the E2 aptamers are G-rich sequences with the possibility of G-quadruplex formation that involve the N7 positions. E2 binding could stabilize the G-quadruplex in the aptamer−E2 complex, decreasing the availability of the N7 position for DMS methylation. However, high-resolution structural information typically obtained from X-ray or NMR studies is necessary to explore all of these possibilities. For EEApt2, the lack of change of guanosine accessibility with EE concentration may be related to the secondary structure of the aptamer (Figure B.6), which is composed of mostly stems and relatively short loop regions.

The submicromolar sensitivities and the selectivities of our new DNA aptamers are fully retained in natural water from a local lake, although the selection process was performed in a well-defined and simple laboratory binding buffer. This outcome is consistent with others' reports, in which in vitro selected aptamers have been identified in laboratory buffers yet retain

useful binding activities in "real" samples such as blood and urine[32-33, 51]. Moreover, the E2 aptamer from ref 35 has been employed in developing an optical sensor that was used to detect E2 as low as 5 nM in wastewater treatment plant effluents without any interference from the matrix[27].

Small-molecule aptamer K_d values ranging from 0.05 to ≥50 μM can be used to create sensors with practical detection limits and dynamic ranges that span concentrations which are much lower than the K_d values of the aptamers used on the sensor platforms[52-54]. Lower K_d values would make more sensitive sensors (Figure B.7), with a dynamic range that enables the detection of EDCs at concentrations observed in natural waters. The sensitivities and selectivities of our new aptamers, especially in natural water, bode well for practical application of the new aptamers as sensor modules. Electrochemical sensor devices that use the newly identified E2 and EE aptamers are under development.

3.6 Table and Figures

Table 3.1. K_d and Hill coefficient values for aptamers studied in this chapter

	K_d value, μM [a] (by equilibrium filtration assay)						K_d value, μM [a] (by DMS probing)	
	in binding buffer			in natural water diluted 2:1 with binding buffer			in probing buffer [b]	
aptamer	E2	EE	E1	E2	EE	E1	E2	EE
E2Apt1	0.60 ± 0.07 *(1.3 ± 0.1)*	≥50	2.5 ± 0.1	0.52 ± 0.09 *(1.4 ± 0.1)*	≥50	2.3 ± 0.1	0.17–0.47 [c]	— [d]
E2Apt2	0.56 ± 0.10 *(1.5 ± 0.1)*	≥50	4.9 ± 0.2	0.44 ± 0.09 *(1.5 ± 0.1)*	≥50	3.8 ± 0.2	0.52–0.80 [c]	— [d]
EEApt1	≥50	0.95 ± 0.09	≥50	≥50	0.79 ± 0.10	≥50	— [d]	1.3 to 4.0 [c]
EEApt2	0.56 ± 0.10 *(1.3 ± 0.1)*	0.46 ± 0.04	1.3 ± 0.1	0.87 ± 0.20 *(1.3 ± 0.1)*	0.50 ± 0.09	1.9 ± 0.2	— [d]	— [d]
Kim et al.[35]	≥50	≥50	≥50	nd	nd	nd	nd	nd

[a] Tabulated values represent the curve fit parameter (K_d) from data such as that in Figure 3.2A, Figure B.3 and Figure B.4. Values in parentheses represent the Hill coefficients n, for which the value is 1 when not explicitly stated. Errors correspond to curve-fit parameter errors or values calculated using covariance matrices as described in Appendix B. nd = not determined. $K_{1/2}$ values are derived from table values i.e. $K_{1/2} = K_d^{1/n}$; $K_{1/2}$ values are used to compute selectivities of aptamers.

[b] See Appendix B for description of the DMS probing buffer and experiment.

[c] Tabulated values represent the range of the best-fit K_d values from individual guanosine nucleotides, from data such as that shown in Figure 3.4C. See Table B.1 for individual nucleotide K_d values.

[d] K_d value could not be determined by this method because no guanosine nucleotide of EEApt2 showed dependence of DMS probing intensity on EE concentration.

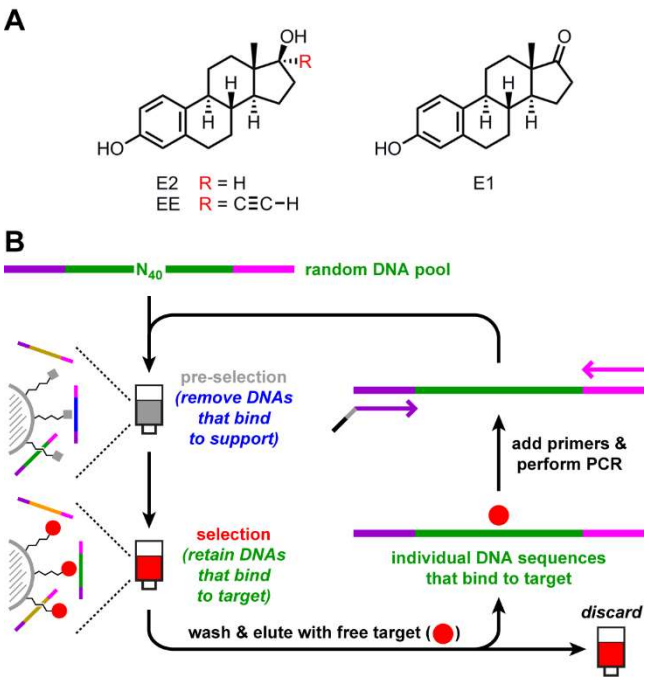

Figure 3.1. 17β-Estradiol (E2) and its derivatives 17α-ethynylestradiol (EE) and estrone (E1), and in vitro selection strategy for identification of aptamers. (A) E2, EE, and E1. (B) In vitro selection strategy.

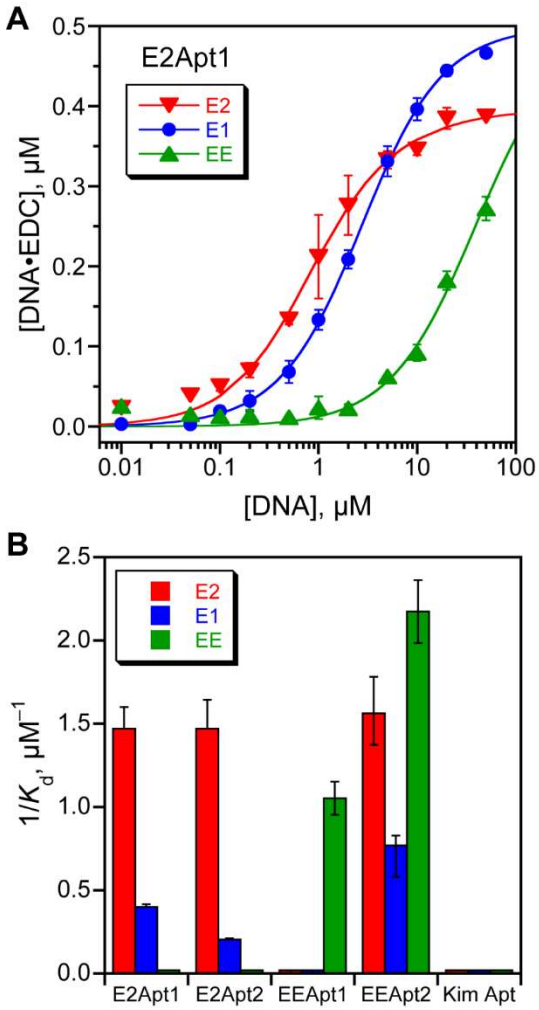

Figure 3.2. Dissociation constants (K_d values) for aptamers with E2 and analogues. (A) Data from equilibrium filtration assays to determine K_d values, obtained at [EDC] = 0.5 μM and plotted to allow fitting to equation (3.3) for EE and E1 data and equation (3.7) for E2 data as described in the Materials and Methods section. These data are for E2Apt1; see Figure B.3 for comprehensive data for all aptamers in this report, as well as the aptamer of Kim et al.[35] Error bars correspond to half of range from two independent measurements. For EE and E1 plots, the midpoint of the fitted curve is found at a DNA aptamer concentration of (K_d + 0.25) μM, as derived in the Materials and Methods section. That is, the actual K_d value is 0.25 μM lower than the apparent midpoint of the curves. The Hill coefficient for binding of E2 is slightly greater than 1 (Figure B.4). See Table 3.1 for K_d and Hill n values. (B) Comparison of dissociation constants for each aptamer with E2 and its two analogues. For ease of comparison (larger values = tighter binding), the K_d values are shown as their reciprocals, i.e., the association constants.

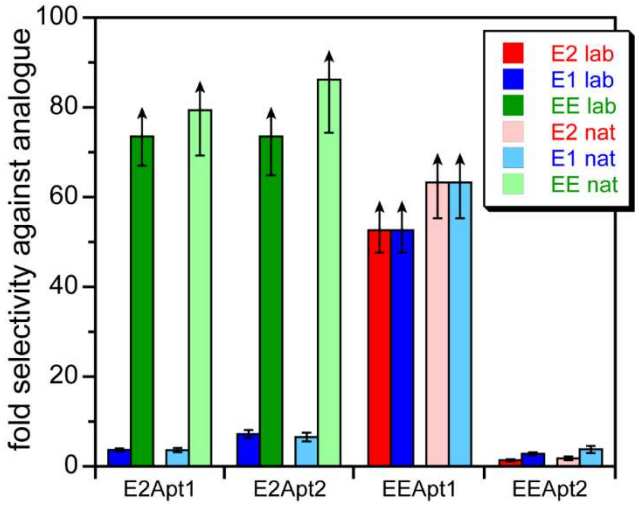

Figure 3.3. Aptamer selectivities, using $K_{1/2}$ values derived from Table 3.1, where $K_{1/2} = K_d^{1/n}$ (n = Hill coefficient). Note that when n = 1, $K_{1/2} = K_d$. For each E2 aptamer, the selectivity against the analogue was quantified as $K_{1/2}$(analogue)/$K_{1/2}$(E2). For each EE aptamer, the selectivity against the analogue was quantified as $K_{1/2}$(analogue)/$K_{1/2}$(EE). Data are shown for each indicated aptamer, labeled with the analogue identity as well as the water source ("lab" = laboratory water; "nat" = natural lake water). Error bars are propagated from the tabulated data by sum in quadrature for fractional error in the quotient. Data values shown with upward-pointing arrows are lower limits, because the K_d(analogue) value is a lower limit. In such cases, the error bar is simply derived from the fractional error in the denominator.

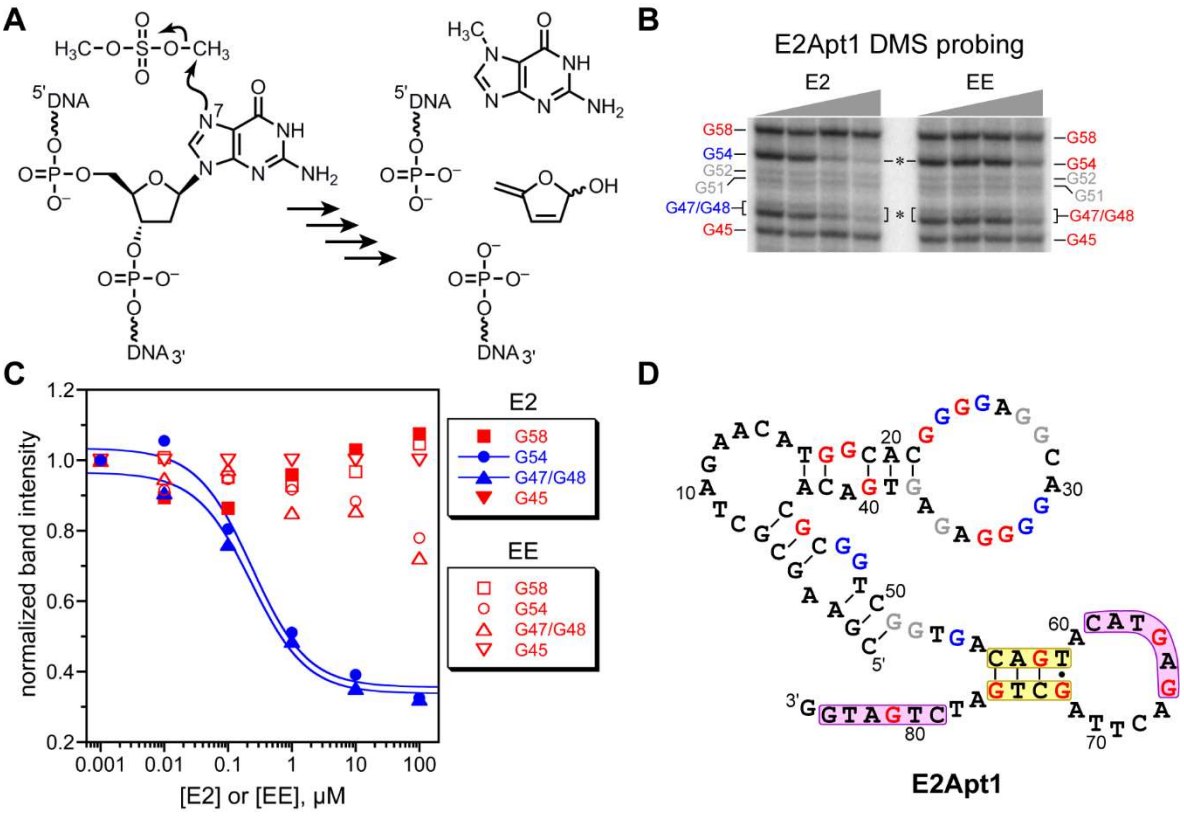

Figure 3.4. Dimethyl sulfate (DMS) probing. (A) Outcome of DMS methylation of guanosine N7, depurination, and strand scission. (B) Representative PAGE image for DMS probing of E2Apt1. Each band intensity correlates directly with the extent of methylation of the corresponding guanosine nucleotide. Lanes are shown for 0, 0.01, 1, and 100 μM E2/EE; see full image in Figure B.5. Asterisks denote the two nucleotide positions visible on this image, G47/G48 and G54, for which E2 and EE led to substantially different concentration dependence profiles. (C) Quantification of data from the panel B experiment. Representative data for DMS probing in the presence of E2 and EE are shown with filled and open symbols, respectively. Blue and red correspond to colors used in panel D for individual guanosines. Data were fit using equation (3.6) as described in the Materials and Methods section. K_d values are in Table 3.1 and Table B.1. (D) The lowest-energy mfold-predicted secondary structure of E2Apt1. Guanosines with substantial change in DMS accessibility as a function of E2 concentration are blue; guanosines with little or no change in accessibility are red; guanosines for which the band intensity was too low to provide useful E2 concentration dependence are grey; all non-guanosine nucleotides (and also several guanosines at the 5′- and 3′-ends for which accessibility information was not obtained) are black. In the next-lowest-energy structure (0.9 kcal/mol higher in free energy), the yellow-highlighted stem is broken, and the purple-highlighted nucleotides form a stem with one G-G mismatch. See Table B.1 and Figure B.6 for K_d values and secondary structures for E2Apt2, EEApt1, and EEApt2.

3.7 REFERENCES

1. Sharpe, R. M.; Skakkebaek, N. E., Are oestrogens involved in falling sperm counts and disorders of the male reproductive tract? *The Lancet* **1993,** *341* (8857), 1392-1396.
2. Folmar, L. C.; Denslow, N. D.; Rao, V.; Chow, M.; Crain, D. A.; Enblom, J.; Marcino, J.; Guillette, L. J., Vitellogenin induction and reduced serum testosterone concentrations in feral male carp (Cyprinus carpio) captured near a major metropolitan sewage treatment plant. *Environmental Health Perspectives* **1996,** *104* (10), 1096-1101.
3. Thayer, K. A.; Ruhlen, R. L.; Howdeshell, K. L.; Buchanan, D. L.; Cooke, P. S.; Preziosi, D.; Welshons, W. V.; Haseman, J.; Saal, F. S., Altered prostate growth and daily sperm production in male mice exposed prenatally to subclinical doses of 17α-ethinyl oestradiol. *APMIS* **2011,** *109* (S103), S278-S288.
4. Jobling, S.; Williams, R.; Johnson, A.; Taylor, A.; Gross-Sorokin, M.; Nolan, M.; Tyler, C. R.; van Aerle, R.; Santos, E.; Brighty, G., Predicted Exposures to Steroid Estrogens in U.K. Rivers Correlate with Widespread Sexual Disruption in Wild Fish Populations. *Environmental Health Perspectives* **2006,** *114* (Suppl 1), 32-39.
5. Kidd, K. A.; Blanchfield, P. J.; Mills, K. H.; Palace, V. P.; Evans, R. E.; Lazorchak, J. M.; Flick, R. W., Collapse of a fish population after exposure to a synthetic estrogen. *Proceedings of the National Academy of Sciences* **2007,** *104* (21), 8897.
6. Vilahur, N.; Bustamante, M.; Byun, H.-M.; Fernandez, M. F.; Santa Marina, L.; Basterrechea, M.; Ballester, F.; Murcia, M.; Tardón, A.; Fernández-Somoano, A.; Estivill, X.; Olea, N.; Sunyer, J.; Baccarelli, A. A., Prenatal exposure to mixtures of xenoestrogens and repetitive element DNA methylation changes in human placenta. *Environment International* **2014,** *71*, 81-87.
7. Kolpin, D. W.; Furlong, E. T.; Meyer, M. T.; Thurman, E. M.; Zaugg, S. D.; Barber, L. B.; Buxton, H. T., Pharmaceuticals, Hormones, and Other Organic Wastewater Contaminants in U.S. Streams, 1999−2000: A National Reconnaissance. *Environmental Science & Technology* **2002,** *36* (6), 1202-1211.
8. Van den Belt, K.; Berckmans, P.; Vangenechten, C.; Verheyen, R.; Witters, H., Comparative study on the in vitro/in vivo estrogenic potencies of 17β-estradiol, estrone, 17α-ethynylestradiol and nonylphenol. *Aquatic Toxicology* **2004,** *66* (2), 183-195.
9. Pillon, A.; Boussioux, A.-M.; Escande, A.; Aït-Aïssa, S.; Gomez, E.; Fenet, H.; Ruff, M.; Moras, D.; Vignon, F.; Duchesne, M.-J.; Casellas, C.; Nicolas, J.-C.; Balaguer, P., Binding of Estrogenic Compounds to Recombinant Estrogen Receptor-α: Application to Environmental Analysis. *Environmental Health Perspectives* **2005,** *113* (3), 278-284.
10. Hutchins, S. R.; White, M. V.; Hudson, F. M.; Fine, D. D., Analysis of Lagoon Samples from Different Concentrated Animal Feeding Operations for Estrogens and Estrogen Conjugates. *Environmental Science & Technology* **2007,** *41* (3), 738-744.
11. Grover, D. P.; Zhang, Z. L.; Readman, J. W.; Zhou, J. L., A comparison of three analytical techniques for the measurement of steroidal estrogens in environmental water samples. *Talanta* **2009,** *78* (3), 1204-1210.
12. Hirobe, M.; Goda, Y.; Okayasu, Y.; Tomita, J.; Takigami, H.; Ike, M.; Tanaka, H., The use of enzyme-linked immunosorbent assays (ELISA) for the determination of pollutants in environmental and industrial wastes. *Water Science and Technology* **2006,** *54* (11-12), 1.
13. Manickum, T.; John, W., The current preference for the immuno-analytical ELISA method for quantitation of steroid hormones (endocrine disruptor compounds) in wastewater in South Africa. *Analytical and Bioanalytical Chemistry* **2015,** *407* (17), 4949-4970.
14. Sawaya, W. N.; Lone, K. P.; Husain, A.; Dashti, B.; Al-Zenki, S., Screening for estrogenic steroids in sheep and chicken by the application of enzyme-linked immunosorbent assay and a comparison with analysis by gas chromatography–mass spectrometry. *Food Chemistry* **1998,** *63* (4), 563-569.

15. Farré, M.; Brix, R.; Kuster, M.; Rubio, F.; Goda, Y.; López de Alda, M. J.; Barceló, D., Evaluation of commercial immunoassays for the detection of estrogens in water by comparison with high-performance liquid chromatography tandem mass spectrometry HPLC–MS/MS (QqQ). *Analytical and Bioanalytical Chemistry* **2006,** *385* (6), 1001-1011.
16. Viganò, L.; Benfenati, E.; Cauwenberge, A. v.; Eidem, J. K.; Erratico, C.; Goksøyr, A.; Kloas, W.; Maggioni, S.; Mandich, A.; Urbatzka, R., Estrogenicity profile and estrogenic compounds determined in river sediments by chemical analysis, ELISA and yeast assays. *Chemosphere* **2008,** *73* (7), 1078-1089.
17. López de Alda, M. J. B., Damià Review of analytical methods for the determination of estrogens and progestogens in waste waters. *Fresenius Journal of Analytical Chemistry* **2001,** *371*, 437-447.
18. Committee on Methods of Producing Monoclonal Antibodies of the Institute for Laboratory Animal Research of the National Research Council. Animal-Welfare Issues Related to the Ascites Method for Producing Monoclonal Antibodies. In *Monoclonal Antibody Production*, National Academy Press: Washington DC, 1999.
19. O'Sullivan, C. K., Aptasensors – the future of biosensing? *Analytical and Bioanalytical Chemistry* **2002,** *372* (1), 44-48.
20. Nutiu, R.; Li, Y., In Vitro Selection of Structure-Switching Signaling Aptamers. *Angewandte Chemie International Edition* **2005,** *44* (7), 1061-1065.
21. Liu, J.; Lu, Y., Fast Colorimetric Sensing of Adenosine and Cocaine Based on a General Sensor Design Involving Aptamers and Nanoparticles. *Angewandte Chemie International Edition* **2006,** *45* (1), 90-94.
22. Zayats, M.; Huang, Y.; Gill, R.; Ma, C.-a.; Willner, I., Label-Free and Reagentless Aptamer-Based Sensors for Small Molecules. *Journal of the American Chemical Society* **2006,** *128* (42), 13666-13667.
23. Baker, B. R.; Lai, R. Y.; Wood, M. S.; Doctor, E. H.; Heeger, A. J.; Plaxco, K. W., An Electronic, Aptamer-Based Small-Molecule Sensor for the Rapid, Label-Free Detection of Cocaine in Adulterated Samples and Biological Fluids. *Journal of the American Chemical Society* **2006,** *128* (10), 3138-3139.
24. Willner, I.; Zayats, M., Electronic Aptamer-Based Sensors. *Angewandte Chemie International Edition* **2007,** *46* (34), 6408-6418.
25. Song, S.; Wang, L.; Li, J.; Fan, C.; Zhao, J., Aptamer-based biosensors. *TrAC Trends in Analytical Chemistry* **2008,** *27* (2), 108-117.
26. Vikesland, P. J.; Wigginton, K. R., Nanomaterial Enabled Biosensors for Pathogen Monitoring - A Review. *Environmental Science & Technology* **2010,** *44* (10), 3656-3669.
27. Yildirim, N.; Long, F.; Gao, C.; He, M.; Shi, H.-C.; Gu, A. Z., Aptamer-Based Optical Biosensor For Rapid and Sensitive Detection of 17β-Estradiol In Water Samples. *Environmental Science & Technology* **2012,** *46* (6), 3288-3294.
28. Kent, A. D.; Spiropulos, N. G.; Heemstra, J. M., General Approach for Engineering Small-Molecule-Binding DNA Split Aptamers. *Analytical Chemistry* **2013,** *85* (20), 9916-9923.
29. Deng, C.; Chen, J.; Nie, Z.; Wang, M.; Chu, X.; Chen, X.; Xiao, X.; Lei, C.; Yao, S., Impedimetric Aptasensor with Femtomolar Sensitivity Based on the Enlargement of Surface-Charged Gold Nanoparticles. *Analytical Chemistry* **2009,** *81* (2), 739-745.
30. Fan, L.; Zhao, G.; Shi, H.; Liu, M.; Wang, Y.; Ke, H., A Femtomolar Level and Highly Selective 17β-estradiol Photoelectrochemical Aptasensor Applied in Environmental Water Samples Analysis. *Environmental Science & Technology* **2014,** *48* (10), 5754-5761.
31. Ke, H.; Liu, M.; Zhuang, L.; Li, Z.; Fan, L.; Zhao, G., A Fetomolar Level 17β-estradiol Electrochemical Aptasensor Constructed On Hierarchical Dendritic Gold Modified Boron-Doped Diamond Electrode. *Electrochimica Acta* **2014,** *137*, 146-153.
32. Swensen, J. S.; Xiao, Y.; Ferguson, B. S.; Lubin, A. A.; Lai, R. Y.; Heeger, A. J.; Plaxco, K. W.; Soh, H. T., Continuous, Real-Time Monitoring of Cocaine in Undiluted Blood Serum via a

Microfluidic, Electrochemical Aptamer-Based Sensor. *Journal of the American Chemical Society* **2009,** *131* (12), 4262-4266.
33. Ferguson, B. S.; Hoggarth, D. A.; Maliniak, D.; Ploense, K.; White, R. J.; Woodward, N.; Hsieh, K.; Bonham, A. J.; Eisenstein, M.; Kippin, T. E.; Plaxco, K. W.; Soh, H. T., Real-Time, Aptamer-Based Tracking of Circulating Therapeutic Agents in Living Animals. *Science Translational Medicine* **2013,** *5* (213), 213ra165.
34. An, J. H.; Park, S. J.; Kwon, O. S.; Bae, J.; Jang, J., High-Performance Flexible Graphene Aptasensor for Mercury Detection in Mussels. *ACS Nano* **2013,** *7* (12), 10563-10571.
35. Kim, Y. S.; Jung, H. S.; Matsuura, T.; Lee, H. Y.; Kawai, T.; Gu, M. B., Electrochemical detection of 17β-estradiol using DNA aptamer immobilized gold electrode chip. *Biosensors and Bioelectronics* **2007,** *22* (11), 2525-2531.
36. Long, F.; Shi, H.; Wang, H., Fluorescence resonance energy transfer based aptasensor for the sensitive and selective detection of 17β-estradiol using a quantum dot-bioconjugate as a nano-bioprobe. *RSC Advances* **2014,** *4* (6), 2935-2941.
37. Liu, J.; Bai, W.; Niu, S.; Zhu, C.; Yang, S.; Chen, A., Highly sensitive colorimetric detection of 17β-estradiol using split DNA aptamers immobilized on unmodified gold nanoparticles. *Scientific Reports* **2014,** *4*, 7571.
38. Lin, Z.; Chen, L.; Zhang, G.; Liu, Q.; Qiu, B.; Cai, Z.; Chen, G., Label-free aptamer-based electrochemical impedance biosensor for 17β-estradiol. *Analyst* **2012,** *137* (4), 819-822.
39. Tuerk, C.; Gold, L., Systematic evolution of ligands by exponential enrichment: RNA ligands to bacteriophage T4 DNA polymerase. *Science* **1990,** *249* (4968), 505.
40. Ellington, A. D.; Szostak, J. W., In vitro selection of RNA molecules that bind specific ligands. *Nature* **1990,** *346* (6287), 818-822.
41. Levy, M.; Ellington, A. D., ATP-Dependent Allosteric DNA Enzymes. *Chemistry & Biology* **2002,** *9* (4), 417-426.
42. Maxam, A. M.; Gilbert, W., A new method for sequencing DNA. *Proceedings of the National Academy of Sciences of the United States of America* **1977,** *74* (2), 560-564.
43. Zuker, M., Mfold web server for nucleic acid folding and hybridization prediction. *Nucleic Acids Research* **2003,** *31* (13), 3406-3415.
44. *Functional Nucleic Acids for Analytical Applications*. Springer Science + Business Media, LLC: New York, 2009.
45. Huy, G. D.; Jin, N.; Yin, B.-C.; Ye, B.-C., A novel separation and enrichment method of 17β-estradiol using aptamer-anchored microbeads. *Bioprocess and Biosystems Engineering* **2011,** *34* (2), 189-195.
46. Langan, T. J.; Nyakubaya, V. T.; Casto, L. D.; Dolan, T. D.; Archer-Hartmann, S. A.; Yedlapalli , S. L.; Sooter, L. J.; Holland, L. A., Assessment of aptamer-steroid binding using stacking-enhanced capillary electrophoresis. *ELECTROPHORESIS* **2012,** *33* (5), 866-869.
47. Jenison, R. D.; Gill, S. C.; Pardi, A.; Polisky, B., High-resolution molecular discrimination by RNA. *Science* **1994,** *263* (5152), 1425.
48. Mehta, J.; Rouah-Martin, E.; Van Dorst, B.; Maes, B.; Herrebout, W.; Scippo, M.-L.; Dardenne, F.; Blust, R.; Robbens, J., Selection and Characterization of PCB-Binding DNA Aptamers. *Analytical Chemistry* **2012,** *84* (3), 1669-1676.
49. Baronti, C.; Curini, R.; D'Ascenzo, G.; Di Corcia, A.; Gentili, A.; Samperi, R., Monitoring Natural and Synthetic Estrogens at Activated Sludge Sewage Treatment Plants and in a Receiving River Water. *Environmental Science & Technology* **2000,** *34* (24), 5059-5066.
50. Lévesque, D.; Beaudoin, J.-D.; Roy, S.; Perreault, J.-P., In vitro selection and characterization of RNA aptamers binding thyroxine hormone. *Biochemical Journal* **2007,** *403* (Pt 1), 129-138.
51. Roncancio, D.; Yu, H.; Xu, X.; Wu, S.; Liu, R.; Debord, J.; Lou, X.; Xiao, Y., A Label-Free Aptamer-Fluorophore Assembly for Rapid and Specific Detection of Cocaine in Biofluids. *Analytical Chemistry* **2014,** *86* (22), 11100-11106.

52. Wu, J.; Chu, H.; Mei, Z.; Deng, Y.; Xue, F.; Zheng, L.; Chen, W., Ultrasensitive one-step rapid detection of ochratoxin A by the folding-based electrochemical aptasensor. *Analytica Chimica Acta* **2012,** *753*, 27-31.
53. Jiang, B.; Wang, M.; Chen, Y.; Xie, J.; Xiang, Y., Highly sensitive electrochemical detection of cocaine on graphene/AuNP modified electrode via catalytic redox-recycling amplification. *Biosensors and Bioelectronics* **2012,** *32* (1), 305-308.
54. Xue, F.; Wu, J.; Chu, H.; Mei, Z.; Ye, Y.; Liu, J.; Zhang, R.; Peng, C.; Zheng, L.; Chen, W., Electrochemical aptasensor for the determination of bisphenol A in drinking water. *Microchimica Acta* **2013,** *180* (1), 109-115.

CHAPTER 4
EFFECTS OF IMMOBILIZING DNA APTAMERS ON BINDING TO ESTRADIOL AND ETHYNYLESTRADIOL

In preparation for submission to *ACS Sensors*

4.1 Abstract

Aptamers are often selected and characterized in their unattached or free state, but are immobilized on gold nanoparticles or electrode surfaces when integrated into an aptasensor. Changes in aptamer binding affinity to target analytes when immobilized may be problematic for aptasensor development. A binding assay was used to determine the dissociation constants (K_d) of immobilized aptamers for 17β-estradiol (E2) and 17α-ethynylestradiol (EE), where biotinylated aptamers were attached to streptavidin-coated magnetic beads (MμBs). The E2 aptamer, E2Apt1, retains its binding affinity when immobilized either at the 5′ or 3′ end. The K_d of the immobilized aptamer is moderately improved (0.14, 0.21 μM) compared to the free aptamer K_d (0.65 μM). On the other hand, the EE aptamer EEApt1 loses all binding ability upon immobilization. The E2 aptamer, E2Apt2, retains its binding affinity when immobilized at its 3′ end (K_d = 0.25 μM) and its affinity is comparable to that of the free aptamer (K_d = 0.77 μM). On 5′ immobilization of E2Apt2, the aptamer binds to E2 up to a loading density (1 μM) beyond which the aptamer loses its binding ability, potentially due to dimerization. E2Apt1 (5′) was immobilized on gold nanoparticles, and it was found that the aptamer retains its binding affinity as with the MμBs. The binding affinity of immobilized aptamers is inversely correlated to the average linear distance of the binding pocket from the immobilized end, suggesting that undesirable interactions between DNA strands and/or other moieties are more likely when the binding pocket is further away from the surface. A favorably binding aptamer (E2Apt1) was

chosen to determine if the conformational change it undergoes upon binding is sufficient to inhibit electrochemical reduction on a 2 mm gold-electrode surface. The 5′ immobilized E2Apt1 did not cause a change in the electrochemical current, suggesting that obtaining sufficient conformational change upon binding to E2 is another challenge in aptasensor development.

4.2 Introduction

A variety of anthropogenic organic compounds have been detected in natural and surface waters[1]. A subset of these contaminants, called endocrine-disrupting compounds (EDCs), have adverse effects on the endocrine system and negatively impact aquatic and human health[2-7]. Among the EDCs, natural hormone 17β-estradiol (E2) and synthetic hormone 17α-ethynylestradiol (EE) are found to exhibit high estrogenic potency[8] and have been detected in surface water samples at nanomolar concentrations[1]. Typically, chromatographic-spectroscopic methods like LC-MS, GC-MS or antibody-based assays like ELISAs (enzyme linked immunosorbent assays) are used to detect these compounds[9-10]. However, the former techniques are expensive, time-consuming and require implementation by an expert. Additionally, ELISAs suffer from false positives due to interference from analogues and/or environmental matrix components[11-13].

An emerging technique employs the use of aptamer-based molecular detection of EDCs[14-16]. Aptamers are synthetic single-stranded oligonucleotides (DNA or RNA) that are selected to bind to a target of interest with desired sensitivity and selectivity[17-18]. DNA aptamers hold promise given their versatility, ability to withstand a broad range of physiological conditions, and low cost of synthesis. They have been identified for a variety of targets ranging from whole cells[19] to metal ions[20-21], including small organics[22-24] and proteins[25-26]. DNA aptamers are identified through a process called Systematic Evolution of Ligands through

EXponential enrichment, or SELEX[18]. In this process, a random pool of single-stranded DNA (ssDNA) is exposed to a column containing the desired target immobilized on resin. The sequences that bind to the target are retained on the column and are subsequently eluted using a denaturant or free target in buffer. These sequences are amplified using PCR, purified, and put through the same cycle until a DNA pool that exhibits high (usually >30%) binding activity is obtained. The ssDNA pool is cloned and sequenced to identify strongly binding aptamers.

Aptamers can be functionalized and are typically coupled with one of a suite of sensor platforms to create aptamer-based sensors (or aptasensors), in some cases with limits of detection as low as 1 fM[14, 27]. Typically, the binding of the target to the aptamer is accompanied with a change in the aptamer's conformation[28-29]. This change is transduced into a measurable signal change using the sensor platform, and the signal change is in turn correlated to the concentration of the target. Conformational change of an aptamer upon binding to a target is essential for most sensor applications. Such changes are potentially less drastic in aptamers for small organics compared to those for proteins, due to the difference in the size of the targets. Additionally, in many of the common platforms, e.g., electrochemical, colorimetric and fluorescence-based, aptamers are immobilized on a surface[30-32] (Figure 4.1). Since aptamer selection (i.e., SELEX method) is often performed using free (i.e., unattached) aptamers, immobilization may negatively affect aptamer conformation upon binding and aptamer binding affinity. Further, target compounds may nonspecifically bind to the immobilization surface, and adjacent DNA strands on the surface may undergo hybridization. Thus, there is a need to study the behavior of immobilized aptamers, particularly for small organics.

The objectives of this study are to evaluate the binding affinities of three immobilized aptamers to targets E2 or EE; to explore structural implications that affect binding due to

aptamer immobilization, and to determine if immobilized aptamers which exhibit suitable binding affinity can be converted into electrochemical aptasensors. Two E2 aptamers, E2Apt1 and E2Apt2, and one EE aptamer, EEApt1, developed in Chapter 3[24], were used in this study. They were immobilized at either end (3′ or 5′) on streptavidin-coated magnetic microbeads, and the binding affinities were determined using a one-step binding assay. Results are compared to those from Chapter 3, where binding affinities of these same aptamers to E2 or EE in solution were determined[24]. In order to probe surface effects, one of the aptamers that showed similar binding in solution and when immobilized on magnetic beads was further tested for target binding after immobilization on gold nanoparticles. Lastly, E2Apt1 (5′) was immobilized on a gold electrode (electrochemical platform), and square wave voltammetry was used to test if sufficient conformational change of the aptamer occurs upon introduction of the target for electrochemical detection.

4.3 Materials and Methods

Materials

The chemicals E2 (>98%), EE (>98%), 6-mercapto-1-hexanol (97%), potassium hexacyanoferrate(III) (>99%), and potassium cyanide (>98%) were obtained from Sigma-Aldrich. Tris(2-carboxyethyl)phosphine hydrochloride (TCEP-HCl) was obtained from Thermo Scientific. Tritiated EDCs 2,4,6,7-^{3}H-E2 (94Ci/mmol) and 6,7-^{3}H-EE (60Ci/mmol) were obtained from PerkinElmer and American Radiolabeled Chemicals, respectively. Scintillation cocktail Ecoscint-O was obtained from National Diagnostics. Thiohexyl-labeled and biotin-labeled DNA oligos were purchased from LGC Biosearch Technologies. Streptavidin-coated COMPEL magnetic beads (2.9μm diameter) were purchased from Bangs Laboratories. 15nm gold nanoparticles (AuNPs) were obtained from Ted Pella. 2mm diameter gold disc electrodes,

platinum wire electrode, Ag/AgCl and $Hg/HgSO_4$ reference electrodes (RE) and electrode polishing kit were obtained from CH Instruments. The DLK-70 potentiostat from Analytical Instrument Systems, Inc. was used for the electrochemical experiments. The Nanodrop 2000c (Thermo Scientific) was used for UV-Vis absorbance measurements for DNA and gold nanoparticle concentration quantification. A liquid scintillation counter (Beckman Coulter LS 6500) was used to quantify ^3H radioactivity.

Binding Assay of Aptamers on Magnetic Beads

Aptamers are often characterized by their dissociation constants (K_d), which is a measure of the strength of binding to a target analyte. A smaller K_d value implies that the aptamer is a strong binder and vice versa. A common approach for determining K_d values with unattached (free) aptamer and free target is the equilibrium filtration method, described in Chapter 3[33]. Here a one-step binding assay with immobilized aptamer and free target was conducted.

A fixed volume of streptavidin-coated magnetic microbeads (MμBs) suspension was aliquoted into a 2 mL low retention tube and washed by magnetically separating the MμBs, pipetting out the supernatant, and resuspending the MμBs in an equal volume of 1× PBS by vortexing for 2 min. The MμBs were washed in PBS two additional times before splitting them into 100 μL aliquots contained in 0.6 mL microcentrifuge tubes. For each sample, the supernatant was pipetted out and the MμBs were resuspended in 10 μL PBS containing biotin-labeled DNA aptamer (0, 0.2, 0.6, 2, 6, 20, 40 and 60 μM quantified by absorbance at 260 nm [$A_{260\text{-ini}}$]). The suspension was incubated for 2 h on a shaker at 1500rpm at room temperature. The supernatant was pipetted out and used to quantify the remaining DNA ($A_{260\text{-fin}}$). The DNA-derivatized MμBs were incubated with biotin in 10 μL PBS, such that the total amount of biotin (biotin-DNA and biotin) exposed to the MμBs was constant (0.6 nmol per sample). The

suspension was incubated for 1 h on a shaker at 1500rpm. The supernatant was pipetted out and stored ($A_{260\text{-}bio}$) and the MμBs were washed three times with 100μL PBS. The MμBs were resuspended in 20 μL selection buffer (50 mM Tris-HCl pH 7.5, 300 mM NaCl, 5 mM $MgCl_2$, 2% (v/v) ethanol) containing 0.05 μM tritiated EDC. This suspension was incubated for 2 h on a shaker at 1500 rpm at room temperature. The MμBs were separated and 10 μL of the supernatant was pipetted out and introduced into a scintillation vial containing 5 mL scintillation fluid to quantify the scintillation counts of free/unbound EDC (SC).

The amount of DNA bound to the MμBs was calculated using equation 4.1 based on Beer-Lambert's law,

$$a = \frac{(A_{260-i} - A_{260-fin} - A_{260-bio})}{\varepsilon\, l} \tag{4.1}$$

where pathlength l is 0.1cm and the extinction coefficient ε of the DNA was obtained from the IDT OligoAnalyzer web-based tool. This allows us to quantify the concentration of DNA aptamer, a, in the 20μL solution for the subsequent binding assay.

In order to estimate the dissociation constant (K_d) of the immobilized aptamer, the data was fit to equation 4.2 based on a target-aptamer binding model[24], where y is the concentration of the aptamer-target complex and c' is the total concentration of available EDC, that is not non-specifically bound to the MμBs.

$$y = \frac{(c'+a+K_d) - \sqrt{(c'+a+K_d)^2 - 4c'a}}{2} \tag{4.2}$$

The concentration of aptamer-target complex y was computed from equation 4.3, where SC_{Bare} and SC_{DNA} are scintillation counts of the supernatant of bare MμBs and DNA-derivatized MμBs, respectively. SC_{total} is the total scintillation counts of the tritiated EDC introduced per tube, and c is the total concentration of the EDC in the binding solution (0.05μM).

$$y = \frac{\mathrm{SC}_{Bare} - \mathrm{SC}_{DNA}}{\mathrm{SC}_{total}} \times c \quad (4.3)$$

Binding Assay of E2 Aptamer on AuNPs

The disulfide bond on the thiohexyl-labeled DNA (aptamer or non-specific DNA) was first reduced by incubation with 10mM TCEP-HCl solution for 1 h at room temperature. The thiolated DNA was extracted using ethanol precipitation followed by dissolution in 1mM Tris-acetate pH 8.2 buffer resulting in a ~30µM thiol-DNA solution. The thiol-DNA was attached to the AuNPs using a previously established protocol[34]. Briefly, 1000µL of AuNP stock was aliquoted into a 1.5mL low retention tube and centrifuged at 14000rpm for 20 minutes at 20°C to precipitate the AuNPs. The supernatant was pipetted out and the AuNPs were resuspended in 500µL of 1 mM Tris-acetate buffer pH 8.2 along with 10uL of the thiol-DNA solution and incubated for 45 minutes at room temperature. 22 µL of 0.5 M citrate buffer pH 3 was introduced and this suspension was incubated for 10 min. 26.5 µL of 3 M NaCl was added and this suspension was incubated for 5 min. The AuNPs were washed two times with 500 µL of 1 mM Tris-acetate buffer pH 8.2 using the centrifugation-resuspension steps, as described before.

In order to quantify the number of DNA strands per AuNP, a previously established UV-Vis absorbance-based protocol[35] was employed. Briefly, 100 µL of the DNA-AuNP composite was used to measure the absorbance at 520 nm (A_{520}) to quantify the concentration of AuNPs in the solution (ε_{AuNP} = 3.64 x 10^8 M^{-1} cm^{-1}) using Beer-Lambert's law. 125 µL of 16 mM KCN solution was added to 375 µL of the composite and incubated for 30 min to decompose the AuNPs. The A_{260} value of this solution (dDNA-AuNPs) was noted to compute the absorbance due to DNA in the sample using equation 4.4, which corrects for background absorbance due to decomposition of unmodified AuNPs (dAuNPs). The corrected absorbance ($A_{260,DNA}$) was used to calculate the concentration of DNA in the sample using Beer-Lambert's law.

$$A_{260,DNA} = A_{260,dDNA-AuNPs} - A_{260,dAuNPs} \quad (4.4)$$

To carry out the binding assay, the desired amount of DNA-AuNP composite in 1mM Tris-acetate buffer pH 8.2 was centrifuged and the supernatant pipetted out. This composite was resuspended in 100 µL of selection buffer containing 0.01 µM tritiated E2. This solution was incubated for 90 min at room temperature with brief vortexing every 30 min. The solution was centrifuged at 25°C and 50 µL of the supernatant was aliquoted into a scintillation vial containing 5 mL scintillation cocktail. The scintillation counts from each sample serves as a measure of the amount of free unbound E2.

Electrochemical Sensor Incorporating E2 Aptamer

In a 90 µL volume, 8 µM thiol-DNA was reduced using 10 mM TCEP-HCl for 1 h at room temperature. An equal volume of buffer (20 mM KH_2PO_4, 1 M NaCl) was added and the solution was adjusted to pH 7 by adding 2.33 µL of 0.77 M NaOH. The gold electrodes were polished using alumina slurry (1, 0.3 and 0.05 µm), followed by sonication in 50% (v/v) ethanol solution for 5 min. Each electrode was cleaned in 0.5M H_2SO_4 using cyclic voltammetry (0 to 1.1 V vs $Hg/HgSO_4$, scan rate 100 mV/s, 5 sweeps), rinsed, and dried under N_2 gas. Each electrode was incubated with 20µL of the thiol-DNA solution for 1 h at room temperature. Each electrode was rinsed with DI water and subsequently incubated with 20 µL of 3 mM 6-mercapto-1-hexanol in buffer (10 mM KH_2PO_4, 500 mM NaCl) for 30 min to displace any non-specifically bound DNA. The electrodes were rinsed with DI water and incubated with 20 µL selection buffer for 15 min. The electrodes were rinsed with selection buffer (no ethanol) and inserted into an electrochemical cell containing 0.5mM potassium ferricyanide, also in selection buffer (no ethanol). A square wave voltammetry (SWV) scan was conducted with the following parameters: initial potential 0.6 V, final potential − 0.3 V (vs Ag/AgCl RE), pulse height 50 mV. The effect

of SW frequency was studied by varying it between 10, 25, 60 and 100Hz. After the initial SWV scan of each electrode, it was rinsed with DI water and incubated with 20 µL of selection buffer containing 10µM E2 for 1 h. Each electrode was rinsed with selection buffer (no ethanol) and immediately used for a final SWV scan. The change in peak current between the initial ($I_{p\text{-}ini}$) and final ($I_{p\text{-}fin}$) SWV scans was computed using equation 4.5.

$$\%\ signal\ change = \frac{I_{p-ini} - I_{p-fin}}{I_{p-ini}} \times 100 \quad (4.5)$$

4.4 Results and Discussion

MµB-Immobilized Aptamer Dissociation Constants

The biotin-labeled DNA was immobilized on the MµBs using the described protocol. At low concentrations of DNA in solution ($\leq$0.2 µM), 60-100% of the DNA is immobilized on the beads via streptavidin-biotin coupling, while at higher concentrations ($\geq$20µM) <20% of the DNA is immobilized (data not shown). Based on the manufacturer's data, each 100µL aliquot of MµBs has a capacity for 240 pmol of a biotinylated compound (biotin-FITC, MW = 831Da). Assuming this is the saturation loading of a biotinylated compound, at high DNA concentrations (60 µM) the surface sites were ~45% saturated. The saturation level is low, potentially due to the lower packing density of DNA strands (MW>26,000Da) compared to the small molecule, biotin-FITC. This finding is consistent with a previous study[36], which shows that long DNA strands have lower packing densities on surfaces compared to short ones. Additionally, the quantification of adsorbed DNA at higher concentrations (>60µM) was associated with large errors.

The percentage of target EDC remaining in the supernatant on equilibration with MµBs, without and with saturation loading of DNA aptamers, is shown in Figure 4.2. There is significant uptake (up to 75%) of EDCs to MµBs without any DNA aptamer immobilized on it, indicating non-specific adsorption to the MµB surface. In the presence of aptamers E2Apt1 and

E2Apt2, additional uptake compared to the underivatized MμBs was observed, suggesting that the aptamers maintain their binding activity upon immobilization. However, EEApt1 did not show any further uptake of EE when immobilized on the MμBs. In the binding model, the assumption is that the amount of non-specifically adsorbed EDC is constant since the number of MμBs and hence surface area introduced in each experiment is constant. Therefore, to compute the concentration of DNA-EDC complex, non-specifically adsorbed EDC was accounted for (equation 4.3), and the concentration of freely available EDC for binding was adjusted to c' (equation 4.2), instead of using the total EDC concentration c (0.05μM).

Binding assays were conducted using a constant concentration of EDC (*c)* and a range of MμBs-immobilized aptamer concentrations. The normalized concentration of aptamer-target complex on MμBs (adjusted for nonspecific adsorption) is plotted against the aptamer concentration for the three aptamers in Figure 4.3. Also plotted are results obtained in Chapter 3 for the unbound aptamer (from equilibrium filtration tests)[24]. For ease of comparison, the concentration of aptamer-target complex, y, was normalized against the available concentration of the EDC. Hence, y was normalized against c' for the MμBs binding assay, and y was normalized against c for the free (unattached) DNA since non-specific binding was not observed. Figure 4.3A shows a plot for aptamer E2Apt1 in its unattached form, as well as when immobilized on either its 5′ or 3′ end. In both cases of immobilization, upon increasing the DNA aptamer concentration, a steady increase in aptamer-target complex concentration was observed. These results indicate that E2Apt1 retains its binding ability when immobilized on either end. On the other hand, a similar plot for EEApt1 (Figure 4.3C) shows a lack of aptamer-target complex formation upon increasing the immobilized aptamer concentration. These results suggest that the aptamer when immobilized on either end entirely loses its binding ability. Figure 4.3B shows the

plot for E2Apt2; this aptamer retains its binding ability when immobilized on its 3′ end, evidenced by the formation of the complex upon increasing the immobilized aptamer concentration. However, 5′ immobilization shows an increase in complex concentration up to 1μM DNA loading, after which it decreases. Further discussion of these results is in the subsequent section.

The MμBs assay data was fit to equation 4.2 to obtain dissociation constants (K_d) for the aptamers that retain their binding affinity. However, the curve fit was poor when c or c' was fixed based on the observed data. Therefore, both parameters were fit i.e., K_d and c', and the inverse of K_d are plotted to compare the binding affinity of immobilized aptamers to unbound aptamers; results are shown in Figure 4.4. Small values of K_d are more favorable and signify better binding affinity of aptamers. The K_d values of immobilized E2Apt1 (3′ and 5′) and E2Apt2 (3′) aptamers are lower than those of unattached aptamers (from equilibrium filtration tests). These results indicate that the K_d values of immobilized aptamers are moderately improved in the case of both the E2 aptamers. This could be an artifact of the difference in concentrations of target used in the bead binding assay (0.05 μM) and equilibrium-filtration assay (0.5μM). The fitted c' values (c'_{fit}) were found to be less than the observed c' values in all cases (Table C.1). This indicates that the complex concentration levels off at a lower value than the maximum available target concentration. The potential implication is that at high DNA loadings, the DNA strands are not able to fold into favorable conformations to bind to the target of interest due to the high packing density[37]. As a result, the effective DNA concentration is lower, yielding lower concentrations of complex.

AuNP-Immobilized E2 Aptamer Binding

The binding characteristics of 5′ immobilized E2Apt1 was tested on AuNPs, since this aptamer exhibited the most favorable K_d in the MμBs assay. Colorimetric aptasensors often use AuNPs, in some cases with the aptamer covalently attached to them through thiol-gold bonds, and electrochemical atpasensors typically immobilize aptamers on a gold electrode surface. Like the MμBs, significant (up to ~90%) non-specific binding of E2 to citrate-capped AuNPs was observed. Also, unmodified AuNPs were unstable in high ionic strength buffers, such as the selection buffer. Therefore, a non-specific DNA sequence [polyAAC or $(AAC)_{16}$] was used as a negative control to stabilize the AuNPs and reduce the non-specific adsorption of the target. A previously established protocol[34] was used to immobilize the DNA on the AuNPs. The polyAAC-AuNPs accommodated 111.2 $\pm$ 1.1 (n=3) DNA strands per AuNP, while the E2Apt1-AuNPs accommodated 42.6 $\pm$ 0.9 (n=3) DNA strands per AuNP. The polyAAC is a 48-mer while the aptamer is an 85-mer. Short DNA strands tend to occupy less area, and our observation is consistent with a previous study[36].

To determine binding to the bound E2Apt1, the assumption is that E2 non-specifically adsorbs to the surface of the AuNPs, and access to these surface sites is independent of the DNA coverage on the AuNPs. From the AuNP binding assay, two adsorption isotherms were constructed – one with the polyAAC-AuNPs and the second with the E2Apt1-AuNPs (Figure C.1). The E2Apt1-AuNPs have more E2 "adsorbed" onto the surface compared to the polyAAC-AuNPs, implying that the aptamer is binding to the E2. From this set of isotherms, the concentration of complex was calculated and normalized against the total concentration of E2 introduced (c) since the available E2 (c') varies with the amount of AuNPs introduced. This normalized aptamer-target concentration is plotted against the total AuNP-immobilized aptamer

concentration in Figure 4.3A along with the results obtained from the equilibrium filtration and the MμBs assays. Increasing aptamer concentration shows an increase in aptamer-target complex concentration. Additionally, there is good agreement between the AuNP assay and the MμBs assay, indicating that the aptamer retains its binding affinity on the AuNP surface. However, the K_d could not be estimated using this data because the non-specific adsorption of E2 onto the AuNPs was very high (>95%) at high concentrations of DNA (more AuNPs introduced to achieve high DNA concentrations). This resulted in large errors in computing complex concentration. Yet, the data indicate that the E2Apt1 retains its binding affinity when immobilized on the AuNP surface.

Structural Insights into Aptamer Immobilization

As discussed in Chapter 3[24], dimethyl sulfate (DMS) was used to probe binding sites between each of the three DNA aptamers and their respective targets. DMS methylates the guanines which then react with an alkaline base causing the DNA strand to cleave. Guanines involved in binding to the target are either less or more prone to methylation resulting in decreased or increased strand cleavage. This difference in base-catalyzed cleavage in the absence and presence of target was observed on a PAGE gel and the guanines involved in binding the target were identified.

The E2 aptamers are guanine-rich and the binding regions were identified to be primarily located in the loops of the aptamers (Figure C.2). The three aptamer configurations that retain their binding activity upon immobilization i.e., E2Apt1 (5′ and 3′) and E2Apt2 (3′) were considered. First the average linear distance of the binding pocket was determined by averaging the linear distance to each guanine from the immobilized end of the aptamer. The assumption is that each base is 0.6nm in length[38] and only the guanines involved in binding with E2 were

accounted for, based on our previous data[24] from Chapter 3. The binding constant was plotted against the average linear distance of the binding "pocket" from the immobilized end of the aptamer, and results are shown in Figure 4.5. The data show that the closer the binding pocket to the immobilized end, the more favorable the binding affinity of the aptamer. The region closer to the immobilized end is probably rigidly held in place and may have less freedom to interact with other moieties (e.g., streptavidin, the polymer coating on the bead, neighboring DNA etc.) compared to the regions that are further away, potentially resulting in better binding closer to the site of immobilization. Modeling the DNA as linear strands on a surface has limitations since the DNA is likely to fold into complex tertiary structures. Therefore, these results are speculative in nature since the state-of-the-art has no means of predicting the 3D structure of the DNA based on the sequence.

Aptamer E2Apt2 (5′) creates a unique binding curve which shows increase in complex concentration up to 1 μM DNA loading, after which the complex concentration decreases (Figure 4.3B). Increased packing density at high concentrations of the DNA could potentially lead to self-dimerization through hybridization, leaving fewer single strands that are available for binding with the target. This dimerizing region (Figure C.2) is farther away from the immobilized end of the aptamer, potentially granting it more freedom to dimerize. Thermodynamically, the difference between free energy of self-folding of the aptamer (ΔG_{fold} = −7.1 kcal/mol) and that of homodimerization (ΔG_{dimer} = −18.0 kcal/mol) is a maximum for E2Apt2 compared to E2Apt1 (ΔG_{fold} = −5.4 kcal/mol, ΔG_{dimer} = −13.1 kcal/mol) and EEApt1 (ΔG_{fold} = − 6.7 kcal/mol, ΔG_{dimer} = −8.3 kcal/mol). This potentially favors dimerization most strongly in the case of E2Apt2. These values were calculated from IDT's oligo analyzer and mfold web-based tools[39]. Additionally, based on our chemical probing data reported

previously[24], the region of the DNA that dimerizes contains guanine bases that are involved in binding to the E2 (Figure C.2); this could lead to disruption of the binding pocket and thus complex formation. The spacing of DNA on the MμBs supports this hypothesis i.e., the length of the 86-nucleotide long aptamer is ~51nm if modeled as a ssDNA[38]. Beyond 1 μM concentration of MμB-immobilized DNA, the distance between DNA strands is <13nm (assuming hexagonal packing), indicating that more than 75% of the length of the strand can interact with its neighbors, resulting in reduced interaction with the target. However, modeling the DNA strands in a linear manner has its limitations because the DNA could fold into complex tertiary structures.

In the case of aptamer EEApt1 (5′ and 3′), complete loss of their binding ability upon immobilization is observed perhaps because the immobilization causes a disruption in the tertiary structure of the aptamers making them incapable of binding to the target.

E2 Aptamer-based Electrochemical Sensor

5′ thiol-labeled E2Apt1 was immobilized on the gold electrode and SWV was conducted. Based on the K_d value of immobilized aptamer and typical DNA packing on gold electrodes[40], >95% of the aptamer should be in complex form at 10 μM E2. However, no significant change in peak current on incubating the aptamer-modified electrodes with target E2 was observed (Figure 4.6). This could be due to insufficient conformational change of the aptamer upon binding to a small molecule such as E2 (MW = 272Da). Alternatively, a conformational change too far away from the electrode could have the same outcome. Additional attempts associated with methylene-blue tagged DNA aptamers and positive controls are reported in Appendix C.

Conformational changes are more pronounced with larger targets (e.g., proteins) due to the sheer size of the target. However, in one case, an immobilized DNA aptamer did not show

significant electrochemical signal change in the presence of target immunoglobulin G (MW= 190,000Da) despite exhibiting binding affinity to the target, evidenced by a change in surface plasmon resonance (SPR) signal[41].

Therefore, factors involving conformational change upon target binding and effect of immobilization on the binding affinity of the aptamer need to be considered while developing aptamers since the ultimate goal is incorporating them into aptasensors. Despite most sensor platforms employing immobilized aptamers, the traditional SELEX process isolates aptamers using free ssDNA. Therefore, testing the aptamer in its sensor configuration prior to sensor development is crucial. Alternatively, a modification of SELEX called capture-SELEX has the ssDNA pool attached to beads via hybridization with a DNA strand during the selection process[42]. Such a construct can be directly applied to a sensor platform, once aptamers are isolated, without testing if aptamers retain their binding affinity upon immobilization. Additionally, capture-SELEX is potentially a better method to isolate aptamers for targets such as small organics that cannot be readily immobilized on a matrix.

4.5 Figures

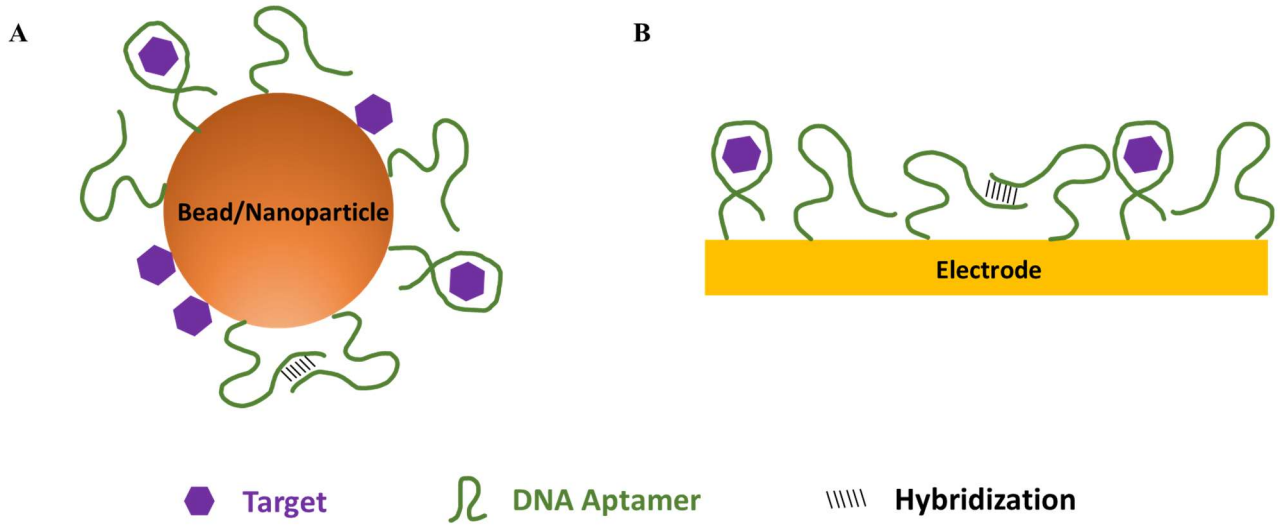

Figure 4.1. Aptamers immobilized on (A) colorimetric and (B) electrochemical platforms. Undesirable interactions include non-specific adsorption of the target on the sensor surface and hybridization of neighboring DNA aptamer strands.

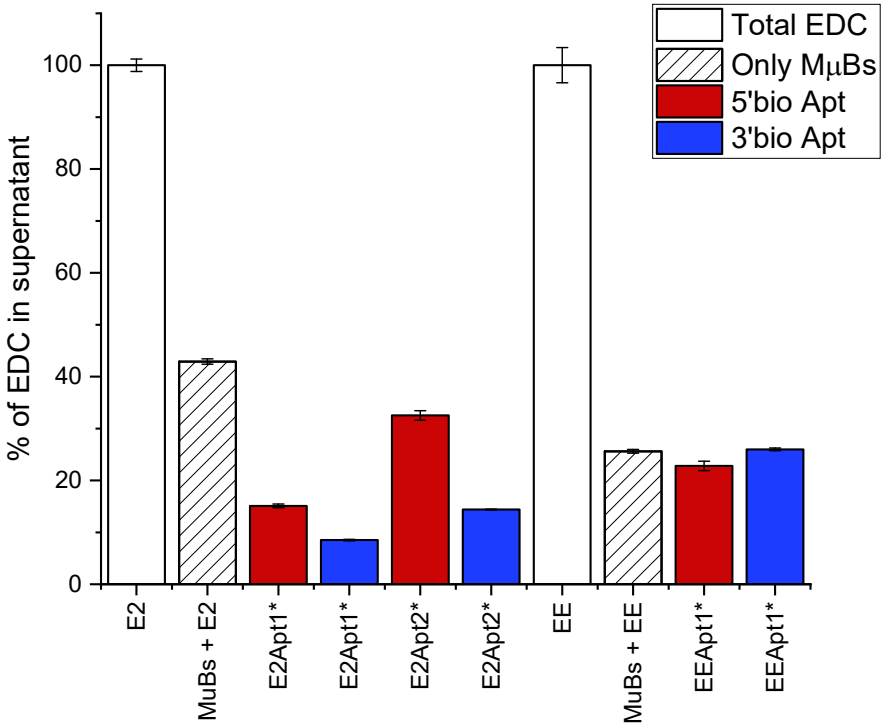

Figure 4.2. Percentage of tritiated EDC remaining in supernatant for the MμBs assays without and with E2 or EE aptamers at saturated loading. The * symbol indicates that the aptamer is immobilized on the MμBs.

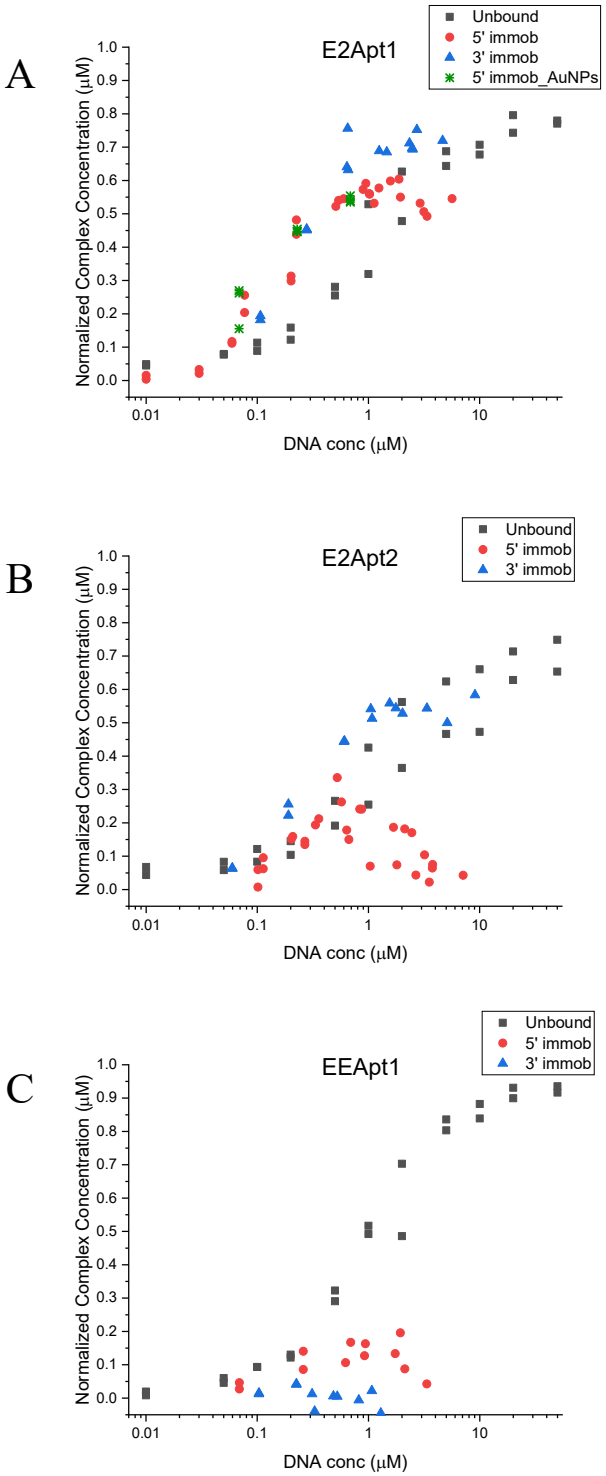

Figure 4.3. Binding curves of unbound, 5′ and 3′ immobilized DNA aptamers. Plots of normalized complex concentration versus concentration of immobilized DNA aptamer (on magnetic beads unless otherwise specified in the legend) for (A) E2Apt1 (B) E2Apt2 and (C) EEApt1.

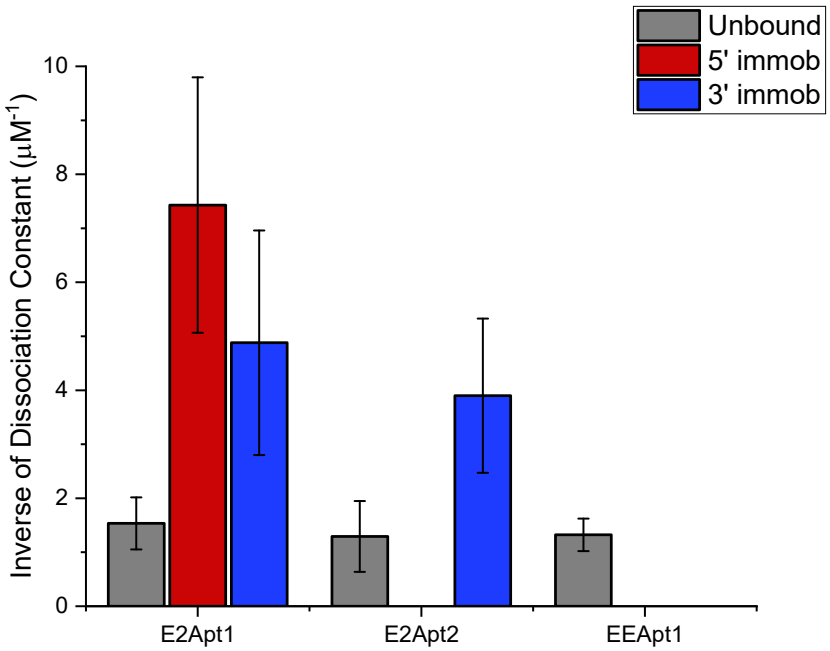

Figure 4.4. Inverse of dissociation constant K_d with 95% confidence intervals for unbound and immobilized aptamers.

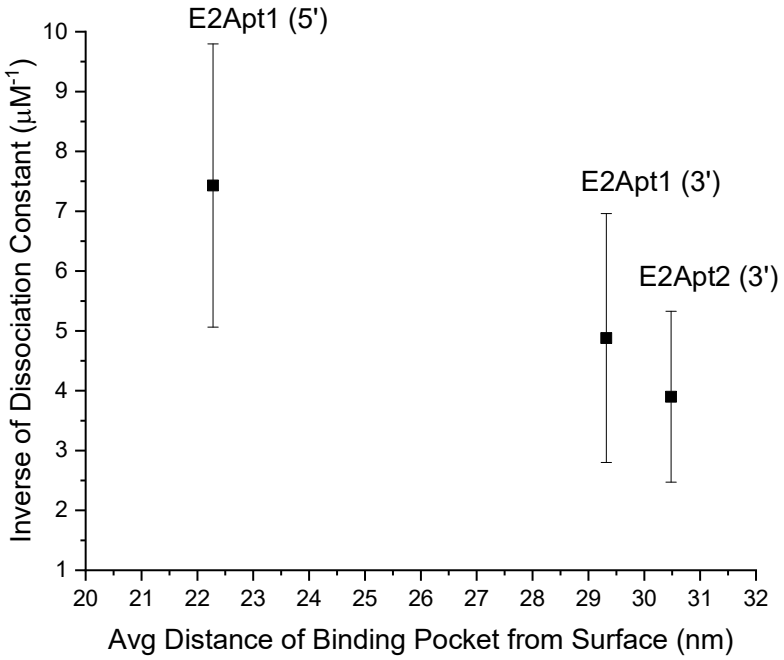

Figure 4.5. Plot of inverse of dissociation constant K_d with 95% confidence intervals versus the average linear distance of the binding pocket from the surface/site of immobilization.

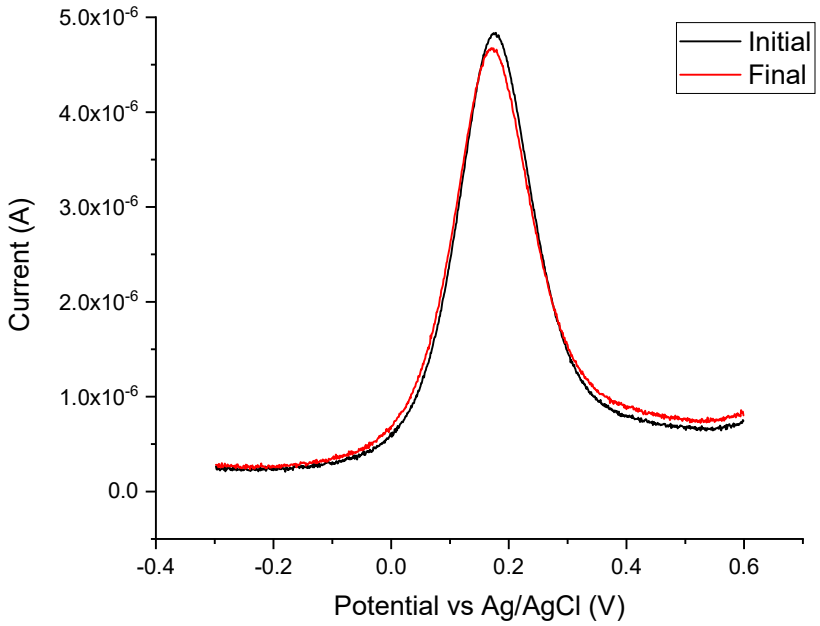

Figure 4.6. SWV (frequency 25Hz) for 5′ immobilized E2Apt1 on gold electrode. The initial and final averaged signals are from three unique electrodes.

4.6 REFERENCES

1. Kolpin, D. W.; Furlong, E. T.; Meyer, M. T.; Thurman, E. M.; Zaugg, S. D.; Barber, L. B.; Buxton, H. T., Pharmaceuticals, Hormones, and Other Organic Wastewater Contaminants in U.S. Streams, 1999−2000: A National Reconnaissance. *Environmental Science & Technology* **2002,** *36* (6), 1202-1211.
2. Sharpe, R. M.; Skakkebaek, N. E., Are oestrogens involved in falling sperm counts and disorders of the male reproductive tract? *The Lancet* **1993,** *341* (8857), 1392-1396.
3. Folmar, L. C.; Denslow, N. D.; Rao, V.; Chow, M.; Crain, D. A.; Enblom, J.; Marcino, J.; Guillette, L. J., Vitellogenin induction and reduced serum testosterone concentrations in feral male carp (Cyprinus carpio) captured near a major metropolitan sewage treatment plant. *Environmental Health Perspectives* **1996,** *104* (10), 1096-1101.
4. Jobling, S.; Williams, R.; Johnson, A.; Taylor, A.; Gross-Sorokin, M.; Nolan, M.; Tyler, C. R.; van Aerle, R.; Santos, E.; Brighty, G., Predicted Exposures to Steroid Estrogens in U.K. Rivers Correlate with Widespread Sexual Disruption in Wild Fish Populations. *Environmental Health Perspectives* **2006,** *114* (Suppl 1), 32-39.
5. Kidd, K. A.; Blanchfield, P. J.; Mills, K. H.; Palace, V. P.; Evans, R. E.; Lazorchak, J. M.; Flick, R. W., Collapse of a fish population after exposure to a synthetic estrogen. *Proceedings of the National Academy of Sciences* **2007,** *104* (21), 8897.
6. Vilahur, N.; Bustamante, M.; Byun, H.-M.; Fernandez, M. F.; Santa Marina, L.; Basterrechea, M.; Ballester, F.; Murcia, M.; Tardón, A.; Fernández-Somoano, A.; Estivill, X.; Olea, N.; Sunyer, J.; Baccarelli, A. A., Prenatal exposure to mixtures of xenoestrogens and repetitive element DNA methylation changes in human placenta. *Environment International* **2014,** *71*, 81-87.
7. Kabir, E. R.; Rahman, M. S.; Rahman, I., A review on endocrine disruptors and their possible impacts on human health. *Environmental Toxicology and Pharmacology* **2015,** *40* (1), 241-258.
8. Van den Belt, K.; Berckmans, P.; Vangenechten, C.; Verheyen, R.; Witters, H., Comparative study on the in vitro/in vivo estrogenic potencies of 17β-estradiol, estrone, 17α-ethynylestradiol and nonylphenol. *Aquatic Toxicology* **2004,** *66* (2), 183-195.
9. Grover, D. P.; Zhang, Z. L.; Readman, J. W.; Zhou, J. L., A comparison of three analytical techniques for the measurement of steroidal estrogens in environmental water samples. *Talanta* **2009,** *78* (3), 1204-1210.
10. Hirobe, M.; Goda, Y.; Okayasu, Y.; Tomita, J.; Takigami, H.; Ike, M.; Tanaka, H., The use of enzyme-linked immunosorbent assays (ELISA) for the determination of pollutants in environmental and industrial wastes. *Water Science and Technology* **2006,** *54* (11-12), 1.
11. Sawaya, W. N.; Lone, K. P.; Husain, A.; Dashti, B.; Al-Zenki, S., Screening for estrogenic steroids in sheep and chicken by the application of enzyme-linked immunosorbent assay and a comparison with analysis by gas chromatography–mass spectrometry. *Food Chemistry* **1998,** *63* (4), 563-569.
12. Sullivan, J. J.; Goh, K. S., Evaluation and Validation of a Commercial ELISA for Diazinon in Surface Waters. *Journal of Agricultural and Food Chemistry* **2000,** *48* (9), 4071-4078.
13. Calisto, V.; Bahlmann, A.; Schneider, R. J.; Esteves, V. I., Application of an ELISA to the quantification of carbamazepine in ground, surface and wastewaters and validation with LC–MS/MS. *Chemosphere* **2011,** *84* (11), 1708-1715.
14. Zhu, B.; Alsager, O. A.; Kumar, S.; Hodgkiss, J. M.; Travas-Sejdic, J., Label-free electrochemical aptasensor for femtomolar detection of 17β-estradiol. *Biosensors and Bioelectronics* **2015,** *70*, 398-403.
15. Fan, L.; Zhao, G.; Shi, H.; Liu, M.; Wang, Y.; Ke, H., A Femtomolar Level and Highly Selective 17β-estradiol Photoelectrochemical Aptasensor Applied in Environmental Water Samples Analysis. *Environmental Science & Technology* **2014,** *48* (10), 5754-5761.

16. Alsager, O. A.; Kumar, S.; Willmott, G. R.; McNatty, K. P.; Hodgkiss, J. M., Small molecule detection in solution via the size contraction response of aptamer functionalized nanoparticles. *Biosensors and Bioelectronics* **2014,** *57*, 262-268.
17. Tuerk, C.; Gold, L., Systematic evolution of ligands by exponential enrichment: RNA ligands to bacteriophage T4 DNA polymerase. *Science* **1990,** *249* (4968), 505.
18. Ellington, A. D.; Szostak, J. W., Selection in vitro of single-stranded DNA molecules that fold into specific ligand-binding structures. *Nature* **1992,** *355* (6363), 850-852.
19. Dwivedi, H. P.; Smiley, R. D.; Jaykus, L.-A., Selection of DNA aptamers for capture and detection of Salmonella Typhimurium using a whole-cell SELEX approach in conjunction with cell sorting. *Applied Microbiology and Biotechnology* **2013,** *97* (8), 3677-3686.
20. Wang, L.; Liu, X.; Hu, X.; Song, S.; Fan, C., Unmodified gold nanoparticles as a colorimetric probe for potassium DNA aptamers. *Chemical Communications* **2006,** (36), 3780-3782.
21. Kim, M.; Um, H.-J.; Bang, S.; Lee, S.-H.; Oh, S.-J.; Han, J.-H.; Kim, K.-W.; Min, J.; Kim, Y.-H., Arsenic Removal from Vietnamese Groundwater Using the Arsenic-Binding DNA Aptamer. *Environmental Science & Technology* **2009,** *43* (24), 9335-9340.
22. Song, K.-M.; Cho, M.; Jo, H.; Min, K.; Jeon, S. H.; Kim, T.; Han, M. S.; Ku, J. K.; Ban, C., Gold nanoparticle-based colorimetric detection of kanamycin using a DNA aptamer. *Analytical Biochemistry* **2011,** *415* (2), 175-181.
23. Ng, A.; Chinnappan, R.; Eissa, S.; Liu, H.; Tlili, C.; Zourob, M., Selection, Characterization, and Biosensing Application of High Affinity Congener-Specific Microcystin-Targeting Aptamers. *Environmental Science & Technology* **2012,** *46* (19), 10697-10703.
24. Akki, S. U.; Werth, C. J.; Silverman, S. K., Selective Aptamers for Detection of Estradiol and Ethynylestradiol in Natural Waters. *Environmental Science & Technology* **2015,** *49* (16), 9905-9913.
25. Tang, J.; Xie, J.; Shao, N.; Yan, Y., The DNA aptamers that specifically recognize ricin toxin are selected by two in vitro selection methods. *Electrophoresis* **2006,** *27* (7), 1303-1311.
26. Tang, J.; Yu, T.; Guo, L.; Xie, J.; Shao, N.; He, Z., In vitro selection of DNA aptamer against abrin toxin and aptamer-based abrin direct detection. *Biosensors and Bioelectronics* **2007,** *22* (11), 2456-2463.
27. Na, W.; Park, J. W.; An, J. H.; Jang, J., Size-controllable ultrathin carboxylated polypyrrole nanotube transducer for extremely sensitive 17β-estradiol FET-type biosensors. *Journal of Materials Chemistry B* **2016,** *4* (29), 5025-5034.
28. Macaya, R. F.; Schultze, P.; Smith, F. W.; Roe, J. A.; Feigon, J., Thrombin-Binding DNA Aptamer Forms a Unimolecular Quadruplex Structure in Solution. *Proceedings of the National Academy of Sciences of the United States of America* **1993,** *90* (8), 3745-3749.
29. Stojanovic, M. N.; de Prada, P.; Landry, D. W., Aptamer-Based Folding Fluorescent Sensor for Cocaine. *Journal of the American Chemical Society* **2001,** *123* (21), 4928-4931.
30. Liu, J.; Lu, Y., Fast Colorimetric Sensing of Adenosine and Cocaine Based on a General Sensor Design Involving Aptamers and Nanoparticles. *Angewandte Chemie International Edition* **2006,** *45* (1), 90-94.
31. Baker, B. R.; Lai, R. Y.; Wood, M. S.; Doctor, E. H.; Heeger, A. J.; Plaxco, K. W., An Electronic, Aptamer-Based Small-Molecule Sensor for the Rapid, Label-Free Detection of Cocaine in Adulterated Samples and Biological Fluids. *Journal of the American Chemical Society* **2006,** *128* (10), 3138-3139.
32. Zhu, Y.; Zhou, C.; Yan, X.; Yan, Y.; Wang, Q., Aptamer-functionalized nanoporous gold film for high-performance direct electrochemical detection of bisphenol A in human serum. *Analytica Chimica Acta* **2015,** *883*, 81-89.
33. Jenison, R. D.; Gill, S. C.; Pardi, A.; Polisky, B., High-resolution molecular discrimination by RNA. *Science* **1994,** *263* (5152), 1425.

34. Zhang, X.; Servos, M. R.; Liu, J., Instantaneous and Quantitative Functionalization of Gold Nanoparticles with Thiolated DNA Using a pH-Assisted and Surfactant-Free Route. *Journal of the American Chemical Society* **2012,** *134* (17), 7266-7269.
35. Baldock, B. L.; Hutchison, J. E., UV–Visible Spectroscopy-Based Quantification of Unlabeled DNA Bound to Gold Nanoparticles. *Analytical Chemistry* **2016,** *88* (24), 12072-12080.
36. Steel, A. B.; Levicky, R. L.; Herne, T. M.; Tarlov, M. J., Immobilization of nucleic acids at solid surfaces: effect of oligonucleotide length on layer assembly. *Biophysical Journal* **2000,** *79* (2), 975-981.
37. White, R. J.; Phares, N.; Lubin, A. A.; Xiao, Y.; Plaxco, K. W., Optimization of Electrochemical Aptamer-Based Sensors via Optimization of Probe Packing Density and Surface Chemistry. *Langmuir* **2008,** *24* (18), 10513-10518.
38. Murphy, M. C.; Rasnik, I.; Cheng, W.; Lohman, T. M.; Ha, T., Probing Single-Stranded DNA Conformational Flexibility Using Fluorescence Spectroscopy. *Biophysical Journal* **2004,** *86* (4), 2530-2537.
39. Zuker, M., Mfold web server for nucleic acid folding and hybridization prediction. *Nucleic Acids Research* **2003,** *31* (13), 3406-3415.
40. Peterson, A. W.; Heaton, R. J.; Georgiadis, R. M., The effect of surface probe density on DNA hybridization. *Nucleic Acids Research* **2001,** *29* (24), 5163-5168.
41. Xiao, Y.; Uzawa, T.; White, R. J.; DeMartini, D.; Plaxco, K. W., On the Signaling of Electrochemical Aptamer-Based Sensors: Collision- and Folding-Based Mechanisms. *Electroanalysis* **2009,** *21* (11), 1267-1271.
42. Stoltenburg, R.; Nikolaus, N.; Strehlitz, B., Capture-SELEX: Selection of DNA Aptamers for Aminoglycoside Antibiotics. *Journal of Analytical Methods in Chemistry* **2012,** *2012*, 14.

CHAPTER 5
CONCLUSIONS

5.1 Summary and Conclusions

This dissertation examined DNA aptamers as potential candidates to develop sensors for small organic contaminants with the following objectives: (1) critically review DNA aptamers and aptasensors developed for small organic molecules and assess their use for monitoring environmentally relevant organics, (2) select and characterize DNA aptamers that bind to E2 and EE and, (3) study the effect of immobilization on the binding affinity of the selected E2 and EE aptamers.

Chapter 2 of this dissertation focused on reviewing ~80 aptamers and ~200 aptasensors developed for small organics. Based on the linear regression results, binding affinity was found to have a weak (proportionality constant = 0.01-0.07) relationship to the hydrophobicity of organics (p-value < 0.05), implying that hydrophobic interactions are significant in aptamer-target interactions for organics. Binding affinity was also directly related to the length of the aptamer (p-value < 0.05, slope = 0.01), indicating that longer aptamers potentially form more specific binding pockets for the target. On comparing the three commonly used sensor platforms – colorimetric, fluorescence and electrochemical, the sensitivity of the electrochemical platform was found to be better than those of the former platforms (p-value < $5x10^{-6}$, d-value >0.8). The aptasensor LOD was found to be directly related to the aptamer dissociation constant, demonstrating the effect of the inherent sensitivity of the aptamer on the sensor's sensitivity (p-value < 10^{-9}, slope = 1.01). Aptasensors have been developed for only a small fraction of environmental contaminants. In many cases[1-4], the reported aptasensors are not sensitive enough to detect these pollutants at environmentally relevant concentrations and in other cases[5-7] the construction of the sensor involves complex fabrication steps. Compared to protein-based

sensors for 11 contaminants, aptasensors do not hold a definitive edge in terms of sensitivity or selectivity. Thus, aptasensor development faces these challenges including reusability, reproducibility and robustness prior to commercialization.

Chapter 3 describes the selection and characterization of E2 and EE selective aptamers. Using in vitro selection or SELEX, 2 E2 aptamers (E2Apt1 and E2Apt2) and 2 EE aptamers (EEApt1 and EEApt2) were identified. An equilibrium-filtration assay was used to determine the dissociation constant K_d of the aptamers. The E2 aptamers were found to have K_d values of 0.6μM and are at least 74-fold more sensitive for E2 than the first reported E2 aptamer[8]. The E2 aptamers bound to analogue estrone (E1) but are at least 74-fold selective over EE. The EE aptamers' K_d values are 0.5-1μM. EEApt1 was found to be 53-fold more selective for EE over E2 or E1 but EEApt2 bound to all three EDCs (E1, E2 and EE) with similar affinity. The aptamers maintained their binding affinity and selectivity in natural water from a local lake. DMS probing enabled further insight into the binding regions of the aptamers and suggests that the single-stranded loop regions of the DNA are involved in interactions with the target.

Chapter 4 deals with the assessment of dissociation constants of immobilized selective aptamers, E2Apt1, E2Apt2 and EEApt1. The biotin-labeled aptamers are immobilized on streptavidin-coated magnetic microbeads and K_d values are determined using a binding assay. E2Apt1 immobilized at either end (5′ or 3′) and E2Apt2 immobilized at the 3′ end retain their binding affinity (K_d values range from 0.14-0.25 μM). The binding affinity is inversely correlated to the average linear distance of the binding pocket from the immobilized end, suggesting that undesirable interactions between the aptamer and other moieties are more likely when the binding pocket is further away from the surface. However, this is based on an oversimplified model which assumes the DNA to be linear and therefore this model is limited.

E2Apt2 immobilized at the 5′ end exhibits a unique binding curve – increasing the immobilized DNA concentration causes an increase in the concentration of the aptamer-target complex up to 1 μM DNA concentration, after which there is a drop in complex concentration. This result potentially implies dimerization of the DNA at high loadings due to increased proximity of the DNA on the beads, making the DNA unavailable for binding to the target. EEApt1 loses its binding affinity upon immobilization at either end. The 5′ immobilized E2Apt1 was tested on a 2 mm gold electrode and no change in the electrochemical current on binding to E2 was observed, indicating that the conformational change upon binding to E2 is insufficient.

5.2 Engineering Significance

Based on the review (Chapter 2), this research highlighted two significant factors that affect the sensitivity or LOD of DNA aptasensors for small organics. One factor is the inherent binding affinity of the aptamer quantified by the dissociation constant K_d. The other factor is the sensor platform employed – the electrochemical platform was found to perform better than the colorimetric and fluorescence-based platforms. The critical analysis identified challenges regarding aptasensor sensitivity, selectivity and commercialization for environmental contaminants.

This research also identified the first selective and sensitive EE aptamer (EEApt1) and supplemented the existing literature on E2 aptamers (Chapter 3). These aptamers were found to maintain their binding affinity in natural waters which contained natural organic matter, implying that the aptamers can be used for in situ detection of the EDCs without any need for additional sample pre-treatment. Selective aptamers were identified by exposing the DNA pool to the region of the target molecule that contained unique functional groups. This strategy could

be extended to other aptamer selections and coupled with counter-selections to identify selective aptamers for various targets.

Typically, aptamers are identified and characterized in their unattached or free state but are immobilized onto sensors platforms in order to develop aptasensors. Observations made in Chapter 4 imply that immobilization of the aptamer could adversely affect its binding affinity, in some cases leading to a complete loss of binding affinity (EEApt1). Therefore, the effect of aptamer immobilization on its binding affinity is an essential factor that needs to be evaluated prior to sensor development. Another factor that needs consideration is the conformational change of the aptamer upon binding to the target. Even if the aptamer retains its binding affinity upon immobilization, perhaps the conformational change is not significant enough to be reflected as an electrochemical signal change (E2Apt1). This could potentially be a result of the size of the target and the length of the aptamer. While long aptamers are more sensitive (Chapter 2), the relative change in aptamer conformation upon target binding might be insignificant. The DMS probing data identifying binding regions of the aptamer (Chapter 3) could be used to truncate the aptamer to a more functional length. However, the potential implication is that shorter aptamers are more suited to be developed into aptasensors to detect small organics.

5.3 Future work

This work presented the selection and characterization of DNA aptamers for two organic contaminants, and the effect of aptamer immobilization on binding affinity. The results highlight the issues in aptasensor development due to the difference in configurations of the aptamer during selections (free or unattached) and when incorporated into a sensor (immobilized or attached to a surface). Additionally, aptamers are less likely to undergo a significant change in conformation upon binding to a small organic due to the sheer size of the target.

Given that the aptamer binding affinity can be compromised upon immobilization (EEApt1), or the conformational change is not sufficient development into an electrochemical sensor (E2Apt1), sensors that employ free or unattached aptamers can be explored. For instance, a study used an indirect competitive assay between a fluorophore-labeled aptamer, free target and target immobilized on a sensor surface[9]. First, the aptamer and free target were incubated together followed by passing this incubation mixture over the sensor surface. If the sample contains a high concentration free target, the aptamer would be unavailable to bind to the surface-immobilized target resulting in a low fluorescence signal. Hence the signal could be correlated to the concentration of free target in the sample. This sensor model could be applied with the aptamers selected in this work to develop a sensor.

Small organics have a limited number of reactive functional groups and hence immobilizing these targets can pose a challenge. Modifications of the SELEX process can be used to overcome this hurdle[10-12]. In capture-SELEX[10], a short strand of DNA (cDNA) is immobilized on the support. The DNA pool attached to the support through hybridization with the cDNA and this construct is incubated with free target during selections. DNA sequences that detach from the surface upon binding to the target are eluted and amplified. This construct of the cDNA and identified DNA aptamer(s) can be directly employed on a sensor platform (Figure 5.1). The structure-switching[13-14] nature of this construct is beneficial since it could potentially improve the magnitude of signal change leading to more sensitive sensors. In case of capture-SELEX, the configuration of the aptamer during the selection process could ideally mirror the eventual arrangement of the aptamer in the aptasensor without any loss in binding affinity. Therefore, a new set of selections using capture-SELEX could be used to identify new E2 and EE aptamers which can then be incorporated onto a sensor platform.

5.4 Figure

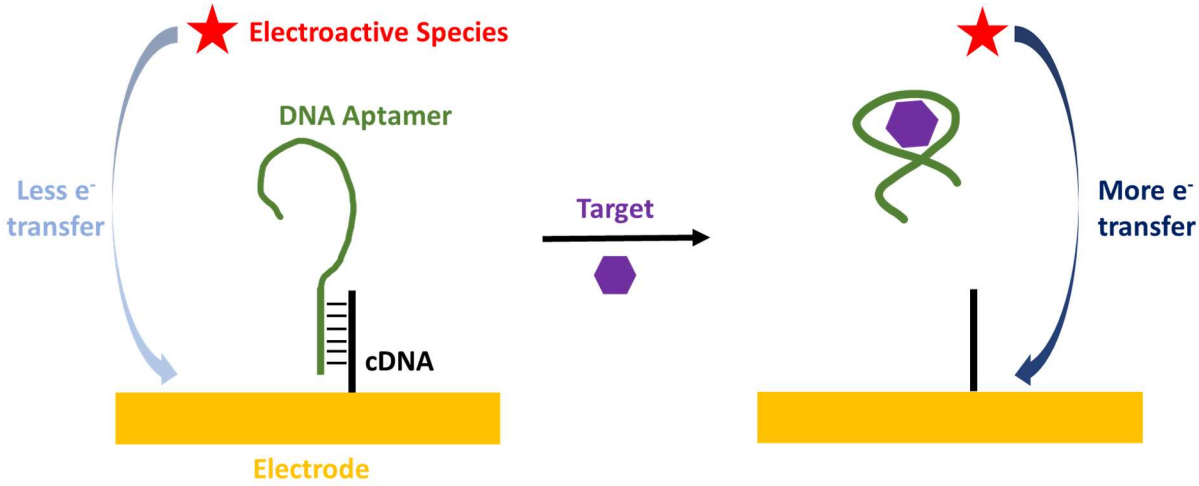

Figure 5.1. Conceptual model of electrochemical sensor based on capture-SELEX aptamer selections where the complementary DNA (cDNA) is immobilized on an electrode and the DNA aptamer is hybridized to the cDNA. This construct undergoes a change upon aptamer binding to the target which is reflected as a change in the electron transfer (current) at the electrode.

5.5 REFERENCES

1. Wang, A.; Zhao, H.; Chen, X.; Tan, B.; Zhang, Y.; Quan, X., A colorimetric aptasensor for sulfadimethoxine detection based on peroxidase-like activity of graphene/nickel@palladium hybrids. *Analytical Biochemistry* **2017,** *525*, 92-99.
2. Du, G.; Wang, L.; Zhang, D.; Ni, X.; Zhou, X.; Xu, H.; Xu, L.; Wu, S.; Zhang, T.; Wang, W., Colorimetric aptasensor for progesterone detection based on surfactant-induced aggregation of gold nanoparticles. *Analytical Biochemistry* **2016,** *514*, 2-7.
3. Du, G.; Zhang, D.; Xia, B.; Xu, L.; Wu, S.; Zhan, S.; Ni, X.; Zhou, X.; Wang, L., A label-free colorimetric progesterone aptasensor based on the aggregation of gold nanoparticles. *Microchimica Acta* **2016,** *183* (7), 2251-2258.
4. Lavaee, P.; Danesh, N. M.; Ramezani, M.; Abnous, K.; Taghdisi, S. M., Colorimetric aptamer based assay for the determination of fluoroquinolones by triggering the reduction-catalyzing activity of gold nanoparticles. *Microchimica Acta* **2017,** *184* (7), 2039-2045.
5. Li, S.; Wu, X.; Liu, C.; Yin, G.; Luo, J.; Xu, Z., Application of DNA aptamers as sensing layers for detection of carbofuran by electrogenerated chemiluminescence energy transfer. *Analytica Chimica Acta* **2016,** *941*, 94-100.
6. Meng, F.; Ma, X.; Duan, N.; Wu, S.; Xia, Y.; Wang, Z.; Xu, B., Ultrasensitive SERS aptasensor for the detection of oxytetracycline based on a gold-enhanced nano-assembly. *Talanta* **2017,** *165*, 412-418.
7. Kim, S.; Lee, H. J., Gold Nanostar Enhanced Surface Plasmon Resonance Detection of an Antibiotic at Attomolar Concentrations via an Aptamer-Antibody Sandwich Assay. *Analytical Chemistry* **2017,** *89* (12), 6624-6630.
8. Kim, Y. S.; Jung, H. S.; Matsuura, T.; Lee, H. Y.; Kawai, T.; Gu, M. B., Electrochemical detection of 17β-estradiol using DNA aptamer immobilized gold electrode chip. *Biosensors and Bioelectronics* **2007,** *22* (11), 2525-2531.
9. Yildirim, N.; Long, F.; Gao, C.; He, M.; Shi, H.-C.; Gu, A. Z., Aptamer-Based Optical Biosensor For Rapid and Sensitive Detection of 17β-Estradiol In Water Samples. *Environmental Science & Technology* **2012,** *46* (6), 3288-3294.
10. Stoltenburg, R.; Nikolaus, N.; Strehlitz, B., Capture-SELEX: Selection of DNA Aptamers for Aminoglycoside Antibiotics. *Journal of Analytical Methods in Chemistry* **2012,** *2012*, 14.
11. Gu, H.; Duan, N.; Wu, S.; Hao, L.; Xia, Y.; Ma, X.; Wang, Z., Graphene oxide-assisted non-immobilized SELEX of okdaic acid aptamer and the analytical application of aptasensor. **2016,** *6*, 21665.
12. Zhang, Y.; You, Y.; Xia, Z.; Han, X.; Tian, Y.; Zhou, N., Graphene oxide-based selection and identification of ofloxacin-specific single-stranded DNA aptamers. *RSC Advances* **2016,** *6* (101), 99540-99545.
13. Nutiu, R.; Li, Y., Structure-Switching Signaling Aptamers. *Journal of the American Chemical Society* **2003,** *125* (16), 4771-4778.
14. Nutiu, R.; Li, Y., In Vitro Selection of Structure-Switching Signaling Aptamers. *Angewandte Chemie International Edition* **2005,** *44* (7), 1061-1065.

APPENDIX A: SUPPLEMENTARY INFORMATION FOR CRITICAL REVIEW

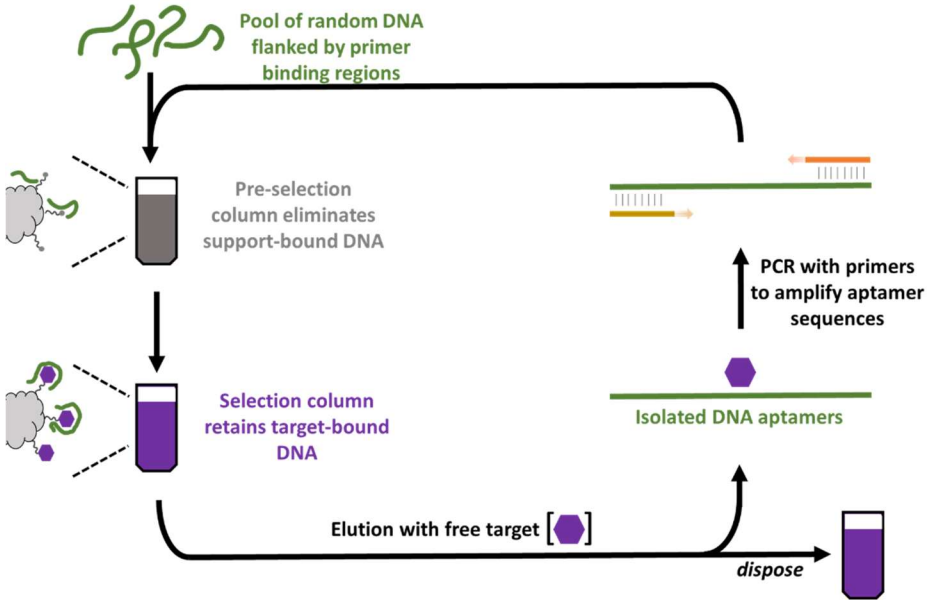

Figure A.1. SELEX process used for DNA aptamer selections modified from [1]

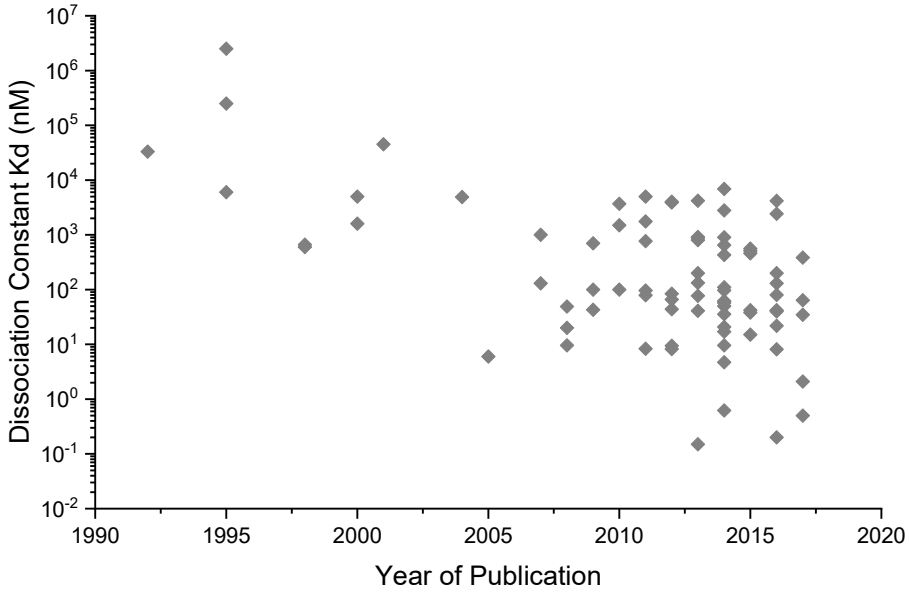

Figure A.2. Dissociation constant (K_d) of aptamers for small molecule targets (MW 60-1700Da) plotted against the year of publication

(i)

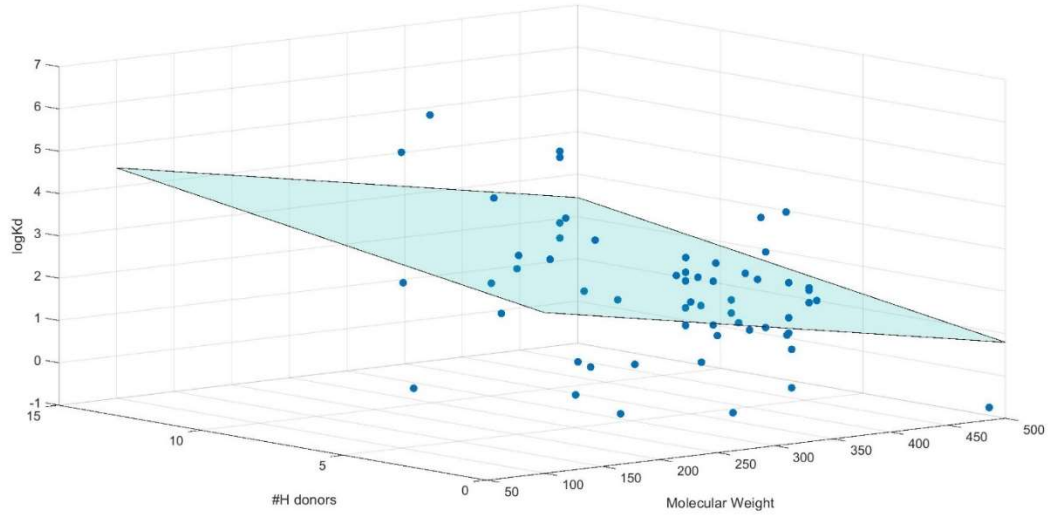

(ii)

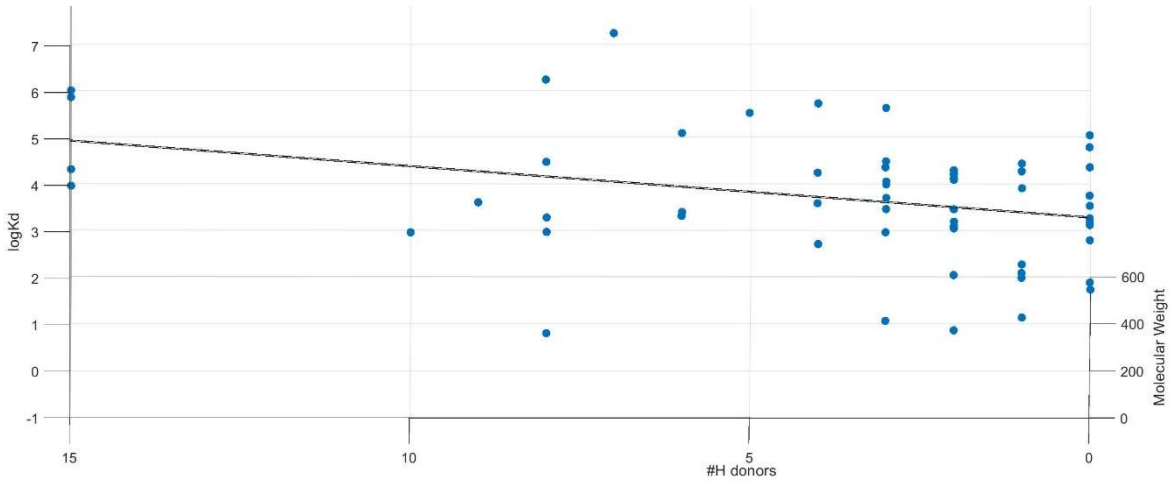

(iii)

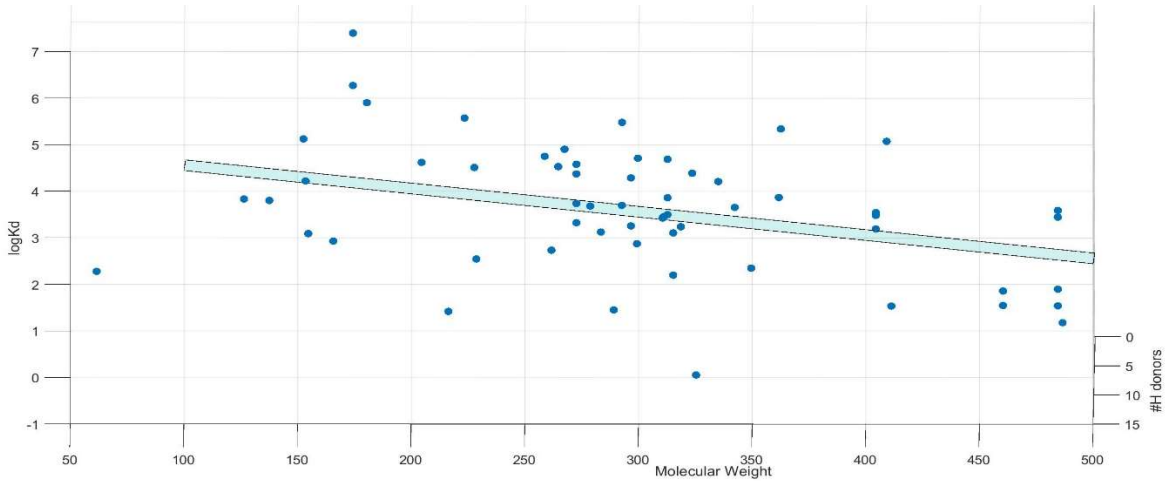

Figure A.3a. (i) Scatter plot showing molecular weight and number of hydrogen bond donors against logK_d. Plane corresponds to the multiple linear regression fit. Side view of plot with (ii) hydrogen donors and (iii) molecular weight on the horizontal axis.

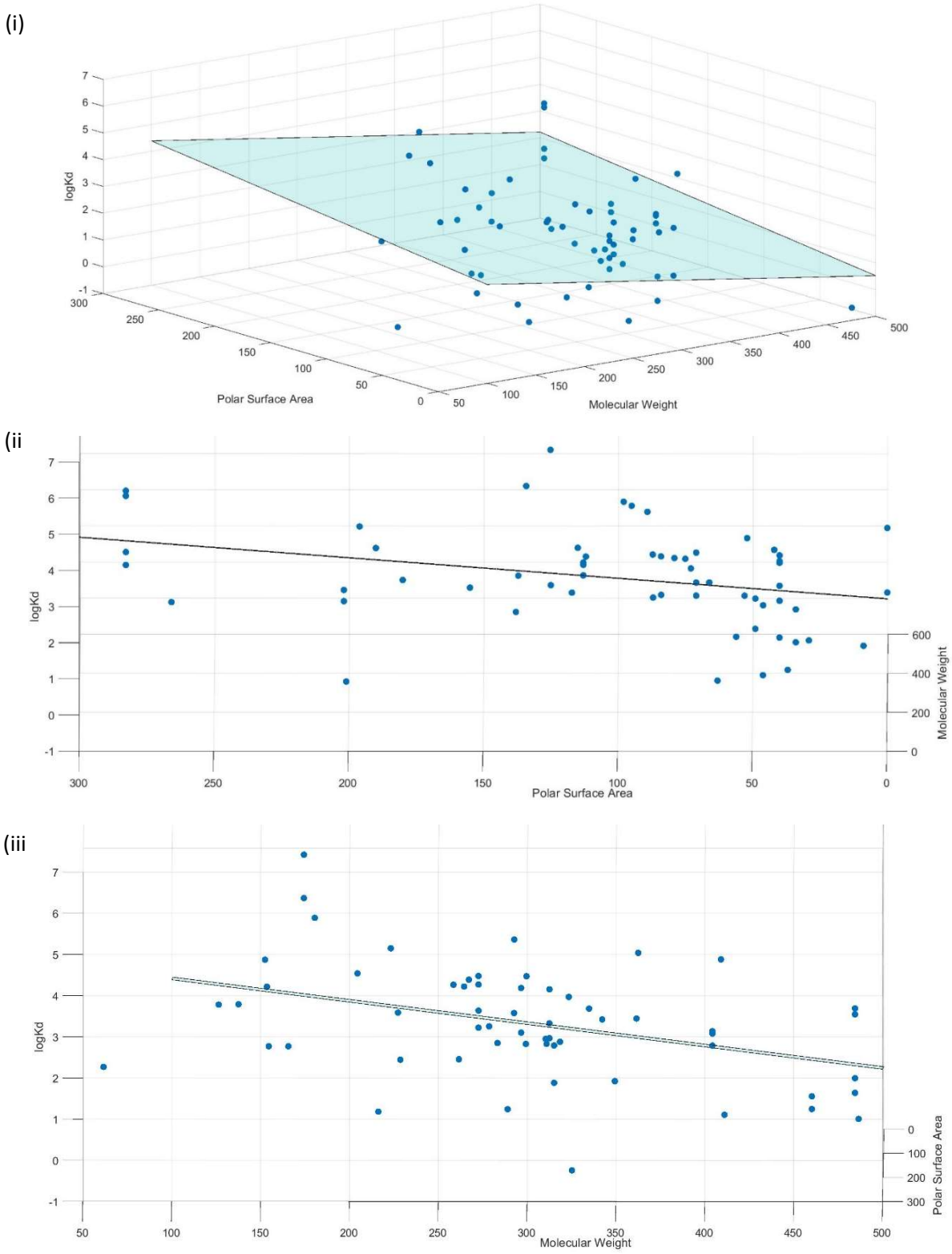

Figure A.3b. (i) Scatter plot showing target molecular weight and polar surface area against logK_d. Plane corresponds to the multiple linear regression fit. Side view of plot with (ii) polar surface area (iii) molecular weight on the horizontal axis.

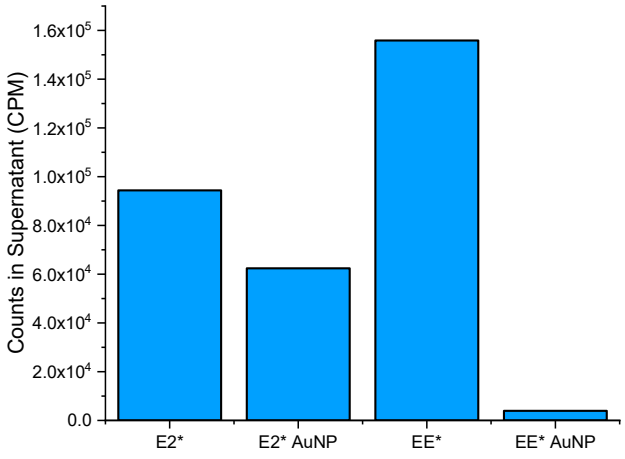

Figure A.4. Non-specific adsorption of 1pmol 2,4,6,7-3H-estradiol (81 Ci/mmol) and 6,7-3H-ethynylestradiol (60 Ci/mmol) to 100uL of 20nM citrate capped gold nanoparticles (AuNPs). Y-axis has the counts (cpm) in the supernatant post-centrifugation in the presence and absence of AuNPs.

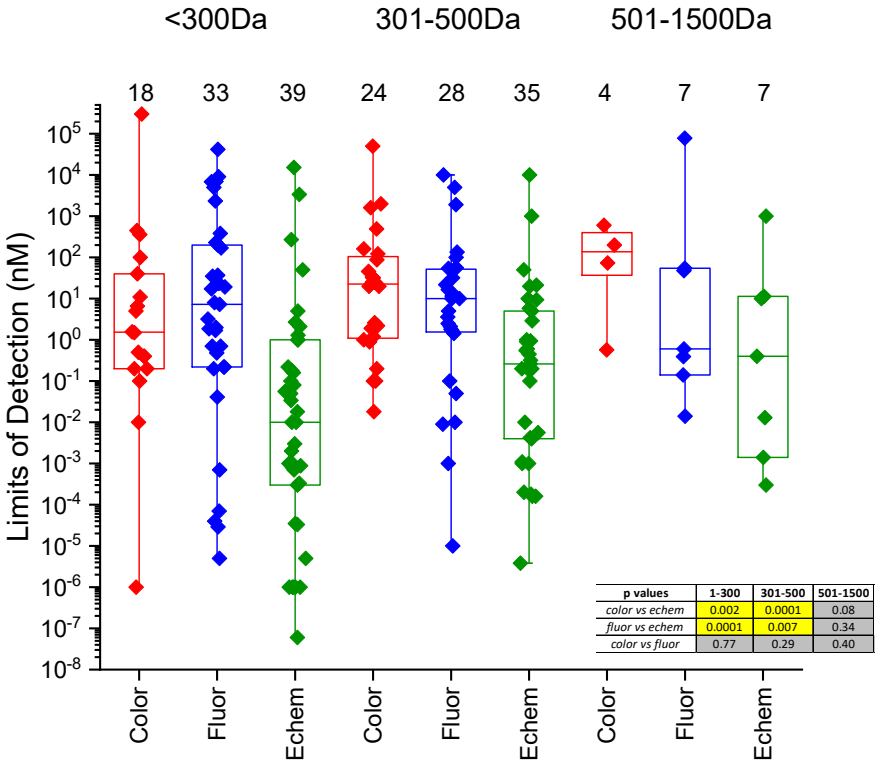

Figure A.5. Box plot of LODs for the colorimetric, fluorescence and electrochemical platforms split into three molecular weight categories. The p-value is obtained by comparing any two platforms using an independent samples t-test. The number against each box indicates the number of samples used to create each box.

Table A.1. Comprehensive list of small organics for which DNA aptamers have been developed between 1992 and 2017 including those noted in the reviews by McKeague & DeRosa[2] and Pfeiffer & Mayer[3]. Molecular weight (MW) of the target, the lowest (best) reported K_d and year of publication are listed.

Target	Mol. Wt	Lowest Kd [nM]	Year	Ref
Reactive green 19	1419	3.3E+04	1992	[4]
Adenosine	267	6.0E+03	1995	[5]
L-argininamide	174	2.5E+05	1995	[6]
L-arginine	174	2.5E+06	1995	[6]
Cellobiose	342	6.0E+02	1998	[7]
Sulforhodamine B	558.7	6.6E+02	1998	[8]
Cholic acid	408.6	5.0E+03	2000	[9]
Hematoporphyrin	598.7	1.6E+03	2000	[10]
L-tyrosinamide	180	4.5E+04	2001	[11]
Sialyllactose	633.6	4.9E+03	2004	[12]
Ethanolamine	61	6.0E+00	2005	[13]
(R)-thalidomide	258	1.0E+03	2007	[14]
17ß-estradiol	272	1.3E+02	2007	[15]
Daunomycin	527.5	2.0E+01	2008	[16]
Ochratoxin A	403.8	4.9E+01	2008	[17]
Oxytetracycline	460	9.6E+00	2008	[18]
8-hydroxy-2-deoxyguanosine	283	1.0E+02	2009	[19]
Diclofenac	296	4.3E+01	2009	[20]
Dopamine	153	7.0E+02	2009	[21]
(S) and (R) ibuprofen	206	1.5E+03	2010	[22]
Adenosine triphosphate	347	3.7E+03	2010	[23]
Fumonisin B1	721.8	1.0E+02	2010	[24]
Acetamiprid	222.7	5.0E+03	2011	[25]
Bisphenol A	228	8.3E+00	2011	[26]
Chloramphenicol	323	7.7E+02	2011	[27]
Kanamycin	484.5	7.9E+01	2011	[28]
L-tryptophan	204	1.8E+03	2011	[29]
Ochratoxin A	403.8	9.6E+01	2011	[30]
Ampicillin	349	9.4E+00	2012	[31]
Digoxin	781	8.2E+00	2012	[32]
Kanamycin A	484	3.9E+03	2012	[33]
Lysergamine	269	4.4E+01	2012	[34]
Polychlorinated biphenyl (PCB77)	292	4.0E+03	2012	[35]
Polychlorinated biphenyls (PCB72 and PCB101)	292	6.6E+01	2012	[36]
Sulfadimethoxine	310	8.4E+01	2012	[37]
Abscisic acid	264	8.0E+02	2013	[38]
Codeine	299	9.1E+02	2013	[39]
N-glycolylneuraminic acid	325	1.5E-01	2013	[40]

Table A.1 continued

N-methyl-mesoporphyrin	580.7	8.8E+02	2013	[41]
Okadaic acid	805	7.7E+01	2013	[42]
Saxitoxin	299	1.3E+02	2013	[43]
Streptomycin	581.6	2.0E+02	2013	[44]
Xanthine	152	4.2E+03	2013	[45]
Zearalenone	318	4.1E+01	2013	[46]
17ß-estradiol	272	9.0E+02	2014	[47]
17ß-estradiol	272	5.0E+01	2014	[48]
Aflatoxin B1	312	9.7E+01	2014	[49]
Aflatoxin B1	312	6.5E+02	2014	[50]
Aflatoxin M1	328	3.6E+01	2014	[49]
Atrazine	215.7	6.2E-01	2014	[51]
Bromacil	261	9.6E+00	2014	[52]
Cortisol	362	6.9E+03	2014	[53]
Cylindrospermopsin	415	5.7E+01	2014	[54]
Fumonisin B-1	721.8	6.2E+01	2014	[55]
Kanamycin A	484	2.8E+03	2014	[56]
Ochratoxin A	403.8	1.1E+02	2014	[57]
Oxytetracycline	460	4.7E+00	2014	[58]
Progesterone	314.5	1.7E+01	2014	[59]
T-2 toxin	466.5	2.1E+01	2014	[60]
Trinitrotoluene	227	4.3E+02	2014	[61]
17ß-estradiol	272	5.6E+02	2015	[1]
17α-ethynylestradiol	296	4.6E+02	2015	[1]
Anatoxin-a	165	1.5E+01	2015	[62]
Brevetoxin-2	895	4.2E+01	2015	[63]
Edifenfos	310.4	3.8E+01	2015	[64]
Melamine	126	5.1E+02	2015	[65]
1-3 beta D glucans	1700	8.0E+01	2016	[66]
Aflatoxin B1	312	4.2E+01	2016	[67]
Bromodiphenyl ether(BDE47)	485.8	2.0E-01	2016	[68]
Gonyautoxin 1/4	411	8.1E+00	2016	[69]
Malachite Green	364.9	2.4E+03	2016	[70]
Okdaic Acid	805	4.0E+01	2016	[71]
Ofloxacin	361	1.3E+02	2016	[72]
Patulin	154	2.2E+01	2016	[73]
Thioflavin T	318.9	4.2E+03	2016	[74]
Tyramine	137	2.0E+02	2016	[75]
Benzylpenicillin	334.4	3.8E+02	2017	[76]
Testosterone	288.4	5.0E-01	2017	[77]

Table A.1 continued

Dibutyl Phthalate (DBP)	278	6.4E+01	2017	[78]
Kanamycin	484.5	3.5E+01	2017	[79]
Progesterone	314.5	2.1E+00	2017	[80]

Table A.2. DNA aptamers developed for some proteins. Molecular weight (MW) of the target, the lowest (best) reported K_d and year of publication are listed.

Target	Mol. Wt	Lowest Kd [nM]	Year	Ref
Thrombin	36,000	2.5×10^{1}	1992	[81]
Human Immunoglobulin E	190,000	6.0×10^{0}	1996	[82]
Platelet Derived Growth Factor	25,000-29,000	9.4×10^{-2}	1996	[83]
Immunoglobulin E	190,000	2.7×10^{1}	2004	[84]
Ricin	62,925	5.8×10^{1}	2006	[85]
Abrin	260,000	2.8×10^{1}	2007	[86]
CFP-10.ESAT-6 (TB)	16,000	1.6×10^{0}	2012	[87]
EpCAM	34,932	3.3×10^{1}	2014	[50]
Protein A	42,000	2.1×10^{2}	2015	[88]

Equations to calculate Cohen's d

Cohen's d-value is calculated using equations A1 and A2, where the means of two data sets are x_1 and x_2. The two data sets contain n_1 and n_2 number of samples with standard deviations SD_1 and SD_2.

$$d = \frac{\bar{x}_1 - \bar{x}_2}{SD_{pooled}} \quad \text{(A1)}$$

$$SD_{pooled} = \sqrt{\frac{(n_1-1)SD_1^2 + (n_2-1)SD_2^2}{n_1+n_2-2}} \quad \text{(A2)}$$

Table A.3. P-values, proportionality constants and intercepts of single and two variable linear regression models with logK_d as the dependent variable.

Regression	Independent Variable(s)	p-value	Proportionality Constant	Intercept
Single Variable Models	log Koc	0.04	-0.20	2.42
	log D	0.05	-0.07	2.12
	Length	0.03	-0.01	3.03
Two Variable Models	MW	0.04	-0.002	2.53
	#h don	0.03	0.081	
	MW	0.02	-0.003	2.56
	PSA	0.04	0.005	
	MW	0.00	-0.006	3.10
	log KH	0.03	-0.051	
	MW	0.05	-0.002	2.73
	log D	0.02	-0.085	
	log D	0.00	-0.149	3.32
	ΔHvap	0.04	-0.013	
	log D	0.00	-0.152	6.23
	ΔSvap	0.04	-37.980	

Table A.4. List of aptasensors developed for various small organic molecules including sensor platform, limit of detection (LOD), upper and lower limits of the detection range and matrices tested. Compounds with an asterisk (*) are EPA regulated. PEC - photoelectrochemical. SERS - surface enhances Raman spectroscopy. SPR - surface plasmon resonance. NR - not reported.

Target	Sensor Platform	LOD [nM]	Detection Range [nM]		Matrices	Year	Ref
Dopamine	Colorimetric	3.6E+02	5.4E+02	5.4E+03	NR	2011	[89]
	Electrochemical	1.0E-02	1.0E-02	1.0E+01	Exocytotic fluid	2013	[90]
	Electrochemical	1.0E+00	5.0E+00	1.5E+02	Human serum	2014	[91]
	Glucose meter	3.0E+00	8.0E+01	1.0E+05	Human serum	2015	[92]
	Electrochemical	3.4E+03	5.0E+03	7.5E+04	Serum	2016	[93]
	Electrochemical	2.1E+00	5.0E+00	3.0E+02	Serum	2016	[94]
L-Tryptophan	Electrochemical	1.5E+04	6.3E+04	2.0E+06	NR	2013	[95]
	Fluorescence	7.0E+03	1.0E+04	5.0E+05	Fetal bovine serum	2015	[96]
	Fluorescence	6.8E+03	1.0E+04	5.0E+05	NR	2015	[96]
Omethoate	SERS	2.4E+04	NR	NR	Apple juice	2014	[97]
	Fluorescence	2.3E+01	2.3E+01	4.7E+04	Cabbage sample	2014	[98]
	Fluorescence	2.4E+03	NR	NR	Tangerine peels	2015	[99]
	Fluorescence	2.3E+02	7.0E+02	1.0E+04	Apple peels	2016	[100]
	Colorimetric	1.0E+02	1.0E+02	1.0E+04	Soil samples	2016	[101]
	Fluorescence	4.1E-02	1.0E-01	1.7E+01	River water, cabbage samples	2017	[102]
	Fluorescence	2.9E-05	1.0E-04	1.0E+03	River water, cabbage samples	2017	[102]
Carbofuran*	ECL	8.8E-04	2.0E-02	8.0E+00	Fruit and vegetable samples	2016	[103]
Acetamiprid	Electrochemical	1.0E+00	5.0E+00	6.0E+02	Wastewater, tomato samples	2013	[104]
	Colorimetric	5.0E+00	7.5E+01	7.5E+03	Soil samples	2013	[105]
	Colorimetric	4.5E+02	4.5E+02	4.5E+04	NR	2014	[106]
	Colorimetric	4.0E+01	1.0E+02	1.0E+04	Wastewater	2015	[107]
	Electrochemical	3.3E-04	1.0E-04	5.0E+00	Wastewater, vegetable samples	2015	[108]
	PEC	1.8E-01	5.0E-01	8.0E+02	Cucumber samples	2016	[109]
	Fluorescence	7.3E+00	5.0E+01	1.0E+03	Vegetable samples	2016	[110]
	Fluorescence	7.0E-01	7.0E-01	1.5E+02	River water, cabbage samples	2016	[111]
	Fluorescence	3.2E+00	5.0E+01	1.0E+03	Tea samples	2016	[112]
	Chemiluminescence	6.2E-02	8.0E-01	6.3E+02	Wastewater, Soil, cucumber	2016	[113]
BPA	Colorimetric	2.0E-01	4.0E-02	4.4E+02	Tap water, lake water	2013	[114]
	Colorimetric	4.0E-01	4.0E+00	4.0E+04	NR	2013	[115]
	Fluorescence	4.0E-05	4.0E-04	4.0E+01	Urine, water samples	2013	[115]
	Electrochemical	1.0E-03	4.0E-04	4.0E+00	Drinking water	2013	[116]
	PEC	1.8E-02	1.8E-02	3.2E+00	Bottled water, livixium of plastic bottles & plastic wraps	2013	[117]

Table A.4 continued

BPA	Electrochemical	5.0E+00	1.0E+01	1.0E+04	Milk	2014	[118]
	SERS	3.0E+00	3.0E+00	3.0E+02	NR	2014	[119]
	Optical	3.5E-02	9.0E-02	2.2E+01	Tap water	2014	[120]
	Electrochemical	1.0E-06	1.0E-06	1.0E-02	NR	2014	[121]
	Fluorescence	1.9E+00	2.0E+00	1.0E+02	Wastewater	2014	[122]
	Fluorescence	2.2E-01	4.4E-01	4.4E+01	Tap water, river water	2015	[123]
	SERS	1.0E-05	1.0E-05	1.0E+02	Tap water	2015	[124]
	Electrochemical	5.6E-02	1.0E-01	1.0E+02	Human serum	2015	[125]
	ECL	2.2E-01	4.4E-01	2.2E+03	NR	2015	[126]
	Colorimetric	5.0E-01	1.5E+02	6.1E+02	Tap water	2015	[127]
	Electrochemical	8.0E-02	1.0E-01	1.0E+02	NR	2015	[128]
	Fluorescence	7.0E-01	2.2E+00	4.4E+02	Bottled water	2015	[129]
	Electrochemical	6.0E-08	1.0E-07	1.0E-03	River water	2016	[130]
	Electrochemical	1.0E-06	1.0E-06	1.0E-02	plastic bottle, printing paper	2016	[131]
	Colorimetric	1.5E+00	1.5E+00	5.0E+02	Tap water, river water	2016	[132]
	Fluorescence	8.0E+00	4.4E+01	3.5E+02	Tap water	2016	[133]
	Fluorescence	5.0E-06	1.0E-05	1.0E+01	Tap, lake, river water	2016	[134]
	ECL	1.6E-01	2.0E-01	4.4E+02	Bottled water	2016	[135]
	SPR	1.6E-02	4.4E-02	2.2E+02	Bottled water	2016	[136]
	Electrochemical	1.0E-02	1.0E-02	1.0E+03	NR	2016	[137]
	Electrochemical	1.0E-06	1.0E-06	1.0E-02	Serum	2017	[138]
	Electrochemical	5.0E-02	1.0E-01	1.0E+01	Bottled water, milk, juice	2017	[139]
	Fluorescence	7.0E-04	4.0E-03	4.4E+01	NR	2017	[140]
	Fluorescence	2.0E+00	2.0E+00	2.0E+01	River water	2017	[141]
	Colorimetric	6.6E+00	1.9E+01	2.9E+02	Plastic bottle extract	2017	[142]
	Electrochemical	3.5E-05	1.0E-04	1.0E-03	Plastic bottle extract	2017	[143]
Phorate	SERS	4.0E+02	4.0E+02	3.8E+03	Apple juice	2014	[97]
	Fluorescence	1.9E+01	1.9E+01	3.8E+04	Cabbage sample	2014	[98]
	Fluorescence	3.8E+02	NR	NR	Tangerine peels	2015	[99]
	Fluorescence	2.0E+02	6.0E+02	1.0E+04	Apple peels	2016	[100]
	Colorimetric	1.0E-02	1.0E-02	1.3E+03	Apple sample	2016	[144]
Adenosine	Colorimetric	3.0E+05	3.0E+05	2.0E+06	NR	2006	[145]
	Fluorescence	5.0E+03	5.0E+03	1.0E+06	NR	2013	[146]
	Fluorescence	9.1E+03	9.1E+03	1.0E+05	NR	2017	[147]
	Fluorescence	2.0E-01	3.0E-01	1.7E+02	Urine	2017	[148]
	Fluorescence	4.2E+04	4.2E+04	1.1E+06	Serum	2017	[149]
Estradiol	Electrochemical	1.0E-01	1.0E-02	1.0E+00	NR	2007	[15]
	Optical	2.1E+00	5.0E+00	8.0E+01	Wastewater	2012	[150]
	Electrochemical	2.0E-03	1.0E-02	1.0E+01	Human urine	2012	[151]
	PEC	3.3E-05	5.0E-05	1.5E-02	Lake water, wastewater	2014	[152]
	Colorimetric	4.0E-01	4.0E-01	4.0E+05	NR	2014	[153]
	Fluorescence	2.2E-01	8.2E-01	2.1E+01	Bottled water, Wastewater	2014	[154]

Table A.4 continued

Estradiol	Electrochemical	5.0E-06	1.0E-05	1.0E+00	Rivulet water	2014	[155]
	Optical	5.0E+00	5.0E+00	1.0E+02	NR	2014	[48]
	Electrochemical	7.0E-04	1.0E-03	1.0E+00	Urine	2015	[156]
	Colorimetric	1.0E-01	1.0E-01	1.0E+04	Synthetic saliva	2015	[157]
	Electrochemical	8.0E-04	5.0E-03	6.0E-01	Wastewater	2015	[158]
	Colorimetric	1.0E-06	1.0E-06	1.0E+01	Tap, lake, river water	2015	[159]
	Colorimetric	1.1E+01	3.6E+01	3.3E+02	Tap water	2015	[160]
	Electrochemical	1.0E-06	1.0E-06	1.0E+01	NR	2015	[161]
	Colorimetric	2.0E-01	2.0E-01	8.0E-01	NR	2015	[162]
	Electrochemical	5.0E+01	5.0E+01	1.6E+03	NR	2015	[163]
	Electrochemical	1.0E-06	1.0E-06	1.0E+03	Urine	2015	[164]
	Fluorescence	7.0E-05	1.0E-04	1.0E+00	NR	2016	[165]
	Colorimetric	1.6E+00	1.6E+00	3.5E+02	Water	2016	[166]
	Fluorescence	3.7E+01	8.0E+01	4.0E+02	Fetal Bovine Serum	2016	[167]
	Fluorescence	4.8E-01	4.8E-01	2.0E+02	Water	2017	[168]
Isocarbophos	SERS	3.4E+03	NR	NR	Apple juice	2014	[97]
	Fluorescence	1.7E+01	1.7E+01	3.5E+04	Cabbage sample	2014	[98]
	Fluorescence	3.5E+01	3.5E+02	3.5E+04	Tangerine peels	2015	[99]
	Fluorescence	1.7E+02	5.0E+02	1.0E+04	Apple peels	2016	[100]
PCB72*	Electrochemical	1.0E-03	3.0E-03	3.4E+02	Fish samples	2015	[169]
	Electrochemical	1.3E+00	1.3E+00	3.4E+02	Fish samples	2016	[170]
PCB 77*	Fluorescence	1.7E+00	1.7E+00	3.4E+02	NR	2012	[35]
	SERS	1.0E+03	1.0E+03	1.0E+06	NR	2014	[171]
	SERS	1.0E+01	1.0E+01	1.0E+05	NR	2015	[172]
	SERS	3.3E+01	3.3E+01	1.0E+03	NR	2016	[173]
	Electrochemical	3.4E-02	7.0E-01	6.9E+02	Tap water	2016	[174]
Diclofenac	Electrochemical	2.7E+02	2.7E+02	5.0E+03	Blood, serum	2012	[175]
	Electrochemical	2.7E+00	1.0E+01	2.0E+02	Urine	2016	[176]
Codeine	Electrochemical	3.0E-03	1.0E-02	1.0E+02	NR	2013	[39]
	Electrochemical	3.0E-04	1.0E-03	1.0E+02	NR	2016	[177]
Cocaine	Fluorescence	1.0E+04	1.0E+04	2.5E+06	Serum	2001	[178]
	Colorimetric	5.0E+04	5.0E+04	5.0E+05	NR	2006	[145]
	Electrochemical	1.0E+04	1.0E+04	5.0E+05	Fetal calf serum, human saliva	2006	[179]
	Colorimetric	2.0E+03	2.0E+04	2.0E+05	NR	2008	[180]
	Electrochemical	1.0E+03	1.0E+03	1.0E+07	Blood, cellular lysate	2009	[181]
	Fluorescence	5.6E+01	1.0E+02	1.0E+04	Saliva, serum, urine	2016	[182]
	Fluorescence	5.0E+01	5.0E+01	1.0E+04	Saliva	2017	[183]
	Electrochemical	5.0E+01	5.0E+01	1.0E+05	Saliva, serum	2017	[184]
	Fluorescence	5.0E+03	5.0E+03	5.0E+06	Serum, urine	2017	[185]
	Electrochemical	1.0E-03	3.0E-03	3.3E+00	Human serum, urine, saliva	2017	[186]
Sulfadimethoxine	Fluorescence	3.2E+01	3.2E+01	1.6E+03	Milk	2012	[37]

Table A.4 continued

Sulfadimethoxine	Colorimetric	1.6E+02	1.6E+02	3.2E+03	NR	2013	[187]
	Colorimetric	1.6E+03	NR	NR	NR	2014	[188]
	PEC	5.5E-01	1.0E+00	1.0E+02	Milk	2016	[189]
	Colorimetric	2.2E+00	3.2E+00	1.6E+03	Lake water	2017	[190]
	Colorimetric	3.2E+01	3.2E+01	3.2E+06	Milk	2017	[191]
Progesterone	Electrochemical	2.9E+00	3.2E+01	1.9E+02	Tap water	2014	[59]
	Colorimetric	2.6E+00	2.6E+00	8.0E+02	Tap water, urine	2016	[192]
	Colorimetric	8.9E-01	8.9E-01	5.0E+02	Human serum, urine	2016	[193]
	Fluorescence	5.0E+00	3.2E+01	3.2E+02	Tap water, artificial urine	2017	[80]
Ciprofloxacin	Colorimetric	1.2E+00	4.0E+00	5.0E+02	Water, serum, milk	2017	[194]
	Electrochemical	2.6E-01	8.0E-01	4.0E+02	Water, serum, milk	2017	[195]
Ampicillin	Fluorescence	1.4E+00	1.4E+00	1.4E+02	Milk	2012	[31]
	Electrochemical	1.0E-01	1.0E-01	1.0E+03	Milk	2013	[196]
	Electrochemical	1.1E-03	5.0E-03	1.0E+01	Milk	2015	[197]
	Electrochemical	4.0E-03	2.0E-02	4.0E+01	Milk	2016	[198]
Chlorpyrifos*	Electrochemical	9.4E-01	2.8E+00	2.9E+05	Vegetable samples	2016	[199]
Profenofos	SERS	1.4E+04	NR	NR	Apple juice	2014	[97]
	Fluorescence	1.3E+01	1.3E+01	2.7E+04	Cabbage sample	2014	[98]
	Fluorescence	1.3E+02	2.7E+02	2.7E+04	Tangerine peels	2015	[99]
	Fluorescence	1.0E+02	3.0E+02	1.0E+04	Apple peels	2016	[100]
DEHP*	Electrochemical	1.0E-02	1.0E-02	1.0E+02	NR	2017	[78]
OTA	Colorimetric	2.0E+01	2.0E+01	6.3E+02	NR	2011	[200]
	Fluorescence	1.9E+03	2.0E+03	3.5E+04	NR	2011	[201]
	Fluorescence	2.2E+01	5.0E+01	5.0E+02	1% red wine	2011	[201]
	Electrochemical	2.0E-01	2.0E+00	2.2E+01	Wheat extracts	2011	[202]
	Fluorescence	5.0E-02	1.0E-01	2.5E+02	Maize samples	2012	[203]
	Fluorescence	2.5E+00	2.5E+00	2.5E+03	Red wine	2017	[204]
	Fluorescence	1.7E+01	2.0E+01	5.0E+02	Red wine, beer	2017	[205]
	Luminescence	2.0E-03	2.0E-03	6.2E+02	Beer	2017	[206]
	Fluorescence	3.6E+00	3.6E+00	5.0E+03	White wine	2017	[207]
	Fluorescence	1.0E-05	2.0E-04	2.0E-01	Cereal samples	2017	[208]
Lincomycin	ECL	1.6E-04	5.0E-03	1.0E+00	Meat samples	2017	[209]
Tetracycline	Electrochemical	1.0E+01	1.0E+01	1.0E+04	NR	2009	[210]
	Electrochemical	5.0E+00	1.0E+01	5.0E+04	Milk	2012	[211]
	Colorimetric	3.3E+01	2.0E+02	1.0E+05	Milk	2012	[212]
	Colorimetric	1.2E+02	1.2E+02	5.0E+03	Milk	2013	[213]
	Colorimetric	4.6E+01	4.6E+01	4.0E+02	Milk	2013	[214]
	Colorimetric	1.8E-02	2.0E-02	2.3E+02	Honey	2014	[215]
	Colorimetric	1.0E-01	1.0E-01	1.0E+00	NR	2014	[216]
	Fluorescence	1.2E+01	1.2E+01	1.3E+02	Milk	2014	[217]
	Electrochemical	3.2E-01	1.0E+00	1.0E+04	Milk	2014	[218]
	Electrochemical	5.6E-03	1.0E-01	1.0E+06	Milk	2014	[219]

Table A.4 continued

Tetracycline	Colorimetric	8.8E+01	4.5E+02	4.5E+03	Milk	2015	[220]
	Colorimetric	2.0E-01	2.0E-01	2.3E+03	Honey	2015	[221]
	Electrochemical	4.2E-03	1.0E-01	1.0E+06	Milk	2015	[222]
	Fluorescence	2.1E+00	2.1E+00	3.0E+02	Rat serum, tap water	2015	[223]
	Electrochemical	4.5E-01	1.5E+00	3.5E+03	Milk, serum	2016	[224]
	Electrochemical	3.8E-06	1.0E-05	1.0E+03	Serum, milk, honey	2016	[225]
	Electrochemical	6.0E-01	1.0E+00	5.0E+03	NR	2016	[226]
	Electrochemical	2.0E+01	1.0E+02	2.0E+03	Milk	2016	[227]
	Chemiluminescence	4.0E-02	1.0E-01	1.1E+01	Milk	2016	[228]
	Fluorescence	1.0E-02	2.0E-02	2.3E+02	Milk, homogenized pork	2017	[229]
	SPR	5.0E-09	5.0E-09	2.0E-07	River water	2017	[230]
Oxytetracycline	Electrochemical	1.0E+00	1.0E+00	1.0E+02	NR	2009	[231]
	Colorimetric	2.5E+01	2.5E+01	1.0E+03	NR	2010	[232]
	Optical	2.2E+02	2.2E+02	2.2E+04	NR	2010	[233]
	Cantilever	2.0E-01	1.0E+00	1.0E+02	NR	2013	[234]
	Fluorescence	1.0E+01	1.0E+02	2.0E+03	Lake water	2013	[235]
	Electrochemical	2.1E+01	2.2E+01	1.3E+03	Mouse blood serum, urine	2013	[236]
	Colorimetric	2.0E+01	2.0E+01	2.2E+03	Milk	2014	[58]
	PEC	9.0E-01	4.0E+00	1.5E+02	NR	2015	[237]
	Fluorescence	1.8E+00	2.2E+00	1.1E+02	Milk, honey, pork	2015	[238]
	Luminescence	8.0E-02	1.0E-01	2.2E+02	Milk	2015	[239]
	Fluorescence	1.0E+01	1.0E+01	2.0E+02	Tap water, milk	2015	[240]
	Colorimetric	1.9E+00	1.9E+00	2.2E+02	Milk, honey, chicken	2015	[241]
	Luminescence	1.0E-01	2.0E-01	2.2E+01	Milk	2015	[242]
	Colorimetric	1.0E+00	1.0E+00	1.0E+03	Tap water	2015	[243]
	Fluorescence	5.4E+01	5.4E+01	2.2E+03	Tap, river water	2016	[244]
	Electrochemical	1.8E-04	5.0E-04	5.0E+01	Milk	2016	[245]
	Fluorescence	1.0E-01	5.0E-01	1.0E+02	Tap water, honey	2016	[246]
	Chemiluminescence	4.0E-02	1.0E-01	1.1E+01	Milk	2016	[228]
	Colorimetric	4.9E+02	4.3E+03	6.1E+04	Milk	2016	[247]
	Electrochemical	2.0E-04	1.0E-03	1.1E+02	Milk	2016	[248]
	Electrochemical	1.0E-03	1.0E-03	4.3E+03	Honey	2016	[249]
	PEC	1.9E-01	2.0E+00	3.0E+02	Tap, lake water, milk, chicken	2017	[250]
	Fluorescence	1.7E+00	1.7E+00	2.5E+02	Milk	2017	[251]
	SERS	9.0E-09	1.0E-07	1.0E-03	Fishmeal	2017	[252]
Kanamycin	Colorimetric	2.5E+01	2.5E+01	8.0E+01	NR	2011	[28]
	Electrochemical	9.4E+00	5.0E+01	9.0E+03	Milk	2012	[253]
	PEC	2.0E-01	1.0E+00	2.3E+02	NR	2014	[254]
	Fluorescence	9.0E-03	1.0E-02	3.0E+00	Human serum	2014	[255]
	Electrochemical	5.8E+00	1.0E+01	1.0E+02	Milk	2014	[256]
	Optical	1.0E+00	1.0E+01	6.0E+02	Milk	2017	[257]
	Colorimetric	1.0E-01	1.0E-01	1.0E+02	Milk, meat samples	2017	[258]

Table A.4 continued

Kanamycin	Electrochemical	2.0E-01	2.5E+00	1.6E+02	Milk	2017	[259]
	Electrochemical	1.6E-04	2.0E-03	1.0E+02	Milk	2017	[260]
	Fluorescence	1.0E-03	1.0E-03	2.0E-02	Milk, blood serum	2017	[261]
Adenosine Triphosphate	Electrochemical	1.0E+01	1.0E+01	1.0E+06	Cell lysate	2007	[262]
	Colorimetric	6.0E+02	4.4E+03	1.3E+05	NR	2007	[263]
	Electrochemical	1.0E+03	1.0E+03	4.0E+06	Cell lysate	2009	[181]
	Fluorescence	7.8E+04	7.8E+04	1.1E+06	Serum	2017	[149]
	qPCR	1.7E+01	5.0E+01	5.0E+06	NR	2017	[264]
Streptomycin	Colorimetric	2.0E+02	2.0E+02	1.2E+03	Honey	2013	[44]
	Electrochemical	1.1E+01	3.0E+01	1.5E+03	Milk, rat serum	2016	[265]
	Colorimetric	7.3E+01	7.3E+01	2.0E+03	Milk, serum	2016	[266]
	Fluorescence	4.8E+01	4.8E+01	2.0E+03	Milk, serum	2016	[266]
	Fluorescence	5.5E+01	5.5E+01	1.1E+03	Milk, blood serum	2016	[267]
Fumonisin B1	Fluorescence	1.4E-01	1.4E-01	6.9E+02	Maize samples	2012	[203]
	Fluorescence	1.4E-02	1.4E-02	1.4E+02	Maize samples	2013	[268]
	ECL	4.0E-01	7.0E-01	6.9E+02	Wheat samples	2014	[269]
	Electrochemical	1.4E-03	1.4E-03	1.4E+03	Wheat samples	2015	[270]
	Cantilever	4.6E+01	1.4E+02	5.5E+04	NR	2015	[271]
Digoxin	Fluorescence	6.0E-01	6.0E-01	6.0E+01	Rat serum	2015	[272]
	Electrochemical	1.3E-02	2.5E-02	2.5E-01	Urine, plasma	2015	[273]
	Fluorescence	3.9E-01	3.9E-01	3.0E+01	Serum	2015	[274]
	Colorimetric	5.7E-01	5.7E-01	3.0E+01	Serum	2015	[274]
	Electrochemical	3.0E-04	1.0E-03	1.0E+02	Serum	2016	[275]

Table A.5. Limits of detection for the most sensitive aptasensors, commercial ELISA kits, lab-based ELISAs and immunosensors developed in lab for environmentally relevant compound detection. Compounds with the * sign are regulated in accordance with the Safe Drinking Water Act.

Target	**Aptasensor**	**Ref**	**Comm ELISA**	**Ref**	**Lab ELISA**	**Ref**	**Immunosensor**	**Ref**
Carbofuran*	8.80E-04	[103]	2.20E+00	[276]	4.50E-02	[277]	4.50E-02	[278]
PCBs*	1.00E-03	[169]	7.70E-01	[279]	2.70E-01	[280]	3.10E-04	[281]
Chlorpyrifos*	9.40E-01	[199]	2.80E-01	[282]	2.80E-01	[283]	1.80E-02	[284]
BPA	6.00E-08	[130]	4.00E-02	[285]	1.30E-01	[286]	5.00E-06	[287]
E2	1.00E-06	[159, 161, 164]	3.10E-04	[288]	2.30E-02	[289]	5.50E-05	[290]
SDM	5.50E-01	[189]	3.20E+00	[291]	1.60E-02	[292]	NR	-
Progesterone	8.90E-01	[193]	1.70E-02	[293]	6.00E-02	[294]	2.00E-04	[295]
Ciprofloxacin	2.60E-01	[195]	2.10E+00	[296]	9.00E-02	[297]	3.00E-02	[298]
Lincomycin	1.60E-04	[209]	4.90E-01	[299]	3.70E-01	[300]	NR	-
TET	5.00E-09	[230]	1.10E-01	[301]	1.00E-01	[302]	1.40E-02	[303]
OTC	9.00E-09	[252]	3.20E+00	[304]	2.80E-01	[305]	NR	-

REFERENCES

1. Akki, S. U.; Werth, C. J.; Silverman, S. K., Selective Aptamers for Detection of Estradiol and Ethynylestradiol in Natural Waters. *Environmental Science & Technology* **2015,** *49* (16), 9905-9913.
2. McKeague, M.; DeRosa, M. C., Challenges and Opportunities for Small Molecule Aptamer Development. *Journal of Nucleic Acids* **2012,** *2012*, 748913.
3. Pfeiffer, F.; Mayer, G., Selection and Biosensor Application of Aptamers for Small Molecules. *Frontiers in Chemistry* **2016,** *4*, 25.
4. Ellington, A. D.; Szostak, J. W., Selection in vitro of single-stranded DNA molecules that fold into specific ligand-binding structures. *Nature* **1992,** *355* (6363), 850-852.
5. Huizenga, D. E.; Szostak, J. W., A DNA Aptamer That Binds Adenosine and ATP. *Biochemistry* **1995,** *34* (2), 656-665.
6. Harada, K.; Frankel, A. D., Identification of two novel arginine binding DNAs. *The EMBO Journal* **1995,** *14* (23), 5798-5811.
7. Yang, Q.; Goldstein, I. J.; Mei, H.-Y.; Engelke, D. R., DNA ligands that bind tightly and selectively to cellobiose. *Proceedings of the National Academy of Sciences* **1998,** *95* (10), 5462-5467.
8. Wilson, C.; Szostak, J. W., Isolation of a fluorophore-specific DNA aptamer with weak redox activity. *Chemistry & Biology* **1998,** *5* (11), 609-617.
9. Kato, T.; Takemura, T.; Yano, K.; Ikebukuro, K.; Karube, I., In vitro selection of DNA aptamers which bind to cholic acid. *Biochimica et Biophysica Acta (BBA) - Gene Structure and Expression* **2000,** *1493* (1), 12-18.
10. Okazawa, A.; Maeda, H.; Fukusaki, E.; Katakura, Y.; Kobayashi, A., In vitro selection of hematoporphyrin binding DNA aptamers. *Bioorganic & Medicinal Chemistry Letters* **2000,** *10* (23), 2653-2656.
11. Vianini, E.; Palumbo, M.; Gatto, B., In vitro selection of DNA aptamers that bind l-tyrosinamide. *Bioorganic & Medicinal Chemistry* **2001,** *9* (10), 2543-2548.
12. Mehedi Masud, M.; Kuwahara, M.; Ozaki, H.; Sawai, H., Sialyllactose-binding modified DNA aptamer bearing additional functionality by SELEX. *Bioorganic & Medicinal Chemistry* **2004,** *12* (5), 1111-1120.
13. Mann, D.; Reinemann, C.; Stoltenburg, R.; Strehlitz, B., In vitro selection of DNA aptamers binding ethanolamine. *Biochemical and Biophysical Research Communications* **2005,** *338* (4), 1928-1934.
14. Shoji, A.; Kuwahara, M.; Ozaki, H.; Sawai, H., Modified DNA Aptamer That Binds the (R)-Isomer of a Thalidomide Derivative with High Enantioselectivity. *Journal of the American Chemical Society* **2007,** *129* (5), 1456-1464.
15. Kim, Y. S.; Jung, H. S.; Matsuura, T.; Lee, H. Y.; Kawai, T.; Gu, M. B., Electrochemical detection of 17β-estradiol using DNA aptamer immobilized gold electrode chip. *Biosensors and Bioelectronics* **2007,** *22* (11), 2525-2531.
16. Wochner, A.; Menger, M.; Orgel, D.; Cech, B.; Rimmele, M.; Erdmann, V. A.; Glökler, J., A DNA aptamer with high affinity and specificity for therapeutic anthracyclines. *Analytical Biochemistry* **2008,** *373* (1), 34-42.
17. Cruz-Aguado, J. A.; Penner, G., Determination of Ochratoxin A with a DNA Aptamer. *Journal of Agricultural and Food Chemistry* **2008,** *56* (22), 10456-10461.
18. Niazi, J. H.; Lee, S. J.; Kim, Y. S.; Gu, M. B., ssDNA aptamers that selectively bind oxytetracycline. *Bioorganic & Medicinal Chemistry* **2008,** *16* (3), 1254-1261.
19. Miyachi, Y.; Shimizu, N.; Ogino, C.; Fukuda, H.; Kondo, A., Selection of a DNA aptamer that binds 8-OHdG using GMP-agarose. *Bioorganic & Medicinal Chemistry Letters* **2009,** *19* (13), 3619-3622.

20. Joeng, C. B.; Niazi, J. H.; Lee, S. J.; Gu, M. B., ssDNA aptamers that recognize diclofenac and 2-anilinophenylacetic acid. *Bioorganic & Medicinal Chemistry* **2009,** *17* (15), 5380-5387.
21. Walsh, R.; DeRosa, M. C., Retention of function in the DNA homolog of the RNA dopamine aptamer. *Biochemical and Biophysical Research Communications* **2009,** *388* (4), 732-735.
22. Kim, Y. S.; Hyun, C. J.; Kim, I. A.; Gu, M. B., Isolation and characterization of enantioselective DNA aptamers for ibuprofen. *Bioorganic & Medicinal Chemistry* **2010,** *18* (10), 3467-3473.
23. Luo, X.; McKeague, M.; Pitre, S.; Dumontier, M.; Green, J.; Golshani, A.; Derosa, M. C.; Dehne, F., Computational approaches toward the design of pools for the in vitro selection of complex aptamers. *RNA* **2010,** *16* (11), 2252-2262.
24. McKeague, M.; Bradley, C. R.; De Girolamo, A.; Visconti, A.; Miller, J. D.; DeRosa, M. C., Screening and Initial Binding Assessment of Fumonisin B(1) Aptamers. *International Journal of Molecular Sciences* **2010,** *11* (12), 4864-4881.
25. He, J.; Liu, Y.; Fan, M.; Liu, X., Isolation and Identification of the DNA Aptamer Target to Acetamiprid. *Journal of Agricultural and Food Chemistry* **2011,** *59* (5), 1582-1586.
26. Jo, M.; Ahn, J.-Y.; Lee, J.; Lee, S.; Hong, S. W.; Yoo, J.-W.; Kang, J.; Dua, P.; Lee, D.-k.; Hong, S.; Kim, S., Development of Single-Stranded DNA Aptamers for Specific Bisphenol A Detection. *Oligonucleotides* **2011,** *21* (2), 85-91.
27. Mehta, J.; Van Dorst, B.; Rouah-Martin, E.; Herrebout, W.; Scippo, M.-L.; Blust, R.; Robbens, J., In vitro selection and characterization of DNA aptamers recognizing chloramphenicol. *Journal of Biotechnology* **2011,** *155* (4), 361-369.
28. Song, K.-M.; Cho, M.; Jo, H.; Min, K.; Jeon, S. H.; Kim, T.; Han, M. S.; Ku, J. K.; Ban, C., Gold nanoparticle-based colorimetric detection of kanamycin using a DNA aptamer. *Analytical Biochemistry* **2011,** *415* (2), 175-181.
29. Yang, X.; Bing, T.; Mei, H.; Fang, C.; Cao, Z.; Shangguan, D., Characterization and application of a DNA aptamer binding to l-tryptophan. *Analyst* **2011,** *136* (3), 577-585.
30. Barthelmebs, L.; Jonca, J.; Hayat, A.; Prieto-Simon, B.; Marty, J.-L., Enzyme-Linked Aptamer Assays (ELAAs), based on a competition format for a rapid and sensitive detection of Ochratoxin A in wine. *Food Control* **2011,** *22* (5), 737-743.
31. Song, K.-M.; Jeong, E.; Jeon, W.; Cho, M.; Ban, C., Aptasensor for ampicillin using gold nanoparticle based dual fluorescence–colorimetric methods. *Analytical and Bioanalytical Chemistry* **2012,** *402* (6), 2153-2161.
32. Kiani, Z.; Shafiei, M.; Rahimi-Moghaddam, P.; Karkhane, A. A.; Ebrahimi, S. A., In vitro selection and characterization of deoxyribonucleic acid aptamers for digoxin. *Analytica Chimica Acta* **2012,** *748*, 67-72.
33. Stoltenburg, R.; Nikolaus, N.; Strehlitz, B., Capture-SELEX: Selection of DNA Aptamers for Aminoglycoside Antibiotics. *Journal of Analytical Methods in Chemistry* **2012,** *2012*, 14.
34. Rouah-Martin, E.; Mehta, J.; van Dorst, B.; de Saeger, S.; Dubruel, P.; Maes, B. U. W.; Lemiere, F.; Goormaghtigh, E.; Daems, D.; Herrebout, W.; van Hove, F.; Blust, R.; Robbens, J., Aptamer-Based Molecular Recognition of Lysergamine, Metergoline and Small Ergot Alkaloids. *International Journal of Molecular Sciences* **2012,** *13* (12), 17138-17159.
35. Xu, S.; Yuan, H.; Chen, S.; Xu, A.; Wang, J.; Wu, L., Selection of DNA aptamers against polychlorinated biphenyls as potential biorecognition elements for environmental analysis. *Analytical Biochemistry* **2012,** *423* (2), 195-201.
36. Mehta, J.; Rouah-Martin, E.; Van Dorst, B.; Maes, B.; Herrebout, W.; Scippo, M.-L.; Dardenne, F.; Blust, R.; Robbens, J., Selection and Characterization of PCB-Binding DNA Aptamers. *Analytical Chemistry* **2012,** *84* (3), 1669-1676.
37. Song, K.-M.; Jeong, E.; Jeon, W.; Jo, H.; Ban, C., A coordination polymer nanobelt (CPNB)-based aptasensor for sulfadimethoxine. *Biosensors and Bioelectronics* **2012,** *33* (1), 113-119.
38. Grozio, A.; Gonzalez, V. M.; Millo, E.; Sturla, L.; Vigliarolo, T.; Bagnasco, L.; Guida, L.; D'Arrigo, C.; De Flora, A.; Salis, A.; Martin, E. M.; Bellotti, M.; Zocchi, E., Selection and

Characterization of Single Stranded DNA Aptamers for the Hormone Abscisic Acid. *Nucleic Acid Therapeutics* **2013,** *23* (5), 322-331.
39. Huang, L.; Yang, X.; Qi, C.; Niu, X.; Zhao, C.; Zhao, X.; Shangguan, D.; Yang, Y., A label-free electrochemical biosensor based on a DNA aptamer against codeine. *Analytica Chimica Acta* **2013,** *787*, 203-210.
40. Gong, S.; Ren, H.-L.; Tian, R.-Y.; Lin, C.; Hu, P.; Li, Y.-S.; Liu, Z.-S.; Song, J.; Tang, F.; Zhou, Y.; Li, Z.-H.; Zhang, Y.-Y.; Lu, S.-Y., A novel analytical probe binding to a potential carcinogenic factor of N-glycolylneuraminic acid by SELEX. *Biosensors and Bioelectronics* **2013,** *49*, 547-554.
41. Yang, J.; Bowser, M. T., Capillary Electrophoresis–SELEX Selection of Catalytic DNA Aptamers for a Small-Molecule Porphyrin Target. *Analytical Chemistry* **2013,** *85* (3), 1525-1530.
42. Eissa, S.; Ng, A.; Siaj, M.; Tavares, A. C.; Zourob, M., Selection and Identification of DNA Aptamers against Okadaic Acid for Biosensing Application. *Analytical Chemistry* **2013,** *85* (24), 11794-11801.
43. Zheng, X.; Hu, B.; Gao, S. X.; Liu, D. J.; Sun, M. J.; Jiao, B. H.; Wang, L. H., A saxitoxin-binding aptamer with higher affinity and inhibitory activity optimized by rational site-directed mutagenesis and truncation. *Toxicon* **2015,** *101*, 41-47.
44. Zhou, N.; Wang, J.; Zhang, J.; Li, C.; Tian, Y.; Wang, J., Selection and identification of streptomycin-specific single-stranded DNA aptamers and the application in the detection of streptomycin in honey. *Talanta* **2013,** *108*, 109-116.
45. Bae, H.; Ren, S.; Kang, J.; Kim, M.; Jiang, Y.; Jin, M. M.; Min, I. M.; Kim, S., Sol-Gel SELEX Circumventing Chemical Conjugation of Low Molecular Weight Metabolites Discovers Aptamers Selective to Xanthine. *Nucleic Acid Therapeutics* **2013,** *23* (6), 443-449.
46. Chen, X.; Huang, Y.; Duan, N.; Wu, S.; Ma, X.; Xia, Y.; Zhu, C.; Jiang, Y.; Wang, Z., Selection and identification of ssDNA aptamers recognizing zearalenone. *Analytical and Bioanalytical Chemistry* **2013,** *405* (20), 6573-6581.
47. Vanschoenbeek, K.; Vanbrabant, J.; Hosseinkhani, B.; Vermeeren, V.; Michiels, L., Aptamers targeting different functional groups of 17β-estradiol. *The Journal of Steroid Biochemistry and Molecular Biology* **2015,** *147*, 10-16.
48. Alsager, O. A.; Kumar, S.; Willmott, G. R.; McNatty, K. P.; Hodgkiss, J. M., Small molecule detection in solution via the size contraction response of aptamer functionalized nanoparticles. *Biosensors and Bioelectronics* **2014,** *57*, 262-268.
49. Malhotra, S.; Pandey, A. K.; Rajput, Y. S.; Sharma, R., Selection of aptamers for aflatoxin M1 and their characterization. *Journal of Molecular Recognition* **2014,** *27* (8), 493-500.
50. Zhu, Z.; Song, Y.; Li, C.; Zou, Y.; Zhu, L.; An, Y.; Yang, C. J., Monoclonal Surface Display SELEX for Simple, Rapid, Efficient, and Cost-Effective Aptamer Enrichment and Identification. *Analytical Chemistry* **2014,** *86* (12), 5881-5888.
51. Williams, R. M.; Crihfield, C. L.; Gattu, S.; Holland, L. A.; Sooter, L. J., In Vitro Selection of a Single-Stranded DNA Molecular Recognition Element against Atrazine. *International Journal of Molecular Sciences* **2014,** *15* (8), 14332-14347.
52. Williams, R. M.; Kulick, A. R.; Yedlapalli, S.; Battistella, L.; Hajiran, C. J.; Sooter, L. J., In Vitro Selection of a Single-Stranded DNA Molecular Recognition Element Specific for Bromacil. *Journal of Nucleic Acids* **2014,** *2014*, 102968.
53. Martin, J. A.; Chávez, J. L.; Chushak, Y.; Chapleau, R. R.; Hagen, J.; Kelley-Loughnane, N., Tunable stringency aptamer selection and gold nanoparticle assay for detection of cortisol. *Analytical and Bioanalytical Chemistry* **2014,** *406* (19), 4637-4647.
54. Elshafey, R.; Siaj, M.; Zourob, M., In Vitro Selection, Characterization, and Biosensing Application of High-Affinity Cylindrospermopsin-Targeting Aptamers. *Analytical Chemistry* **2014,** *86* (18), 9196-9203.

55. Chen, X.; Huang, Y.; Duan, N.; Wu, S.; Xia, Y.; Ma, X.; Zhu, C.; Jiang, Y.; Ding, Z.; Wang, Z., Selection and characterization of single stranded DNA aptamers recognizing fumonisin B1. *Microchimica Acta* **2014,** *181* (11), 1317-1324.
56. Nikolaus, N.; Strehlitz, B., DNA-Aptamers Binding Aminoglycoside Antibiotics. *Sensors (Basel, Switzerland)* **2014,** *14* (2), 3737-3755.
57. McKeague, M.; Velu, R.; Hill, K.; Bardóczy, V.; Mészáros, T.; DeRosa, M. C., Selection and Characterization of a Novel DNA Aptamer for Label-Free Fluorescence Biosensing of Ochratoxin A. *Toxins* **2014,** *6* (8), 2435-2452.
58. Kim, C.-H.; Lee, L.-P.; Min, J.-R.; Lim, M.-W.; Jeong, S.-H., An indirect competitive assay-based aptasensor for detection of oxytetracycline in milk. *Biosensors and Bioelectronics* **2014,** *51*, 426-430.
59. Contreras Jiménez, G.; Eissa, S.; Ng, A.; Alhadrami, H.; Zourob, M.; Siaj, M., Aptamer-Based Label-Free Impedimetric Biosensor for Detection of Progesterone. *Analytical Chemistry* **2015,** *87* (2), 1075-1082.
60. Chen, X.; Huang, Y.; Duan, N.; Wu, S.; Xia, Y.; Ma, X.; Zhu, C.; Jiang, Y.; Wang, Z., Screening and Identification of DNA Aptamers against T-2 Toxin Assisted by Graphene Oxide. *Journal of Agricultural and Food Chemistry* **2014,** *62* (42), 10368-10374.
61. Priyanka; Shorie, M.; Bhalla, V.; Pathania, P.; Suri, C. R., Nanobioprobe mediated DNA aptamers for explosive detection. *Chemical Communications* **2014,** *50* (9), 1080-1082.
62. Elshafey, R.; Siaj, M.; Zourob, M., DNA aptamers selection and characterization for development of label-free impedimetric aptasensor for neurotoxin anatoxin-a. *Biosensors and Bioelectronics* **2015,** *68*, 295-302.
63. Eissa, S.; Siaj, M.; Zourob, M., Aptamer-based competitive electrochemical biosensor for brevetoxin-2. *Biosensors and Bioelectronics* **2015,** *69*, 148-154.
64. Kwon, Y. S.; Nguyen, V.-T.; Park, J. G.; Gu, M. B., Detection of Iprobenfos and Edifenphos using a new Multi-aptasensor. *Analytica Chimica Acta* **2015,** *868*, 60-66.
65. Gu, C.; Lan, T.; Shi, H.; Lu, Y., Portable Detection of Melamine in Milk Using a Personal Glucose Meter Based on an in Vitro Selected Structure-Switching Aptamer. *Analytical Chemistry* **2015,** *87* (15), 7676-7682.
66. Tang, X. L.; Hua, Y.; Guan, Q.; Yuan, C. H., Improved detection of deeply invasive candidiasis with DNA aptamers specific binding to (1→3)-β-D-glucans from Candida albicans. *European Journal of Clinical Microbiology & Infectious Diseases* **2016,** *35* (4), 587-595.
67. Setlem, K.; Mondal, B.; Ramlal, S.; Kingston, J., Immuno Affinity SELEX for Simple, Rapid, and Cost-Effective Aptamer Enrichment and Identification against Aflatoxin B1. *Frontiers in Microbiology* **2016,** *7*, 1909.
68. Kim, U.-J.; Kim, B. C., DNA aptamers for selective identification and separation of flame retardant chemicals. *Analytica Chimica Acta* **2016,** *936*, 208-215.
69. Gao, S.; Hu, B.; Zheng, X.; Cao, Y.; Liu, D.; Sun, M.; Jiao, B.; Wang, L., Gonyautoxin 1/4 aptamers with high-affinity and high-specificity: From efficient selection to aptasensor application. *Biosensors and Bioelectronics* **2016,** *79*, 938-944.
70. Wang , H.; Wang, J.; Sun, N.; Cheng , H.; Chen, H.; Pei, R., Selection and Characterization of Malachite Green Aptamers for the Development of Light–up Probes. *ChemistrySelect* **2016,** *1* (8), 1571-1574.
71. Gu, H.; Duan, N.; Wu, S.; Hao, L.; Xia, Y.; Ma, X.; Wang, Z., Graphene oxide-assisted non-immobilized SELEX of okdaic acid aptamer and the analytical application of aptasensor. **2016,** *6*, 21665.
72. Zhang, Y.; You, Y.; Xia, Z.; Han, X.; Tian, Y.; Zhou, N., Graphene oxide-based selection and identification of ofloxacin-specific single-stranded DNA aptamers. *RSC Advances* **2016,** *6* (101), 99540-99545.
73. Wu, S.; Duan, N.; Zhang, W.; Zhao, S.; Wang, Z., Screening and development of DNA aptamers as capture probes for colorimetric detection of patulin. *Analytical Biochemistry* **2016,** *508*, 58-64.

74. Wang, H.; Wang, J.; Xu, L.; Zhang, Y.; Chen, Y.; Chen, H.; Pei, R., Selection and characterization of thioflavin T aptamers for the development of light-up probes. *Analytical Methods* **2016,** *8* (48), 8461-8465.
75. Valenzano, S.; De Girolamo, A.; DeRosa, M. C.; McKeague, M.; Schena, R.; Catucci, L.; Pascale, M., Screening and Identification of DNA Aptamers to Tyramine Using in Vitro Selection and High-Throughput Sequencing. *ACS Combinatorial Science* **2016,** *18* (6), 302-313.
76. Lee, A. Y.; Ha, N.-R.; Jung, I.-P.; Kim, S.-H.; Kim, A. R.; Yoon, M.-Y., Development of a ssDNA aptamer for detection of residual benzylpenicillin. *Analytical Biochemistry* **2017,** *531*, 1-7.
77. Skouridou, V.; Jauset-Rubio, M.; Ballester, P.; Bashammakh, A. S.; El-Shahawi, M. S.; Alyoubi, A. O.; O'Sullivan, C. K., Selection and characterization of DNA aptamers against the steroid testosterone. *Microchimica Acta* **2017,** *184* (6), 1631-1639.
78. Han, Y.; Diao, D.; Lu, Z.; Li, X.; Guo, Q.; Huo, Y.; Xu, Q.; Li, Y.; Cao, S.; Wang, J.; Wang, Y.; Zhao, J.; Li, Z.; He, M.; Luo, Z.; Lou, X., Selection of Group-Specific Phthalic Acid Esters Binding DNA Aptamers via Rationally Designed Target Immobilization and Applications for Ultrasensitive and Highly Selective Detection of Phthalic Acid Esters. *Analytical Chemistry* **2017,** *89* (10), 5270-5277.
79. Ha, N.-R.; Jung, I.-P.; La, I.-J.; Jung, H.-S.; Yoon, M.-Y., Ultra-sensitive detection of kanamycin for food safety using a reduced graphene oxide-based fluorescent aptasensor. **2017,** *7*, 40305.
80. Alhadrami, H. A.; Chinnappan, R.; Eissa, S.; Rahamn, A. A.; Zourob, M., High affinity truncated DNA aptamers for the development of fluorescence based progesterone biosensors. *Analytical Biochemistry* **2017,** *525*, 78-84.
81. Bock, L. C.; Griffin, L. C.; Latham, J. A.; Vermaas, E. H.; Toole, J. J., Selection of single-stranded DNA molecules that bind and inhibit human thrombin. *Nature* **1992,** *355* (6360), 564-566.
82. Wiegand, T. W.; Williams, P. B.; Dreskin, S. C.; Jouvin, M. H.; Kinet, J. P.; Tasset, D., High-affinity oligonucleotide ligands to human IgE inhibit binding to Fc epsilon receptor I. *The Journal of Immunology* **1996,** *157* (1), 221.
83. Green, L. S.; Jellinek, D.; Jenison, R.; Östman, A.; Heldin, C.-H.; Janjic, N., Inhibitory DNA Ligands to Platelet-Derived Growth Factor B-Chain. *Biochemistry* **1996,** *35* (45), 14413-14424.
84. Mendonsa, S. D.; Bowser, M. T., In Vitro Evolution of Functional DNA Using Capillary Electrophoresis. *Journal of the American Chemical Society* **2004,** *126* (1), 20-21.
85. Tang, J.; Xie, J.; Shao, N.; Yan, Y., The DNA aptamers that specifically recognize ricin toxin are selected by two in vitro selection methods. *Electrophoresis* **2006,** *27* (7), 1303-1311.
86. Tang, J.; Yu, T.; Guo, L.; Xie, J.; Shao, N.; He, Z., In vitro selection of DNA aptamer against abrin toxin and aptamer-based abrin direct detection. *Biosensors and Bioelectronics* **2007,** *22* (11), 2456-2463.
87. Rotherham, L. S.; Maserumule, C.; Dheda, K.; Theron, J.; Khati, M., Selection and Application of ssDNA Aptamers to Detect Active TB from Sputum Samples. *PLOS ONE* **2012,** *7* (10), e46862.
88. Stoltenburg, R.; Schubert, T.; Strehlitz, B., In vitro Selection and Interaction Studies of a DNA Aptamer Targeting Protein A. *PLoS ONE* **2015,** *10* (7), e0134403.
89. Zheng, Y.; Wang, Y.; Yang, X., Aptamer-based colorimetric biosensing of dopamine using unmodified gold nanoparticles. *Sensors and Actuators B: Chemical* **2011,** *156* (1), 95-99.
90. Li, B.-R.; Hsieh, Y.-J.; Chen, Y.-X.; Chung, Y.-T.; Pan, C.-Y.; Chen, Y.-T., An Ultrasensitive Nanowire-Transistor Biosensor for Detecting Dopamine Release from Living PC12 Cells under Hypoxic Stimulation. *Journal of the American Chemical Society* **2013,** *135* (43), 16034-16037.
91. Zhou, J.; Wang, W.; Yu, P.; Xiong, E.; Zhang, X.; Chen, J., A simple label-free electrochemical aptasensor for dopamine detection. *RSC Advances* **2014,** *4* (94), 52250-52255.

92. Hun, X.; Xu, Y.; Xie, G.; Luo, X., Aptamer biosensor for highly sensitive and selective detection of dopamine using ubiquitous personal glucose meters. *Sensors and Actuators B: Chemical* **2015,** *209*, 596-601.
93. Jarczewska, M.; Sheelam, S. R.; Ziółkowski, R.; Górski, Ł., A Label-Free Electrochemical DNA Aptasensor for the Detection of Dopamine. *Journal of The Electrochemical Society* **2016,** *163* (3), B26-B31.
94. Azadbakht, A.; Roushani, M.; Abbasi, A. R.; Menati, S.; Derikvand, Z., A label-free aptasensor based on polyethyleneimine wrapped carbon nanotubes in situ formed gold nanoparticles as signal probe for highly sensitive detection of dopamine. *Materials Science and Engineering: C* **2016,** *68*, 585-593.
95. Huang, R.; Xiong, W.; Wang, D.; Guo, L.; Lin, Z.; Yu, L.; Chu, K.; Qiu, B.; Chen, G., Label-free aptamer-based partial filling technique for enantioseparation and determination of dl-tryptophan with micellar electrokinetic chromatography. *ELECTROPHORESIS* **2013,** *34* (2), 254-259.
96. Yang, X.; Han, Q.; Zhang, Y.; Wu, J.; Tang, X.; Dong, C.; Liu, W., Determination of free tryptophan in serum with aptamer—Comparison of two aptasensors. *Talanta* **2015,** *131*, 672-677.
97. Pang, S.; Labuza, T. P.; He, L., Development of a single aptamer-based surface enhanced Raman scattering method for rapid detection of multiple pesticides. *Analyst* **2014,** *139* (8), 1895-1901.
98. Zhang, C.; Wang, L.; Tu, Z.; Sun, X.; He, Q.; Lei, Z.; Xu, C.; Liu, Y.; Zhang, X.; Yang, J.; Liu, X.; Xu, Y., Organophosphorus pesticides detection using broad-specific single-stranded DNA based fluorescence polarization aptamer assay. *Biosensors and Bioelectronics* **2014,** *55*, 216-219.
99. Dou, X.; Chu, X.; Kong, W.; Luo, J.; Yang, M., A gold-based nanobeacon probe for fluorescence sensing of organophosphorus pesticides. *Analytica Chimica Acta* **2015,** *891*, 291-297.
100. Tang, T.; Deng, J.; Zhang, M.; Shi, G.; Zhou, T., Quantum dot-DNA aptamer conjugates coupled with capillary electrophoresis: A universal strategy for ratiometric detection of organophosphorus pesticides. *Talanta* **2016,** *146*, 55-61.
101. Wang, P.; Wan, Y.; Ali, A.; Deng, S.; Su, Y.; Fan, C.; Yang, S., Aptamer-wrapped gold nanoparticles for the colorimetric detection of omethoate. *Science China Chemistry* **2016,** *59* (2), 237-242.
102. Zhang, C.; Lin, B.; Cao, Y.; Guo, M.; Yu, Y., Fluorescence Determination of Omethoate Based on a Dual Strategy for Improving Sensitivity. *Journal of Agricultural and Food Chemistry* **2017,** *65* (14), 3065-3073.
103. Li, S.; Wu, X.; Liu, C.; Yin, G.; Luo, J.; Xu, Z., Application of DNA aptamers as sensing layers for detection of carbofuran by electrogenerated chemiluminescence energy transfer. *Analytica Chimica Acta* **2016,** *941*, 94-100.
104. Fan, L.; Zhao, G.; Shi, H.; Liu, M.; Li, Z., A highly selective electrochemical impedance spectroscopy-based aptasensor for sensitive detection of acetamiprid. *Biosensors and Bioelectronics* **2013,** *43*, 12-18.
105. Shi, H.; Zhao, G.; Liu, M.; Fan, L.; Cao, T., Aptamer-based colorimetric sensing of acetamiprid in soil samples: Sensitivity, selectivity and mechanism. *Journal of Hazardous Materials* **2013,** *260*, 754-761.
106. Weerathunge, P.; Ramanathan, R.; Shukla, R.; Sharma, T. K.; Bansal, V., Aptamer-Controlled Reversible Inhibition of Gold Nanozyme Activity for Pesticide Sensing. *Analytical Chemistry* **2014,** *86* (24), 11937-11941.
107. Yang, Z.; Qian, J.; Yang, X.; Jiang, D.; Du, X.; Wang, K.; Mao, H.; Wang, K., A facile label-free colorimetric aptasensor for acetamiprid based on the peroxidase-like activity of hemin-functionalized reduced graphene oxide. *Biosensors and Bioelectronics* **2015,** *65*, 39-46.
108. Jiang, D.; Du, X.; Liu, Q.; Zhou, L.; Dai, L.; Qian, J.; Wang, K., Silver nanoparticles anchored on nitrogen-doped graphene as a novel electrochemical biosensing platform with enhanced sensitivity for aptamer-based pesticide assay. *Analyst* **2015,** *140* (18), 6404-6411.

109. Li, H.; Qiao, Y.; Li, J.; Fang, H.; Fan, D.; Wang, W., A sensitive and label-free photoelectrochemical aptasensor using Co-doped ZnO diluted magnetic semiconductor nanoparticles. *Biosensors and Bioelectronics* **2016,** *77*, 378-384.
110. Guo, J.; Li, Y.; Wang, L.; Xu, J.; Huang, Y.; Luo, Y.; Shen, F.; Sun, C.; Meng, R., Aptamer-based fluorescent screening assay for acetamiprid via inner filter effect of gold nanoparticles on the fluorescence of CdTe quantum dots. *Analytical & Bioanalytical Chemistry* **2016,** *408* (2), 557-566.
111. Lin, B.; Yu, Y.; Li, R.; Cao, Y.; Guo, M., Turn-on sensor for quantification and imaging of acetamiprid residues based on quantum dots functionalized with aptamer. *Sensors and Actuators B: Chemical* **2016,** *229*, 100-109.
112. Hu, W.; Chen, Q.; Li, H.; Ouyang, Q.; Zhao, J., Fabricating a novel label-free aptasensor for acetamiprid by fluorescence resonance energy transfer between NH2-NaYF4: Yb, Ho@SiO2 and Au nanoparticles. *Biosensors and Bioelectronics* **2016,** *80*, 398-404.
113. Qi, Y.; Xiu, F.-R.; Zheng, M.; Li, B., A simple and rapid chemiluminescence aptasensor for acetamiprid in contaminated samples: Sensitivity, selectivity and mechanism. *Biosensors and Bioelectronics* **2016,** *83*, 243-249.
114. Mei, Z.; Chu, H.; Chen, W.; Xue, F.; Liu, J.; Xu, H.; Zhang, R.; Zheng, L., Ultrasensitive one-step rapid visual detection of bisphenol A in water samples by label-free aptasensor. *Biosensors and Bioelectronics* **2013,** *39* (1), 26-30.
115. Ragavan, K. V.; Selvakumar, L. S.; Thakur, M. S., Functionalized aptamers as nano-bioprobes for ultrasensitive detection of bisphenol-A. *Chemical Communications* **2013,** *49* (53), 5960-5962.
116. Xue, F.; Wu, J.; Chu, H.; Mei, Z.; Ye, Y.; Liu, J.; Zhang, R.; Peng, C.; Zheng, L.; Chen, W., Electrochemical aptasensor for the determination of bisphenol A in drinking water. *Microchimica Acta* **2013,** *180* (1), 109-115.
117. Zhang, Y.; Cao, T.; Huang, X.; Liu, M.; Shi, H.; Zhao, G., A Visible-Light Driven Photoelectrochemical Aptasensor for Endocrine Disrupting Chemicals Bisphenol A with High Sensitivity and Specificity. *Electroanalysis* **2013,** *25* (7), 1787-1795.
118. Zhou, L.; Wang, J.; Li, D.; Li, Y., An electrochemical aptasensor based on gold nanoparticles dotted graphene modified glassy carbon electrode for label-free detection of bisphenol A in milk samples. *Food Chemistry* **2014,** *162*, 34-40.
119. Marks, H. L.; Pishko, M. V.; Jackson, G. W.; Coté, G. L., Rational Design of a Bisphenol A Aptamer Selective Surface-Enhanced Raman Scattering Nanoprobe. *Analytical Chemistry* **2014,** *86* (23), 11614-11619.
120. Kuang, H.; Yin, H.; Liu, L.; Xu, L.; Ma, W.; Xu, C., Asymmetric Plasmonic Aptasensor for Sensitive Detection of Bisphenol A. *ACS Applied Materials & Interfaces* **2014,** *6* (1), 364-369.
121. Lee, J. S.; Kim, S. G.; Jun, J.; Shin, D. H.; Jang, J., Aptamer-Functionalized Multidimensional Conducting-Polymer Nanoparticles for an Ultrasensitive and Selective Field-Effect-Transistor Endocrine-Disruptor Sensors. *Advanced Functional Materials* **2014,** *24* (39), 6145-6153.
122. Yildirim, N.; Long, F.; He, M.; Shi, H.-C.; Gu, A. Z., A portable optic fiber aptasensor for sensitive, specific and rapid detection of bisphenol-A in water samples. *Environmental Science: Processes & Impacts* **2014,** *16* (6), 1379-1386.
123. Zhu, Y.; Cai, Y.; Xu, L.; Zheng, L.; Wang, L.; Qi, B.; Xu, C., Building An Aptamer/Graphene Oxide FRET Biosensor for One-Step Detection of Bisphenol A. *ACS Applied Materials & Interfaces* **2015,** *7* (14), 7492-7496.
124. Chung, E.; Jeon, J.; Yu, J.; Lee, C.; Choo, J., Surface-enhanced Raman scattering aptasensor for ultrasensitive trace analysis of bisphenol A. *Biosensors and Bioelectronics* **2015,** *64*, 560-565.
125. Zhu, Y.; Zhou, C.; Yan, X.; Yan, Y.; Wang, Q., Aptamer-functionalized nanoporous gold film for high-performance direct electrochemical detection of bisphenol A in human serum. *Analytica Chimica Acta* **2015,** *883*, 81-89.

126. Chen, L.; Zeng, X.; Ferhan, A. R.; Chi, Y.; Kim, D.-H.; Chen, G., Signal-on electrochemiluminescent aptasensors based on target controlled permeable films. *Chemical Communications* **2015,** *51* (6), 1035-1038.
127. Xu, J.; Li, Y.; Bie, J.; Jiang, W.; Guo, J.; Luo, Y.; Shen, F.; Sun, C., Colorimetric method for determination of bisphenol A based on aptamer-mediated aggregation of positively charged gold nanoparticles. *Microchimica Acta* **2015,** *182* (13), 2131-2138.
128. Ding, J.; Gu, Y.; Li, F.; Zhang, H.; Qin, W., DNA Nanostructure-Based Magnetic Beads for Potentiometric Aptasensing. *Analytical Chemistry* **2015,** *87* (13), 6465-6469.
129. Duan, N.; Zhang, H.; Nie, Y.; Wu, S.; Miao, T.; Chen, J.; Wang, Z., Fluorescence resonance energy transfer-based aptamer biosensors for bisphenol A using lanthanide-doped KGdF4 nanoparticles. *Analytical Methods* **2015,** *7* (12), 5186-5192.
130. Cheng, C.; Wang, S.; Wu, J.; Yu, Y.; Li, R.; Eda, S.; Chen, J.; Feng, G.; Lawrie, B.; Hu, A., Bisphenol A Sensors on Polyimide Fabricated by Laser Direct Writing for Onsite River Water Monitoring at Attomolar Concentration. *ACS Applied Materials & Interfaces* **2016,** *8* (28), 17784-17792.
131. Kim, S. G.; Lee, J. S.; Jun, J.; Shin, D. H.; Jang, J., Ultrasensitive Bisphenol A Field-Effect Transistor Sensor Using an Aptamer-Modified Multichannel Carbon Nanofiber Transducer. *ACS Applied Materials & Interfaces* **2016,** *8* (10), 6602-6610.
132. Zhang, D.; Yang, J.; Ye, J.; Xu, L.; Xu, H.; Zhan, S.; Xia, B.; Wang, L., Colorimetric detection of bisphenol A based on unmodified aptamer and cationic polymer aggregated gold nanoparticles. *Analytical Biochemistry* **2016,** *499*, 51-56.
133. Li, Y.; Xu, J.; Wang, L.; Huang, Y.; Guo, J.; Cao, X.; Shen, F.; Luo, Y.; Sun, C., Aptamer-based fluorescent detection of bisphenol A using nonconjugated gold nanoparticles and CdTe quantum dots. *Sensors and Actuators B: Chemical* **2016,** *222*, 815-822.
134. Chen, J.; Zhou, S., Label-free DNA Y junction for bisphenol A monitoring using exonuclease III-based signal protection strategy. *Biosensors and Bioelectronics* **2016,** *77*, 277-283.
135. Guo, X.; Wu, S.; Duan, N.; Wang, Z., Mn2+-doped NaYF4:Yb/Er upconversion nanoparticle-based electrochemiluminescent aptasensor for bisphenol A. *Analytical and Bioanalytical Chemistry* **2016,** *408* (14), 3823-3831.
136. Luo, Z.; Zhang, J.; Wang, Y.; Chen, J.; Li, Y.; Duan, Y., An aptamer based method for small molecules detection through monitoring salt-induced AuNPs aggregation and surface plasmon resonance (SPR) detection. *Sensors and Actuators B: Chemical* **2016,** *236*, 474-479.
137. Kazane, I.; Gorgy, K.; Gondran, C.; Spinelli, N.; Zazoua, A.; Defrancq, E.; Cosnier, S., Highly Sensitive Bisphenol-A Electrochemical Aptasensor Based on Poly(Pyrrole-Nitrilotriacetic Acid)-Aptamer Film. *Analytical Chemistry* **2016,** *88* (14), 7268-7273.
138. Lin, X.; Cheng, C.; Terry, P.; Chen, J.; Cui, H.; Wu, J., Rapid and sensitive detection of bisphenol a from serum matrix. *Biosensors and Bioelectronics* **2017,** *91*, 104-109.
139. Deiminiat, B.; Rounaghi, G. H.; Arbab-Zavar, M. H.; Razavipanah, I., A novel electrochemical aptasensor based on f-MWCNTs/AuNPs nanocomposite for label-free detection of bisphenol A. *Sensors and Actuators B: Chemical* **2017,** *242*, 158-166.
140. Lee, E.-H.; Lim, H. J.; Lee, S.-D.; Son, A., Highly Sensitive Detection of Bisphenol A by NanoAptamer Assay with Truncated Aptamer. *ACS Applied Materials & Interfaces* **2017,** *9* (17), 14889-14898.
141. He, M.-Q.; Wang, K.; Wang, J.; Yu, Y.-L.; He, R.-H., A sensitive aptasensor based on molybdenum carbide nanotubes and label-free aptamer for detection of bisphenol A. *Analytical and Bioanalytical Chemistry* **2017,** *409* (7), 1797-1803.
142. Zhang, Y.; Wang, Y.; Zhu, W.; Wang, J.; Yue, X.; Liu, W.; Zhang, D.; Wang, J., Simultaneous colorimetric determination of bisphenol A and bisphenol S via a multi-level DNA circuit mediated by aptamers and gold nanoparticles. *Microchimica Acta* **2017,** *184* (3), 951-959.

143. Beiranvand, Z. S.; Abbasi, A. R.; Dehdashtian, S.; Karimi, Z.; Azadbakht, A., Aptamer-based electrochemical biosensor by using Au-Pt nanoparticles, carbon nanotubes and acriflavine platform. *Analytical Biochemistry* **2017,** *518*, 35-45.
144. Bala, R.; Sharma, R. K.; Wangoo, N., Development of gold nanoparticles-based aptasensor for the colorimetric detection of organophosphorus pesticide phorate. *Analytical and Bioanalytical Chemistry* **2016,** *408* (1), 333-338.
145. Liu, J.; Lu, Y., Fast Colorimetric Sensing of Adenosine and Cocaine Based on a General Sensor Design Involving Aptamers and Nanoparticles. *Angewandte Chemie International Edition* **2006,** *45* (1), 90-94.
146. Zhu, C.; Zeng, Z.; Li, H.; Li, F.; Fan, C.; Zhang, H., Single-Layer MoS2-Based Nanoprobes for Homogeneous Detection of Biomolecules. *Journal of the American Chemical Society* **2013,** *135* (16), 5998-6001.
147. Zhang, Z.; Oni, O.; Liu, J., New insights into a classic aptamer: binding sites, cooperativity and more sensitive adenosine detection. *Nucleic Acids Research* **2017,** *45* (13), 7593-7601.
148. Song, Y.; Tang, T.; Wang, X.; Xu, G.; Wei, F.; Wu, Y.; Song, Q.; Ma, Y.; Ma, Y.; Cen, Y.; Hu, Q., Highly selective and sensitive detection of adenosine utilizing signal amplification based on silver ions-assisted cation exchange reaction with CdTe quantum dots. *Sensors and Actuators B: Chemical* **2017,** *247*, 305-311.
149. Sergelen, K.; Liedberg, B.; Knoll, W.; Dostalek, J., A surface plasmon field-enhanced fluorescence reversible split aptamer biosensor. *Analyst* **2017,** *142* (16), 2995-3001.
150. Yildirim, N.; Long, F.; Gao, C.; He, M.; Shi, H.-C.; Gu, A. Z., Aptamer-Based Optical Biosensor For Rapid and Sensitive Detection of 17β-Estradiol In Water Samples. *Environmental Science & Technology* **2012,** *46* (6), 3288-3294.
151. Lin, Z.; Chen, L.; Zhang, G.; Liu, Q.; Qiu, B.; Cai, Z.; Chen, G., Label-free aptamer-based electrochemical impedance biosensor for 17[small beta]-estradiol. *Analyst* **2012,** *137* (4), 819-822.
152. Fan, L.; Zhao, G.; Shi, H.; Liu, M.; Wang, Y.; Ke, H., A Femtomolar Level and Highly Selective 17β-estradiol Photoelectrochemical Aptasensor Applied in Environmental Water Samples Analysis. *Environmental Science & Technology* **2014,** *48* (10), 5754-5761.
153. Liu, J.; Bai, W.; Niu, S.; Zhu, C.; Yang, S.; Chen, A., Highly sensitive colorimetric detection of 17β-estradiol using split DNA aptamers immobilized on unmodified gold nanoparticles. *Scientific Reports* **2014,** *4*, 7571.
154. Long, F.; Shi, H.; Wang, H., Fluorescence resonance energy transfer based aptasensor for the sensitive and selective detection of 17[small beta]-estradiol using a quantum dot-bioconjugate as a nano-bioprobe. *RSC Advances* **2014,** *4* (6), 2935-2941.
155. Ke, H.; Liu, M.; Zhuang, L.; Li, Z.; Fan, L.; Zhao, G., A Fetomolar Level 17β-estradiol Electrochemical Aptasensor Constructed On Hierachical Dendritic Gold Modified Boron-Doped Diamond Electrode. *Electrochimica Acta* **2014,** *137*, 146-153.
156. Huang, K.-J.; Liu, Y.-J.; Zhang, J.-Z.; Cao, J.-T.; Liu, Y.-M., Aptamer/Au nanoparticles/cobalt sulfide nanosheets biosensor for 17β-estradiol detection using a guanine-rich complementary DNA sequence for signal amplification. *Biosensors and Bioelectronics* **2015,** *67*, 184-191.
157. Soh, J. H.; Lin, Y.; Rana, S.; Ying, J. Y.; Stevens, M. M., Colorimetric Detection of Small Molecules in Complex Matrixes via Target-Mediated Growth of Aptamer-Functionalized Gold Nanoparticles. *Analytical Chemistry* **2015,** *87* (15), 7644-7652.
158. Fan, L.; Zhao, G.; Shi, H.; Liu, M., A simple and label-free aptasensor based on nickel hexacyanoferrate nanoparticles as signal probe for highly sensitive detection of 17β-estradiol. *Biosensors and Bioelectronics* **2015,** *68*, 303-309.
159. Chen, J.; Wen, J.; Yang, G.; Zhou, S., A target-induced three-way G-quadruplex junction for 17[small beta]-estradiol monitoring with a naked-eye readout. *Chemical Communications* **2015,** *51* (62), 12373-12376.

160. Li, Y.; Xu, J.; Jia, M.; Yang, Z.; Liang, Z.; Guo, J.; Luo, Y.; Shen, F.; Sun, C., Colorimetric determination of 17β-estradiol based on the specific recognition of aptamer and the salt-induced aggregation of gold nanoparticles. *Materials Letters* **2015,** *159*, 221-224.
161. Na, W.; Park, J. W.; An, J. H.; Jang, J., Size-controllable ultrathin carboxylated polypyrrole nanotube transducer for extremely sensitive 17[small beta]-estradiol FET-type biosensors. *Journal of Materials Chemistry B* **2016,** *4* (29), 5025-5034.
162. Alsager, O. A.; Kumar, S.; Zhu, B.; Travas-Sejdic, J.; McNatty, K. P.; Hodgkiss, J. M., Ultrasensitive Colorimetric Detection of 17β-Estradiol: The Effect of Shortening DNA Aptamer Sequences. *Analytical Chemistry* **2015,** *87* (8), 4201-4209.
163. Zheng, H. Y.; Alsager, O. A.; Wood, C. S.; Hodgkiss, J. M.; Plank, N. O. V., Carbon nanotube field effect transistor aptasensors for estrogen detection in liquids. *Journal of Vacuum Science & Technology B, Nanotechnology and Microelectronics: Materials, Processing, Measurement, and Phenomena* **2015,** *33* (6), 06F904.
164. Zhu, B.; Alsager, O. A.; Kumar, S.; Hodgkiss, J. M.; Travas-Sejdic, J., Label-free electrochemical aptasensor for femtomolar detection of 17β-estradiol. *Biosensors and Bioelectronics* **2015,** *70*, 398-403.
165. Dou, M.; Garcia, J. M.; Zhan, S.; Li, X., Interfacial nano-biosensing in microfluidic droplets for high-sensitivity detection of low-solubility molecules. *Chemical Communications* **2016,** *52* (17), 3470-3473.
166. Zhang, D.; Zhang, W.; Ye, J.; Zhan, S.; Xia, B.; Lv, J.; Xu, H.; Du, G.; Wang, L., A Label-Free Colorimetric Biosensor for 17β-Estradiol Detection Using Nanoparticles Assembled by Aptamer and Cationic Polymer. *Australian Journal of Chemistry* **2016,** *69* (1), 12-19.
167. Huang, H.; Shi, S.; Gao, X.; Gao, R.; Zhu, Y.; Wu, X.; Zang, R.; Yao, T., A universal label-free fluorescent aptasensor based on Ru complex and quantum dots for adenosine, dopamine and 17β-estradiol detection. *Biosensors and Bioelectronics* **2016,** *79*, 198-204.
168. Ni, X.; Xia, B.; Wang, L.; Ye, J.; Du, G.; Feng, H.; Zhou, X.; Zhang, T.; Wang, W., Fluorescent aptasensor for 17β-estradiol determination based on gold nanoparticles quenching the fluorescence of Rhodamine B. *Analytical Biochemistry* **2017,** *523*, 17-23.
169. Yan, Z.; Gan, N.; Wang, D.; Cao, Y.; Chen, M.; Li, T.; Chen, Y., A "signal-on'' aptasensor for simultaneous detection of chloramphenicol and polychlorinated biphenyls using multi-metal ions encoded nanospherical brushes as tracers. *Biosensors and Bioelectronics* **2015,** *74*, 718-724.
170. Chen, M.; Gan, N.; Zhang, H.; Yan, Z.; Li, T.; Chen, Y.; Xu, Q.; Jiang, Q., Electrochemical simultaneous assay of chloramphenicol and PCB72 using magnetic and aptamer-modified quantum dot-encoded dendritic nanotracers for signal amplification. *Microchimica Acta* **2016,** *183* (3), 1099-1106.
171. Lu, Y.; Huang, Q.; Meng, G.; Wu, L.; Jingjing, Z., Label-free selective SERS detection of PCB-77 based on DNA aptamer modified SiO2@Au core/shell nanoparticles. *Analyst* **2014,** *139* (12), 3083-3087.
172. Fu, C.; Wang, Y.; Chen, G.; Yang, L.; Xu, S.; Xu, W., Aptamer-Based Surface-Enhanced Raman Scattering-Microfluidic Sensor for Sensitive and Selective Polychlorinated Biphenyls Detection. *Analytical Chemistry* **2015,** *87* (19), 9555-9558.
173. Sun, K.; Huang, Q.; Meng, G.; Lu, Y., Highly Sensitive and Selective Surface-Enhanced Raman Spectroscopy Label-free Detection of 3,3′,4,4′-Tetrachlorobiphenyl Using DNA Aptamer-Modified Ag-Nanorod Arrays. *ACS Applied Materials & Interfaces* **2016,** *8* (8), 5723-5728.
174. Wu, L.; Qi, P.; Fu, X.; Liu, H.; Li, J.; Wang, Q.; Fan, H., A novel electrochemical PCB77-binding DNA aptamer biosensor for selective detection of PCB77. *Journal of Electroanalytical Chemistry* **2016,** *771*, 45-49.
175. Kashefi-Kheyrabadi, L.; Mehrgardi, M. A., Design and construction of a label free aptasensor for electrochemical detection of sodium diclofenac. *Biosensors and Bioelectronics* **2012,** *33* (1), 184-189.

176. Derikvand, H.; Roushani, M.; Abbasi, A. R.; Derikvand, Z.; Azadbakht, A., Design of folding-based impedimetric aptasensor for determination of the nonsteroidal anti-inflammatory drug. *Analytical Biochemistry* **2016,** *513*, 77-86.
177. Niu, X.; Huang, L.; Zhao, J.; Yin, M.; Luo, D.; Yang, Y., An ultrasensitive aptamer biosensor for the detection of codeine based on a Au nanoparticle/polyamidoamine dendrimer-modified screen-printed carbon electrode. *Analytical Methods* **2016,** *8* (5), 1091-1095.
178. Stojanovic, M. N.; de Prada, P.; Landry, D. W., Aptamer-Based Folding Fluorescent Sensor for Cocaine. *Journal of the American Chemical Society* **2001,** *123* (21), 4928-4931.
179. Baker, B. R.; Lai, R. Y.; Wood, M. S.; Doctor, E. H.; Heeger, A. J.; Plaxco, K. W., An Electronic, Aptamer-Based Small-Molecule Sensor for the Rapid, Label-Free Detection of Cocaine in Adulterated Samples and Biological Fluids. *Journal of the American Chemical Society* **2006,** *128* (10), 3138-3139.
180. Zhang, J.; Wang, L.; Pan, D.; Song, S.; Boey, F. Y. C.; Zhang, H.; Fan, C., Visual Cocaine Detection with Gold Nanoparticles and Rationally Engineered Aptamer Structures. *Small* **2008,** *4* (8), 1196-1200.
181. Zuo, X.; Xiao, Y.; Plaxco, K. W., High Specificity, Electrochemical Sandwich Assays Based on Single Aptamer Sequences and Suitable for the Direct Detection of Small-Molecule Targets in Blood and Other Complex Matrices. *Journal of the American Chemical Society* **2009,** *131* (20), 6944-6945.
182. Wang, J.; Song, J.; Wang, X.; Wu, S.; Zhao, Y.; Luo, P.; Meng, C., An ATMND/SGI based label-free and fluorescence ratiometric aptasensor for rapid and highly sensitive detection of cocaine in biofluids. *Talanta* **2016,** *161*, 437-442.
183. Yu, H.; Canoura, J.; Guntupalli, B.; Lou, X.; Xiao, Y., A cooperative-binding split aptamer assay for rapid, specific and ultra-sensitive fluorescence detection of cocaine in saliva. *Chemical Science* **2017,** *8* (1), 131-141.
184. Rauf, S.; Zhang, L.; Ali, A.; Liu, Y.; Li, J., Label-Free Nanopore Biosensor for Rapid and Highly Sensitive Cocaine Detection in Complex Biological Fluids. *ACS Sensors* **2017,** *2* (2), 227-234.
185. Liu, Y.; Zhao, Q., Direct fluorescence anisotropy assay for cocaine using tetramethylrhodamine-labeled aptamer. *Analytical and Bioanalytical Chemistry* **2017,** *409* (16), 3993-4000.
186. Su, F.; Zhang, S.; Ji, H.; Zhao, H.; Tian, J.-Y.; Liu, C.-S.; Zhang, Z.; Fang, S.; Zhu, X.; Du, M., Two-Dimensional Zirconium-Based Metal–Organic Framework Nanosheet Composites Embedded with Au Nanoclusters: A Highly Sensitive Electrochemical Aptasensor toward Detecting Cocaine. *ACS Sensors* **2017,** *2* (7), 998-1005.
187. Chen, A.; Jiang, X.; Zhang, W.; Chen, G.; Zhao, Y.; Tunio, T. M.; Liu, J.; Lv, Z.; Li, C.; Yang, S., High sensitive rapid visual detection of sulfadimethoxine by label-freeaptasensor. *Biosensors and Bioelectronics* **2013,** *42*, 419-425.
188. Niu, S.; Lv, Z.; Liu, J.; Bai, W.; Yang, S.; Chen, A., Colorimetric Aptasensor Using Unmodified Gold Nanoparticles for Homogeneous Multiplex Detection. *PLOS ONE* **2014,** *9* (10), e109263.
189. Okoth, O. K.; Yan, K.; Liu, Y.; Zhang, J., Graphene-doped Bi2S3 nanorods as visible-light photoelectrochemical aptasensing platform for sulfadimethoxine detection. *Biosensors and Bioelectronics* **2016,** *86*, 636-642.
190. Wang, A.; Zhao, H.; Chen, X.; Tan, B.; Zhang, Y.; Quan, X., A colorimetric aptasensor for sulfadimethoxine detection based on peroxidase-like activity of graphene/nickel@palladium hybrids. *Analytical Biochemistry* **2017,** *525*, 92-99.
191. Yan, J.; Huang, Y.; Zhang, C.; Fang, Z.; Bai, W.; Yan, M.; Zhu, C.; Chen, A., Aptamer based photometric assay for the antibiotic sulfadimethoxine based on the inhibition and reactivation of the peroxidase-like activity of gold nanoparticles. *Microchimica Acta* **2017,** *184* (1), 59-63.
192. Du, G.; Zhang, D.; Xia, B.; Xu, L.; Wu, S.; Zhan, S.; Ni, X.; Zhou, X.; Wang, L., A label-free colorimetric progesterone aptasensor based on the aggregation of gold nanoparticles. *Microchimica Acta* **2016,** *183* (7), 2251-2258.

193. Du, G.; Wang, L.; Zhang, D.; Ni, X.; Zhou, X.; Xu, H.; Xu, L.; Wu, S.; Zhang, T.; Wang, W., Colorimetric aptasensor for progesterone detection based on surfactant-induced aggregation of gold nanoparticles. *Analytical Biochemistry* **2016,** *514*, 2-7.
194. Lavaee, P.; Danesh, N. M.; Ramezani, M.; Abnous, K.; Taghdisi, S. M., Colorimetric aptamer based assay for the determination of fluoroquinolones by triggering the reduction-catalyzing activity of gold nanoparticles. *Microchimica Acta* **2017,** *184* (7), 2039-2045.
195. Abnous, K.; Danesh, N. M.; Alibolandi, M.; Ramezani, M.; Taghdisi, S. M.; Emrani, A. S., A novel electrochemical aptasensor for ultrasensitive detection of fluoroquinolones based on single-stranded DNA-binding protein. *Sensors and Actuators B: Chemical* **2017,** *240*, 100-106.
196. Daprà, J.; Lauridsen, L. H.; Nielsen, A. T.; Rozlosnik, N., Comparative study on aptamers as recognition elements for antibiotics in a label-free all-polymer biosensor. *Biosensors and Bioelectronics* **2013,** *43*, 315-320.
197. Wang, H.; Wang, Y.; Liu, S.; Yu, J.; Xu, W.; Guo, Y.; Huang, J., Target-aptamer binding triggered quadratic recycling amplification for highly specific and ultrasensitive detection of antibiotics at the attomole level. *Chemical Communications* **2015,** *51* (39), 8377-8380.
198. Wang, X.; Dong, S.; Gai, P.; Duan, R.; Li, F., Highly sensitive homogeneous electrochemical aptasensor for antibiotic residues detection based on dual recycling amplification strategy. *Biosensors and Bioelectronics* **2016,** *82*, 49-54.
199. Jiao, Y.; Jia, H.; Guo, Y.; Zhang, H.; Wang, Z.; Sun, X.; Zhao, J., An ultrasensitive aptasensor for chlorpyrifos based on ordered mesoporous carbon/ferrocene hybrid multiwalled carbon nanotubes. *RSC Advances* **2016,** *6* (63), 58541-58548.
200. Yang, C.; Wang, Y.; Marty, J.-L.; Yang, X., Aptamer-based colorimetric biosensing of Ochratoxin A using unmodified gold nanoparticles indicator. *Biosensors and Bioelectronics* **2011,** *26* (5), 2724-2727.
201. Sheng, L.; Ren, J.; Miao, Y.; Wang, J.; Wang, E., PVP-coated graphene oxide for selective determination of ochratoxin A via quenching fluorescence of free aptamer. *Biosensors and Bioelectronics* **2011,** *26* (8), 3494-3499.
202. Bonel, L.; Vidal, J. C.; Duato, P.; Castillo, J. R., An electrochemical competitive biosensor for ochratoxin A based on a DNA biotinylated aptamer. *Biosensors and Bioelectronics* **2011,** *26* (7), 3254-3259.
203. Wu, S.; Duan, N.; Ma, X.; Xia, Y.; Wang, H.; Wang, Z.; Zhang, Q., Multiplexed Fluorescence Resonance Energy Transfer Aptasensor between Upconversion Nanoparticles and Graphene Oxide for the Simultaneous Determination of Mycotoxins. *Analytical Chemistry* **2012,** *84* (14), 6263-6270.
204. Lu, Z.; Chen, X.; Hu, W., A fluorescence aptasensor based on semiconductor quantum dots and MoS2 nanosheets for ochratoxin A detection. *Sensors and Actuators B: Chemical* **2017,** *246*, 61-67.
205. Lv, L.; Li, D.; Liu, R.; Cui, C.; Guo, Z., Label-free aptasensor for ochratoxin A detection using SYBR Gold as a probe. *Sensors and Actuators B: Chemical* **2017,** *246*, 647-652.
206. Dai, S.; Wu, S.; Duan, N.; Chen, J.; Zheng, Z.; Wang, Z., An ultrasensitive aptasensor for Ochratoxin A using hexagonal core/shell upconversion nanoparticles as luminophores. *Biosensors and Bioelectronics* **2017,** *91*, 538-544.
207. Samokhvalov, A. V.; Safenkova, I. V.; Eremin, S. A.; Zherdev, A. V.; Dzantiev, B. B., Use of anchor protein modules in fluorescence polarisation aptamer assay for ochratoxin A determination. *Analytica Chimica Acta* **2017,** *962*, 80-87.
208. Yang, Y.; Li, W.; Shen, P.; Liu, R.; Li, Y.; Xu, J.; Zheng, Q.; Zhang, Y.; Li, J.; Zheng, T., Aptamer fluorescence signal recovery screening for multiplex mycotoxins in cereal samples based on photonic crystal microsphere suspension array. *Sensors and Actuators B: Chemical* **2017,** *248*, 351-358.

209. Li, S.; Liu, C.; Yin, G.; Zhang, Q.; Luo, J.; Wu, N., Aptamer-molecularly imprinted sensor base on electrogenerated chemiluminescence energy transfer for detection of lincomycin. *Biosensors and Bioelectronics* **2017,** *91*, 687-691.
210. Kim, Y.-J.; Kim, Y. S.; Niazi, J. H.; Gu, M. B., Electrochemical aptasensor for tetracycline detection. *Bioprocess and Biosystems Engineering* **2009,** *33* (1), 31.
211. Zhou, L.; Li, D.-J.; Gai, L.; Wang, J.-P.; Li, Y.-B., Electrochemical aptasensor for the detection of tetracycline with multi-walled carbon nanotubes amplification. *Sensors and Actuators B: Chemical* **2012,** *162* (1), 201-208.
212. Jeong, S.; Rhee Paeng, I., Sensitivity and Selectivity on Aptamer-Based Assay: The Determination of Tetracycline Residue in Bovine Milk. *The Scientific World Journal* **2012,** *2012*, 10.
213. He, L.; Luo, Y.; Zhi, W.; Wu, Y.; Zhou, P., A Colorimetric Aptamer Biosensor Based on Gold Nanoparticles for the Ultrasensitive and Specific Detection of Tetracycline in Milk. *Australian Journal of Chemistry* **2013,** *66* (4), 485-490.
214. He, L.; Luo, Y.; Zhi, W.; Zhou, P., Colorimetric Sensing of Tetracyclines in Milk Based on the Assembly of Cationic Conjugated Polymer-Aggregated Gold Nanoparticles. *Food Analytical Methods* **2013,** *6* (6), 1704-1711.
215. Wang, S.; Yong, W.; Liu, J.; Zhang, L.; Chen, Q.; Dong, Y., Development of an indirect competitive assay-based aptasensor for highly sensitive detection of tetracycline residue in honey. *Biosensors and Bioelectronics* **2014,** *57*, 192-198.
216. Kwon, Y. S.; Ahmad Raston, N. H.; Gu, M. B., An ultra-sensitive colorimetric detection of tetracyclines using the shortest aptamer with highly enhanced affinity. *Chemical Communications* **2014,** *50* (1), 40-42.
217. Luo, Y.; He, L.; Zhan, S.; Wu, Y.; Liu, L.; Zhi, W.; Zhou, P., Ultrasensitive Resonance Scattering (RS) Spectral Detection for Trace Tetracycline in Milk Using Aptamer-Coated Nanogold (ACNG) as a Catalyst. *Journal of Agricultural and Food Chemistry* **2014,** *62* (5), 1032-1037.
218. Shen, G.; Guo, Y.; Sun, X.; Wang, X., Electrochemical Aptasensor Based on Prussian Blue-Chitosan-Glutaraldehyde for the Sensitive Determination of Tetracycline. *Nano-Micro Letters* **2014,** *6* (2), 143-152.
219. Guo, Y.; Shen, G.; Sun, X.; Wang, X., Electrochemical Aptasensor Based on Multiwalled Carbon Nanotubes and Graphene for Tetracycline Detection. *IEEE Sensors Journal* **2015,** *15* (3), 1951-1958.
220. Luo, Y.; Xu, J.; Li, Y.; Gao, H.; Guo, J.; Shen, F.; Sun, C., A novel colorimetric aptasensor using cysteamine-stabilized gold nanoparticles as probe for rapid and specific detection of tetracycline in raw milk. *Food Control* **2015,** *54*, 7-15.
221. Wang, S.; Liu, J.; Yong, W.; Chen, Q.; Zhang, L.; Dong, Y.; Su, H.; Tan, T., A direct competitive assay-based aptasensor for sensitive determination of tetracycline residue in Honey. *Talanta* **2015,** *131*, 562-569.
222. Guo, Y.; Wang, X.; Sun, X., *A label-free electrochemical aptasensor based on electrodeposited gold nanoparticles and methylene blue for tetracycline detection*. 2015; Vol. 10, p 3668-3679.
223. Jalalian, S. H.; Taghdisi, S. M.; Danesh, N. M.; Bakhtiari, H.; Lavaee, P.; Ramezani, M.; Abnous, K., Sensitive and fast detection of tetracycline using an aptasensor. *Analytical Methods* **2015,** *7* (6), 2523-2528.
224. Taghdisi, S. M.; Danesh, N. M.; Ramezani, M.; Abnous, K., A novel M-shape electrochemical aptasensor for ultrasensitive detection of tetracyclines. *Biosensors and Bioelectronics* **2016,** *85*, 509-514.
225. Jahanbani, S.; Benvidi, A., Comparison of two fabricated aptasensors based on modified carbon paste/oleic acid and magnetic bar carbon paste/Fe3O4@oleic acid nanoparticle electrodes for tetracycline detection. *Biosensors and Bioelectronics* **2016,** *85*, 553-562.
226. Zhan, X.; Hu, G.; Wagberg, T.; Zhan, S.; Xu, H.; Zhou, P., Electrochemical aptasensor for tetracycline using a screen-printed carbon electrode modified with an alginate film containing

reduced graphene oxide and magnetite (Fe3O4) nanoparticles. *Microchimica Acta* **2016,** *183* (2), 723-729.
227. Xue, J.; Liu, J.; Wang, C.; Tian, Y.; Zhou, N., Simultaneous electrochemical detection of multiple antibiotic residues in milk based on aptamers and quantum dots. *Analytical Methods* **2016,** *8* (9), 1981-1988.
228. Hao, L.; Gu, H.; Duan, N.; Wu, S.; Wang, Z., A chemiluminescent aptasensor for simultaneous detection of three antibiotics in milk. *Analytical Methods* **2016,** *8* (44), 7929-7936.
229. Ouyang, Q.; Liu, Y.; Chen, Q.; Guo, Z.; Zhao, J.; Li, H.; Hu, W., Rapid and specific sensing of tetracycline in food using a novel upconversion aptasensor. *Food Control* **2017,** *81*, 156-163.
230. Kim, S.; Lee, H. J., Gold Nanostar Enhanced Surface Plasmon Resonance Detection of an Antibiotic at Attomolar Concentrations via an Aptamer-Antibody Sandwich Assay. *Analytical Chemistry* **2017,** *89* (12), 6624-6630.
231. Kim, Y. S.; Niazi, J. H.; Gu, M. B., Specific detection of oxytetracycline using DNA aptamer-immobilized interdigitated array electrode chip. *Analytica Chimica Acta* **2009,** *634* (2), 250-254.
232. Kim, Y. S.; Kim, J. H.; Kim, I. A.; Lee, S. J.; Jurng, J.; Gu, M. B., A novel colorimetric aptasensor using gold nanoparticle for a highly sensitive and specific detection of oxytetracycline. *Biosensors and Bioelectronics* **2010,** *26* (4), 1644-1649.
233. Kim, K.; Gu, M.-B.; Kang, D.-H.; Park, J.-W.; Song, I.-H.; Jung, H.-S.; Suh, K.-Y., High-sensitivity detection of oxytetracycline using light scattering agglutination assay with aptasensor. *ELECTROPHORESIS* **2010,** *31* (18), 3115-3120.
234. Hou, H.; Bai, X.; Xing, C.; Gu, N.; Zhang, B.; Tang, J., Aptamer-Based Cantilever Array Sensors for Oxytetracycline Detection. *Analytical Chemistry* **2013,** *85* (4), 2010-2014.
235. Zhao, H.; Gao, S.; Liu, M.; Chang, Y.; Fan, X.; Quan, X., Fluorescent assay for oxytetracycline based on a long-chain aptamer assembled onto reduced graphene oxide. *Microchimica Acta* **2013,** *180* (9), 829-835.
236. Zheng, D.; Zhu, X.; Zhu, X.; Bo, B.; Yin, Y.; Li, G., An electrochemical biosensor for the direct detection of oxytetracycline in mouse blood serum and urine. *Analyst* **2013,** *138* (6), 1886-1890.
237. Yan, K.; Liu, Y.; Yang, Y.; Zhang, J., A Cathodic "Signal-off" Photoelectrochemical Aptasensor for Ultrasensitive and Selective Detection of Oxytetracycline. *Analytical Chemistry* **2015,** *87* (24), 12215-12220.
238. Liu, C.; Lu, C.; Tang, Z.; Chen, X.; Wang, G.; Sun, F., Aptamer-functionalized magnetic nanoparticles for simultaneous fluorometric determination of oxytetracycline and kanamycin. *Microchimica Acta* **2015,** *182* (15), 2567-2575.
239. Fang, C.; Wu, S.; Duan, N.; Dai, S.; Wang, Z., Highly sensitive aptasensor for oxytetracycline based on upconversion and magnetic nanoparticles. *Analytical Methods* **2015,** *7* (6), 2585-2593.
240. Yuan, F.; Zhao, H.; Zhang, Z.; Gao, L.; Xu, J.; Quan, X., Fluorescent biosensor for sensitive analysis of oxytetracycline based on an indirectly labelled long-chain aptamer. *RSC Advances* **2015,** *5* (72), 58895-58901.
241. Lu, C.; Tang, Z.; Liu, C.; Kang, L.; Sun, F., Magnetic-nanobead-based competitive enzyme-linked aptamer assay for the analysis of oxytetracycline in food. *Analytical and Bioanalytical Chemistry* **2015,** *407* (14), 4155-4163.
242. Zhang, H.; Fang, C.; Wu, S.; Duan, N.; Wang, Z., Upconversion luminescence resonance energy transfer-based aptasensor for the sensitive detection of oxytetracycline. *Analytical Biochemistry* **2015,** *489*, 44-49.
243. Seo, H. B.; Kwon, Y. S.; Lee, J.-e.; Cullen, D.; Noh, H.; Gu, M. B., A novel reflectance-based aptasensor using gold nanoparticles for the detection of oxytetracycline. *Analyst* **2015,** *140* (19), 6671-6675.
244. Tan, B.; Zhao, H.; Du, L.; Gan, X.; Quan, X., A versatile fluorescent biosensor based on target-responsive graphene oxide hydrogel for antibiotic detection. *Biosensors and Bioelectronics* **2016,** *83*, 267-273.

245. Chen, M.; Gan, N.; Zhou, Y.; Li, T.; Xu, Q.; Cao, Y.; Chen, Y., An electrochemical aptasensor for multiplex antibiotics detection based on metal ions doped nanoscale MOFs as signal tracers and RecJf exonuclease-assisted targets recycling amplification. *Talanta* **2016,** *161*, 867-874.
246. Hosseini, M.; Mehrabi, F.; Ganjali, M. R.; Norouzi, P., A fluorescent aptasensor for sensitive analysis oxytetracycline based on silver nanoclusters. *Luminescence* **2016,** *31* (7), 1339-1343.
247. Su, R.; Xu, J.; Luo, Y.; Li, Y.; Liu, X.; Bie, J.; Sun, C., Highly selective and sensitive visual detection of oxytetracycline based on aptamer binding-mediated the anti-aggregation of positively charged gold nanoparticles. *Materials Letters* **2016,** *180*, 31-34.
248. Yan, Z.; Gan, N.; Li, T.; Cao, Y.; Chen, Y., A sensitive electrochemical aptasensor for multiplex antibiotics detection based on high-capacity magnetic hollow porous nanotracers coupling exonuclease-assisted cascade target recycling. *Biosensors and Bioelectronics* **2016,** *78*, 51-57.
249. Liu, S.; Wang, Y.; Xu, W.; Leng, X.; Wang, H.; Guo, Y.; Huang, J., A novel sandwich-type electrochemical aptasensor based on GR-3D Au and aptamer-AuNPs-HRP for sensitive detection of oxytetracycline. *Biosensors and Bioelectronics* **2017,** *88*, 181-187.
250. Li, Y.; Tian, J.; Yuan, T.; Wang, P.; Lu, J., A sensitive photoelectrochemical aptasensor for oxytetracycline based on a signal "switch off-on" strategy. *Sensors and Actuators B: Chemical* **2017,** *240*, 785-792.
251. Babaei, M.; Jalalian, S. H.; Bakhtiari, H.; Ramezani, M.; Abnous, K.; Taghdisi, S. M., Aptamer-Based Fluorescent Switch for Sensitive Detection of Oxytetracycline. *Australian Journal of Chemistry* **2017,** *70* (6), 718-723.
252. Meng, F.; Ma, X.; Duan, N.; Wu, S.; Xia, Y.; Wang, Z.; Xu, B., Ultrasensitive SERS aptasensor for the detection of oxytetracycline based on a gold-enhanced nano-assembly. *Talanta* **2017,** *165*, 412-418.
253. Zhu, Y.; Chandra, P.; Song, K.-M.; Ban, C.; Shim, Y.-B., Label-free detection of kanamycin based on the aptamer-functionalized conducting polymer/gold nanocomposite. *Biosensors and Bioelectronics* **2012,** *36* (1), 29-34.
254. Li, R.; Liu, Y.; Cheng, L.; Yang, C.; Zhang, J., Photoelectrochemical Aptasensing of Kanamycin Using Visible Light-Activated Carbon Nitride and Graphene Oxide Nanocomposites. *Analytical Chemistry* **2014,** *86* (19), 9372-9375.
255. Li, H.; Sun, D.-e.; Liu, Y.; Liu, Z., An ultrasensitive homogeneous aptasensor for kanamycin based on upconversion fluorescence resonance energy transfer. *Biosensors and Bioelectronics* **2014,** *55*, 149-156.
256. Sun, X.; Li, F.; Shen, G.; Huang, J.; Wang, X., Aptasensor based on the synergistic contributions of chitosan-gold nanoparticles, graphene-gold nanoparticles and multi-walled carbon nanotubes-cobalt phthalocyanine nanocomposites for kanamycin detection. *Analyst* **2014,** *139* (1), 299-308.
257. Wang, C.; Wang, C.; Wang, Q.; Chen, D., Resonance light scattering method for detecting kanamycin in milk with enhanced sensitivity. *Analytical and Bioanalytical Chemistry* **2017,** *409* (11), 2839-2846.
258. Wang, C.; Chen, D.; Wang, Q.; Tan, R., Kanamycin detection based on the catalytic ability enhancement of gold nanoparticles. *Biosensors and Bioelectronics* **2017,** *91*, 262-267.
259. Sharma, A.; Istamboulie, G.; Hayat, A.; Catanante, G.; Bhand, S.; Marty, J. L., Disposable and portable aptamer functionalized impedimetric sensor for detection of kanamycin residue in milk sample. *Sensors and Actuators B: Chemical* **2017,** *245*, 507-515.
260. Chen, M.; Gan, N.; Zhou, Y.; Li, T.; Xu, Q.; Cao, Y.; Chen, Y., A novel aptamer- metal ions-nanoscale MOF based electrochemical biocodes for multiple antibiotics detection and signal amplification. *Sensors and Actuators B: Chemical* **2017,** *242*, 1201-1209.
261. Ha, N.-R.; Jung, I.-P.; La, I.-J.; Jung, H.-S.; Yoon, M.-Y., Ultra-sensitive detection of kanamycin for food safety using a reduced graphene oxide-based fluorescent aptasensor. *Scientific Reports* **2017,** *7*, 40305.

262. Zuo, X.; Song, S.; Zhang, J.; Pan, D.; Wang, L.; Fan, C., A Target-Responsive Electrochemical Aptamer Switch (TREAS) for Reagentless Detection of Nanomolar ATP. *Journal of the American Chemical Society* **2007,** *129* (5), 1042-1043.
263. Wang, J.; Wang, L.; Liu, X.; Liang, Z.; Song, S.; Li, W.; Li, G.; Fan, C., A Gold Nanoparticle-Based Aptamer Target Binding Readout for ATP Assay. *Advanced Materials* **2007,** *19* (22), 3943-3946.
264. Modh, H.; Witt, M.; Urmann, K.; Lavrentieva, A.; Segal, E.; Scheper, T.; Walter, J.-G., Aptamer-based detection of adenosine triphosphate via qPCR. *Talanta* **2017,** *172*, 199-205.
265. Mohammad Danesh, N.; Ramezani, M.; Sarreshtehdar Emrani, A.; Abnous, K.; Taghdisi, S. M., A novel electrochemical aptasensor based on arch-shape structure of aptamer-complimentary strand conjugate and exonuclease I for sensitive detection of streptomycin. *Biosensors and Bioelectronics* **2016,** *75*, 123-128.
266. Emrani, A. S.; Danesh, N. M.; Lavaee, P.; Ramezani, M.; Abnous, K.; Taghdisi, S. M., Colorimetric and fluorescence quenching aptasensors for detection of streptomycin in blood serum and milk based on double-stranded DNA and gold nanoparticles. *Food Chemistry* **2016,** *190*, 115-121.
267. Taghdisi, S. M.; Danesh, N. M.; Nameghi, M. A.; Ramezani, M.; Abnous, K., A label-free fluorescent aptasensor for selective and sensitive detection of streptomycin in milk and blood serum. *Food Chemistry* **2016,** *203*, 145-149.
268. Wu, S.; Duan, N.; Li, X.; Tan, G.; Ma, X.; Xia, Y.; Wang, Z.; Wang, H., Homogenous detection of fumonisin B1 with a molecular beacon based on fluorescence resonance energy transfer between NaYF4: Yb, Ho upconversion nanoparticles and gold nanoparticles. *Talanta* **2013,** *116*, 611-618.
269. Zhao, Y.; Luo, Y.; Li, T.; Song, Q., Au NPs driven electrochemiluminescence aptasensors for sensitive detection of fumonisin B1. *RSC Advances* **2014,** *4* (101), 57709-57714.
270. Shi, Z.-Y.; Zheng, Y.-T.; Zhang, H.-B.; He, C.-H.; Wu, W.-D.; Zhang, H.-B., DNA Electrochemical Aptasensor for Detecting Fumonisins B1 Based on Graphene and Thionine Nanocomposite. *Electroanalysis* **2015,** *27* (5), 1097-1103.
271. Chen, X.; Bai, X.; Li, H.; Zhang, B., Aptamer-based microcantilever array biosensor for detection of fumonisin B-1. *RSC Advances* **2015,** *5* (45), 35448-35452.
272. Emrani, A. S.; Taghdisi, S. M.; Danesh, N. M.; Jalalian, S. H.; Ramezani, M.; Abnous, K., A novel fluorescent aptasensor for selective and sensitive detection of digoxin based on silica nanoparticles. *Analytical Methods* **2015,** *7* (9), 3814-3818.
273. Bagheri, H.; Talemi, R. P.; Afkhami, A., Gold nanoparticles deposited on fluorine-doped tin oxide surface as an effective platform for fabricating a highly sensitive and specific digoxin aptasensor. *RSC Advances* **2015,** *5* (72), 58491-58498.
274. Sarreshtehdar Emrani, A.; Danesh, N. M.; Lavaee, P.; Jalalian, S. H.; Ramezani, M.; Abnous, K.; Taghdisi, S. M., Sensitive and selective detection of digoxin based on fluorescence quenching and colorimetric aptasensors. *Analytical Methods* **2015,** *7* (8), 3419-3424.
275. Mashhadizadeh, M. H.; Naseri, N.; Mehrgardi, M. A., A digoxin electrochemical aptasensor using Ag nanoparticle decorated graphene oxide. *Analytical Methods* **2016,** *8* (39), 7247-7253.
276. Creative Diagnostics Carbofuran ELISA kit. http://www.creative-diagnostics.com/Carbofuran-EIA-Kit-244088-471.htm.
277. Razak, C. N. A.; Salam, F.; Ampon, K.; Basri, M.; Salleh, A. B., Development of an ELISA for Detection of Parathion, Carbofuran, and 2,4-Dichlorophenoxyacetic Acid in Water, Soil, Vegetables, and Fruits. *Annals of the New York Academy of Sciences* **1998,** *864* (1), 479-484.
278. Sun, X.; Du, S.; Wang, X., Amperometric immunosensor for carbofuran detection based on gold nanoparticles and PB-MWCNTs-CTS composite film. *European Food Research and Technology* **2012,** *235* (3), 469-477.
279. Modernwater Monitoring Rapid Assay for PCBs. http://www.modernwater-monitoring.com/pdf/MW_Factsheet_Rapid-Assay_PCB.pdf.

280. Inui, H.; Takeuchi, T.; Uesugi, A.; Doi, F.; Takai, M.; Nishi, K.; Miyake, S.; Ohkawa, H., Enzyme-Linked Immunosorbent Assay with Monoclonal and Single-Chain Variable Fragment Antibodies Selective to Coplanar Polychlorinated Biphenyls. *Journal of Agricultural and Food Chemistry* **2012,** *60* (7), 1605-1612.
281. Endo, T.; Okuyama, A.; Matsubara, Y.; Nishi, K.; Kobayashi, M.; Yamamura, S.; Morita, Y.; Takamura, Y.; Mizukami, H.; Tamiya, E., Fluorescence-based assay with enzyme amplification on a micro-flow immunosensor chip for monitoring coplanar polychlorinated biphenyls. *Analytica Chimica Acta* **2005,** *531* (1), 7-13.
282. Strategic Diagnostics Inc Chlorpyrifos RaPID assay https://www.nemi.gov/methods/method_pdf/7261/.
283. Liu, Y. H.; Chen, J.; Guo, Y. R.; Wang, C. M.; Liang, X.; Zhu, G. N., A sensitive monoclonal antibody-based enzyme-linked immunosorbent assay for chlorpyrifos residue determination in Chinese agricultural samples. *Journal of Environmental Science and Health, Part B* **2011,** *46* (4), 313-320.
284. Sun, Z.; Wang, W.; Wen, H.; Gan, C.; Lei, H.; Liu, Y., Sensitive electrochemical immunoassay for chlorpyrifos by using flake-like Fe3O4 modified carbon nanotubes as the enhanced multienzyme label. *Analytica Chimica Acta* **2015,** *899* (Supplement C), 91-99.
285. Creative Diagnostics Bisphenol A ELISA kit. http://www.creative-diagnostics.com/Bisphenol-A-EIA-Kit-3972-464.htm.
286. Lei, Y.; Fang, L.; Hamid Akash, M. S.; Liu, Z.; Shi, W.; Chen, S., Development and comparison of two competitive ELISAs for the detection of bisphenol A in human urine. *Analytical Methods* **2013,** *5* (21), 6106-6113.
287. Kim, K. S.; Jang, J.-r.; Choe, W.-S.; Yoo, P. J., Electrochemical detection of Bisphenol A with high sensitivity and selectivity using recombinant protein-immobilized graphene electrodes. *Biosensors and Bioelectronics* **2015,** *71* (Supplement C), 214-221.
288. DRG International Salivary Estradiol ELISA https://store.drg-international.com/shop/salivary-estradiol-elisa.asp.
289. Lacorn, M.; Fleischer, K.; Willig, S.; Gremmel, S.; Steinhart, H.; Claus, R., Use of biotinylated 17β-estradiol in enzyme-immunoassay development: Spacer length and chemical structure of the bridge are the main determinants in simultaneous streptavidin–antibody binding. *Journal of Immunological Methods* **2005,** *297* (1), 225-236.
290. Zhang, S.; Du, B.; Li, H.; Xin, X.; Ma, H.; Wu, D.; Yan, L.; Wei, Q., Metal ions-based immunosensor for simultaneous determination of estradiol and diethylstilbestrol. *Biosensors and Bioelectronics* **2014,** *52* (Supplement C), 225-231.
291. Creative Diagnostics Sulfadimethoxine ELISA kit. http://www.creative-diagnostics.com/Sulfadimethoxine-ELISA-Kit-3575-464.htm.
292. Peng, C.-F.; Duan, X.-H.; Pan, Q.-L.; Liu, L.-Q.; Xue, F., Ultrasensitive Nano-ELISA for Detecting Sulfadimethoxine in Chicken Tissue. *Journal of Chemistry* **2013,** *2013*, 5.
293. DRG International Salivary Progesterone ELISA. https://store.drg-international.com/shop/salivary-progesterone-elisa.asp.
294. Saha, B.; Das, C., Development of a Highly Sensitive Enzyme Linked Immunosorbent Assay for Human Serum Progesterone using Penicillinase. *Journal of Immunoassay* **1991,** *12* (3), 391-412.
295. Dong, X.-X.; Yuan, L.-P.; Liu, Y.-X.; Wu, M.-F.; Liu, B.; Sun, Y.-M.; Shen, Y.-D.; Xu, Z.-L., Development of a progesterone immunosensor based on thionine-graphene oxide composites platforms: Improvement by biotin-streptavidin-amplified system. *Talanta* **2017,** *170* (Supplement C), 502-508.
296. BiooScientific MaxSignal Ciprofloxacin ELISA kit. http://www.biooscientific.com/Antibiotic-Residue-Test-Kits/MaxSignal-Ciprofloxacin-ELISA-Test-Kit.
297. Chen, J.-J.; Jiang, J.-Q., Monoclonal antibody-based solvent tolerable indirect competitive ELISA for monitoring ciprofloxacin residue in poultry samples. *Food and Agricultural Immunology* **2013,** *24* (3), 331-344.

298. Ionescu, R. E.; Jaffrezic-Renault, N.; Bouffier, L.; Gondran, C.; Cosnier, S.; Pinacho, D. G.; Marco, M. P.; Sánchez-Baeza, F. J.; Healy, T.; Martelet, C., Impedimetric immunosensor for the specific label free detection of ciprofloxacin antibiotic. *Biosensors and Bioelectronics* **2007,** *23* (4), 549-555.
299. Creative Diagnostics Lincomycin EIA kit. http://www.creative-diagnostics.com/Lincomycin-EIA-Kit-244064-471.htm.
300. Wang, Y.; Wang, R.; Wang, J.; Yang, H.; Song, J.; Wang, Y.; Deng, A., A sensitive and specific enzyme-linked immunosorbent assay for the detection of lincomycin in food samples. *Journal of the Science of Food and Agriculture* **2010,** *90* (12), 2083-2089.
301. MyBioSource Tetracyclines ELISA kit. https://www.mybiosource.com/prods/ELISA-Kit/Tetracyclines/TET/datasheet.php?products_id=280466.
302. Jeon, M.; Kim, J.; Paeng, K.-J.; Park, S.-W.; Paeng, I. R., Biotin–avidin mediated competitive enzyme-linked immunosorbent assay to detect residues of tetracyclines in milk. *Microchemical Journal* **2008,** *88* (1), 26-31.
303. Que, X.; Chen, X.; Fu, L.; Lai, W.; Zhuang, J.; Chen, G.; Tang, D., Platinum-catalyzed hydrogen evolution reaction for sensitive electrochemical immunoassay of tetracycline residues. *Journal of Electroanalytical Chemistry* **2013,** *704* (Supplement C), 111-117.
304. BiooScientific MaxSignal Oxytetracycline ELISA kit. http://www.biooscientific.com/Antibiotic-Residue-Test-Kits/MaxSignal-Oxytetracycline-ELISA-Kit.
305. Le, T.; Yu, H.; Zhao, Z.; Wei, W., Development of a Monoclonal Antibody-Based ELISA for the Detection of Oxytetracycline and 4-Epi-Oxytetracycline Residues in Chicken Tissues. *Analytical Letters* **2012,** *45* (4), 386-394.

APPENDIX B: SUPPLEMENTARY INFORMATION FOR APTAMER SELECTION AND CHARACTERIZATION

Materials

The DNA oligonucleotides (random pools) used for the E2 and EE aptamer selections were, respectively, 5′-CGAAGCGCTAGAACAT-N40-AGTACATGAGACTTAGCTGATCC TGATGG-3′ and 5′-CGAAGTCGCCATCTCTTC-N40-ATAGTGAGTCGTATTAAGCTGATC CTGAT GG-3′, where N40 denotes 40 consecutive random nucleotides. In the PCR step of each selection, the primers were E2 forward 5′-CGAAGCGCTAGAACAT-3′, E2 reverse 5′(AAC)4XCCATCAGGATCAGCTAAGTCTCATGTACT-3′, EE forward 5′-CGAAGTCGCC ATCTCTTC-3′, and EE reverse 5′-(AAC)4XCCATCAGGATCAGCT-3′, where X = HEG spacer to stop Taq polymerase (thereby allowing separation of the two DNA single strands). For cloning the E2 selection, the forward and reverse primers were respectively modified to 5′-TAATTAATTAATTACGAAGCGCTAGAACAT-3′ and 5′-TAATTAATTAATTACCCA TCAGGATCAGCT-3′, each containing stop codons in all three reading frames. For cloning of the EE selection, only the reverse primer was modified by inclusion of stop codons.

Immobilization of E2 and EE on Agarose Support

For immobilization, approximately 25 mL of distilled water was added to 6 g of epoxy-activated agarose support in a 50 mL plastic (polyethylene) tube until the combined volume of swelled support and water was 33 mL (~15–20 min). The suspension was transferred to a 60 mL medium-porosity sintered glass funnel and washed by suction with 1200 mL of water in 30 mL portions with manual agitation over 3 h. The support (~15 mL volume) was transferred to a 50 mL plastic tube and washed with 3 × 15 mL of immobilization buffer [100 mM Na_2CO_3, 50% (v/v) isopropyl alcohol, pH 13], centrifuging at 250 × *g* for 5 min after each addition. The

immobilization reaction was performed in a 15 mL plastic tube using 5 mL of support and 5 mL of immobilization buffer containing 20 mM E2 or EE for 8 h (E2) or 26 h (EE) at 37 °C; the EE immobilization was found empirically to require the longer time. The sample was centrifuged as above, and the immobilization buffer was decanted. The support was washed with 3 × 5 mL of immobilization buffer. The unreacted epoxy groups were capped by incubation with 5 mL of 1 M ethanolamine for 20 h at 23 °C, followed by centrifugation, decanting, and washing with three complete cycles of 5 mL of 0.1 M sodium acetate, pH 4.0, 5 mL of 0.1 M Tris, pH 8.0, and 5 mL of water. For preparation of the pre-selection support with only immobilized ethanolamine, the support was directly derivatized via the capping procedure. The stock of derivatized support was stored in 5 mL of 20% (v/v) ethanol at 4 °C.

To obtain a portion of derivatized support, the stock sample was vortexed, and a 400 µL aliquot of the suspension was removed to a 1.7 mL tube. The sample was centrifuged at 2000 × *g* for 10 s and the supernatant was removed by pipet, providing 200 µL of derivatized support.

The extent of derivatization of the support was quantified by UV-visible spectroscopy, by measuring the absorbance at 280 nm (A280) of 75 µL of the support suspended in 225 µL of 50% (w/v) poly(ethylene glycol) (PEG 4000, Fluka). A calibration plot was constructed by measuring the A_{280} values of a series of suspensions of 75 µL of unmodified support (Sepharose 6B, Sigma, catalog number 6B100) in 222 µL of 50% (w/v) PEG 4000 containing 60–300 nmol of aqueous phase E2 or EE, along with 3 µL of ethanol for solubility. The calibration plot indicated that typically 50–100 nmol of E2 or EE was immobilized on 75 µL of support, equivalent to 133–267 nmol of E2 or EE on 200 µL of support, which was the amount used in each selection round.

In vitro Selection Procedure

The in vitro selection procedure was performed as follows.

Procedure for Initiating Selection (Round 1)

The selection strategy for DNA aptamers is shown in Figure 3.1B. In the first selection round, 50 μL of pre-selection support was transferred to a Micro Bio-Spin chromatography column (Bio-Rad) and washed with 5 × 250 μL of binding buffer (50 mM Tris, pH 7.5, 5 mM $MgCl_2$, and 300 mM NaCl), each time centrifuging at 3000 × *g* for 30 s. To suppress nonspecific binding of DNA to the support, a "blocking" DNA oligonucleotide, $(AAC)_{20}$, was used. Approximately 100 pmol of the blocking oligonucleotide in 400 μL of binding buffer was added to the washed support in the pre-selection column. The suspension was transferred to a 2 mL tube sealed with an O-ring and incubated on a nutator at 23 °C for 10 min. The suspension was returned to the pre-selection column, which was centrifuged, and the filtrate was discarded. In a separate 1.7 mL tube, 500 pmol of a random DNA pool (~3×10^{14} unique sequences, of which 5 pmol was 5′-^{32}P-radiolabeled to enable monitoring of binding activity) in 400 μL of binding buffer was annealed by heating at 95 °C for 5 min and cooling at 23 °C for 30 min. The annealed DNA pool was added to the washed support containing the blocking oligonucleotide. The suspension was transferred to the 2 mL O-ring tube, incubated on the nutator for 10 min, returned to the pre-selection column, and centrifuged. The pre-selection support was suspended in 400 μL of binding buffer, and the suspension was transferred to a 7 mL scintillation vial (sample A). The flow-through from the pre-selection column was retained for incubation with the selection support.

Into a separate column was placed 200 μL of E2/EE-derivatized selection support, which was washed with 10 × 500 μL of binding buffer, centrifuging each time. The support was treated with

400 pmol of $(AAC)_{20}$ blocking oligonucleotide as described above. The retained flow-through from the pre-selection column was added to the blocking oligonucleotide-treated selection support. This suspension was transferred to a 2 mL O-ring tube, incubated on the nutator for 1 h, returned to the selection column, and centrifuged. The flow-through was transferred to a scintillation vial (sample B), and the selection support was retained for subsequent washes.

The selection support was washed with 10 × 200 μL of wash buffer, which was the binding buffer containing 20% (v/v) ethanol for E2 support or 2% (v/v) ethanol for EE support. For each wash, the buffer was incubated in the column for 3 min followed by centrifugation. Two consecutive washes were combined and transferred to a scintillation vial (sample C). The selection support was eluted twice with free E2/EE in solution. For both elutions, 300 μL of the appropriate wash buffer containing 200 μM E2 or 20 μM EE was transferred to the selection column. The suspension was transferred to a 2 mL O-ring tube, incubated on the nutator for 2 h, returned to the selection column, and centrifuged. The two elutions were combined and transferred to a scintillation vial (sample D). A suspension of the E2/EE support in 400 μL of binding buffer was transferred to a scintillation vial (sample E).

A scintillation counter (Beckman Coulter LS 6500) was used to quantify the amount of ^{32}P in each of the five samples A–E. To track the selection progression (Figure B.1), the fraction of total counts (samples A–E) that bound to the selection column and subsequently were eluted specifically with free E2/EE (sample D only) was used as quantification of the pool binding activity.

After counting, sample D was divided between two 1.7 mL tubes and precipitated with ethanol. Two PCR reactions were performed, i.e., 10-cycle PCR followed by 30-cycle PCR. First, a 100 μL sample was prepared containing the ethanol-precipitated product, 200 pmol of

forward primer, 50 pmol of reverse primer, 20 nmol of each dNTP, and 10 μL of 10× Taq polymerase buffer (1× = 20 mM Tris-HCl, pH 8.8, 10 mM $(NH_4)_2SO_4$, 10 mM KCl, 2 mM $MgSO_4$, and 0.1% Triton X-100). This sample was cycled 10 times according to the following PCR program: 94 °C for 2 min, 10× (94 °C for 30 s, 47 °C for 30 s, 72 °C for 30 s), 72 °C for 5 min. Taq polymerase was removed by phenol/chloroform extraction. Second, a 50 μL sample was prepared containing 1 μL of the 10-cycle PCR product, 100 pmol of forward primer, 25 pmol of reverse primer, 10 nmol of each dNTP, 20 μCi of α-^{32}P-dCTP (800 Ci/mmol), and 5 μL of 10× Taq polymerase buffer. This sample was cycled 30 times according to the following PCR program: 94 °C for 2 min, 30× (94 °C for 30 s, 47 °C for 30 s, 72 °C for 30 s), 72 °C for 5 min. The sample was separated by 8% PAGE, extracted with TEN buffer, and precipitated with ethanol.

Procedure for Subsequent Selection Rounds 2+

Each subsequent selection round was performed as described for Round 1, with the following modifications. The pre-selection support was incubated simultaneously with annealed 30-cycle PCR product (~5-10 pmol) and 100 pmol of blocking oligonucleotide in 400 μL of binding buffer. 400 pmol of blocking oligonucleotide in 5 μL of binding buffer was added to the flow-through from the pre-selection column, before the sample was incubated with the selection support. After the selection support was washed with the appropriate wash buffer, the two elution steps were each performed for 30 min (1 h total). For rounds 9+ of the E2 selection, a longer elution time of 3 h for each elution step (6 h total) was used to promote elution of tighter-binding sequences.

Cloning and Sequencing

After 10 rounds for both the E2 and EE selections, the 30-cycle PCR was performed as described above, with the following modifications: 1 μL of 1/1000 dilution of the 10-cycle PCR product was used; α-^{32}P-dCTP was omitted; one or two cloning primers incorporating stop codons were used (see Materials); and 25 pmol of each cloning primer was used. The resulting 114 bp (from E2 selection) and 104 bp (from EE selection) double-stranded DNA product with single adenosine overhangs as added by Taq polymerase was isolated by 2% agarose gel (Fermentas gel extraction kit). Individual aptamers were cloned using a TOPO TA kit (Life Technologies). Miniprep DNA (Fermentas) was prepared, and the presence of the expected aptamer insert was confirmed by EcoRI digestion and 2% agarose gel electrophoresis. Sequencing was performed at the UIUC Biotechnology Center. Aptamers for preliminary binding studies were prepared by 30-cycle PCR directly from the miniprep DNA. For subsequent studies, aptamers were prepared by solid-phase synthesis (IDT). Aptamer sequences that were studied in detail are shown in Figure B.2.

Preliminary Assays for Binding of Aptamers to Immobilized E2/EE

As a preliminary screen of individual clones, binding assays were performed. The pre-selection step was omitted; the E2/EE-derivatized support was incubated with an individual clone (obtained by 30 cycles of PCR using the miniprep DNA as template) followed by washing with the appropriate wash buffer as described above in the selection procedure. The column was eluted with 300 μL portions of appropriate wash buffer containing increasing concentrations of E2/EE, ranging from 0.1 to 300 μM. Each elution was collected separately for scintillation counting. Individual clones were characterized further when they showed substantial binding

activity, as assessed by an increase in the amount of material eluted with increasing concentration of E2/EE.

Equilibrium Filtration Assay

The rationale for arriving at equation (3.4) in the main text is described here. Because of the molecular weight cutoff membrane, the retentate contains both A•L and free L, whereas the filtrate has only free L. The two experimentally measureable concentrations of L are total L in the retentate and free L in the filtrate, noting that there is no bound L in the filtrate (which has no aptamer). Moreover, the concentration of free L is the same in the retentate and filtrate, because the EDC passes freely through the cutoff filter. The scintillation counting data were correlated to molar concentrations by $(c_R + c_F)/(v_R + v_F) = c$ (= 0.5 μM). From the experimental values of c_F/v_F, the concentration of free L was calculated and used to determine the concentration of A•L in the retentate. Finally, noting that the concentration, y, of A•L in the full sample is defined in reference to the total volume of the full sample ($v_R + v_F$), the value of y was calculated and plotted according to equation (3.3), as shown in Figure 3.2A.

DMS Probing

Each aptamer was probed using dimethyl sulfate (DMS) in the presence of varying concentrations of E2 or EE. In a 1.7 mL tube, 0.4 pmol of 5′-^{32}P-radiolabeled aptamer in 10 μL of modified binding buffer (50 mM HEPES, pH 7.5, 5 mM $MgCl_2$, and 300 mM NaCl, where HEPES replaces Tris in the original binding buffer because Tris can be methylated by DMS) was annealed by heating at 95 °C for 5 min followed by cooling at 23 °C for 1.5 h. To this sample was added 10 μL of modified binding buffer containing 5% (v/v) of ethanol and a particular concentration of E2/EE (final concentration 1 nM to 100 μM). As a standard, a sample of 0.4 pmol of 5′-^{32}P-radiolabeled aptamer in 20 μL of TE (10 mM Tris, pH 8.0, and 1 mM EDTA)

without E2/EE was prepared and annealed. To 15 µL of the aptamer sample was added 10 µL of methylation buffer [50 mM sodium cacodylate, pH 8.0, 300 mM NaCl, 2.43% (v/v) ethanol, 1.25 % (v/v) DMSO, and 0.075% (v/v) Triton X-100] containing 0.27% (v.v) DMS. The 25 µL sample was incubated at 23 °C for 30 min and precipitated with ethanol. The product was dissolved in 50 µL of 10% (v/v) piperidine and heated at 95 °C for 30 min followed by cooling on dry ice for 5 min. The samples were dried under vacuum overnight and separated by 12% PAGE, with imaging by PhosphorImager and quantification by ImageQuant (GE Healthcare).

Selection progressions

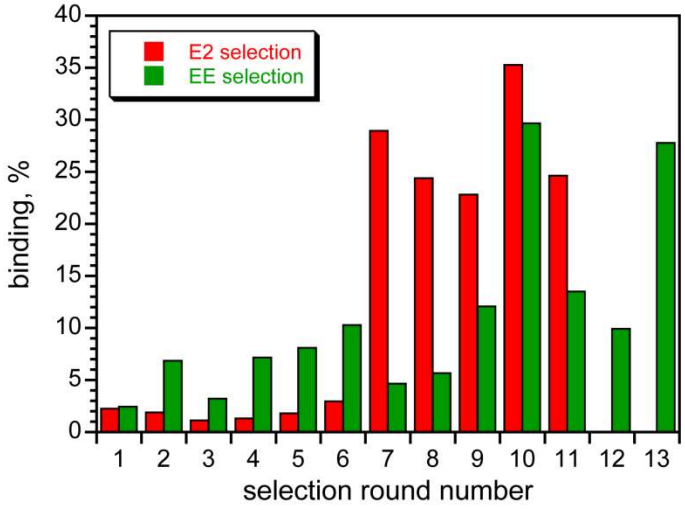

Figure B.1. Selection progressions for E2 and EE selections. Long elution time pressure was applied from Round 9 for E2 selections only. Individual aptamers were cloned from the Round 10 pools in both selections once sustained stable activity was observed.

Sequences of individual deoxyribozymes

```
                          10                  20                  30                  40
E2Apt1  GGCACGGGGA GGCAGGGG-A GAGTGACACG CGGTCGGTGA C 40
E2Apt2  ......T.AC ..GG.ATCTG .GA.AC.TG. ...ATCCGTG T 41
EEApt1  A..CATC.AC ..TC.AAA-G CTAAC.T..A ..CAAA.C.G T 40
EEApt2  A..GGAAC.T ..GGA.CT-T .C.G.CATAC AAACTATG.G A 40
```

Figure B.2. Sequences of E2 and EE aptamers that were characterized by equilibrium filtration and DMS probing assays. Only the initially random (N_{40}) sequences are shown. All aptamers were used as 5′-CGAAGCGCTAGAACAT-N_{40}-AGTACATGAGACTTAGCTGATCCTGATGG-3′ (E2Apt1, E2Apt2) and 5′-CGAAGTCGCCATCTCTTC-N_{40}-ATAGTGAGTCGTATTAAGCTGATCCTGATGG-3′ (EEApt1, EEApt2). Identical residues in comparison to E2Apt1 are represented as dots. Gaps are depicted as dashes. The E2Apt2 sequence includes one additional nucleotide (41 nt), apparently due to a spontaneous insertion by Taq polymerase during an unknown selection round.

Equilibrium filtration assay data

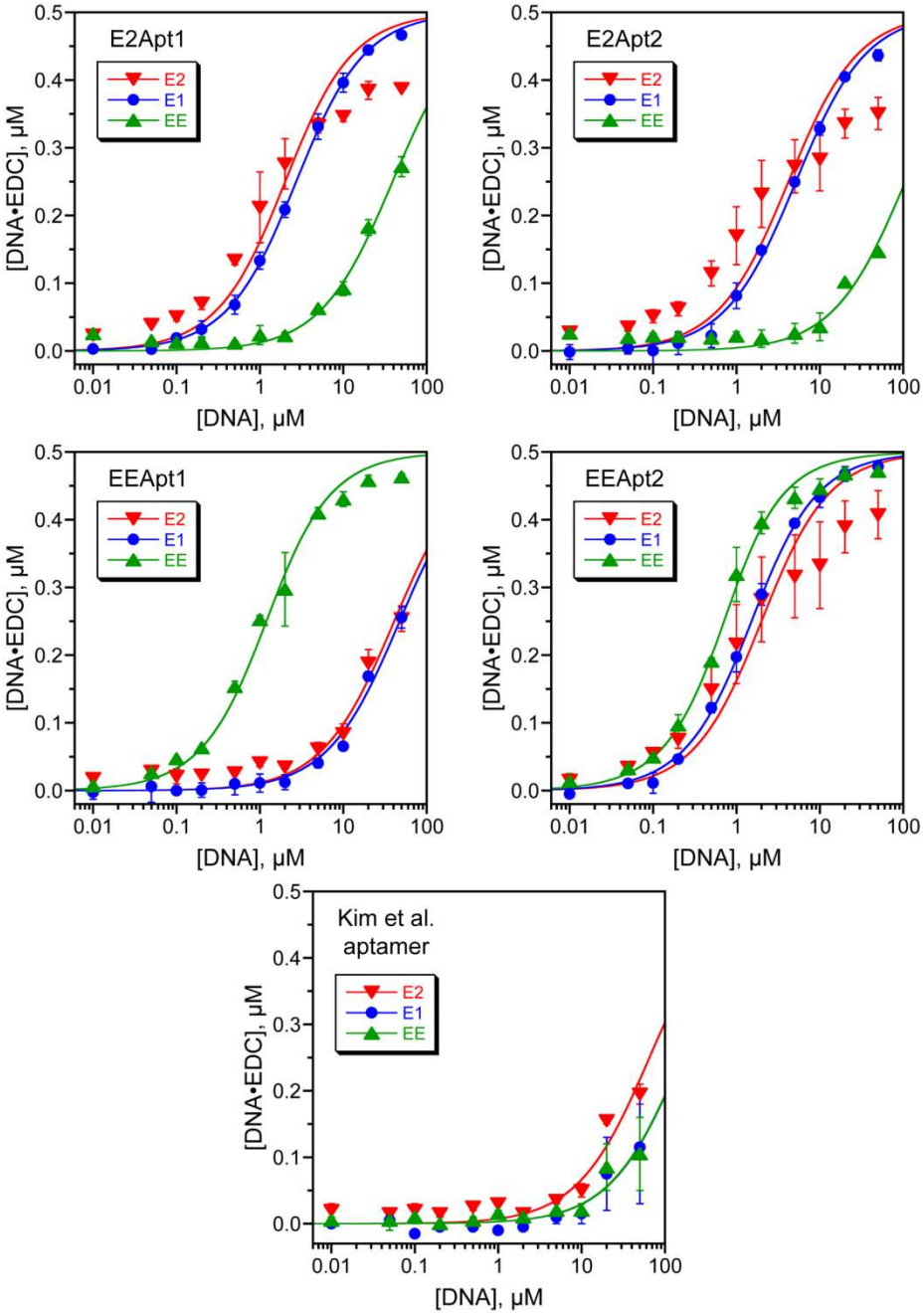

Figure B.3. Equilibrium filtration assay data for the E2Apt1, E2Apt2, EEApt1, and EEApt2 aptamers as well as the E2 aptamer identified by Kim et al.[1] These data are fit using the model that assumes Hill coefficient $n = 1$. K_d values are tabulated in Table 3.1. See Figure B.4 for alternate fitting approach with Hill coefficient $n \neq 1$ for the E2 data.

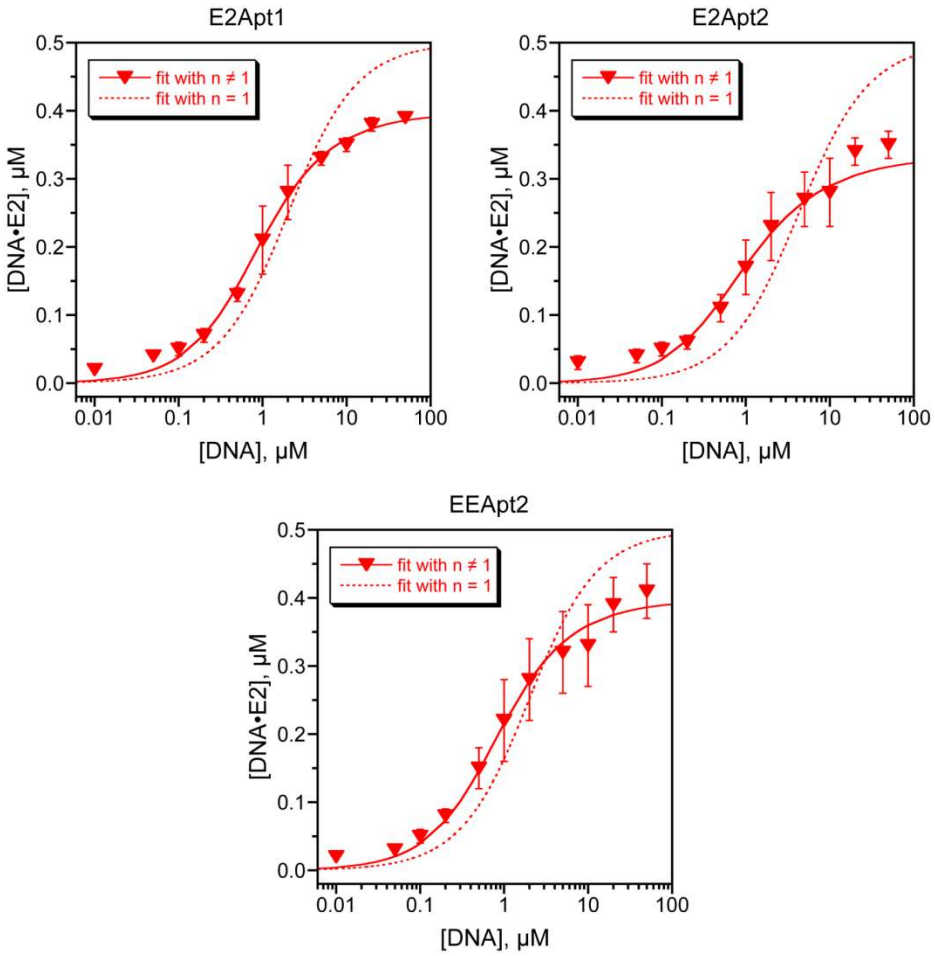

Figure B.4. Equilibrium filtration assay data for the E2Apt1, E2Apt2 and EEApt2 aptamers binding to E2, fit using the model with Hill coefficient $n \neq 1$. K_d and n values are tabulated in Table 3.1. Fits to the same data with $n = 1$ from Figure B.3 are shown for comparison. There is no plot for EEApt1 because this aptamer did not bind appreciably to E2.

Errors for equilibrium filtration assay parameters

Best-fit parameter values (K_d, n) were obtained using equation (3.7) and minimizing the root mean square error (RMSE) given by

$$RMSE = \sqrt{\frac{\sum \left(y_{\text{expt}} - y_{pred} \right)^2}{N}}$$

where N is the number of data points ($N = 11$), y_{expt} is the experimentally obtained value of A•L, and y_{pred} is the value of A•L computed using specific values of K_d and n. In order to obtain error bars (standard errors) for the best-fit values of parameters, K_d and n, first the covariance matrix V was calculated. V is computed using variance (σ^2) and the first derivative matrix X for each data point, where

$$V = (\mathrm{X}^T . \mathrm{X})^{-1} \sigma^2$$

$$\sigma^2 = \frac{RMSE^2 \times N}{N - p}$$

$$X_{i1} = \frac{\partial y_{i,pred}}{\partial K_d} = \frac{y_{pred}(K_d + \Delta K_d) - y_{pred}(K_d)}{\Delta K_d}$$

$$X_{i2} = \frac{\partial y_{i,pred}}{\partial n} = \frac{y_{pred}(n + \Delta n) - y_{pred}(n)}{\Delta n}$$

where p is the number of parameters ($p = 2$ in this case), and the parameters are increased by 15% to compute the first derivatives, e.g., $\Delta K_d = 0.15 * K_d$. The standard error for K_d is given by $\sqrt{V_{11}}$ and that for n is given by $\sqrt{V_{22}}$.

DMS probing data

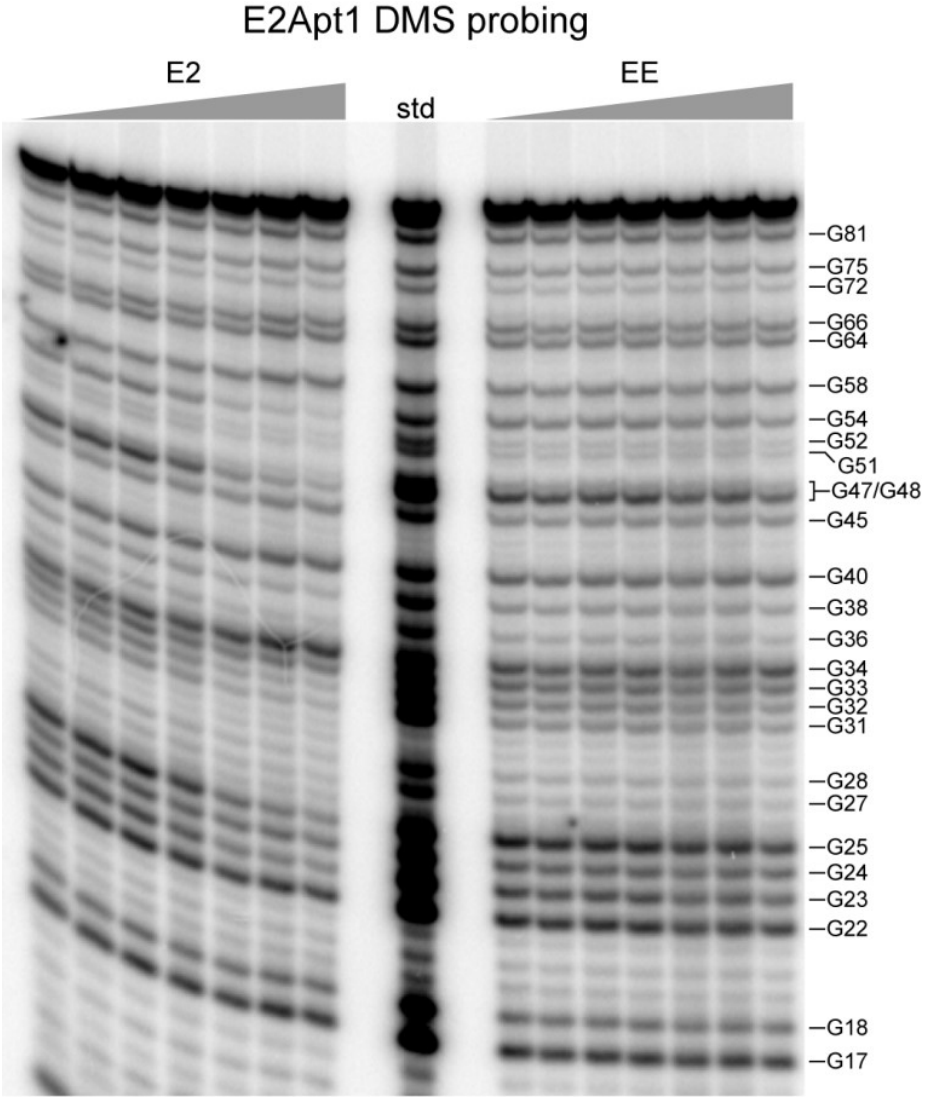

Figure B.5. Full PAGE image for the experiment shown in Figure 3.4B. For each set of lanes, E2/EE concentrations are (left to right) 0, 0.001, 0.01, 0.1, 1, 10, and 100 μM.

Table B.1. K_d values determined from DMS probing data for individual guanosine nucleotides of E2Apt1, E2Apt2, and EEApt1 with E2, E2, and EE, respectively. Values were derived from data such as that shown in Figure 3.4C. Error bars are from the fits to equation (3.6) as described in the Experimental Section. For nucleotide G64 of EEApt1, the normalized band intensity was observed to increase two-fold as the EE concentration was increased; this was the only nucleotide in any of these aptamers for which the normalized band intensity increased rather than decreased.

E2Apt1 nt	E2 K_d, μM
G54	0.24 ± 0.08
G47/G48	0.23 ± 0.07
G32	0.17 ± 0.04
G31	0.47 ± 0.13
G25	0.31 ± 0.07

E2Apt2 nt	E2 K_d, μM
G54	0.65 ± 0.21
G48	0.75 ± 0.35
G46	0.77 ± 0.14
G45	0.80 ± 0.10
G31	0.52 ± 0.12
G30	0.80 ± 0.16
G29	0.65 ± 0.15
G28	0.70 ± 0.19
G27	0.78 ± 0.15
G24	0.63 ± 0.28

EEApt1 nt	EE K_d, μM
G64	1.5 ± 0.5
G62	3.7 ± 1.0
G37	4.0 ± 1.9
G30	1.3 ± 0.5

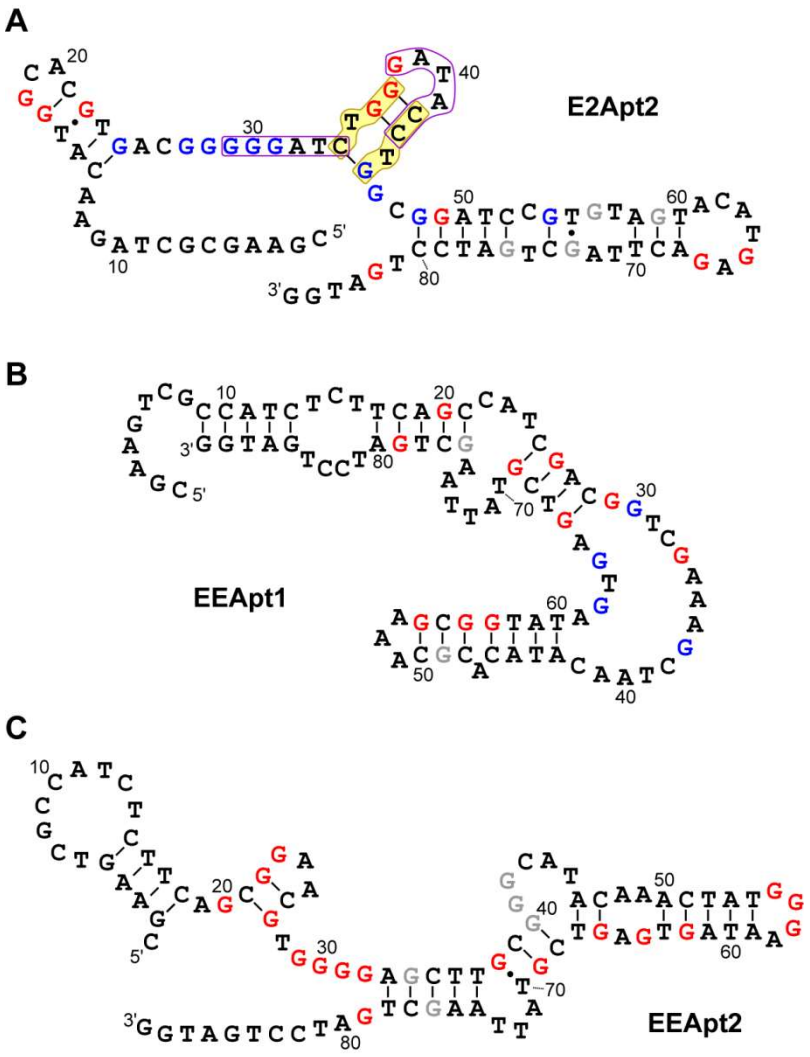

Figure B.6. mfold-predicted secondary structures for E2Apt2, EEApt1, and EEApt2, similar to Figure 3.4D for E2Apt1. For each aptamer, only the lowest-energy structure is illustrated. Blue G nucleotides = substantial concentration-dependent change in DMS accessibility with E2 (E2Apt2) or EE (EEApt1 and EEApt2); red = no change in DMS accessibility; grey = band intensity too low to quantify; black = non-G nucleotides and G nucleotides at the 5′- and 3′-ends. For E2Apt2, the structure with the purple instead of yellow stem is 0.5 kcal/mol higher in free energy.

Lake and tap water characteristics

Table B.2. Characteristics of the lake and tap waters used in the equilibrium filtration assay. The water samples were characterized by the Illinois State Water Survey lab facility in Champaign. nd = not detected.

Component	Units	Lake	Tap
pH		8.29	8.47
alkalinity	mg/L as $CaCO_3$	141	135
B	mg/L	0.11	0.36
Ba	mg/L	0.06	0.08
Ca	mg/L	47.4	13.8
Cu	mg/L	nd	0.08
K	mg/L	3.40	2.58
Mg	mg/L	15.9	12.5
Mn	mg/L	0.003	nd
Na	mg/L	113	32
S	mg/L	5.38	nd
Si	mg/L	0.99	3.63
Sr	mg/L	0.10	0.15
Tl	mg/L	0.02	nd
F	mg/L	0.18	0.86
Cl	mg/L	182.1	13.2
NO_3 (as N)	mg/L	nd	0.05
SO_4	mg/L	14.69	0.32
TDS	mg/L	477	166
dissolved TOC	mg/L	4.43	1.25

Relationship between K_d and LOD

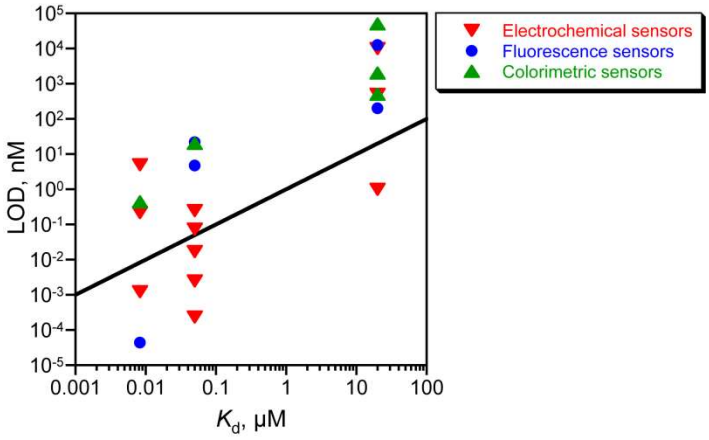

Figure B.7. LOD versus K_d for three broad categories of platforms: electrochemical sensors, fluorescence sensors, and colorimetric sensors. The cited studies involve aptasensors developed for three small molecules: bisphenol A (K_d = 8.3 nM),[2-6] ochratoxin A (K_d = 50 nM),[7-13] and cocaine (K_d = 20 µM).[14-22] The slope of the straight line is 1.

REFERENCES

1. Kim, Y. S.; Jung, H. S.; Matsuura, T.; Lee, H. Y.; Kawai, T.; Gu, M. B. Electrochemical detection of 17β-estradiol using DNA aptamer immobilized gold electrode chip. *Biosens. Bioelectron.* **2007**, *22*, 2525-2531.
2. Xue, F.; Wu, J.; Chu, H.; Mei, Z.; Ye, Y.; Liu, J.; Zhang, R.; Peng, C.; Zheng, L.; Chen, W. Electrochemical aptasensor for the determination of bisphenol A in drinking water. *Microchim. Acta* **2013**, *180*, 109-115.
3. Ragavan, K. V.; Selvakumar, L. S.; Thakur, M. S. Functionalized aptamers as nano-bioprobes for ultrasensitive detection of bisphenol-A. *Chem. Commun.* **2013**, *49*, 5960-5962.
4. Mei, Z.; Chu, H.; Chen, W.; Xue, F.; Liu, J.; Xu, H.; Zhang, R.; Zheng, L. Ultrasensitive one-step rapid visual detection of bisphenol A in water samples by label-free aptasensor. *Biosens. Bioelectron.* **2013**, *39*, 26-30.
5. Zhou, L.; Wang, J.; Li, D.; Li, Y. An electrochemical aptasensor based on gold nanoparticles dotted graphene modified glassy carbon electrode for label-free detection of bisphenol A in milk samples. *Food Chem.* **2014**, *162*, 34-40.
6. Chen, L.; Zeng, X.; Ferhan, A. R.; Chi, Y.; Kim, D.-H.; Chen, G. Signal-on electrochemiluminescent aptasensors based on target controlled permeable films. *Chem. Commun.* **2015**, *51*, 1035-1038.
7. Wang, Z.; Duan, N.; Hun, X.; Wu, S. Electrochemiluminescent aptamer biosensor for the determination of ochratoxin A at a gold-nanoparticles-modified gold electrode using *N*-(aminobutyl)-*N*-ethylisoluminol as a luminescent label. *Anal. Bioanal. Chem.* **2010**, *398*, 2125-2132.
8. Kuang, H.; Chen, W.; Xu, D.; Xu, L.; Zhu, Y.; Liu, L.; Chu, H.; Peng, C.; Xu, C.; Zhu, S. Fabricated aptamer-based electrochemical "signal-off" sensor of ochratoxin A. *Biosens. Bioelectron.* **2010**, *26*, 710-716.
9. Yang, C.; Wang, Y.; Marty, J.-L.; Yang, X. Aptamer-based colorimetric biosensing of Ochratoxin A using unmodified gold nanoparticles indicator. *Biosens. Bioelectron.* **2011**, *26*, 2724-2727.
10. Sheng, L.; Ren, J.; Miao, Y.; Wang, J.; Wang, E. PVP-coated graphene oxide for selective determination of ochratoxin A via quenching fluorescence of free aptamer. *Biosens. Bioelectron.* **2011**, *26*, 3494-3499.
11. Prabhakar, N.; Matharu, Z.; Malhotra, B. D. Polyaniline Langmuir-Blodgett film based aptasensor for ochratoxin A detection. *Biosens. Bioelectron.* **2011**, *26*, 4006-4011.
12. Tong, P.; Zhang, L.; Xu, J.-J.; Chen, H.-Y. Simply amplified electrochemical aptasensor of ochratoxin A based on exonuclease-catalyzed target recycling. *Biosens. Bioelectron.* **2011**, *29*, 97-101.
13. Wu, J.; Chu, H.; Mei, Z.; Deng, Y.; Xue, F.; Zheng, L.; Chen, W. Ultrasensitive one-step rapid detection of ochratoxin A by the folding-based electrochemical aptasensor. *Anal. Chim. Acta* **2012**, *753*, 27-31.
14. Stojanovic, M. N.; de Prada, P.; Landry, D. W. Aptamer-based folding fluorescent sensor for cocaine. *J. Am. Chem. Soc.* **2001**, *123*, 4928-4931.
15. Stojanovic, M. N.; Landry, D. W. Aptamer-based colorimetric probe for cocaine. *J. Am. Chem. Soc.* **2002**, *124*, 9678-9679.
16. Baker, B. R.; Lai, R. Y.; Wood, M. S.; Doctor, E. H.; Heeger, A. J.; Plaxco, K. W. An electronic, aptamer-based small-molecule sensor for the rapid, label-free detection of cocaine in adulterated samples and biological fluids. *J. Am. Chem. Soc.* **2006**, *128*, 3138-3139.
17. Liu, J.; Lu, Y. Fast Colorimetric Sensing of Adenosine and Cocaine Based on a General Sensor Design Involving Aptamers and Nanoparticles. *Angew. Chem. Int. Ed.* **2006**, *45*, 90-94.
18. Li, Y.; Qi, H.; Peng, Y.; Yang, J.; Zhang, C. Electrogenerated chemiluminescence aptamer-based biosensor for the determination of cocaine. *Electrochem. Commun.* **2007**, *9*, 2571-2575.
19. Li, X.; Qi, H.; Shen, L.; Gao, Q.; Zhang, C. Electrochemical Aptasensor for the Determination of Cocaine Incorporating Gold Nanoparticles Modification. *Electroanalysis* **2008**, *20*, 1475-1482.

20. Zhang, J.; Wang, L.; Pan, D.; Song, S.; Boey, F. Y. C.; Zhang, H.; Fan, C. Visual cocaine detection with gold nanoparticles and rationally engineered aptamer structures. *Small* **2008**, *4*, 1196-1200.
21. Jiang, B.; Wang, M.; Chen, Y.; Xie, J.; Xiang, Y. Highly sensitive electrochemical detection of cocaine on graphene/AuNP modified electrode via catalytic redox-recycling amplification. *Biosens. Bioelectron.* **2012**, *32*, 305-308.
22. Roncancio, D.; Yu, H.; Xu, X.; Wu, S.; Liu, R.; Debord, J.; Lou, X.; Xiao, Y. A label-free aptamer-fluorophore assembly for rapid and specific detection of cocaine in biofluids. *Anal. Chem.* **2014**, *86*, 11100-11106.

APPENDIX C: SUPPLEMENTARY INFORMATION FOR IMMOBILIZED APTAMER CHARACTERIZATION AND APTASENSOR DEVELOPMENT

Methylene blue (MB) tagged DNA aptamer experiments

Methylene blue (MB) is a redox active species and DNA can be tagged at either the 5′ or 3′ end with MB for electrochemical sensor development. The MB and thiohexyl labeled DNA were purchased from Biosearch Technologies. The thiolated end of the DNA is used for attachment to gold electrodes. The MB and thiohexyl labeled DNA aptamer was reduced using TCEP, the gold electrodes were cleaned and the DNA was immobilized on the electrodes as described in Chapter 4. Instead of SWV, for the MB experiments alternating current voltammetry (ACV) was conducted using CH Instruments' potentiostat (Model 760b). The following parameters for ACV were used: initial potential −0.1 V, final potential −0.38 V, potential step 4 mV, amplitude 25 mV. The RE was Ag/AgCl and the frequency was varied between 10, 25, 50, 75 and 100 Hz. A positive control from a previous study[1] was employed where a short stem-loop DNA sequence (DNA1) was immobilized on the electrode. The DNA1, on binding to the target DNA sequence (DNA2), undergoes a conformational change (Figure C.3) that reflects as a change in peak current.

The presence of peak current due to the reduction of MB indicates the successful immobilization of DNA on the electrodes since MB is only present in association with the DNA. Figure C.4(A) shows the ACV current prior and post introduction of target DNA and Figure C.4(B) shows the ACV current prior and post introduction of target EE. The percent peak current change at different frequencies was plotted for the EE aptamers as well as the positive control (Figure C.5). Neither of the EE aptamers (EEApt1 and EEApt2) showed a significant change in signal on binding to EE. The ~30% signal change at 10Hz for EEApt1 (3′ MB) was not a reproducible result.

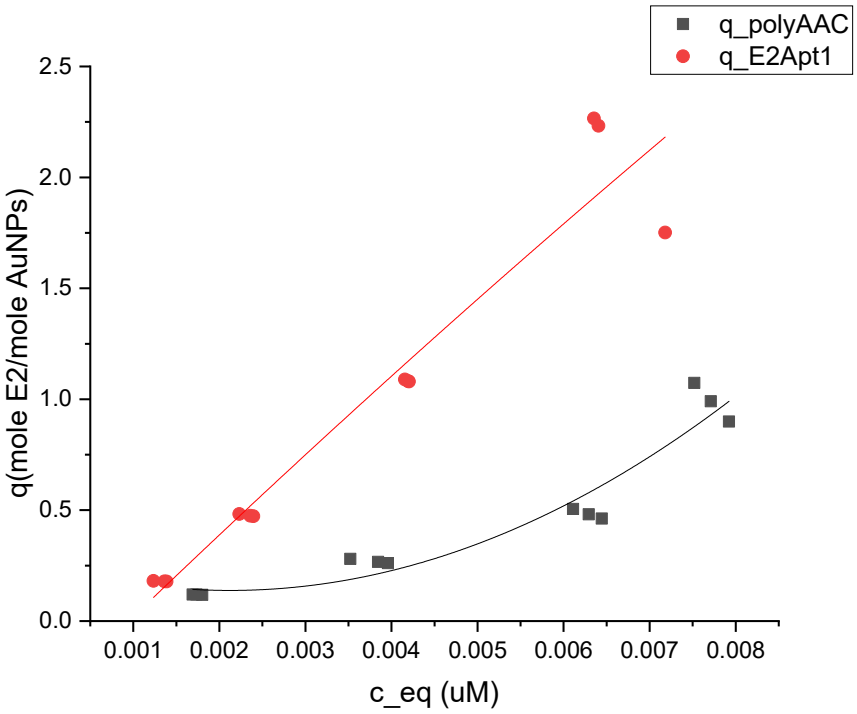

Figure C.1. Adsorption isotherms of AuNPs modified with polyAAC DNA and E2Apt1 (5′). Sorbed concentrations (q) versus solution concentrations (c_eq) of E2.

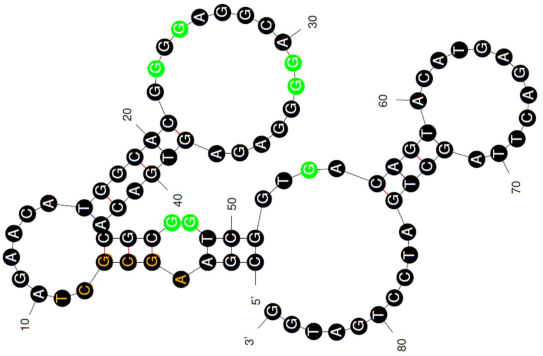

E2Apt1

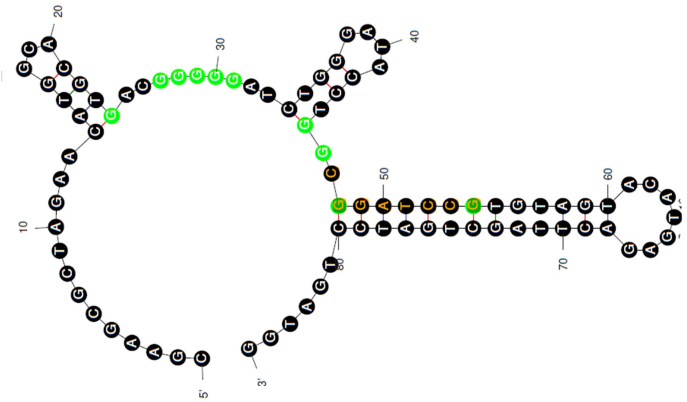

E2Apt2

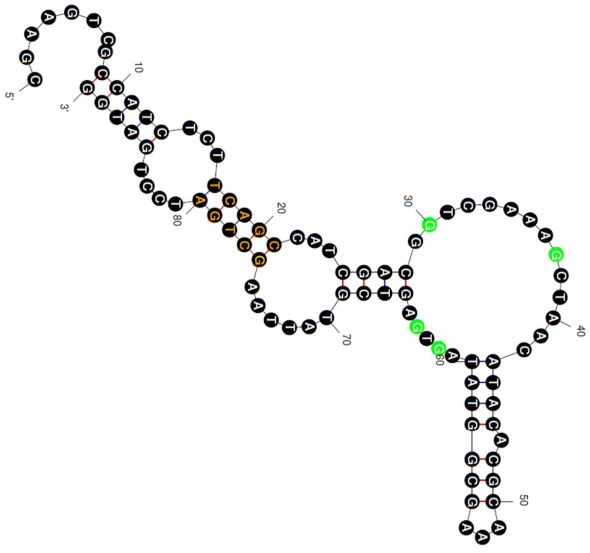

EEApt1

Figure C.2. Secondary structures of aptamers as predicted from mfold. The yellow highlighted bases are self-dimerizing regions. Fluorescent green guanines are involved in binding the target based on my previous chemical probing data.

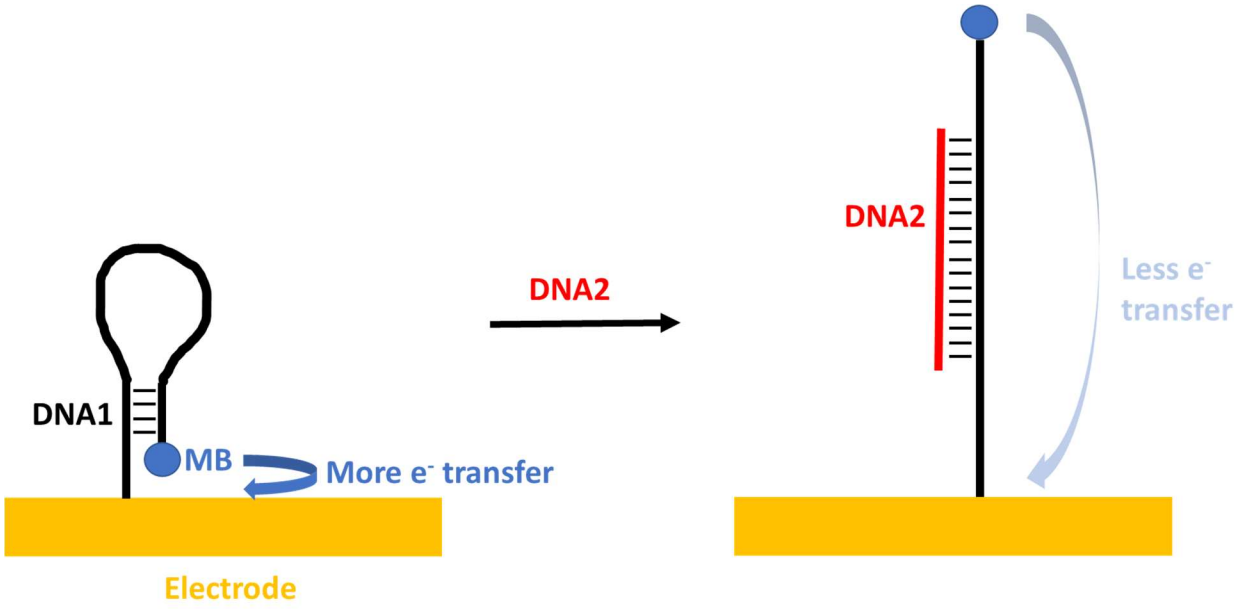

Figure C.3. Positive control for MB-labeled electrochemical experiments employing stem-loop DNA (DNA1) and target DNA (DNA2).

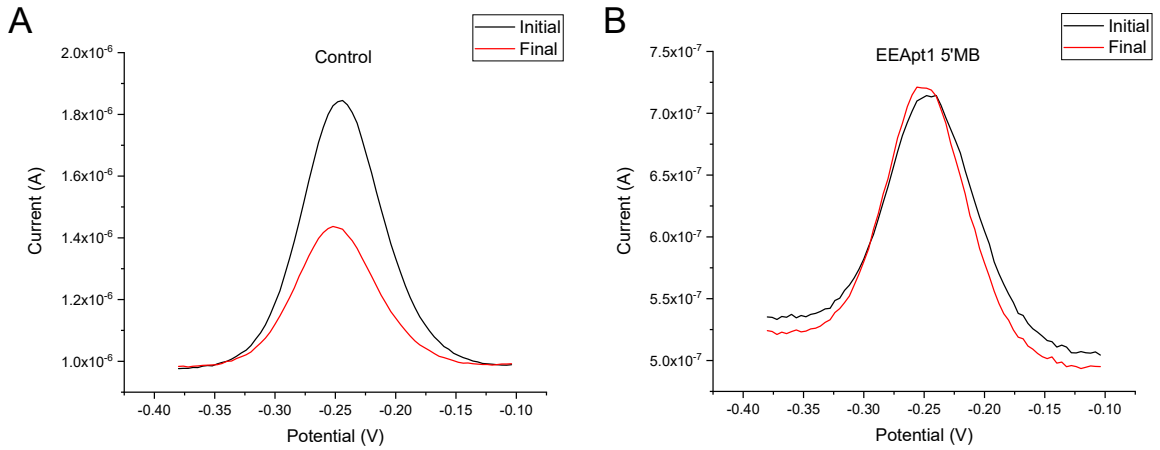

Figure C.4. Initial and final currents for (A) positive control and (B) EEApt1 5′ MB. Presence of peak current indicates immobilization of DNA on the electrode. Change in current shows conformational change upon binding. Frequency of ACV = 25Hz.

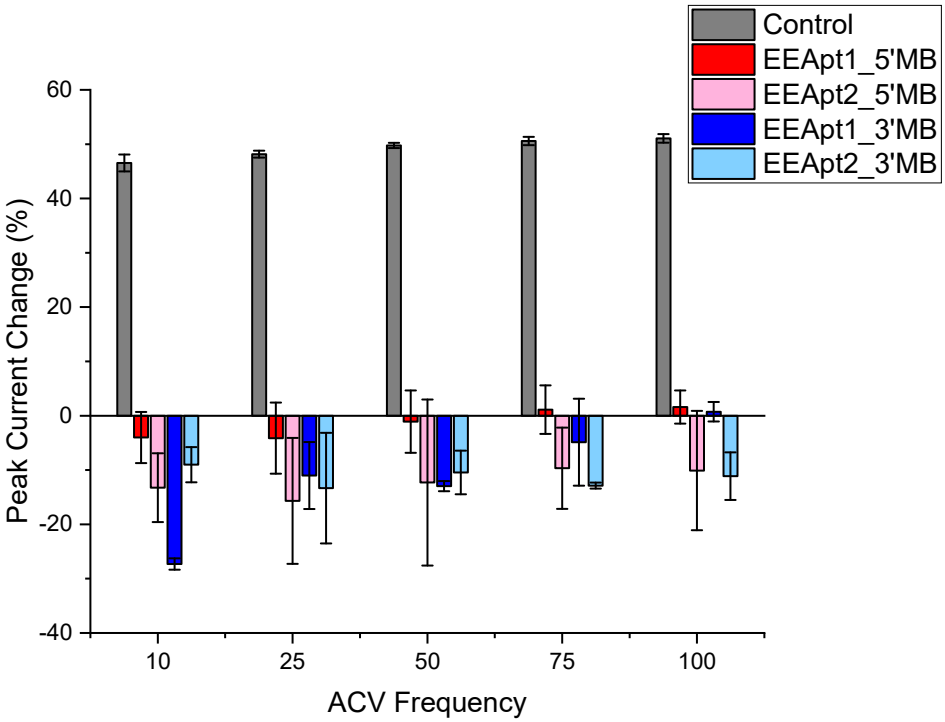

Figure C.5. Bar plot showing percentage peak current change at different ACV frequencies for positive control and 2 EE aptamers.

Table C.1. Tabulated values for K_d (fit value), c'_{fit} (fit value) and c' (experimentally determined)

	Unbound	**5′ immob**	**3′ immob**
		***K*d**	
E2Apt1	0.65	0.13	0.20
E2Apt2	0.77	---	0.26
EEApt1	0.76	---	---
		***c′*fit**	
E2Apt1	0.38	0.011	0.012
E2Apt2	0.33	---	0.011
EEApt1	0.47	---	---
		c′	
E2Apt1	0.5	0.018	0.016
E2Apt2	0.5	0.018	0.018
EEApt1	0.5	0.013	0.012

REFERENCES

1. Cunningham, J. C.; Brenes, N. J.; Crooks, R. M., Paper Electrochemical Device for Detection of DNA and Thrombin by Target-Induced Conformational Switching. *Analytical Chemistry* **2014,** *86* (12), 6166-6170.